



# "Sensing supraphysiological levels of MYC"

## Mechanisms of MIZ1-dependent MYC-induced Apoptosis in Mammary Epithelial Cells

Mechanismen der MIZ1-abhängigen MYC-induzierten Apoptose in  
Brustepithelzellen

### **Doctoral thesis**

for a doctoral degree

at the Graduate School of Life Sciences

Julius-Maximilians-Universität Würzburg

Section Biomedicine

submitted by

**Katrin Evelyn Wiese**

from Hannover

Würzburg, 2015



Submitted on:

**Members of the Thesis Committee**

Chairperson: Prof. Dr. Manfred Gessler

Primary Supervisor: Prof. Dr. Martin Eilers

Second Supervisor: Prof. Dr. Dr. Manfred Scharl

Third Supervisor: Prof. Dr. Andreas Trumpp

Date of Public Defense:

Date of Receipt of Certificates:

"And I wondered if hurdlers ever thought, you know, *This would go faster if we just got rid of the hurdles.*"

John Green, *The Fault in Our Stars*

# Contents

|   |           |
|---|-----------|
| List of Figures . . . . .                                       | i         |
| Abstract . . . . .  | iii       |
| Zusammenfassung . . . . .                                       | iv        |
| <b>1 Introduction</b>   | <b>1</b>  |
| 1.1 Apoptosis - 'everything returns into everything' . . . . .  | 1         |
| 1.1.1 The extrinsic apoptotic pathway . . . . .                 | 2         |
| 1.1.2 The intrinsic apoptotic pathway . . . . .                 | 3         |
| 1.1.3 Regulation of apoptosis by BCL-2 family members . . . . . | 3         |
| 1.1.4 Apoptosis in cancer biology . . . . .                     | 5         |
| 1.2 MYC - 'everything connects to everything else' . . . . .    | 8         |
| 1.2.1 Regulation and deregulation of MYC . . . . .              | 8         |
| 1.2.2 Chromatin binding of MYC . . . . .                        | 9         |
| 1.2.3 Transcriptional regulation by MYC . . . . .               | 11        |
| 1.2.4 Molecular functions of MYC . . . . .                      | 15        |
| 1.3 Objectives of this thesis . . . . .                         | 20        |
| <b>2 Materials</b>  | <b>21</b> |
| 2.1 Strains and cell lines . . . . .                            | 21        |
| 2.1.1 <i>Escherichia coli</i> strains . . . . .                 | 21        |
| 2.1.2 Mammalian cell lines . . . . .                            | 21        |
| 2.2 Cultivation media and supplements . . . . .                 | 22        |
| 2.2.1 Bacterial growth media and antibiotics . . . . .          | 22        |
| 2.2.2 Media and additives for mammalian cell culture . . . . .  | 22        |
| 2.3 Oligonucleotides . . . . .                                  | 24        |
| 2.3.1 Oligonucleotides for sequencing and cloning . . . . .     | 24        |
| 2.3.2 Primers for qRT-PCR . . . . .                             | 24        |
| 2.3.3 Primers for qPCR after ChIP . . . . .                     | 25        |
| 2.3.4 Oligonucleotides for shRNA-mediated depletion . . . . .   | 25        |
| 2.4 Plasmids . . . . .  | 26        |
| 2.4.1 Empty vector backbones . . . . .                          | 26        |
| 2.4.2 Packaging systems . . . . .                               | 26        |
| 2.4.3 Expression vectors . . . . .                              | 26        |
| 2.5 Antibodies . . . . .  | 28        |
| 2.5.1 Primary antibodies . . . . .                              | 28        |
| 2.5.2 Secondary antibodies . . . . .                            | 29        |

|          |   |           |
|----------|---|-----------|
| 2.6      | Chemicals . . . . .   | 29        |
| 2.6.1    | Markers and ladders . . . . .                                 | 29        |
| 2.6.2    | Enzymes . . . . .   | 30        |
| 2.6.3    | Kits . . . . .  | 30        |
| 2.7      | Solutions and buffers . . . . .                               | 30        |
| 2.8      | Consumables and equipment . . . . .                           | 34        |
| 2.9      | Software and web-based programs . . . . .                     | 35        |
| <b>3</b> | <b>Methods</b>  | <b>37</b> |
| 3.1      | Cell biology methods . . . . .                                | 37        |
| 3.1.1    | Maintaining cultured mammalian cells . . . . .                | 37        |
| 3.1.2    | 3D cell culture . . . . .                                     | 38        |
| 3.1.3    | Mammosphere culture . . . . .                                 | 38        |
| 3.1.4    | Production of amphotrophic retroviruses . . . . .             | 38        |
| 3.1.5    | Production of lentiviruses . . . . .                          | 39        |
| 3.1.6    | Transduction of cells with viruses . . . . .                  | 40        |
| 3.1.7    | Cumulative growth curve . . . . .                             | 40        |
| 3.1.8    | Transwell migration assay . . . . .                           | 40        |
| 3.1.9    | Flow cytometry . . . . .                                      | 40        |
| 3.2      | Molecular biology methods . . . . .                           | 41        |
| 3.2.1    | Annealing of oligonucleotides . . . . .                       | 41        |
| 3.2.2    | PCR for cloning of DNA fragments . . . . .                    | 42        |
| 3.2.3    | Restriction digest of DNA fragments . . . . .                 | 42        |
| 3.2.4    | Separation of DNA fragments via gel electrophoresis . . . . . | 43        |
| 3.2.5    | Purification of DNA from agarose gels . . . . .               | 43        |
| 3.2.6    | Ligation of DNA fragments . . . . .                           | 43        |
| 3.2.7    | Transformation of bacteria . . . . .                          | 43        |
| 3.2.8    | Isolation of plasmid DNA from bacteria . . . . .              | 44        |
| 3.2.9    | Isolation of RNA from mammalian cells . . . . .               | 44        |
| 3.2.10   | cDNA synthesis . . . . .                                      | 44        |
| 3.2.11   | Quantitative PCR . . . . .                                    | 45        |
| 3.2.12   | Microarray . . . . .  | 45        |
| 3.3      | Biochemistry methods . . . . .                                | 46        |
| 3.3.1    | Preparation of whole cell lysates . . . . .                   | 46        |
| 3.3.2    | Preparation of nuclear extracts . . . . .                     | 46        |
| 3.3.3    | Quantification of protein concentration . . . . .             | 46        |
| 3.3.4    | SDS polyacrylamide gel electrophoresis . . . . .              | 47        |
| 3.3.5    | Western blot . . . . .  | 47        |
| 3.3.6    | Stripping PVDF membranes . . . . .                            | 47        |
| 3.3.7    | Chromatin immunoprecipitation . . . . .                       | 47        |
| 3.3.8    | ChIP-sequencing . . . . .                                     | 49        |
| 3.4      | Bioinformatic and statistical analyses . . . . .              | 49        |
| 3.4.1    | Bioinformatic analysis of ChIP-seq data . . . . .             | 50        |
| 3.4.2    | Functional analysis of microarray data . . . . .              | 52        |

|          |   |               |
|----------|---|---------------|
| <b>4</b> | <b>Results</b>  | <b>53</b>     |
| 4.1      | Different levels of MYC produce diverse biological outputs . . . . .                                  | 53            |
| 4.1.1    | Biological functions of MYC in MECs at moderate expression levels . . .                               | 54            |
| 4.1.2    | Biological functions of MYC in MECs at oncogenic expression levels . . .                              | 58            |
| 4.2      | Characterisation of MYC/MIZ1-mediated apoptosis . . . . .   | 63            |
| 4.2.1    | MYC/MIZ1-mediated apoptosis is dose-dependent . . . . .   | 63            |
| 4.2.2    | Molecular players involved in MYC-mediated apoptosis . . . . .  | 64            |
| 4.3      | MIZ1-dependent transcriptional changes . . . . .  | 69            |
| 4.3.1    | MIZ1-dependent repression of target genes . . . . .   | 71            |
| 4.4      | Chromatin binding of MYC/MIZ1 complexes . . . . .   | 75            |
| 4.4.1    | Global analysis of MIZ1, MYC-ER and MYCVD-ER binding sites . . . . .                                  | 77            |
| 4.4.2    | MYC and MIZ1 bind cooperatively to core promoters . . . . .   | 79            |
| 4.4.3    | MYC/MIZ1 complexes can bind to low-affinity sites . . . . .   | 81            |
| 4.5      | SRF-regulated genes are repressed by MYC/MIZ1 . . . . .   | 83            |
| 4.5.1    | Repression of SRF target genes is rescued by constitutively active MRTF-A                             | 87            |
| <b>5</b> | <b>Discussion</b>   | <b>90</b>     |
| 5.1      | Why levels matter: MIZ1-dependent and -independent functions of MYC in MECs                           | 90            |
| 5.1.1    | Regulation of proliferation . . . . .   | 91            |
| 5.1.2    | Regulation of self-renewal . . . . .  | 92            |
| 5.1.3    | MYC-induced apoptosis requires association with MIZ1 . . . . .  | 93            |
| 5.2      | Sensing danger: MYC/MIZ1-mediated repression puts cells on the alert . . . . .                        | 95            |
| 5.2.1    | Inhibition of SRF blocks survival signalling via AKT . . . . .  | 96            |
| 5.2.2    | Joint invasion of new genomic territories . . . . .   | 100           |
| 5.3      | Balancing act: oncogenic and tumour suppressive consequences of the MYC/MIZ1<br>interaction . . . . . | 104           |
|          | <b>Bibliography</b>   | <b>I</b>      |
|          | <b>Abbreviations</b>  | <b>XXVII</b>  |
|          | <b>Acknowledgements</b>   | <b>XXXI</b>   |
|          | <b>Publications</b>   | <b>XXXIII</b> |
|          | <b>Curriculum vitae</b>   | <b>XXXIV</b>  |
|          | <b>Affidavit</b>  | <b>XXXV</b>   |

# List of Figures

|      |  |    |
|------|--|----|
| 1.1  | The extrinsic or death receptor pathway . . . . .  | 2  |
| 1.2  | The intrinsic or mitochondrial pathway . . . . .   | 4  |
| 1.3  | Regulation of BCL-2 family members . . . . .   | 6  |
| 1.4  | Regulation of the tumour suppressor p53 . . . . .  | 7  |
| 1.5  | MYC: a key signalling node in cancer . . . . .   | 10 |
| 1.6  | Structure of the MYC/MAX heterodimer . . . . .   | 11 |
| 1.7  | Schematic model of MYC-mediated transcriptional activation . . . . .   | 12 |
| 1.8  | Schematic models of MIZ1-mediated transcriptional activation and repression . .                                  | 14 |
| 1.9  | MYC target genes contribute to the hallmarks of cancer . . . . .   | 17 |
| 1.10 | Crosstalk between MYC and the apoptotic machinery . . . . .  | 18 |
| 4.1  | Comparison of different Myc expression levels <sup>1</sup> . . . . .   | 54 |
| 4.2  | MYC and MYC VD accelerate cell cycle re-entry after starvation <sup>1</sup> . . . . .                            | 55 |
| 4.3  | MYC and MYC VD enhance mammosphere formation <sup>1</sup> . . . . .  | 56 |
| 4.4  | Inhibition of migration by MYC is partially MIZ1-dependent . . . . .   | 57 |
| 4.5  | Sensitisation to apoptosis by MYC is mostly MIZ1-dependent <sup>1</sup> . . . . .                                | 58 |
| 4.6  | MYC and MYC VD induce a mammary stem cell surface marker profile <sup>1</sup> . . . . .                          | 59 |
| 4.7  | Epithelial cells select against high levels of MYC WT but not MYC VD <sup>1</sup> . . . . .                      | 60 |
| 4.8  | Inducible expression of MYC but not MYC VD increases apoptosis <sup>1</sup> . . . . .                            | 62 |
| 4.9  | Dose- and MIZ1-dependent induction of apoptosis <sup>1</sup> . . . . .   | 63 |
| 4.10 | MYC/MIZ1-mediated apoptosis in HMLE cells is p53-independent but could be mediated by ARF <sup>1</sup> . . . . . | 65 |
| 4.11 | Differential induction of p53 between MYC-ER and MYCVD-ER <sup>1</sup> . . . . .                                 | 66 |
| 4.12 | Apoptosis is rescued by knockdown of BIM or overexpression of BCL-2 <sup>1</sup> . . . . .                       | 67 |
| 4.13 | Apoptosis is rescued by knockdown of p53 <sup>1</sup> . . . . .  | 68 |
| 4.14 | Apoptosis is rescued by knockdown of MAX or inhibition of DNA binding <sup>1</sup> . . .                         | 70 |
| 4.15 | Identification of MIZ1-dependent transcriptional changes <sup>1</sup> . . . . .                                  | 71 |
| 4.16 | MYC VD is selectively impaired in gene repression <sup>1</sup> . . . . .   | 72 |
| 4.17 | MIZ1-mediated repression occurs at high levels of MYC <sup>1</sup> . . . . .                                     | 73 |
| 4.18 | Overexpression of MYC VD and MIZ1 depletion have similar effects on MYC target genes <sup>1</sup> . . . . .      | 74 |
| 4.19 | DNA binding of MYC-ER and MIZ1 <sup>1</sup> . . . . .  | 76 |
| 4.20 | Binding of MYCVD-ER to standard MYC targets is weaker . . . . .  | 77 |
| 4.21 | ChIP-sequencing identifies direct target genes of MYC and MIZ1 in MCF10A cells <sup>1</sup>                      | 79 |

---

<sup>1</sup>Parts of this figure were published in similar form in Wiese et al. [2015].

---

|      |  |     |
|------|--|-----|
| 4.22 | Overlap of MYC/MIZ1 bound genes in MCF10A cells . . . . .  | 80  |
| 4.23 | MYC WT but not MYC VD enhances MIZ1 binding to core promoters <sup>1</sup> . . . . .                         | 81  |
| 4.24 | Different DNA binding motifs are enriched in subgroups of MYC-bound genes . . . . .                          | 82  |
| 4.25 | MYC/MIZ1 ratio changes on activated and repressed genes <sup>1</sup> . . . . .                               | 82  |
| 4.26 | Identification of enriched promoter motifs in MYC-repressed genes <sup>1</sup> . . . . .                     | 83  |
| 4.27 | MYC represses genes regulated by SRF and its coactivator MRTF-A <sup>1</sup> . . . . .                       | 84  |
| 4.28 | MYC-mediated repression of SRF targets is downstream of RhoA <sup>1</sup> . . . . .                          | 85  |
| 4.29 | SRF target genes are bound by MYC/MIZ1 complexes <sup>1</sup> . . . . .                                      | 86  |
| 4.30 | $\Delta$ N-MAL rescues expression of SRF target genes <sup>1</sup> . . . . .                                 | 87  |
| 4.31 | MYC represses MRTF/SRF-induced survival signalling via AKT <sup>1</sup> . . . . .                            | 88  |
|      |  |     |
| 5.1  | Proposed model for the continuum of MYC functions with increasing levels . . . . .                           | 95  |
| 5.2  | A cofactor switch determines differential SRF activity and function . . . . .                                | 97  |
| 5.3  | Repression of adhesion and cytoskeleton dependent survival signalling by MYC . . . . .                       | 101 |
| 5.4  | Mechanistic model for the differential effects on target gene expression after MYC<br>deregulation . . . . . | 103 |



## Abstract

Deregulated MYC expression contributes to cellular transformation as well as progression and maintenance of human tumours. Interestingly, in the absence of additional genetic alterations, potentially oncogenic levels of MYC sensitise cells to a variety of apoptotic stimuli. Hence, MYC-induced apoptosis has long been recognised as a major barrier against cancer development.

However, it is largely unknown how cells discriminate physiological from supraphysiological levels of MYC in order to execute an appropriate biological response.

The experiments described in this thesis demonstrate that induction of apoptosis in mammary epithelial cells depends on the repressive actions of MYC/MIZ1 complexes. Analysis of gene expression profiles and ChIP-sequencing experiments reveals that high levels of MYC are required to invade low-affinity binding sites and repress target genes of the serum response factor SRF. These genes are involved in cytoskeletal dynamics as well as cell adhesion processes and are likely needed to transmit survival signals to the AKT kinase. Restoration of SRF activity rescues MIZ1-dependent gene repression and increases AKT phosphorylation and downstream function.

Collectively, these results indicate that association with MIZ1 leads to an expansion of MYC's transcriptional response that allows sensing of oncogenic levels, which points towards a tumour-suppressive role for the MYC/MIZ1 complex in epithelial cells.

## Zusammenfassung

Eine Deregulation der *MYC* Expression trägt entscheidend zur malignen Transformation und Progression humaner Tumoren bei. In Abwesenheit von zusätzlichen genetischen Läsionen machen potentiell onkogene *MYC* Proteinmengen Zellen jedoch anfällig für eine Reihe Apoptose-auslösender Reize. Daher kann *MYC*-induzierte Apoptose als bedeutende tumorsuppressive Maßnahme und wichtige Barriere gegen die Entstehung von Krebs betrachtet werden.

Mechanistisch unklar ist allerdings wie genau Zellen physiologische von supraphysiologischen *MYC*-Mengen unterscheiden um adäquat darauf reagieren zu können.

Die Experimente in dieser Dissertation zeigen, dass die repressive Eigenschaft von *MYC*/*MIZ1* Komplexen für die Induktion von Apoptose in Brustepithelzellen essentiell ist. Die Analyse von Genexpressions- und ChIP-Sequenzier-Experimenten verdeutlicht, dass hohe Level an *MYC* benötigt werden um niedrig-affine Bindestellen im Genom zu besetzen und Zielgene des SRF (*serum response factor*) Transkriptionsfaktors zu reprimieren. Diese Gene haben eine wichtige Funktion in Prozessen wie Zytoskelettdynamik und Zelladhäsion und sind vermutlich daran beteiligt notwendige Überlebenssignale an die Kinase AKT weiterzuleiten. Eine Wiederherstellung der SRF Aktivität revertiert die *MIZ1*-abhängige Repression der Zielgene und führt zu einer vermehrten AKT Phosphorylierung und Funktion.

Insgesamt deuten diese Resultate auf eine tumorsuppressive Rolle des *MYC*/*MIZ1* Komplexes in epithelialen Zellen hin, da eine Veränderung der genregulatorischen Aktivität als Folge der Assoziation mit *MIZ1* dazu beitragen könnte onkogene Mengen an *MYC* zu erkennen.

# Chapter 1

## Introduction

According to the World Health Organization WHO, cancer is the second leading cause of death after cardiovascular diseases, causing 26 % of all fatal casualties in Germany [WHO, 2014].

During normal development and tissue homeostasis, a multitude of stimulatory and inhibitory signals are constantly integrated on a molecular level to decide whether a cell should divide. Hence, normal human cells only reproduce, when they receive the appropriate growth signals. If genetic mutations compromise these control systems, cells proliferate excessively. Further corruption of regulated processes as diverse as replicative immortality, angiogenesis and energy metabolism, can lead to outgrowth of cell clones and, ultimately, tumour formation [Hanahan and Weinberg, 2011].

Fortunately, cell-internal fail-safe mechanisms have evolved, providing additional surveillance in order to protect multicellular organisms from potentially malignant cells. One such backup system, triggered by DNA damage as well as corrupted growth signals, is the induction of apoptosis.

### 1.1 Apoptosis - 'everything returns into everything'

Apoptosis is a tightly regulated conserved process that is essential during both embryonic development and adult tissue homeostasis. Controlled by a defined genetic programme, apoptotic cells undergo an ordered series of molecular events, which can be triggered by intrinsic or extrinsic stimuli. Morphologically, apoptosis is characterised by chromatin condensation, cell shrinkage and DNA fragmentation [Kerr et al., 1972].

Central to the mechanism of apoptosis is a family of cysteine-dependent proteases that cleave their substrates after aspartate residues, hence the name "caspases". These proteases initiate as well as execute most of the morphological and biochemical changes associated with programmed cell death. All caspases reside as inactive precursors in the cytoplasm and can be activated by proteolytic cleavage, close proximity to each other or by association with a cofactor [Hengartner, 2000].

Two major pathways link apoptotic stimuli to activation of the most upstream or "initiator" caspases: the extrinsic or death receptor pathway, and the intrinsic or mitochondrial pathway. Activated initiator caspases start a signalling or "caspase cascade" and amplify the apoptotic signal by activating "executioner" caspases which in turn cleave multiple key substrates, leading to induction of cell death [Adams, 2003].

### 1.1.1 The extrinsic apoptotic pathway

The activation of pro-apoptotic cell surface receptors by so called "death ligands" initiates the extrinsic apoptotic programme (Fig. 1.1). These ligands are members of the tumour necrosis factor (TNF) family and include TNF- $\alpha$ , TRAIL and Fas Ligand [Ashkenazi, 2002].

Once activated, death receptors like TNFR1, DR4 or FAS aggregate and attract the adaptor proteins FADD (Fas-associated death domain protein) or TRADD (tumor necrosis factor receptor type 1-associated death domain protein) to a shared cytoplasmic structure, the so-called "death domain". FADD / TRADD in turn are able to recruit procaspase 8 molecules. This structure, termed death-inducing signalling complex (DISC), arranges the procaspases in a close enough proximity to trigger self-cleavage of the inactive zymogens into active initiator caspases [Boatright et al., 2003].

Subsequent activation of the downstream effector caspases 3, 6 and 7 results in cleavage of various target proteins, which are responsible for the characteristic features of apoptosis. Among them

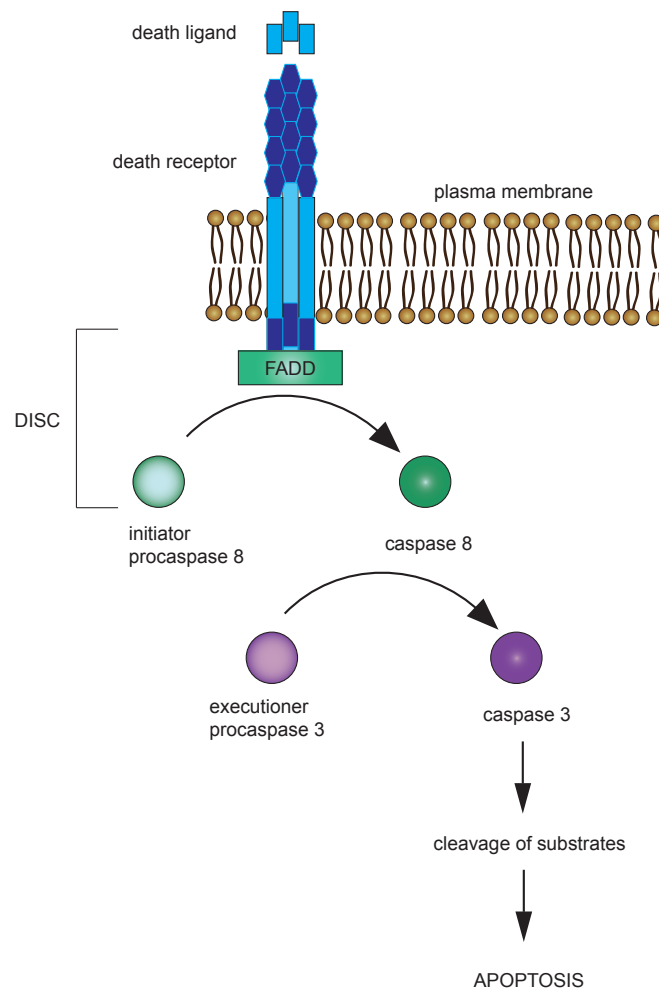


**Figure 1.1: The extrinsic or death receptor pathway**

Binding of their cognate ligands to members of the death receptor superfamily, such as FAS or tumour necrosis factor receptor 1 (TNFR1), induces receptor clustering. The cytoplasmic tails of these receptors bind adaptor molecules, FADD or TRADD (not shown), which recruit multiple procaspase 8 molecules to form a death-inducing signalling complex (DISC). Due to close proximity and cross-activation, procaspases are converted to their active form: caspase 8. Next, a "caspase cascade" is initiated, leading to activation of the executioner caspase 3 and subsequent cleavage of procaspases 6 and 7 (not shown). Substrates of these caspases include nucleases, nuclear lamina and cytoskeletal proteins. Their cleavage creates the morphological and biochemical features associated with the apoptotic phenotype.

are caspase-activated DNase (CAD), which is the main nuclease causing DNA fragmentation and chromatin condensation, as well as nuclear lamina and cytoskeletal proteins [Hengartner, 2000]. Although death receptor and mitochondrial pathways operate largely independently from each other, mechanistically, they merge at the initiation of the caspase cascade by cleavage of caspase 3.

### 1.1.2 The intrinsic apoptotic pathway

Various cellular stress stimuli, including DNA damage, hypoxia and cytokine deprivation, represent pro-apoptotic signals that converge on mitochondria. Being essential for cell survival by generating ATP on the one hand, on the other hand, these organelles also sequester a potent mixture of pro-apoptotic molecules in their intermembrane space. The decision to release these factors is primarily regulated by a complex interplay of the BCL-2 family of proteins (Fig. 1.2 and section 1.1.3). When pro-apoptotic stimuli outweigh pro-survival signals, the outer mitochondrial membrane is permeabilised by the formation of pores. Subsequently, cytochrome c is released into the cytosol, leading to the formation of a large holoenzyme complex, the apoptosome. In an ATP-dependent process, cytochrome c and the adaptor protein Apaf-1 (apoptotic protease-activating factor 1) activate caspase 9, which in turn cleaves caspase 3. This initiates the execution phase of the apoptotic programme that is shared with the extrinsic pathway [Liu et al., 1996; Cain et al., 1999; Rodriguez and Lazebnik, 1999].

Caspase 3 activation can be antagonised by a family of caspase inhibitors, known as inhibitors-of-apoptosis proteins (IAPs). However, among pro-apoptotic molecules released from the mitochondrial compartment are Smac/DIABLO proteins, which are neutralising the anti-apoptotic activity of IAPs, thereby ensuring full execution of apoptosis [Du et al., 2000; Verhagen et al., 2000].

### 1.1.3 Regulation of apoptosis by BCL-2 family members

One of the most complex and sophisticated regulatory mechanisms during apoptosis is the control of mitochondrial outer membrane permeabilisation (MOMP).

This critical step is governed and coordinated by the BCL-2 (B cell lymphoma gene 2) family of proteins. Its members can be divided into three functionally distinct subgroups (Fig. 1.3 A): Pro-survival proteins like BCL-2 itself; pro-apoptotic effector proteins like BAX and BAK; and BH3-only family members, like BIM, which are also pro-apoptotic. From a structural point of view, pro-survival as well as pro-apoptotic effector proteins share four BCL-2 homology (BH) domains, termed BH1 to BH4, whereas BH3-only proteins contain only the third homologous region [Czabotar et al., 2014].

Crucial for permeabilisation of the mitochondrial outer membrane (MOM) are the two pro-apoptotic family members BAX and BAK. In healthy cells, BAX is permanently translocating back and forth between mitochondria and cytosol, whereas BAK is inserted into the MOM. Once activated, BAX and BAK monomers undergo conformational changes, allowing the assembly of homo-oligomers and formation of pores in the outer membrane [Griffiths et al., 1999; Edlich et al., 2011].

Understandably, BAX and BAK are strictly regulated by an intricate interplay of the other pro- and anti-apoptotic family members.

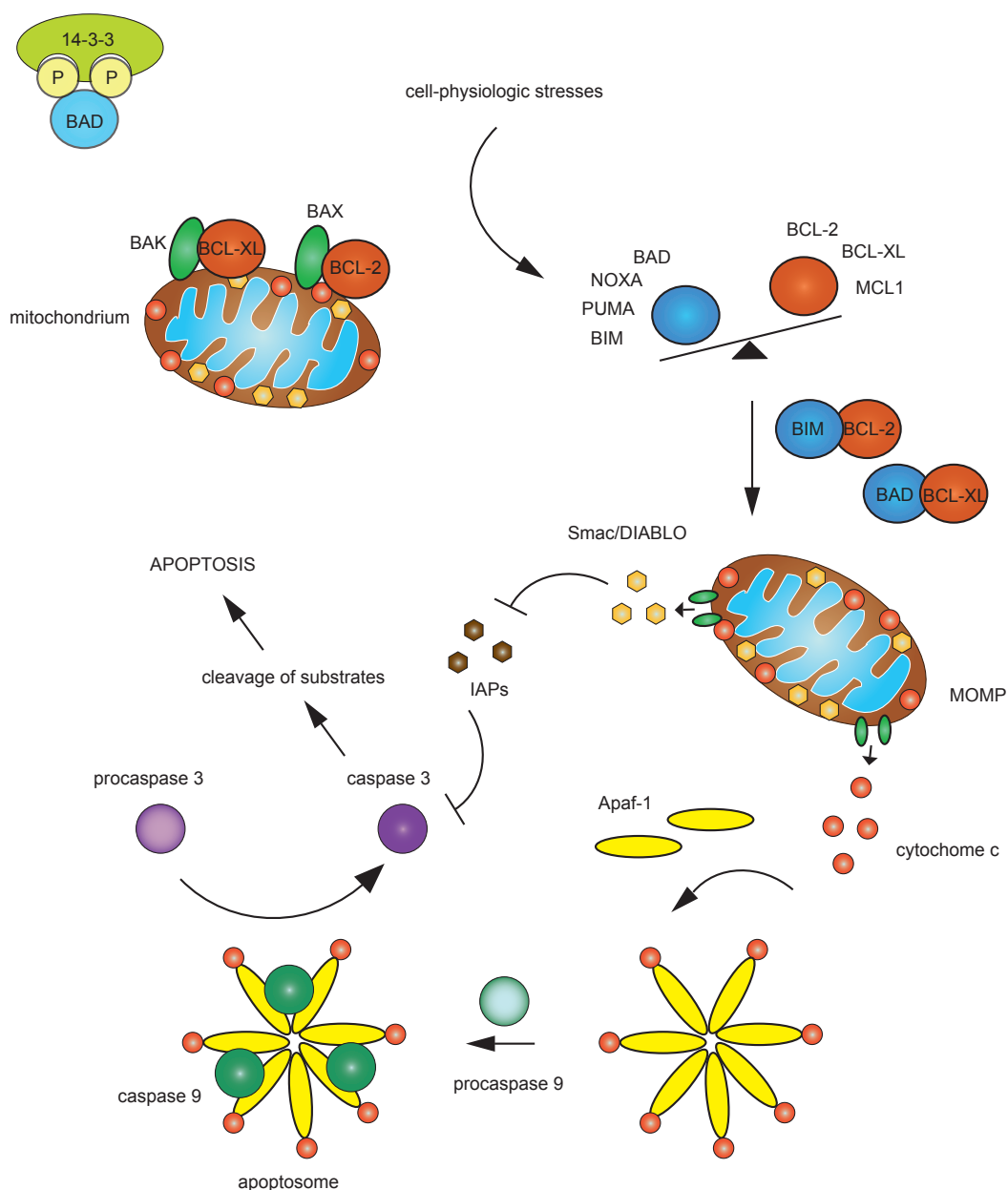


**Figure 1.2: The intrinsic or mitochondrial pathway**

In healthy cells, pro-apoptotic members of the BCL-2 family are retained in an inactive form in the cytoplasm by various mechanisms (e.g. sequestration by 14-3-3, as shown here for BAD). Anti-apoptotic proteins like BCL-2 or BCL-XL are therefore able to neutralise BAK and BAX at the outer mitochondrial membrane. The mitochondrial apoptosis pathway is initiated in response to multiple stress stimuli that alter the balance between pro- and anti-apoptotic BCL-2 family members. Activation of BIM and BAD, for example, antagonises anti-apoptotic members, thereby preventing them from interacting with BAX and BAK at the mitochondria. The result is the permeabilisation of the outer mitochondrial membrane (MOMP) and the release of cytochrome c and other pro-apoptotic molecules. In an ATP-dependent process, cytochrome c associates with Apaf-1 and procaspase 9 to form the apoptosome, leading to an activation of caspase 9 and subsequently, caspase 3.

BH3-only proteins serve as a link between sensors that monitor functional integrity of a cell and the downstream pro-apoptotic effector proteins. Parameters "measured" include access to growth factors, structure of DNA and cell attachment. Therefore, diverse cytotoxic stimuli result in transcriptional induction or post-translational stabilisation of proteins, like BIM, PUMA and BID.

Essentially, the pro-apoptotic functions of these family members are mediated via protein-protein interactions; either by direct binding and activation of BAX and BAK, or by sequestration of

pro-survival BCL-2 proteins, which competes off other bound BH3-only proteins or activated BAX/BAK (blue boxes in Fig. 1.3 B).

Usually, both of these actions are antagonised by multiple members of the pro-survival subgroup, which each bind a subset of pro-apoptotic family members. Sequestration of BH3-only proteins by pro-survival members prevents them from activating BAX/BAK (upper red box in Fig. 1.3 B). In addition, if BAX and BAK are already activated, anti-apoptotic BCL-2 family members prevent the homo-oligomerisation that is necessary for pore formation (lower red box in Fig. 1.3 B and Llambi et al. [2011]). Finally, it has been shown that BAX can be actively translocated from the mitochondria to the cytosol by BCL-XL, adding yet another mode of regulation [Edlich et al., 2011].

Interestingly, also the extrinsic apoptotic pathway can involve cytochrome c release from the mitochondria in some cell types. This is due to caspase 8-mediated proteolytic cleavage of the BH3-only protein BID, which is sufficient to neutralise BCL-2 and activate BAX [Luo et al., 1998].

Taken together, the cellular concentration of each family member is variable and it is the balance between those subgroups in addition to the intensity of the apoptotic stimulus, that determines whether the apoptotic threshold is crossed [Westphal et al., 2014].

#### 1.1.4 Apoptosis in cancer biology

Tumourigenesis is a multistep process during which excessive proliferation provides the basis for accumulation of additional genomic changes, ultimately enabling single cells to acquire all traits necessary for malignant transformation.

Initially proposed already in the very publication that defined the term "apoptosis" by Kerr et al. [1972], it is now unequivocally accepted that the elimination of potentially malignant cells by apoptosis represents a natural barrier against tumour formation [Lowe et al., 2004]. Among the apoptosis-inducing, cell-physiologic stress signals encountered by pre-neoplastic cells during transformation are oncogene-induced hyperproliferation and DNA damage, as well as low oxygen tension. Hence, evasion of programmed cell death is a key step during cancer development and progression [Hanahan and Weinberg, 2011].

General mechanisms contributing to apoptosis resistance include: 1) Disruption of BCL-2 family balance by overexpression of anti-apoptotic BCL-2 family proteins or reduction of pro-apoptotic members; 2) Inhibition of caspase function, e.g. due to increased expression of IAPs; 3) Impairment of death receptor signalling; 4) Loss or mutation of p53 function [Wong, 2011].

#### The tumour suppressor p53

A common way to resist apoptosis is inactivation of the p53 tumour suppressor pathway, a complex network of signalling proteins designed to respond to basically all cell-physiologic stress signals [Horn and Vousden, 2007].

Often referred to as the "guardian of the genome", TP53 (p53) is a short-lived transcription factor with a proteolytic half-life of about 20 min. In normal, unstressed cells, p53 is marked for destruction by attachment of ubiquitin molecules and rapidly degraded in the nucleus and cytosol. The E3 ligase MDM2 (mouse double minute 2, or HDM2 in human cells) is responsible for this fast turnover [Kubbutat et al., 1997]. In addition, MDM2 can also actively represses p53

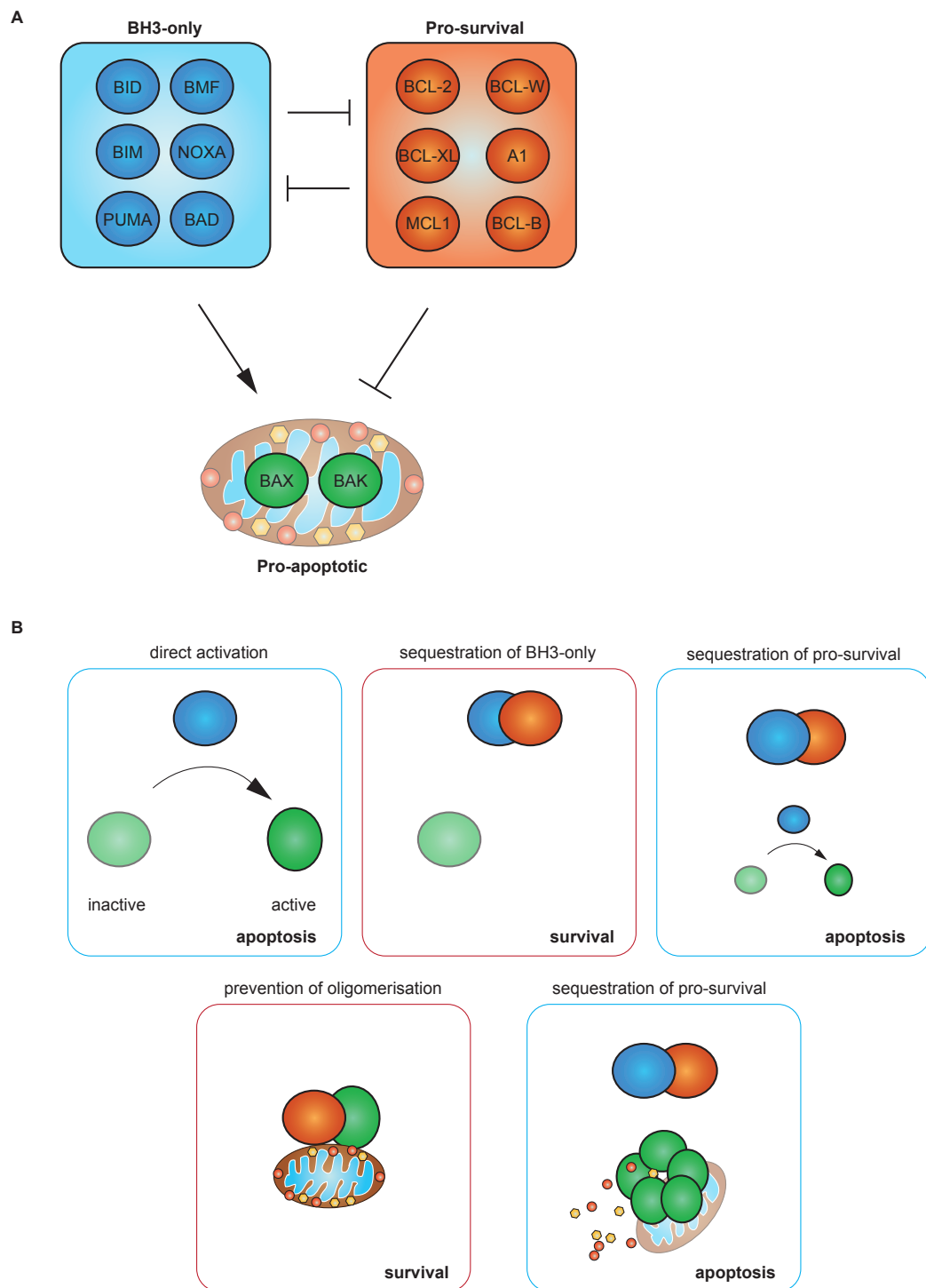


**Figure 1.3: Regulation of BCL-2 family members**

- A BCL-2 family members form a complex interaction network and can be divided into three different classes: Pro-apoptotic BAX and BAK localise to the mitochondria and are responsible for MOMP. BH3-only proteins are also pro-apoptotic and can inhibit the pro-survival members or activate BAX and BAK (see below). Pro-survival proteins inhibit the activity of all the pro-apoptotic family members. Not all existing members are shown.
- B Different modes of regulation exist between BCL-2 family members. Some BH3-only proteins (blue), such as BIM, can directly activate BAX or BAK (green). Action of pro-survival members (red) can prevent this. Other BH3-only proteins like BAD, act primarily through sequestration of anti-apoptotic members, thereby indirectly allowing BAX/BAK activation (upper right blue box). BCL-2 proteins can also directly inhibit activated BAX/BAK proteins and this can be antagonised by BH3-only proteins as well (lower boxes). Adapted from Westphal et al. [2014].



function on target gene promoters by recruiting histone deacetylases, methyltransferases and co-repressors [Ito et al., 2002; Chen et al., 2010b].

Under stress conditions, several checkpoint mechanisms are operational that activate regulatory proteins which in turn protect p53 from degradation (see Fig. 1.4 for examples). Stabilisation and activation are mostly achieved via post-translational modification of p53. For instance, upon DNA damage, the ATM and Chk2 kinases are activated, phosphorylate p53 and thereby prevent the interaction with MDM2 [Canman et al., 1998; Hirao et al., 2000].

Another important regulator of p53 is the tumour suppressor p14<sup>ARF</sup>, the alternate reading frame product of the INK4a/ARF locus. This mode of p53 stabilisation is particularly important after disruption of proper cell cycle regulation by oncogenic signalling. Upon oncogenic stress, ARF is induced and promotes p53 stabilisation by interfering with the MDM2-p53 interaction [Weber et al., 1999; Llanos et al., 2001]. Consequently, for example in the case of lymphoma, it has been shown that the protective function of p53 against tumourigenesis is crucially dependent on ARF [Christophorou et al., 2006].

Following activation by upstream stress response pathways, p53 homo-tetramers regulate target genes involved in various downstream processes. Cell cycle arrest, senescence and apoptosis are considered to be the three major roadblocks limiting the proliferation of pre-cancerous cells. A decision between the different transcriptional programmes is made based on the availability of survival signals. Furthermore, specific post-translational modifications, co-factor recruitment and

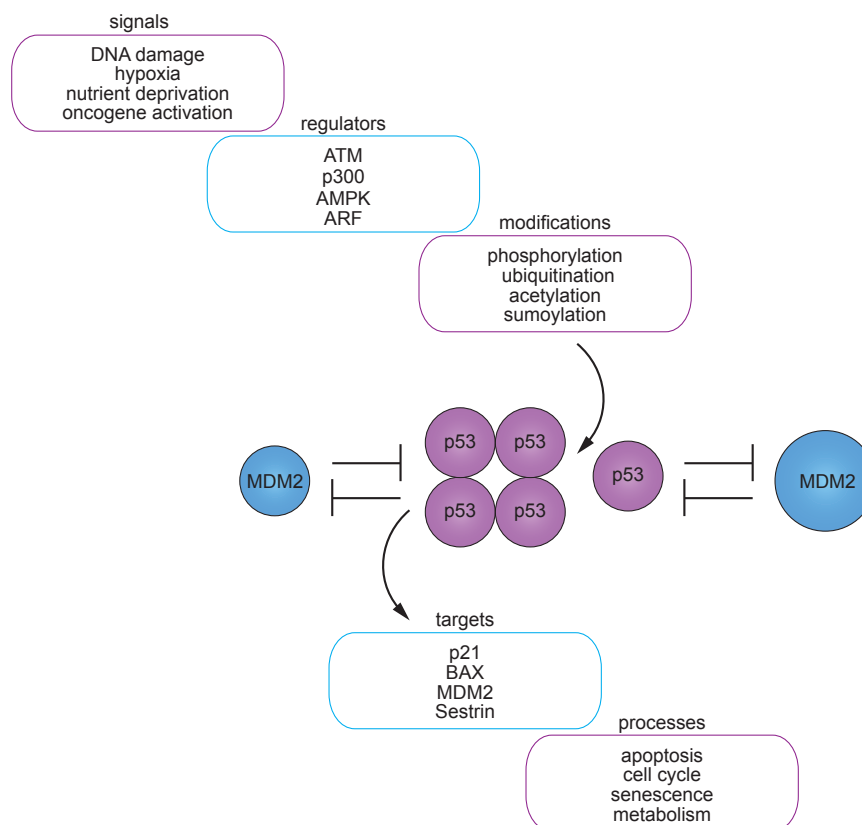


**Figure 1.4: Regulation of the tumour suppressor p53**

Core regulation of p53 is achieved via ubiquitin-mediated proteolysis through the MDM2 / HDM2 E3 ligase. A variety of cellular stress signals are monitored via specific checkpoints and effector proteins of these pathways regulate p53 via a multitude of post-translational modifications. p53 is stabilised, activated and can regulate expression of target genes, thereby inducing a number of cellular responses. A negative feedback loop with MDM2 keeps the increase in p53 levels transient. Adapted from Whibley et al. [2009].

affinity-differences for certain target gene promoters influence the transcriptional and biological output of p53 [Espinosa and Emerson, 2001; Kruse and Gu, 2008; Schlereth et al., 2010].

Although p53 can directly act at the mitochondria to promote apoptosis, most commonly, activation of target genes like *BAX*, *BBC3/PUMA* and *NOXA* is responsible for mitochondrial cytochrome c release [Benchimol, 2001; Mihara et al., 2003]. In addition, regulation of death receptor family members can contribute to p53-mediated apoptosis.

Considering its central role in maintaining the genomic integrity of a cell, it is not surprising that functional inactivation or mutation of p53 is one of the most frequent alterations found in human cancers [Olivier et al., 2010]. Once this protective barrier to prevent propagation of "damaged" cells is overcome, the tumourigenic potential of oncogenes such as *MYC* can no longer be restrained.

## 1.2 *MYC* - 'everything connects to everything else'

Ever since its discovery as a *bona fide* human oncogene in the early 1980s, researchers have been trying to unravel the diversified molecular functions of *MYC*, with the ultimate aim of exploiting this knowledge for cancer therapy.

All three members of the vertebrate *MYC* family, *MYC*, *MYCN* and *MYCL1*, encode transcriptional regulators that integrate multiple cellular signals to influence proliferation and replication, growth, metabolism and differentiation, at multiple steps from development to tissue homeostasis. While it has become clear that *MYC* expression is deregulated and elevated by various mechanisms across many human cancer types, it has been difficult to pinpoint the exact features that distinguish the normal and essential properties of these transcription factors, from the ones unleashing their oncogenic potential [Dang, 2012].

### 1.2.1 Regulation and deregulation of *MYC*

Considering the wide variety of tumour-relevant biological processes influenced by *MYC* (see section 1.2.4), it is not surprising that stringent and sophisticated surveillance networks monitor every step of *MYC* biology. To restrict *MYC*'s actions to an exact developmental stage or tissue-specific needs, the available pool of active *MYC* proteins is controlled at all times, from RNA synthesis to protein stability [Liu and Levens, 2006; Farrell and Sears, 2014].

#### Coordination of *MYC* expression with cellular requirements

Under physiological circumstances, *MYC* is only transcribed in response to defined environmental signals. As a prototype immediate-early gene, preloaded polymerase II at the transcriptional start site ensures a rapid induction of *MYC* transcription upon stimulation with growth factors like PDGF and EGF [Bentley and Groudine, 1986]. In addition, a considerable number of transcription factors, acting downstream of almost all major signalling pathways, has been shown to bind and regulate the *MYC* promoter in specific spatio-temporal patterns. For example, TCF-4/LEF-1 directly activates *MYC* to regulate intestinal homeostasis and regeneration downstream of WNT signalling [He et al., 1998; Konsavage et al., 2012]. Furthermore, a transcriptional activation complex of CSL and ICN, the intracellular domain of NOTCH1, can bind to responsive elements in the promoter and activate *MYC* during self-renewal of hematopoietic stem cells [Sato et al., 2004; Weng et al., 2006].

It is likely, however, that in most cases signals from a variety of upstream inputs are integrated through the widely distributed regulatory elements present at the genomic locus on chromosome 8q24 [Liu and Levens, 2006].

Following transcription, a response element in the 3' UTR controls eIF4E-dependent nuclear export of the *MYC* mRNA [Culjkovic et al., 2006]. Additionally, the mRNA is rapidly degraded after translational pausing through a so called coding region instability determinant (CRD), whereas translation itself can be regulated in response to PI3K/AKT/mTORC1 signalling [Lemm and Ross, 2002; Wall et al., 2008].

On protein level, posttranslational modifications like acetylation and phosphorylation have been shown to influence *MYC*'s transcriptional activity [Vervoorts et al., 2003; Wang et al., 2011].

Finally, *MYC* levels are tightly regulated by the ubiquitin proteasome system. Most prominently, stability is controlled by an N-terminal phosphodegron that is located in a conserved region surrounding threonine 58 and serine 62, known as *MYC* box I. After sequential phosphorylation events, *MYC* is recognised by the F-box protein FBW7, the substrate-recognition subunit of the SCF E3 ubiquitin ligase, and subsequently degraded by the 26S proteasome [Welcker et al., 2004; Yada et al., 2004]. Other E3 ligases, like SCF<sup>Skp2</sup> or HUWE1, do not only control *MYC* turnover but also directly affect its biological activity [Kim et al., 2003; Adhikary et al., 2005; Peter et al., 2014].

### **Failure of surveillance mechanisms on the road to transformation**

Abnormal *MYC* expression contributes to the pathogenesis of most types of human tumours [Vita and Henriksson, 2006; Gabay et al., 2014]. Depending on the type of tumour, chromosomal aberrations involving the *MYC* locus are frequently found and range from translocations in haematological malignancies (e.g. 100% of Burkitt's lymphoma), to amplifications in solid tumours (e.g. up to 48% of breast cancer cases). In up to 70% of human cancers, however, inappropriate expression of *MYC* is observed without any noticeable change to the genomic sequence and is most commonly achieved by alterations in the various upstream signalling pathways that usually control its fate (see Fig. 1.5 for examples).

Several of the most prominent proto-oncogenic pathways, like the Ras/MAPK and PI3K signalling cascades that are frequently mutated in a range of human tumours, are upstream of *MYC*, directly influencing its transcription, stability and activity in response to growth factor signalling [Pylayeva-Gupta et al., 2011; Samuels et al., 2004; Sears et al., 1999; Zhu et al., 2008]. In other cases, *MYC* is deregulated by alterations that are specifically found in only certain tumour types. In colorectal cancer for example, TCF-driven accumulation of *MYC* is the critical downstream event after loss of the tumour suppressor APC [Sansom et al., 2007]. Furthermore, aberrant *MYC* gene expression has also been described as an essential downstream mediator of the NOTCH1 proto-oncogene during the pathogenesis of human T-ALL [Palomero et al., 2006].

### **1.2.2 Chromatin binding of *MYC***

Cell-type-specific gene expression patterns in multicellular organisms are maintained by the sequence-specific binding of transcriptional regulators to their respective target sites in the genome.

*MYC* proteins belong to a conserved class of dimeric transcription factors with a basic helix-loop-helix (bHLH) motif [Murre et al., 1989; Blackwell et al., 1990]. As the name suggests,

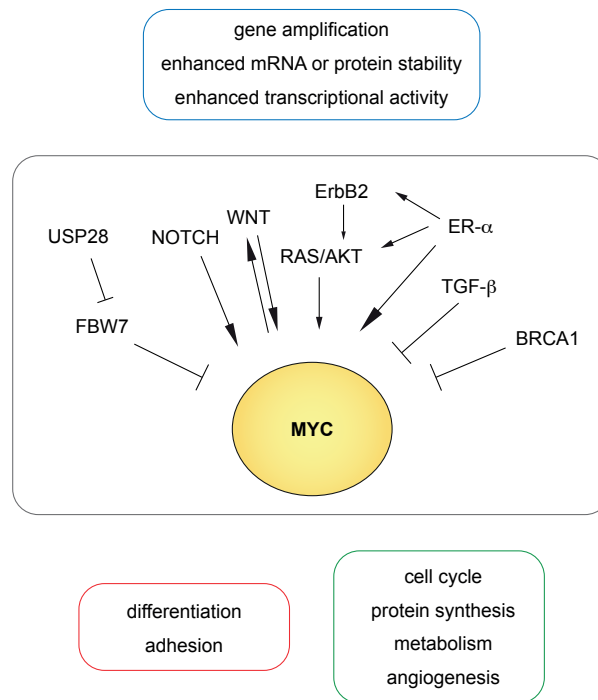


**Figure 1.5: MYC: a key signalling node in cancer**

The tight control mechanisms that usually confine MYC activity to meet exact cellular requirements are frequently impaired in cancer cells. Apart from gene amplifications, alterations in upstream signalling pathways influence MYC on RNA as well as protein levels and can also affect its transcriptional activity. Several proteins and upstream pathways with impact on MYC in human tumours are shown (grey box). The variety of cellular processes affected (red box: repressed; green box: activated), illustrates the far-ranging consequences of deregulated MYC for cells which can eventually lead to transformation and tumour development. Adapted from Hynes and Staelzle [2009].

all members of this family share two functionally distinct domains: A basic region, that is responsible for DNA binding at a consensus hexanucleotide sequence called Enhancer-box (E-box); and the helix-loop-helix domain, that mediates dimerisation with other family members and therefore indirectly determines the relative binding affinity of each functional dimer [Jones, 2004]. The bHLH motif is located in the C-terminal part of all MYC proteins, followed by a so-called leucine-zipper. This additional dimerisation domain is a feature that is only shared among a subgroup of bHLH transcription factors.

The obligate dimerisation partner of MYC proteins is the small bHLHZ protein MAX, and the resulting stable heterodimers make base-specific contact with E-box motifs located within the major groove of DNA (Fig. 1.6 and Blackwell et al. [1990]; Blackwood and Eisenman [1991]; Nair and Burley [2003]). In addition to the palindromic canonical sequence 5'-CACGTG-3', several so-called non-canonical E-box variants are also bound by MYC/MAX heterodimers, e.g. 5'CATGCG-3' and 5'CAACGTG-3' [Blackwell et al., 1993; Haggerty et al., 2003].

Interestingly, recent work has challenged the view that genomic occupancy of MYC/MAX heterodimers solely relies on sequence recognition via E-box binding [Guo et al., 2014]. Instead, binding in promoter regions significantly correlates with the presences of RNA polymerase II, suggesting that MYC might be recruited to active promoters via indirect protein-protein interactions.

Indeed, it has already been demonstrated that recruitment of MYC/MAX dimers to alternative binding sites can be mediated through binding to other transcription factors such as MIZ1, SP1/SP3 and SMAD proteins [Staller et al., 2001; Gartel et al., 2001; Feng et al., 2002].

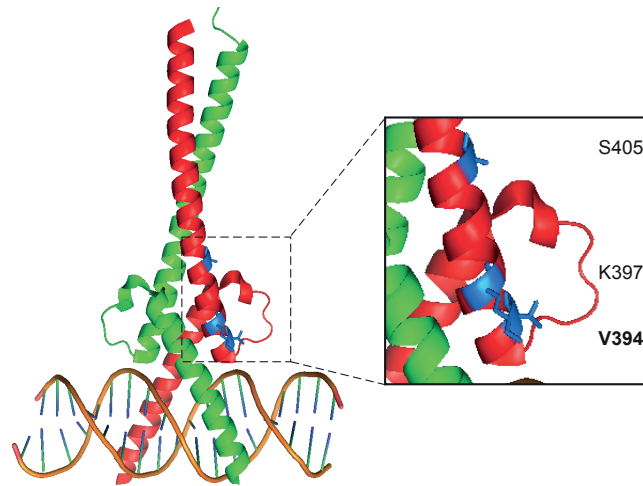


**Figure 1.6: Structure of the MYC/MAX heterodimer**

Crystal structure of the C-terminal DNA binding and dimerization domain of MYC (red) and MAX (green) bound to DNA. The magnified view on the right indicates certain residues within the Myc protein (blue) that disrupt or weaken the interaction with MIZ1 if mutated (see section 1.2.3 for details). Adapted from Wiese et al. [2013].

These findings also match studies showing that MYC preferentially binds to regions of open chromatin as well as promoters pre-loaded with basal transcription machinery, and that E-boxes are only present in a fraction of these binding sites [Guccione et al., 2006; Zeller et al., 2006]. Sequence-specificity seems to become even less important, when MYC is overexpressed [Fernandez et al., 2003].

With the development of high-throughput ChIP-sequencing methods, occupancy of MYC proteins could finally be analysed on a genome-wide level. Studies performed in different cell types and at different expression levels confirmed, that MYC/MAX dimers bind genomic sites marked by H3K4 methylation as well as H3K27 acetylation [Lin et al., 2012a; Nie et al., 2012; Sabò et al., 2014; Walz et al., 2014]. The majority of binding sites is located within promoter-proximal regions [Zeller et al., 2006; Walz et al., 2014]. Moreover, with higher expression levels, the amount of binding sites increases until almost all accessible genomic regions are occupied. This "invasion" happens at both promoters as well as distal elements classified as enhancers [Lin et al., 2012a; Sabò et al., 2014].

However, the steady state binding pattern of MYC does not correlate with regulation of all of its potential 'target genes'. While recent studies indicate that the change in occupancy on a given promoter predicts the magnitude of the transcriptional response, the net effect of MYC on target genes is likely to be further modulated by cell type- and context-specific interactions with other factors [Levens, 2003; Walz et al., 2014].

### 1.2.3 Transcriptional regulation by MYC

Although some aspects of MYC biology seem to be independent from its transcriptional activity and/or its interaction with MAX, most of the described functions have been attributed to the regulation of specific target genes [Cole and Cowling, 2008; Steiger et al., 2008; Eilers and Eisenman, 2008]. First described as a weak transcriptional activator of only a few genes, the picture

of MYC-dependent transcriptional regulation has become increasingly more complex in the last years [Wolf et al., 2015].

### Activation

Typically, transcriptional activators bind to their respective consensus motif in the genome, followed by the recruitment of co-activators as well as chromatin remodelling complexes. In that way, the chromatin structure becomes accessible for components of the general transcription machinery. Although an 'open' chromatin structure seems to precede DNA recognition and binding of MYC/MAX, the dimer mediates additional modifications and remodelling at target sites that are consistent with a role as transcriptional activator.

In general, MYC recruits several universal chromatin modifying proteins and causes hyperacetylation (Fig. 1.7). For example, MYC binds the adaptor protein TRRAP which provides a binding scaffold for two different histone acetyltransferases: GCN5 and TIP60. GCN5 is a part of the conserved STAGA co-activator complex and responsible for acetylation of several lysines on histone H3 (K9/K14/K18) [McMahon et al., 2000; Liu et al., 2003; Knoepfler et al., 2006]. Furthermore, acetylation of histone H4 on lysine 5, 8 and 12 (K5/K8/K12) is mediated via a different complex containing TIP60 as well as the ATPase/helicases TIP48/TIP49, and the SWI/SNF-related chromatin remodelling protein p400 [Frank et al., 2003; Martinato et al., 2008]. Additionally, the acetylases CBP and p300, and the SWI/SNF complex have been identified as positive cofactors for MYC-mediated transcriptional activation [Cheng et al., 1999; Vervoorts et al., 2003].

RNA polymerase II (Pol II) dependent transcriptional activation of eukaryotic genes is a multi-step process that includes the formation of a pre-initiation complex, initiation, promoter clearance, transcriptional elongation and subsequent termination [Weake and Workman, 2010]. Through recruitment of TFIID and P-TEFb, which phosphorylate the carboxy-terminal domain (CTD) of Pol II, MYC plays a significant role in promoter clearance and stimulation of

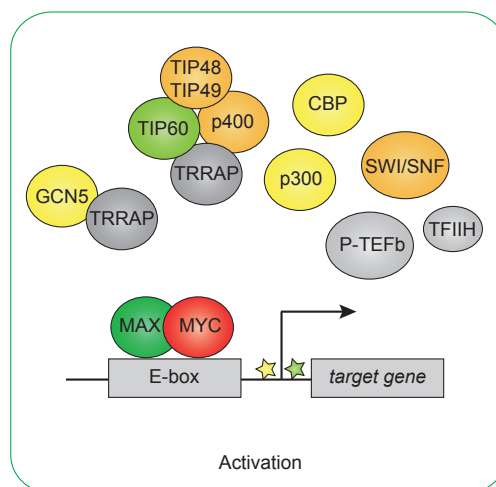


**Figure 1.7: Schematic model of MYC-mediated transcriptional activation**

MYC/MAX dimers bind E-box sequences in the vicinity of target gene promoters. Interaction with a multitude of regulatory cofactors results in chromatin remodelling, histone H3/H4 acetylation (yellow/green stars) and target gene activation. MYC can also stimulate pause release by regulating the activity of RNA polymerase II through recruitment of P-TEFb (not shown).

transcriptional elongation [Eberhardy and Farnham, 2001, 2002; Bouchard et al., 2004; Rahl et al., 2010]. These data are consistent with the finding that Pol II and additional components of the general transcription machinery can be present at promoters prior to MYC binding [Guccione et al., 2006; Lin et al., 2012a; Nie et al., 2012]. However, changes in gene expression after MYC activation do also correlate with the recruitment of total Pol II, suggesting that, in addition to its role in elongation, MYC can regulate transcriptional initiation [Walz et al., 2014].

Apart from stimulating transcription of protein-coding genes transcribed by RNA polymerase II, MYC has also been shown to substantially regulate RNA polymerases I and III [Gomez-Roman et al., 2003; Arabi et al., 2005]. In fact, ribosome biogenesis and RNA processing genes are part of a core signature of MYC-responsive genes in all mammals [Ji et al., 2011].

### **Transcriptional amplification**

With the aim of identifying the target genes responsible for the oncogenic actions of MYC, a huge number of gene expression data sets has been generated following MYC manipulation in many different cellular systems [Schuhmacher et al., 2001; Schlosser et al., 2005; Dang et al., 2006; Kim et al., 2006]. Interestingly, with the exception of ribosomal, metabolic and protein synthesis genes, these datasets are largely non-overlapping, suggesting that most of the genes regulated by MYC are cell-type specific [Rahl and Young, 2014].

In 2003, a role for MYC as a general regulator of gene transcription was first proposed in Burkitt's lymphoma cells [Li et al., 2003]. Subsequently, based on the observation that the primary role of MYC in embryonic stem cells seems to be a genome-wide stimulation of transcriptional pause release, two studies from the Young and Levens laboratories proposed an interesting new model: Instead of regulating specific sets of target genes, the predominant function of MYC appears to be the transcriptional amplification of all genes that are already actively transcribed in a given cell [Rahl et al., 2010; Lin et al., 2012a; Nie et al., 2012]. The observed effect was independent of the MYC levels investigated (physiological versus oncogenic levels).

While this transcriptional amplification, or 'nonlinear amplifier' model is intriguing and can also account for the apparent variation in 'MYC target gene' definition between cell types, it cannot yet explain all aspects of MYC biology. For example, it does not explain, why some biological processes are usually enhanced (e.g. proliferation) while others (e.g. adhesion and differentiation) are always attenuated by MYC (see section 1.2.4). More importantly, an inherent consequence of the model is that the existence of direct MYC-dependent repression is challenged [Lovén et al., 2012].

### **Repression**

The mechanisms of MYC-mediated gene repression are certainly less well understood than its function as transcriptional activator. However, analyses of MYC-dependent gene expression changes in different cellular contexts provide substantial experimental evidence for a model in which MYC can be recruited to target gene promoters for both induction and repression of selective target genes [Lüscher and Vervoorts, 2012; Sabò et al., 2014; Walz et al., 2014].

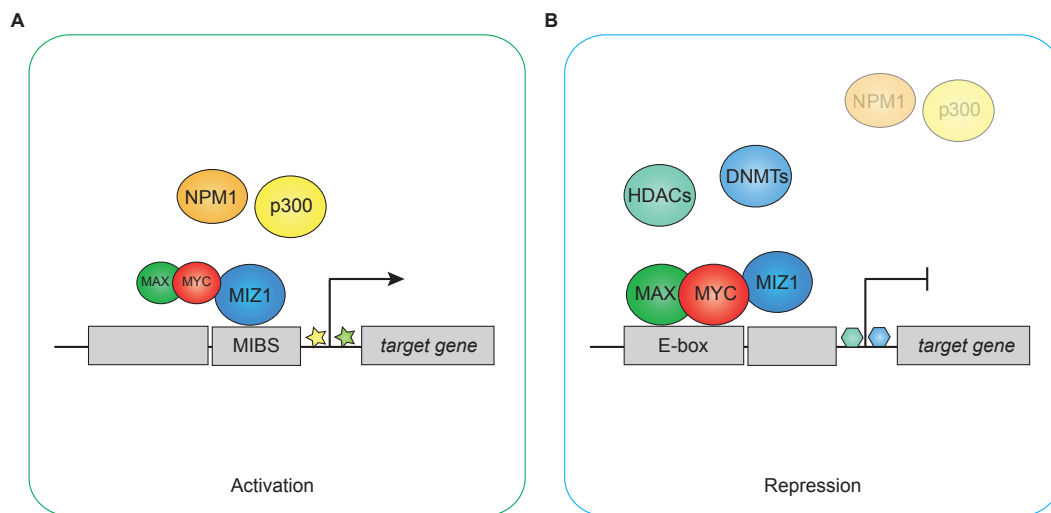


**Figure 1.8: Schematic models of MIZ1-mediated transcriptional activation and repression**

- A Target genes that are activated by MIZ1 are characterised by the presence of MIBS (MIZ1-binding sequences) close to their transcriptional start site. NPM1 and p300 function as positive regulatory co-activators for MIZ1. A fraction of MYC/MAX complexes can be recruited via indirect protein-protein interaction without affecting the transcriptional response.
- B Formation of a MYC/MIZ1 complex on E-box containing genes is correlated with repression of target genes. Mechanisms include displacement of co-activators as well as recruitment of DNA-methyltransferases (DNMTs) and histone deacetylases (HDACs).

From a historical perspective, the first evidence of MYC-induced repression was a negative feedback loop involving the *MYC* gene itself [Grignani et al., 1990]. In the case of the *Drosophila* ortholog *dmyc*, autorepression as well as repression of a significant amount of target genes is dependent on repressive Polycomb group proteins [Goodliffe et al., 2005]. Similarly, MYC may act via the EZH2 histone methyltransferase to promote H3K27 repressive chromatin modifications on its own promoter and other genomic targets in mammalian cells [Kaur and Cole, 2013]. Mechanistically, repression by MYC is often correlated with the recruitment of HDAC (histone deacetylase) containing co-repressor complexes [Satou et al., 2001; Kurland and Tansey, 2008]. For example, MYC-induced repression of differentiation in iPSCs (induced pluripotent stem cells) has been suggested to involve the HDAC1 containing NURD repressive complex [Smith et al., 2010, 2011].

Furthermore, MYC can bind directly to the promoters of a broad range of miRNAs and repress their expression [Chang et al., 2008].

Most prominently, however, MYC-induced repression is the result of an antagonising effect on other transcription factors, such as SP1/SP3 and MIZ1 [Gartel et al., 2001; Staller et al., 2001].

### MIZ1-dependent transcription

In search of cofactors that could mediate repression of MYC target genes, the BTB/POZ-domain containing zinc finger protein MIZ1 was identified in a yeast two-hybrid screen [Peukert et al., 1997]. Point mutagenesis studies suggested that both proteins interact via the helix-loop-helix domain of MYC and are able to bind DNA adjacent to each other (Fig. 1.6 and Herold et al. [2002]).

In primary cells, MIZ1 binds an extended non-palindromic consensus sequence close to the tran-



scriptional start site of target promoters (Fig. 1.8 A and Wolf et al. [2013]). If only low levels of MYC are present, MIZ1 acts as a strong transcriptional activator and regulates target genes involved in cell cycle progression, cell adhesion and autophagy [Staller et al., 2001; Gebhardt et al., 2006; Wolf et al., 2013].

Association with MYC displaces the co-activators p300 and nucleophosmin (NPM1) from MIZ1 and leads to the formation of a repressive complex [Staller et al., 2001; Wanzel et al., 2008]. Point mutants of MYC that disrupt the interaction with MIZ1, like MYC V394D (Fig. 1.6), are not able to repress transcription of cell cycle inhibitors anymore [Herold et al., 2002; van Riggelen et al., 2010].

At least for a subset of shared MYC/MIZ1 target genes, repression might involve DNA methylation [Licchesi et al., 2010]. For example, recruitment of the DNA-methyltransferase DNMT3A contributes to repression of the p21Cip1 promoter (*CDKN1A*) by the MYC/MIZ1 complex [Brenner et al., 2005].

As demonstrated for the C/EBP $\delta$  promoter, repression of genes after association of MYC with MIZ1 can also occur although MIZ1 alone does not influence expression of that particular target gene [Si et al., 2010].

Notably, MYC/MIZ1 can also form heterotrimeric complexes with additional transcription factors such as the zinc finger proteins Gfi-1 and SP1. While Gfi-1 collaborates with MYC to antagonise TGF $\beta$  signalling via repression of *cdkn2b* (encoding p15Ink4b), a repressive complex of SP1/MIZ1 and N-MYC forms to regulate neurotrophin receptor genes in neuroblastoma cells [Basu et al., 2009; Iraci et al., 2011].

Recent genome-wide surveys of MYC and MIZ1 occupancy in human and murine cancer cells revealed that binding of the MYC/MIZ1 complex might not be limited to the small number of previously described target genes. Instead, with high levels of MYC protein present, thousands of promoters are cooperatively bound by MYC/MIZ1 and MAX, suggesting that repressive MYC/MIZ complexes are present as a minor fraction on most MYC regulated genes. Indeed, the ratio of MYC to MIZ1 proteins on a given promoter seems to directly affect the transcriptional output (Fig. 1.8 B; Walz et al. [2014]).

These findings could be of considerable significance for the development of cancer cell-specific inhibitors of MYC function. Especially the HUWE1 ubiquitin ligase seems an attractive therapeutic opportunity as it is required to degrade MIZ1 and thereby prevent the repression of MYC targets genes specifically in cancer cells [Peter et al., 2014].

#### 1.2.4 Molecular functions of MYC

Despite considerable divergences between different studies, analyses of MYC-associated gene signatures reveal at least one consistent set of targets: Genes involved in ribosome biogenesis, RNA processing and biomass accumulation [Ji et al., 2011]. Taking studies from *Drosophila* into account, the most conserved role for MYC seems to revolve around regulation of cell growth, proliferation and differentiation [Gallant, 2013].

Deletion of *Myc* is embryonically lethal between day 9.5 and 10.5 of gestation, mainly as a result of placental insufficiency [Davis et al., 1993; Dubois et al., 2008]. An epiblast-specific knockout further revealed that *Myc* is essential for survival of erythroblasts and hematopoietic stem and progenitor cells [Dubois et al., 2008].

MYC is also required for adult tissue homeostasis in different organs. Knockout of *Myc* in the

murine epidermis for example, leads to loss of the proliferative compartment and premature differentiation. In addition, cell size and growth of keratinocytes are severely impaired [Zanet et al., 2005].

Surprisingly, deregulated expression of MYC in epidermal stem cells leads to loss of adhesive interactions with the stem cell niche and promotes differentiation, suggesting that the consequences of elevated MYC levels are context dependent and influenced by the differentiation status of that particular cell type [Waikel et al., 2001; Frye et al., 2003].

Despite its complex and diverse nature, several fundamental processes are consistently altered during tumorigenesis [Hanahan and Weinberg, 2011]. While some open questions regarding mechanistic details of transcriptional regulation and the definition of "MYC targets" remain, the tumorigenic potential of *MYC* oncogenes is unquestionable. It seems that it is also intimately connected to the regulation, activation and repression, of specific genes, as most of them can be associated with one of the hallmarks of cancer (Fig. 1.9 and Dang et al. [2006]).

An enhanced metabolic capacity is essential for cancer cells to grow and proliferate and MYC can activate multiple genes involved in energy metabolism, including key genes of glycolysis and glutaminolysis [Osthus et al., 2000; Gao et al., 2009]. Target genes like *E2F2* and *CCND2* enable MYC to sustain proliferation of tumour cells even in the absence of appropriate upstream signals [Sears et al., 1997; Bouchard et al., 1999]. In line with this, blocking antimitogenic signals is one of the best characterised consequences of MYC-mediated repression and has been demonstrated for *CDKN1A* and *CDKN2B* *in vivo* [Oskarsson et al., 2006; van Riggelen et al., 2010]. Additionally, direct activation of the telomerase gene *TERT* as well as the RecQ helicase (*WRN*) has been shown to help tumour cells avoid replicative senescence [Wu et al., 1999; Grandori et al., 2003]. This is also connected to an increase in genomic instability which can be promoted either by induction of reactive oxygen species (ROS) and DNA damage via upregulation of *CYP2C9*, or by deregulating mitosis progression via *MAD2* and *BubR1* [Ray et al., 2006; Menssen et al., 2007].

The interaction between tumour cells and their microenvironment has become an additional focus of cancer research in recent years. On the one hand, suppression of critical signalling pathways (*Stat1*, *IFN1b*) by MYC can help tumour cells to evade an immune response [Schlee et al., 2007]. On the other hand, inflammation can also promote tumour development and several cytokines implicated in this process are targets of MYC [Soucek et al., 2007]. Finally, activation and repression of Interleukin-1 $\beta$  and thrombospondin, respectively, has been shown to promote angiogenesis in a mouse model of Myc-dependent beta-cell carcinogenesis [Shchors et al., 2006]. Collectively, it is not surprising that most tumours depend on elevated levels of MYC and MYC activation itself has been proposed to be a "Hallmark of Cancer" [Gabay et al., 2014].

### **MIZ1-dependent functions of MYC**

The murine *miz1* knockout is embryonically lethal at E7.5 [Adhikary et al., 2003]. Apart from one study describing Myc/Miz1-dependent suppression of *Hox* differentiation genes as critical for ES cell maintenance, there is not much evidence that the complex plays a role during normal development [Varlakhanova et al., 2011; Wiese et al., 2013].

Interestingly, MIZ1 seems to mediate several of MYC's oncogenic actions. For example, sup-

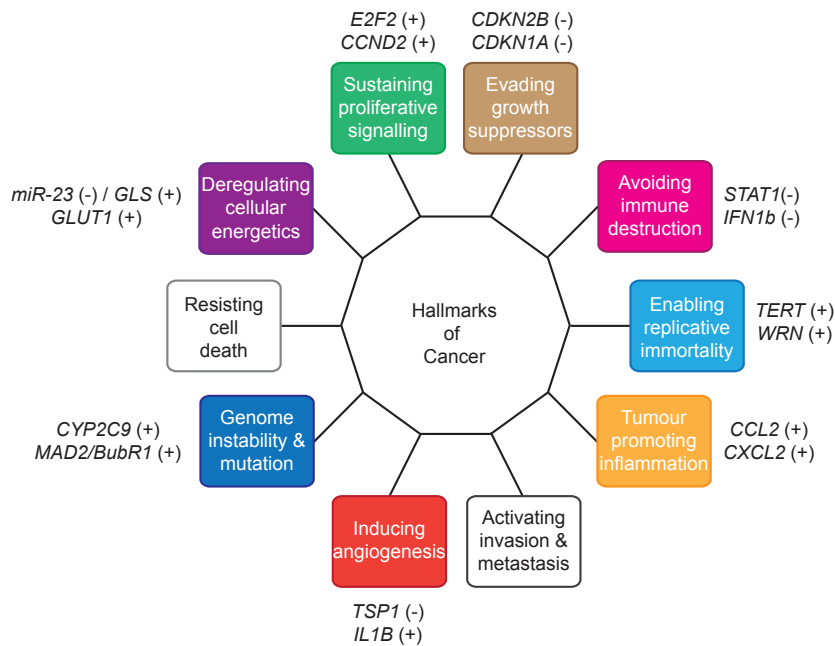


**Figure 1.9: MYC target genes contribute to the hallmarks of cancer**

Examples of MYC target genes (activated (+), repressed (-)) that are connected to the different biological capabilities underlying neoplastic transformation. Two of the hallmarks, namely resisting cell death and activating invasion and metastasis, seem to be inhibited by MYC instead of being promoted. They might be the target of tumour-suppressive fail-safe mechanisms against oncogenic MYC. Illustration of the 'Hallmarks of Cancer' is adapted from Hanahan and Weinberg [2011]. See text for further details and references to individual target genes.

pression of the cell cycle inhibitor p21Cip1 is a critical function of the complex in a murine skin carcinogenesis model [Hönnemann et al., 2012]. In a similar system, absence of the E3 ligase Huwe1 leads to an accumulation of Myc/Miz1 transcriptional complexes and repression of both p21 and p15 [Inoue et al., 2013]. During lymphomagenesis, MYC and MIZ1 associate to block TGF- $\beta$ -induced senescence via downregulation of *Cdkn2b* (p15) and *Cdkn1c* (p57Kip2) [van Riggelen et al., 2010].

However, several observations suggest that the MYC/MIZ1 interaction could also serve as a tumour-suppressive mechanism: Regulation of cell adhesion via repression of integrins  $\alpha6$  and  $\beta1$  is a key role of Myc/Miz1 in the skin [Gebhardt et al., 2006]. As described above, overexpression of MYC in the basal layer depletes epidermal stem cells, most likely due to repression of integrins and a disruption of stem cell - niche interactions [Waikel et al., 2001]. These data point towards a model, in which MIZ1-mediated repression provides an alarm signal to prevent oncogenic MYC accumulation in the stem cell compartment. Importantly, repression of other integrins by MYC has been connected to suppression of metastasis and invasion in breast cancer [Liu et al., 2012a]. In addition, elevated levels of MYC induce the tumour suppressor protein p14<sup>ARF</sup> which promotes assembly of the MYC/MIZ1 complex, leading to repression of cell adhesion genes and the induction of apoptosis [Herkert et al., 2010].

### MYC-induced apoptosis

Considering the central role of MYC in multiple tumour-relevant processes (Fig. 1.9), it is quite obvious why sophisticated networks have evolved to keep it in check.

MYC's ability to induce - or sensitise cells to - apoptosis was discovered almost 25 years ago [Askew et al., 1991; Evan et al., 1992]. Since then, it has become clear that apoptosis-suppressing

genetic or epigenetic events are required to enable the full transforming potential of *MYC* oncogenes.

*In vivo*, this cooperation has been elegantly demonstrated in different models of *MYC*-induced lymphomagenesis: On the one hand, spontaneous inactivation of the tumour suppressive ARF-MDM2-p53 pathway is frequently observed [Eischen et al., 1999]. On the other hand, overexpression of anti-apoptotic BCL-2-family members is sufficient to accelerate *Myc*-induced tumour development [Beverly and Varmus, 2009].

Although many mechanistic details about the molecular interactions between *MYC* and the players of death-regulatory networks have been proposed (Fig. 1.10), they appear to be highly cell-type and context dependent.

In most cases, however, induction of apoptosis seems to require association with *MAX* and therefore involve *MYC*-mediated transcriptional regulation [Amati et al., 1993].

In many tissues, apoptosis is also dependent on p53 stabilisation which is most prominently regulated by *MYC* via the ARF - MDM2 axis [Zindy et al., 1998]. *MYC* can also increase expression of p53, either directly, or indirectly via induction of DNA damage [Reisman et al.,

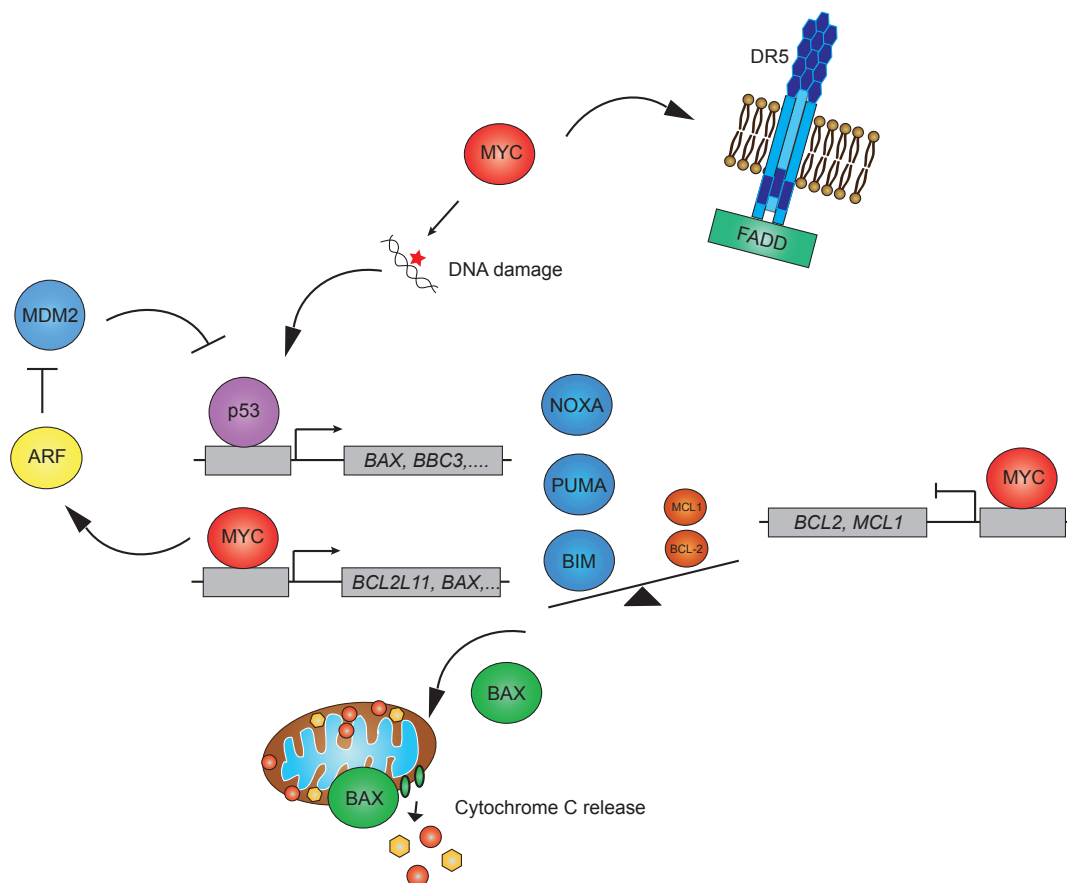


**Figure 1.10: Crosstalk between *MYC* and the apoptotic machinery**

*MYC* affects apoptotic pathways on multiple levels. Examples include induction of pro-apoptotic BH3-only proteins (e.g. *BCL2L11* encoding BIM) and repression of anti-apoptotic BCL-2-like family members, which shifts the balance between these opposing parties in favour of apoptosis. This is mainly executed by BAX due to formation of pores in the outer mitochondrial membrane and cytochrome c release. *MYC* can also lead to an accumulation of ARF, which antagonises MDM2 to promote stabilisation of p53 and subsequent pro-apoptotic target gene activation. In addition, stabilisation of p53 is a consequence of *MYC*-induced DNA damage. Furthermore, *MYC* has been shown to influence the extrinsic apoptotic pathway via upregulation of death receptors.

1993; Vafa et al., 2002]. In addition, due to MIZ1-mediated repression of p21, MYC shifts the p53 response from cell cycle arrest towards apoptosis [Seoane et al., 2002].

ARF transcription is induced by MYC indirectly via FOXO transcription factors [Bouchard et al., 2007]. In turn, ARF enhances the pro-apoptotic activity of MYC in a p53-independent way via repression of Skp2-mediated ubiquitination of the MYC N-terminus [Boone et al., 2011; Zhang et al., 2013].

The apoptotic threshold of a cell can be lowered by altering the balance between pro- and anti-apoptotic BCL-2 proteins (see section 1.1.3) and multiple family members are direct targets of MYC. For instance, the BH3-only protein BIM (encoded by the *BCL2L11* gene) is a mediator of MYC-induced apoptosis in lymphomas, breast cancer and multiple primary tissues [Hemann et al., 2005; Campone et al., 2011; Muthalagu et al., 2014]. Conversely, anti-apoptotic BCL-2 is repressed by MYC in a MIZ1-dependent manner [Patel and McMahon, 2007].

Permeabilisation of the outer mitochondrial membrane can be facilitated by MYC through direct regulation of BAX as well as activation of BAK [Mitchell et al., 2000; Nieminen et al., 2007].

MYC is also able to influence the extrinsic apoptotic pathway, for example by upregulating the expression of death receptor 5 (DR5) [Wang et al., 2004]. Finally, there is also evidence that cytochrome c release from the mitochondria can be triggered by MYC directly [Juin et al., 1999].

Interestingly, although in most cases apoptosis only occurs in response to deregulated and oncogenic levels of MYC, there might be a physiological basis for this phenomenon: MYC regulates apoptosis during involution of the mammary gland and is also essential for DNA-damage induced apoptosis *in vivo* [Sutherland et al., 2006; Phesse et al., 2014].

### 1.3 Objectives of this thesis

To maintain homeostasis, tissues need to balance two essential processes: proliferation and apoptosis. A shift of this balance towards sustained proliferation and concurrent impairment of apoptosis-inducing pathways are two of the biological capabilities that define cancer cells [Hanahan and Weinberg, 2011].

In primary cells, regulated *MYC* expression stimulates G1 to S phase progression. Deregulation or overexpression of *MYC*, however, often results in uncontrolled proliferation and can lead to cellular transformation. Hence, normal *MYC* function is essential during development and tissue homeostasis whereas its uncontrolled activities are a common feature of almost all human tumour types. Intriguingly, cells have evolved mechanisms that couple the occurrence of these latter, inappropriate signals to the induction of apoptosis, a phenomenon called "intrinsic tumour suppression" [Lowe et al., 2004].

Most likely, cells distinguish physiological levels of *MYC* from potentially oncogenic ones based on increased protein abundance and signalling output, but the precise molecular mechanisms have remained unclear.

Therefore, the main aim of this thesis was to characterise which molecular traits, quantitative or qualitative, enable cells to differentiate between varying levels of *MYC*.

Because *MYC* is an important oncogene in breast cancer and might regulate apoptosis in the mammary gland in a physiological context, we chose mammary epithelial cells as a model system to study *MYC* function at different expression levels.

Specifically, it should be determined, whether specific sets of target genes are responsible for mediating the apoptotic phenotype induced by *MYC*. Furthermore, the question whether high levels of *MYC* lead to the acquisition of new targets or merely an amplification of existing ones should be addressed. Finally, the impact of MIZ1-dependent repression should be investigated.

# Chapter 2

## Materials

### 2.1 Strains and cell lines

#### 2.1.1 *Escherichia coli* strains

|                               |   |
|-------------------------------|---|
| <b>DH5<math>\alpha</math></b> | F <sup>-</sup> $\Phi$ 80 <i>lacZ</i> $\Delta$ M15 $\Delta$ ( <i>lacZYA-argF</i> ) U169 <i>recA1 endA1 hsdR17</i> (r <sub>K</sub> <sup>-</sup> , m <sub>K</sub> <sup>+</sup> )<br><i>phoA supE44 <math>\lambda</math>-thi-1 gyrA96 relA1</i> |
| <b>XL1-Blue</b>               | <i>recA1 endA1 gyrA96 thi-1 hsdR17 supE44 relA1 lac</i> [F' <i>proAB lacI</i> <sup>q</sup> Z $\Delta$ M15 Tn10 (Tet <sup>r</sup> )]   |

#### 2.1.2 Mammalian cell lines

|                   |  |
|-------------------|--|
| <b>HMLE</b>       | Human breast epithelial cell line;<br>immortalised through introduction of SV40 small t and large T antigens and hTERT [Elenbaas et al., 2001];<br>kind gift from RA. Weinberg, Whitehead Institute; Cambridge, MA, USA          |
| <b>MCF10A</b>     | Human breast epithelial cell line;<br>derived from human fibrocystic mammary tissue and immortalised after extended cultivation [Soule et al., 1990];<br>kind gift from M. Bentires-Alj, Friedrich Miescher Institute; Basel, CH |
| <b>MDA-MB-231</b> | Human breast cancer cell line;<br>derived from metastatic pleural effusion (ATCC®);<br>kind gift from A. Schulze, Theodor-Boveri-Institute; Würzburg, DE   |
| <b>MDA-MB-468</b> | Human breast cancer cell line;<br>derived from metastatic pleural effusion (ATCC®);<br>kind gift from A. Schulze, Theodor-Boveri-Institute; Würzburg, DE   |
| <b>HeLa</b>       | Human cervix adenocarcinoma cell line (ATCC®);   |
| <b>HCT 116</b>    | Human colorectal carcinoma cell line (ATCC®);  |
| <b>HEK293T</b>    | Human embryonic kidney cell line;<br>carries temperature sensitive gene for SV40 T-antigen (ATCC®);  |

## 2.2 Cultivation media and supplements

### 2.2.1 Bacterial growth media and antibiotics

#### LB medium

|             |                |
|-------------|----------------|
| 1 % (w/v)   | Bacto Tryptone |
| 0.5 % (w/v) | yeast extract  |
| 1 % (w/v)   | NaCl           |

#### LB agar

|             |            |
|-------------|------------|
|             | LB Medium  |
| 1.2 % (w/v) | Bacto Agar |

#### Antibiotics

|           |            |  |
|-----------|------------|--|
| 100 µg/ml | Ampicillin | for selection of bacterial <i>amp<sup>r</sup></i> gene                 |
| 30 µg/ml  | Kanamycin  | for selection of bacterial <i>neo<sup>r</sup>/kan<sup>r</sup></i> gene |

### 2.2.2 Media and additives for mammalian cell culture

A pyruvate and pyridoxine supplemented high glucose version of Dulbecco's Modified Eagle's medium (DMEM) was used as a basal medium for HEK293T, HeLa and HCT 116 cells (Sigma-Aldrich). It was supplemented with 10 % FCS (fetal calf serum; Biochrom) and 10 ml/l Penicillin-Streptomycin solution (10.000 units penicillin, 10 mg/ml streptomycin, Sigma-Aldrich).

All other cell lines were grown in a 1:1 mixture of DMEM and Ham's F-12 (DMEM/F-12, Life Technologies).

#### Growth medium for MCF10A cells

|           |  |
|-----------|--|
|           | DMEM/F-12                                |
| 5 % (v/v) | Donor Horse Serum (Sigma-Aldrich)        |
| 10 ml/l   | Penicillin-Streptomycin                  |
| 20 ng/ml  | Epidermal Growth Factor (rHuEGF, Biomol) |
| 0.5 µg/ml | Hydrocortisone (Sigma-Aldrich)           |
| 10 µg/ml  | Insulin (Sigma-Aldrich)                  |
| 100 ng/ml | Cholera Toxin (Sigma-Aldrich)            |

The growth medium for culture of HMLE cells was only supplemented with EGF, hydrocortisone, insulin and Pen/Strep; breast cancer cell lines were grown in DMEM/F-12 supplemented with insulin, Pen/Strep and 10 % FCS.

Starvation medium for MCF10A cells only contained 0.05 % (v/v) horse serum, insulin and Pen/Strep.

For glutamine deprivation experiments, MCF10A cells were cultured in DMEM without glucose or glutamine, supplemented with 5 % dialysed FCS, 4.5 mg/ml glucose and the usual additional supplements. In the control condition, 2 mM glutamine were added.



**3D Assay medium**

|                      |   |
|----------------------|---|
|                      | DMEM/F-12   |
| 2 % (v/v)            | Donor Horse Serum (Sigma-Aldrich)                     |
| 10 ml/l              | Penicillin-Streptomycin                               |
| 0.5 µg/ml            | Hydrocortisone (Sigma-Aldrich)                        |
| 10 µg/ml             | Insulin (Sigma-Aldrich)                               |
| 100 ng/ml            | Cholera Toxin (Sigma-Aldrich)                         |
| fresh at time of use |   |
| 5 ng/ml              | Epidermal Growth Factor (rHuEGF, Biomol)              |
| 2 % (v/v)            | BD Matrigel <sup>TM</sup> (Growth Factor Reduced, BD) |

**Mammosphere medium**

|           |  |
|-----------|--|
|           | DMEM/F-12                                |
| 1 % (v/v) | Methylcellulose (Sigma-Aldrich)          |
| 2 % (v/v) | B27 (Invitrogen)                         |
| 10 ml/l   | Penicillin-Streptomycin                  |
| 20 ng/ml  | Epidermal Growth Factor (rHuEGF, Biomol) |
| 0.5 µg/ml | Hydrocortisone (Sigma-Aldrich)           |
| 5 µg/ml   | Insulin (Sigma-Aldrich)                  |
| 4 µg/ml   | Heparin (Sigma-Aldrich)                  |

**Antibiotics**

|             |                          |   |
|-------------|--------------------------|---|
| 0.5-2 µg/ml | Puromycin (InvivoGen)    | for selection of bacterial <i>pac<sup>r</sup></i> gene            |
| 85 µg/ml    | Hygromycin B (InvivoGen) | for selection of bacterial <i>hph<sup>r</sup></i> gene            |
| 200 µg/ml   | G 418 (Millipore)        | for selection of bacterial <i>neo<sup>r</sup>/kan<sup>r</sup></i> |

**Additional additives**

|               |  |
|---------------|--|
| 5-200 nM      | 4-Hydroxytamoxifen (4-OHT, Sigma-Aldrich), to induce ER-fusion proteins                |
| 0.025-1 µg/ml | Doxycycline (Dox, Sigma), to activate expression of tet-inducible shRNAs or transgenes |
| 100 µg/ml     | Cycloheximid (Chx, Sigma), to inhibit protein translation                              |
| 8 µg/ml       | Protamine sulfate (Sigma), to increase infection efficiency                            |
| 25 µM         | Chloroquine (Sigma), to increase transfection efficiency                               |
| 25 µM         | CCG-100602 (Biomol), to inhibit RhoA-dependent SRF signalling                          |

## 2.3 Oligonucleotides

DNA oligonucleotides (oligos) were purchased in lyophilised format from Sigma-Aldrich. Standard desalted oligos were ordered in an 0.025  $\mu\text{mol}$  scale and dissolved in *Aqua ad injectabilia* (100  $\mu\text{M}$ ).

In the following tables, *f* refers to a 5' or forward, *r* to a 3' or reverse primer.

### 2.3.1 Oligonucleotides for sequencing and cloning

| Oligo               | sequence (5' to 3')                            |
|---------------------|--|
| SFFV_seq <i>f</i>   | cttctgcttcccagctcta                            |
| pJet_seq <i>f</i>   | aacttggagcaggttccattc                          |
| pJet_seq <i>r</i>   | cctgatgaggtggttagcatag                         |
| IRES_seq <i>f</i>   | tggctctcctcaagcgatt                            |
| IRES_seq <i>r</i>   | cctcacattgccaaaagacg                           |
| pRRL_MCS <i>f</i>   | gatccaccggtattttaaatataaataacgcgtactagtgtcgacg |
| pRRL_MCS <i>r</i>   | gatccgtcgacactagtacgcgtttaataaatttaaataccggtg  |
| Sal_IRES <i>f</i>   | acgtgtcgacggatccgccctctccct                    |
| Puro_IRES <i>r</i>  | gtgggcttgtactcggatcatggttgtggccatattatcat      |
| IRES_Puro <i>f</i>  | atgataaatatggccacaacatgaccgagtacaagcccacg      |
| Puro_Sal <i>r</i>   | acgtgtcgactcaggcaccgggcttgcggg                 |
| Hygro_IRES <i>r</i> | ggctttccggatctatccatggttgtggccatattatcat       |
| IRES_Hygro <i>f</i> | atgataaatatggccacaacatggatagatccggaaagcc       |
| Hygro_Sal <i>r</i>  | acgtgtcgacctattcctttgccctcggac                 |
| V394D_mut <i>f</i>  | gaaaaggcccccaagtagatataccttaaaaaagcc           |
| V394D_mut <i>r</i>  | ggctttttaaggatatactaccttgggggccttttc           |
| Age_Myc <i>f</i>    | gctaccggtatttaaatatgccctcaacgttagctt           |
| Spe_Myc <i>r</i>    | gcgttaattaaactagtttacgcacaagagttccgta          |
| Spe_ER <i>r</i>     | gcgttaattaaactagttcagactgtggcagggaaac          |
| Bam_RhoA <i>f</i>   | gctggatccatggctgccatccgg                       |
| Eco_RhoA <i>r</i>   | gcggaattctcacaagacaaggca                       |

pRRL\_MCS oligos were used to introduce additional restriction sites (e.g. *AgeI*, *SpeI*) into the *BamHI* site of pRRL. This vector was further modified by inserting IRES-Puromycin or IRES-Hygromycin resistance cassettes into the *SalI* site. The fragments were created by annealing of overlapping PCR products. With the same technique, fusions of MYC VD with the modified estrogen binding domain were generated. MYC or MYC-ER proteins were amplified from existing expression vectors and cloned into the newly created *AgeI* - *SpeI* sites of pRRL. RhoA Q63L was cloned into the pLeGo lentiviral vector (*BamHI* - *EcoRI*).

Successful cloning was validated by sequencing with the listed primers ( LGC Genomics).

### 2.3.2 Primers for qRT-PCR

Primers for quantitative reverse transcriptase PCR were designed with the web-based ProbeFinder software from the Universal Probe Library (Roche). If possible, intron-spanning primers were selected to avoid co-amplification of genomic DNA contaminations.

| Primer               | sequence (5' to 3')                              |
|----------------------|--|
| <i>BAK1 f + r</i>    | atggtcaccttacctctgcaa + tcatagcgtcggttgatgctg    |
| <i>BAX f + r</i>     | caagaccagggtggttg + cactcccgccacaaagat           |
| <i>BBC3 f + r</i>    | gacctcaacgcacagtacga + gagattgtacaggacctcca      |
| <i>BCL2 f + r</i>    | cacgctgggagaacagggta + ggatgtacttcatcactatctccc  |
| <i>BCL2L1 f + r</i>  | aagagaacaggactgaggccc + gggctctccatctccgattca    |
| <i>BCL2L11 f + r</i> | ccccgcttttcatctttatg + gggctctgtctgtgtaa         |
| <i>CCND2 f + r</i>   | ggacatccaaccctacatgc + cgcacttctgttctcacag       |
| <i>CLIC4 f + r</i>   | gaattcaaggccagaggcta + cctccatactattttcatcaattca |
| <i>DKK1 f + r</i>    | caggcgtgcaaactgtct + aatgattttgatcagaagacacacata |
| <i>HMGA2 f + r</i>   | ccctctaaagcagctcaaaaga + ggtagtagattgtcccatttcc  |
| <i>ITGB3 f + r</i>   | ggcaagtgtgaatgtggcag + taaagggtcaggcatctggg      |
| <i>ITGB4 f + r</i>   | cacactgcccagggactac + cagcagtcaggcgagagtc        |
| <i>LAMB3 f + r</i>   | gaagatgtcagacgcacacg + catcagtgtcggggtctgt       |
| <i>MCL1 f + r</i>    | aagccaatgggcaggtct + gaactccacaaaccatcctt        |
| <i>MDM2 f + r</i>    | tttttgtgccacaacagacttt + atggtgaggagcaggcaaat    |
| <i>MYL9 f + r</i>    | ggacctgcacgacatgct + acccatggtggtgagcag          |
| <i>MYO1B f + r</i>   | aacaaacatggcctcattgg + cattaataggacctccacacca    |
| <i>ODC1 f + r</i>    | aaagttggttttgcggattg + cgaaggctcaggatcgta        |
| <i>PLAU f + r</i>    | ttgctcaccacaacgacatt + ggcaggcagatggtctgtat      |
| <i>PLEKHG2 f + r</i> | gtggcaccgtgtgtgaga + actgtgctcagggatgtgg         |
| <i>RPS14 f + r</i>   | ggcagaccgagatgaatcctca + caggctccagggtcttggctc   |
| <i>TP53 f + r</i>    | ccgcagtcagatcctagcg + aatcatccattgcttgggacg      |

### 2.3.3 Primers for qPCR after ChIP

| Primer               | sequence (5' to 3')                        |
|----------------------|--|
| <i>CONTROL f + r</i> | ttttctcacattgccctgt + tcaatgctgtaccaggcaaa |
| <i>FBXW8 f + r</i>   | gtgataggcagcagagctga + tgtacgcacgtggtgctc  |
| <i>GNL3 f + r</i>    | gtgacgctcgtcagtg + catattggtgtagaaggaagc   |
| <i>MRPS23 f + r</i>  | aaggatcgtgggctttc + cctgaacctggcaagtaacc   |
| <i>NCL f + r</i>     | ctaccaccctcatctgaatcc + ttgtctcgctgggaaagg |

Design of primers for qPCR after a ChIP was performed with ProbeFinder or PrimerQuest software. Only the genomic sequence of a given promoter that surrounded the binding site of the respective transcription factor was used. An intergenic "control" region on chromosome 11 was amplified to estimate unspecific binding.

### 2.3.4 Oligonucleotides for shRNA-mediated depletion

shRNA mediated knockdown of the indicated genes was achieved by cloning the following target sequences into pLKO (simple hairpin structures from a Pol III U6 promoter) or pInducer11 (pGIPZ-based, uses Pol II CMV promoter to express mir30-based hairpins). shRNAs were designed and cloned by Björn von Eyss.

| Target            | sequence (5' to 3')   |
|-------------------|-----------------------|
| <i>Luciferase</i> | catcacgtacgcggaataact |
| <i>BCL2L11</i>    | gaccgagaaggtagacaattg |
| <i>MAX</i>        | ccacatcaaagacagctttca |
| <i>TP53</i>       | ccacatcaaagacagctttca |

## 2.4 Plasmids

### 2.4.1 Empty vector backbones

- pMSCVpuro** Retroviral vector with a Puromycin resistance marker for LTR driven transgene expression (Clontech)
- pRRL** 3rd generation lentiviral expression vectors with either IRES-Hygromycin or IRES-Puromycin resistance markers or IRES-Tomato or IRES-GFP fluorescent selection markers. Transgene expression is driven by SFFV (spleen focus forming virus) or PGK (phosphoglycerate kinase) promoters. pRRL was generated in the Naldini lab (Addgene # 12252) Promoter cassettes were provided by Johannes Kühle and Axel Schambach (Hannover Medical School).
- pLeGO-iG2-Puro** 3rd generation lentiviral vector for expression of cDNA under control of SFFV promoter. Contains a T2A fusion of eGFP and Puromycin resistance marker (Fehse lab, Addgene # 27341)
- pLKO.1** 3rd generation lentiviral vector for shRNA expression driven by Pol III U6 promoter (Weinberg lab, Addgene # 8453)
- pInducer11** 3rd generation lentiviral vector for inducible, mir30-based shRNA expression. Contains EGFP and tRFP as selectable markers (Westbrook lab, Addgene # 44363)

### 2.4.2 Packaging systems

2nd generation lentiviral packaging vectors generated in the Trono lab were used to produce viral particles by transient transfection of HEK293T cells. Amphotropic VSV-G pseudotyped retroviral particles were generated the same way.

- psPAX2** Plasmid with CAG promoter for efficient expression of HIV-based packaging proteins (*gag*, *pol*, *rev*, *tat*, Addgene # 12260)
- MLV-GP** Packaging vector encoding Moloney murine leukemia virus *gag* and *pol* genes for production of retroviruses (Axel Schambach, Hannover Medical School)
- pMD2.G** Envelope plasmid (VSV-G, Addgene # 12259)

### 2.4.3 Expression vectors

Unless indicated otherwise, expression vectors listed below were generated during this thesis.

---

|                                      |   |
|--------------------------------------|---|
| <b>pMSCVpuro BCL-2</b>               | Retroviral expression of human BCL-2 cloned into <i>EcoRI</i> site (Judith Müller)  |
| <b>pRRL-PGK-IRES-Puro MYC WT</b>     | Lentiviral, PGK-driven expression of human MYC cloned into <i>AgeI</i> - <i>SpeI</i> site. IRES element allows simultaneous expression of Puromycin selection marker.   |
| <b>pRRL-PGK-IRES-Puro MYC VD</b>     | Lentiviral, PGK-driven expression of human MYC V394D cloned into <i>AgeI</i> - <i>SpeI</i> site. IRES element allows simultaneous expression of Puromycin selection marker  |
| <b>pRRL-SFFV-IRES-Puro MYC WT</b>    | Lentiviral, SFFV-driven expression of human MYC cloned into <i>AgeI</i> - <i>SpeI</i> site. IRES element allows simultaneous expression of Puromycin selection marker   |
| <b>pRRL-SFFV-IRES-Puro MYC VD</b>    | Lentiviral, SFFV-driven expression of human MYC V394D cloned into <i>AgeI</i> - <i>SpeI</i> site. IRES element allows simultaneous expression of Puromycin selection marker   |
| <b>pRRL-SFFV-IRES-Hygro MYC WT</b>   | Lentiviral, SFFV-driven expression of human MYC cloned into <i>AgeI</i> - <i>SpeI</i> site. IRES element allows simultaneous expression of Hygromycin selection marker  |
| <b>pRRL-SFFV-IRES-Hygro MYC VD</b>   | Lentiviral, SFFV-driven expression of human MYC V394D cloned into <i>AgeI</i> - <i>SpeI</i> site. IRES element allows simultaneous expression of Hygromycin selection marker  |
| <b>pRRL-SFFV-IRES-Tomato MYC WT</b>  | Lentiviral, SFFV-driven expression of human MYC cloned into <i>AgeI</i> - <i>SpeI</i> site. IRES element allows simultaneous expression of tdTomato red fluorescence marker   |
| <b>pRRL-SFFV-IRES-Tomato MYC VD</b>  | Lentiviral, SFFV-driven expression of human MYC V394D cloned into <i>AgeI</i> - <i>SpeI</i> site. IRES element allows simultaneous expression of tdTomato red selection marker  |
| <b>pRRL-SFFV-IRES-GFP MYC WT</b>     | Lentiviral, SFFV-driven expression of human MYC cloned into <i>AgeI</i> - <i>SpeI</i> site. IRES element allows simultaneous expression of eGFP green fluorescence marker   |
| <b>pRRL-SFFV-IRES-GFP MYC VD</b>     | Lentiviral, SFFV-driven expression of human MYC V394D cloned into <i>AgeI</i> - <i>SpeI</i> site. IRES element allows simultaneous expression of eGFP green selection marker  |
| <b>pRRL-SFFV-IRES-Hygro MYC-ER</b>   | Lentiviral, SFFV-driven expression of human MYC-ER cloned into <i>AgeI</i> - <i>SpeI</i> site. IRES element allows simultaneous expression of Hygromycin selection marker   |
| <b>pRRL-SFFV-IRES-Hygro MYCVD-ER</b> | Lentiviral, SFFV-driven expression of human MYCV394D-ER cloned into <i>AgeI</i> - <i>SpeI</i> site. IRES element allows simultaneous expression of Hygromycin selection marker  |
| <b>pRRL-tRFP-Puro</b>                | Lentiviral, CMV-driven expression of tRFP. IRES element allows simultaneous expression of Puromycin selection marker. Suitable for colour competition experiments. CMV-tRFP-IRES-Puro cassette was excised from an existing pGIPZ plasmid (generated by Joachim Nickel) |
| <b>pLeGO RhoA Q63L</b>               | Lentiviral vector mediating SFFV-driven expression of constitutive active RhoA, together with Puromycin and GFP selectable markers. RhoA was PCR-amplified from an existing plasmid (in pcDNA3 from Stefan Gaubatz)   |

---

|                                  |  |
|----------------------------------|--|
| <b>pLeGO MYC ΔBR</b>             | Lentiviral vector mediating SFFV-driven expression of human MYC missing the basic region (Björn von Eyss)  |
| <b>pLeGO MYC D</b>               | Lentiviral vector mediating SFFV-driven expression of MYC T358D/S373D/T400D, a triple aspartate-substitution mutant (Björn von Eyss)                               |
| <b>pInducer20<br/>ΔN-MAL-GFP</b> | Tet-inducible lentiviral vector with Neomycin selectable marker for expression of a constitutive active allele of MRTF-A with GFP-tag (gift from Dominique Brandt) |
| <b>pLKO.1 shLuci</b>             | Lentiviral vector with a target sequence against Luciferase as control (Björn von Eyss)  |
| <b>pLKO.1 shBIM</b>              | Lentiviral vector for shRNA-mediated depletion of human <i>BCL2L1</i> (Björn von Eyss)   |
| <b>pLKO.1 shp53</b>              | Lentiviral vector for shRNA-mediated depletion of human <i>TP53</i> (Björn von Eyss)   |
| <b>pInducer shMAX</b>            | Lentiviral vector for inducible shRNA-mediated depletion of human <i>MAX</i> (Björn von Eyss)  |

## 2.5 Antibodies

Purified IgG from rabbit or mouse serum (Sigma-Aldrich) was used as control for ChIP experiments.

Matching fluorophore-coupled isotype control antibodies for flow cytometry stainings were purchased from BD Biosciences.

Antibodies for all other applications are listed below.

### 2.5.1 Primary antibodies

| Antigen      | Clone     | Type         | Application | Dilution        | Manufacturer      |
|--------------|-----------|--------------|-------------|-----------------|-------------------|
| MYC          | Y69       | rabbit, mono | WB          | 1:1000          | Abcam             |
| MYC          | 9E10      | mouse, mono  | WB          | 1:500           | Hybridoma         |
| MIZ1         | 10E2      | mouse, mono  | WB, ChIP    | 1:500,<br>2 μg  | Hybridoma         |
| ERα          | HC20      | rabbit, poly | WB, ChIP    | 1:1000,<br>2 μg | Santa Cruz        |
| p14ARF       | NB200-111 | rabbit, poly | WB          | 1:1000          | Novus Biologicals |
| cleaved PARP | F-21-852  | mouse, mono  | WB          | 1:1000          | BD Biosciences    |
| p53          | DO-1      | mouse, mono  | WB          | 1:1000          | Santa Cruz        |
| p53 P-S15    | #9284     | rabbit, poly | WB          | 1:1000          | Cell Signaling    |
| BIM          | C34C5     | rabbit, mono | WB          | 1:1000          | Cell Signaling    |
| BCL-2        | C 21      | rabbit, poly | WB          | 1:1000          | Santa Cruz        |
| GFP          | B-2       | mouse, mono  | WB          | 1:1000          | Santa Cruz        |
| MAX          | C-17      | rabbit, poly | WB          | 1:1000          | Santa Cruz        |

| Antigen              | Clone                    | Type         | Application | Dilution | Manufacturer   |
|----------------------|--------------------------|--------------|-------------|----------|----------------|
| SRF                  | G20                      | rabbit, poly | WB          | 1:1000   | Santa Cruz     |
| AKT P-S473           | #9271                    | rabbit, poly | WB          | 1:1000   | Cell Signaling |
| AKT P-T308           | #9275                    | rabbit, poly | WB          | 1:1000   | Cell Signaling |
| AKT                  | #9272                    | rabbit, poly | WB          | 1:1000   | Cell Signaling |
| GSK3 $\beta$ P-S9    | #9336                    | rabbit, poly | WB          | 1:1000   | Cell Signaling |
| GSK3 $\beta$         | #27C10                   | rabbit, poly | WB          | 1:1000   | Cell Signaling |
| VINCULIN             | hVIN-1                   | mouse, mono  | WB          | 1:10.000 | Sigma-Aldrich  |
| $\alpha$ TUBULIN     | (E-19)-R                 | rabbit, poly | WB          | 1:5000   | Santa Cruz     |
| CDK2                 | M2                       | rabbit, poly | WB          | 1:10.000 | Santa Cruz     |
| HELLS                |                          | rabbit, poly | WB          | 1:2000   | Björn von Eyss |
| MEK1/2<br>P-S271/221 | #9121                    | rabbit, poly | WB          | 1:1000   | Cell Signaling |
| CD44                 | G44-26<br>(APC,<br>FITC) | mouse, mono  | FACS        | 1:5      | BD Biosciences |
| CD24                 | ML5<br>(FITC,<br>PE)     | mouse, mono  | FACS        | 1:5      | BD Biosciences |
| CD326 (Ep-<br>CAM)   | EBA-1<br>(APC)           | mouse, mono  | FACS        | 1:10     | BD Biosciences |

### 2.5.2 Secondary antibodies

Horseshradish peroxidase conjugated secondary antibodies for Western Blot were purchased from Santa Cruz and used at a dilution of 1:10.000.

anti-mouse        donkey anti-mouse IgG HRP  
anti-rabbit        donkey anti-rabbit IgG HRP

## 2.6 Chemicals

Unless indicated otherwise, all laboratory chemicals were purchased in appropriate quality and purity from the companies Thermo Fisher Scientific, Merck Millipore, GE Healthcare, Peqlab, Qiagen, Roche, Carl Roth or Sigma.

### 2.6.1 Markers and ladders

#### DNA molecular weight standards

100 bp DNA Ladder (NEB)  
1kb Plus DNA ladder (Invitrogen)

#### Protein molecular weight standard

PageRuler Prestained Protein Ladder (Thermo Scientific)

### 2.6.2 Enzymes

All restriction enzymes used for molecular cloning were purchased from Thermo Fisher Scientific (Fermentas) or New England Biolabs (NEB).

|   |                   |
|---|-------------------|
| DNase-free RNase A                          | Sigma             |
| RNase-free DNase I                          | QIAGEN            |
| Proteinase K                                | Roth              |
| M-MLV Reverse Transcriptase                 | Promega           |
| Phusion High Fidelity DNA Polymerase        | Thermo Scientific |
| T4 DNA ligase                               | Thermo Scientific |
| FastAP Thermosensitive Alkaline Phosphatase | Thermo Scientific |

### 2.6.3 Kits

|   |                   |
|---|-------------------|
| PureLink® HiPure Plasmid Maxiprep Kit                     | Life Technologies |
| PicoGreen® dsDNA Assay Kit                                | Life Technologies |
| ABsolute QPCR SYBR Green Mix                              | Thermo Scientific |
| GeneJET PCR Purification Kit                              | Thermo Scientific |
| GeneJET Gel Extraction Kit                                | Thermo Scientific |
| MinElute PCR Purification Kit                             | QIAGEN            |
| QIAquick PCR Purification Kit                             | QIAGEN            |
| QIAquick Gel Extraction Kit                               | QIAGEN            |
| RNeasy Mini Kit   | QIAGEN            |
| Experion RNA StdSense Analysis Kit T                      | Bio-Rad           |
| Experion RNA HighSense Analysis Kit                       | Bio-Rad           |
| Experion DNA 1K Analysis Kit                              | Bio-Rad           |
| TruSeq SR Cluster Kit v5-CS-GA                            | Illumina          |
| TrueSeq SBS Kit v5 - GA (36 cycle)                        | Illumina          |
| NEBNext Multiplex Oligos for Illumina                     | NEB               |
| NEBNext ChIP-Seq Library Prep Master Mix Set for Illumina | NEB               |
| Immobilon™ Western Chemiluminescent HRP Substrate         | Merck Millipore   |

## 2.7 Solutions and buffers

Unless indicated otherwise, buffers and solutions were prepared with ddH<sub>2</sub>O from a Milli-Q® Ultrapure Water Purification System (Merck Millipore).



**Annexin V binding buffer**

10 mM HEPES  
10 mM NaCl  
2.5 mM CaCl<sub>2</sub>

**Blocking buffer** for PVDF membranes

5 % powdered milk (Carl Roth) or BSA (Roth)  
in TBS-T

**Bradford solution**

8.5 % (v/v) orthophosphoric acid  
4.75 % (v/v) ethanol  
0.01 % (w/v) Coomassie Brilliant Blue G-250

**Crystal Violet solution**

0.1 % (w/v) Crystal Violet  
20 % (v/v) ethanol

**DNA loading buffer (6x)**

40 % (w/v) Sucrose  
0.2 % (w/v) Orange G  
10 mM EDTA

**Elution buffer** for ChIP

50 mM Tris, pH 8.0  
1 mM EDTA  
1 % SDS  
50 mM NaHCO<sub>3</sub>

**FACS buffer** for cell surface staining

10 % FCS  
in PBS

**FACS buffer** for PI-FACS-staining

36 µg/ml Propidium iodide (Sigma)  
24 µg/ml RNaseA  
in 38 mM sodium citrate or PBS

**Fractionation buffer A**

340 mM Sucrose  
10 mM HEPES  
10 mM KCl  
1.5 mM MgCl<sub>2</sub>  
10 % (w/v) Glycerol  
fresh at time of use:  
0.1 % (v/v) Triton X-100  
1 mM DTT  
1:100 Protease Inhibitor Cocktail (Sigma)  
1:1000 Phosphatase Inhibitor Cocktails 2+3 (Sigma)

**HBS (2x)** for transfection

280 mM NaCl  
1.5 mM Na<sub>2</sub>HPO<sub>4</sub>  
50 mM HEPES  
pH 7.4

**High Salt buffer** for ChIP

50 mM HEPES  
500 mM NaCl  
1 mM EDTA  
1 % Triton X-100  
0.1 % Na-deoxcholate  
0.1 % SDS  
fresh at time of use:  
0.5 mM PMSF

**LiCl buffer** for ChIP

250 mM LiCl  
20 mM Tris, pH 8.0  
1 mM EDTA  
0.5 % NP-40  
0.5 % Na-deoxycholate  
fresh at time of use:  
0.5 mM PMSF

**Mini prep resuspension buffer** (E1)

50 mM Tris, pH 8.0  
10 mM EDTA  
200 µg/ml RNaseA

**Mini prep lysis buffer** (E2)

200 mM NaOH  
1 % (w/v) SDS

**Mini prep neutralisation buffer** (E3)

3.1 M Potassium acetate, pH 5.5

**PEI solution** for transfection

1 mg/ml Polyethylenimine (MW 25.000, linear, Sigma-Aldrich)  
pH adjusted to 7.0 with HCl  
filtered through 0.22 µm membrane filters

**PBS**

137 mM NaCl  
2.7 mM KCl  
10.1 mM Na<sub>2</sub>HPO<sub>4</sub>  
1.76 mM KH<sub>2</sub>PO<sub>4</sub>

**RIPA lysis buffer**

150 mM NaCl  
50 mM Tris  
1 % (v/v) NP-40  
0.5 % (w/v) Na-deoxycholate  
0.1 % (w/v) SDS  
fresh at time of use:  
1:100 Protease Inhibitor Cocktail (Sigma)  
1:1000 Phosphatase Inhibitor Cocktails 2+3 (Sigma)

**SDS sample buffer** (3x, Laemmli)

187.5 mM Tris pH 6.8  
2 M  $\beta$ MerCaptoethanol  
30 % (v/v) glycerine  
6 % SDS  
0.03 % Bromphenol blue

**SDS running buffer** (Tris-Glycine)

25 mM Tris Base  
250 mM glycine  
0.1 % SDS

**Stripping buffer** for PVDF membranes (10x)

2 M glycine  
1 % SDS  
10 % Tween-20  
pH adjusted to 2.3

**Separating gel solution**

7.5-15 % (v/v) acrylamide/bis-acrylamide  
375 mM Tris-HCl pH 8.8  
0.1 % SDS  
0.1 % APS  
0.1 % TEMED

**Sonication buffer** for ChIP

50 mM HEPES  
140 mM NaCl  
1 mM EDTA  
1 % Triton X-100  
0.1 % Na-deoxycholate  
0.1 % SDS  
fresh at time of use:  
0.5 mM PMSF  
1:100 Protease Inhibitor Cocktail (Sigma)  
1:1000 Phosphatase Inhibitor Cocktails 2+3 (Sigma)

**Stacking gel solution**

4 % (v/v) acrylamide/bis-acrylamide  
125 mM Tris-HCl pH 6.8  
0.1 % SDS  
0.1 % APS  
0.1 % TEMED

**Swelling buffer** for ChIP

25 mM HEPES  
1.5 mM  $MgCl_2$   
10 mM KCl  
0.1 % NP-40  
fresh at time of use:  
1 mM DTT  
0.5 mM PMSF  
1:100 Protease Inhibitor Cocktail (Sigma)  
1:1000 Phosphatase Inhibitor Cocktails 2+3 (Sigma)

**TBS (20x)**

500 mM Tris base  
2.8 M NaCl  
adjusted to pH 7.4

**TBS-T**

25 mM Tris base  
140 mM NaCl  
2 % Tween-20

**TE**

10 mM Tris  
1 M EDTA

**TAE (50x)**

2 M Tris acetate  
1 M acetic acid  
50 mM EDTA

**Transfer buffer** for tank blot (10x)

250 mM Tris Base  
1.92 M glycine  
fresh at time of use (to 1x buffer):  
15 % (v/v) methanol

**Trypsin solution**

0.25 % Trypsin  
5 mM EDTA  
22.3 mM Tris pH 7.4  
125 mM NaCl

## 2.8 Consumables and equipment

All laboratory disposables as well as other plastic- and glassware products were purchased from Greiner Bio-One, Nunc, Sarstedt, Corning, Roth, VWR International, A.Hartenstein, Merck Millipore and Starlab.

|  |   |
|--|---|
| <b>Biosafety cabinet</b>                         | Herasafe KS Class II (Thermo Scientific)  |
| <b>Blotting apparatus</b>                        | PerfectBlue Tank-Elektroblotter Web S (Peqlab)  |
| <b>Cell counter</b>                              | CASY® Cell Counter Model DT (Innovatis/Roche)   |
| <b>Centrifuges</b>                               | Galaxy MiniStar (VWR International)<br>Centrifuges 5424 + 5430 R (Eppendorf)<br>Multifuge 1SR (Thermo Scientific)<br>Avanti J-26 XP (Beckman Coulter) |
| <b>CO<sub>2</sub> incubator</b> for cell culture | BBD 6220 (Thermo Scientific)  |
| <b>Digital imaging system</b>                    | LAS4000 mini (Fuji / GE Healthcare Life Sciences)   |
| <b>Electrophoresis chamber</b>                   | Mini-PROTEAN Tetra Cell (Bio-Rad)   |
| <b>Electrophoresis system</b>                    | Experion® Automated Electrophoresis Station,<br>Priming Station, Vortex Station II<br>(Bio-Rad)   |
| <b>Flow cytometer</b>                            | BD FACSCanto®II cell analyser (BD Biosciences)  |

---

|                                     |   |
|-------------------------------------|---|
| <b>Heating block</b>                | Single Block Dry Bath Heating System (Starlab)                          |
| <b>Heat sealer</b>                  | ALPS™ 50V Microplate Sealer (Thermo Scientific)                         |
| <b>Incubation shaker</b>            | Multitron Standard (Infors HT)  |
| <b>Microscope</b>                   | Axiovert 40 CFL (Carl Zeiss)  |
| <b>Orbital shaker</b>               | Universal Shaker SM 30 A (Edmund Bühler GmbH)                           |
| <b>PCR thermal cyclers</b>          | Mastercycler®pro S (Eppendorf)  |
| <b>Electrophoresis power supply</b> | PowerPack™ (Bio-Rad)<br>Consort EV265 (Isogen)                          |
| <b>qPCR system</b>                  | Mx3000P (Agilent Technologies)  |
| <b>Sequencing platform</b>          | Genome Analyzer IIx (Illumina)  |
| <b>Sonifier</b>                     | Digital Sonifier® S-250D<br>(Branson Ultrasonics Corporation)           |
| <b>Spectrophotometers</b>           | NanoDrop 1000 (Thermo Scientific)<br>Ultrospec 2100 pro (GE Healthcare) |
| <b>Thermoshaker</b>                 | ThermoMixer comfort (Eppendorf)   |
| <b>UV transilluminator</b>          | Maxi UV Fluorescent table (Peqlab)                                      |
| <b>Vortex mixer</b>                 | Vortex-Genie 2 (Scientific Industries)                                  |
| <b>Waterbath</b>                    | model WNB (Memmert)<br>ED-5M Heating Circulator (Julabo)                |

## 2.9 Software and web-based programs

|  |   |
|--|---|
| <b>Adobe Acrobat Pro, Illustrator, Photoshop</b> | Adobe Systems Inc.  |
| <b>ApE</b>                                       | A plasmid Editor, by M. Wayne Davis                                       |
| <b>AxioVision</b>                                | Microscopy software, Zeiss  |
| <b>BD FACSDiva 6.1.2</b>                         | Flow cytometry software, BD Biosciences                                   |
| <b>BEDTools</b>                                  | by Aaron R. Quinlan and Ira M. Hall                                       |
| <b>Bowtie</b>                                    | by Ben Langmead and Cole Trapnell   |
| <b>DAVID</b>                                     | <a href="http://david.abcc.ncifcrf.gov">http://david.abcc.ncifcrf.gov</a> |
| <b>GSEA</b>                                      | <a href="http://www.broadinstitute.org">www.broadinstitute.org</a>        |
| <b>Integrated Genome Browser</b>                 | <a href="http://bioviz.org">bioviz.org</a>                                |
| <b>JabRef v2.9.2</b>                             | open source bibliography reference manager                                |
| <b>Java TreeView</b>                             | by Alok Saldanha  |
| <b>LAS-3000</b>                                  | ImageReader software, FUJIFILM  |
| <b>Mac OS X</b>                                  | Apple Inc.  |
| <b>MACS</b>                                      | by Yong Zhang and Tao Liu   |
| <b>MEME-ChIP</b>                                 | by Philip Machanick and Timothy L. Bailey                                 |
| <b>Microsoft Office 2011</b>                     | Microsoft Corporation   |

|                                      |  |
|--------------------------------------|--|
| <b>Multi Gauge</b>                   | Image analysis software, FUJIFILM                                    |
| <b>MxPro</b>                         | qPCR Software, Agilent Technologies                                  |
| <b>R</b>                             | The R Foundation for Statistical Computing                           |
| <b>PrimerQuest® Design Tool</b>      | <a href="http://www.idtdna.com/SciTools">www.idtdna.com/SciTools</a> |
| <b>ProbeFinder</b>                   | Universal ProbeLibrary, Roche Diagnostics                            |
| <b>SAMtools</b>                      | by Heng Li   |
| <b>seqMINER</b>                      | by Tao Ye and Arnaud R. Krebs  |
| <b>TeXShop v3.18</b>                 | TeX previewer for Mac OS X, by Richard Koch                          |
| <b>UCSC Genome Browser Utilities</b> | <a href="http://genome.ucsc.edu">genome.ucsc.edu</a>                 |

# Chapter 3

## Methods

### 3.1 Cell biology methods

All cell culture work was performed in a biological safety cabinet. Cell lines were cultured in CO<sub>2</sub> incubators at 37 °C, 95 % humidity and 5 % CO<sub>2</sub>.

#### 3.1.1 Maintaining cultured mammalian cells

Adherent cell lines were cultured on sterile cell culture dishes using appropriate media. Growth medium was renewed every 2 to 3 days. For subculturing, growth medium was removed, the monolayer was rinsed with PBS and trypsin solution was added. Cells were incubated at 37 °C until they detached and subsequently, DMEM containing 10 % FCS was added to neutralize trypsin. The cell suspension was centrifuged for 5 min at 125 x *g*. Pelleted cells were resuspended in an appropriate volume of complete culture medium and aliquots of the suspension were added to new culture dishes to maintain a subcultivation ratio of 1:4 to 1:8. If applicable, cells were counted in a Neubauer chamber or an automated CASY cell counter.

#### Freezing and thawing cells

For cryopreservation of cells, subconfluent cultures were brought into suspension as described above and then resuspended in 500 µl of serum (FCS or Donor horse serum), supplemented with 5 % DMSO. Cell suspensions were transferred to cryogenic storage vials and placed into a –80 °C freezer inside a passive freezing container to assure a cooling rate of 1 °C/min. Frozen vials were transferred to a liquid nitrogen tank for longterm storage.

To thaw frozen cells, cryovials were placed into a 37 °C water bath and then transferred to a 15 ml centrifuge tube containing 10 ml of growth medium to dilute the DMSO. Cells were centrifuged for 5 min at 125 x *g*, resuspended in complete growth medium and seeded onto appropriate cell culture dishes. After cell attachment, monolayers were rinsed with PBS to remove residual debris and DMSO and fresh medium was added.

#### Synchronization of MCF10A cells by starvation

MCF10A cells can be synchronised in the G1 phase of the cell cycle by serum and growth factor deprivation. For this purpose, cells were plated on 10 cm dishes and cultured until approximately 60 % confluence was reached. Growth medium was removed from the dishes and monolayers were

rinsed twice with PBS to remove residual traces of the old medium. Then, cells were incubated with starvation medium containing only 0.05 % donor horse serum and 10  $\mu\text{g}/\text{ml}$  insulin for 24 h to arrest them in G1 phase. Cells were stimulated with complete growth medium and harvested at different time points to follow cell cycle re-entry kinetics.

### 3.1.2 3D cell culture

Three-dimensional culture of human mammary epithelial cells on reconstituted basement membrane leads to the formation of polarized, acinar-like structures with a central hollow lumen. This 3D-morphogenesis process recapitulates steps of mammary gland development occurring *in vivo* and is therefore useful to investigate cellular behaviour in a biologically more relevant context [Debnath and Brugge, 2005].

To monitor three-dimensional morphogenesis, MCF10A cells were cultured in Matrigel according to a published protocol [Debnath et al., 2003]. Briefly, 8-well chamber slides were pre-coated with 50  $\mu\text{l}$  of Matrigel. MCF10A cells were trypsinized, pelleted, resuspended in 3D Assay medium, counted and diluted to get a concentration of 2.500 cells/100  $\mu\text{l}$ . This suspension was then mixed with Assay medium containing 5 % Matrigel and 10 ng/ml EGF in a ratio of 1:1. 400  $\mu\text{l}$  containing 5.000 cells were plated per well. Fresh Assay medium containing 2.5 % Matrigel and 5 ng/ml EGF was added every 3 days and phase contrast images were taken on several days to document acinar structure formation.

### 3.1.3 Mammosphere culture

*In vitro* sphere-forming assays are used for the quantification of self-renewal and stem cell activity in different tissue types. Hence, the formation of mammospheres has been used to assess stem cell/progenitor activity and self-renewal in mammary tissue and breast cancer cell lines.

To generate primary mammospheres, MCF10A cells were detached as described above and the cell pellet was washed with PBS once, to remove residual traces of serum. Cells were resuspended in Mammosphere Assay medium, counted and then plated into ultra-low attachment 24-well plates at a density of  $1 \times 10^4$  cells per well. Fresh medium was added every 3 days and the number of spheres per  $10^3$  plated cells was counted 10 days after plating.

To assess self-renewal capability, primary mammospheres were harvested, digested with trypsin to generate single cells and then replated as above at a density of  $5 \times 10^3$  cells per well. Fresh medium was added every 3 days and secondary mammosphere formation per  $10^3$  plated cells was scored at day 10.

### 3.1.4 Production of amphotropic retroviruses

Stable delivery of DNA expression constructs into dividing mammalian cells can be achieved by using Moloney Murine Leukemia Virus (MMULV) - based retroviruses. Transfection of retroviral vector constructs into HEK293T-based producer lines containing retroviral gag/pol and envelope proteins will lead to production of viral supernatants.

To produce recombinant retroviral particles capable of transducing human cells, the second generation packaging cell line Phoenix Ampho was used ([www.stanford.edu/group/nolan](http://www.stanford.edu/group/nolan)). 24 h before transfection,  $4 \times 10^6$  Phoenix Ampho cells were plated per 10 cm dish.



The next day, either calcium phosphate mediated or polyethylenimine (PEI) based transfection protocols were used to transfect the cells.

### **Transfection using calcium phosphate**

Prior to calcium phosphate transfection, 8 ml fresh growth medium containing 25  $\mu\text{M}$  chloroquine were added to each dish. 25  $\mu\text{g}$  of retroviral vector construct DNA was mixed with 50  $\mu\text{l}$  of 2.5 M  $\text{CaCl}_2$  and filled up to a total volume of 500  $\mu\text{l}$  with sterile  $\text{H}_2\text{O}$ . Then, 500  $\mu\text{l}$  of 2 x HBS in a 15 ml centrifuge tube were placed on a vortex mixer and the DNA containing transfection mix was added dropwise. Immediately afterwards, the HBS/DNA solution was carefully spread onto the dishes. 12 to 16 h later, the medium was changed to 6 ml fresh growth medium.

### **Transfection using PEI**

In case of PEI based transfection, the old medium was replaced with transfection medium containing 2% FCS, 25  $\mu\text{M}$  chloroquine and no antibiotics. A mix of 25  $\mu\text{g}$  retroviral vector construct DNA and 500  $\mu\text{l}$  Opti-MEM medium was prepared in one tube. In a separate tube, 50  $\mu\text{l}$  PEI were added to 500  $\mu\text{l}$  Opti-MEM medium, maintaining a 2:1 ratio of PEI to total DNA. Both mixes were incubated for 5 min at room temperature (RT) before combining them in one tube and further 15 min incubation. The solution was added dropwise to the cells and incubated for 3 to 6 h after which the medium was changed to 6 ml fresh growth medium as well.

Viral particles in the supernatant were harvested twice, between 36 and 72 h after transfection by using a syringe and filtering them through a 0.45  $\mu\text{m}$  membrane filter. Supernatants were either used directly for transduction (see below) or snap-frozen in liquid nitrogen and stored at  $-80^\circ\text{C}$ .

### **3.1.5 Production of lentiviruses**

In contrast to retroviruses, lentiviral vectors can mediate more efficient delivery, integration and longer stable expression of transgenes in dividing as well as non-dividing cells.

To reduce the risk of helper virus production, lentiviral particles were generated by transiently co-expressing second generation packaging elements and self-inactivating (SIN) HIV-1-derived vectors in HEK293T cells.

The following components were mixed and then transfected according to the transfection protocols described for retrovirus production (3.1.4):

10  $\mu\text{g}$  lentiviral vector DNA  
10  $\mu\text{g}$  packaging system (psPAX2)  
2.5  $\mu\text{g}$  envelope plasmid (pMD2G)

Viral supernatants were harvested 2 - 3 times between 36 and 72 h after transfection by using a syringe and filtering them through a 0.45  $\mu\text{m}$  membrane filter. Supernatants were either used directly for transduction (see below) or aliquoted into cryotubes and stored at  $-80^\circ\text{C}$ . In case a higher virus titer was needed, lentiviral supernatants were concentrated in an ultracentrifuge.

### 3.1.6 Transduction of cells with viruses

To stably infect adherent cells with retro - or lentiviruses, cells were seeded on 10 cm dishes, reaching approximately 60 - 70% confluence upon transduction. If frozen, viral supernatants were thawed in a 37°C water bath.

For lentiviral transduction, the medium was replaced with 3 - 5 ml of fresh growth medium, supplemented with a final concentration of 8 µg/ml protamine sulfate to facilitate interaction between viral particles and target cells. Depending on the vector construct and desired multiplicity of infection (MOI), 100 µl to 2 ml of viral supernatant were used for transduction. The next day, viral supernatants were removed, cells were washed with PBS and then passaged onto new dishes to achieve the optimal density for selection with antibiotics 24 h later.

The protocol for retroviral transduction was equivalent to the method described above, except that, in any case, 3 ml of viral supernatant were combined with 2 ml of fresh medium and 8 µg/ml protamine sulfate, due to lower infection efficiencies.

### 3.1.7 Cumulative growth curve

To compare whether transduction with different vector constructs affected the proliferation rate of MCF10A cells,  $1.5 \times 10^5$  cells from 3 biological infections were plated in triplicates onto 6 cm dishes. After 3 days, cells were trypsinized and the total amount of cells per dish was counted.  $1.5 \times 10^5$  cells were replated from each condition and the described procedure was repeated three more times. Subsequently, the cumulative growth rate was calculated.

### 3.1.8 Transwell migration assay

The migratory behaviour of cultured cells can be investigated using a transwell migration assay, also known as Boyden chamber assay. Cells are seeded on a permeable membrane with a defined pore size and are allowed to migrate through this filter towards a specific stimulus, e.g. serum or a chemoattractant. To study migration of MCF10A cells in response to MYC overexpression, transduced cell pools were starved over night, trypsinized and then seeded in starvation medium at a density of  $1 \times 10^5$  per 24-well into 8 µm-pore size permeable cell culture inserts. Full medium was added to the bottom of the 24-well plates. After 20 h, cells that had not migrated were removed by wiping the upper side of the membrane with cotton swabs. Migrated cells at the bottom of the membrane were fixed in 1% formaldehyde and stained with crystal violet. For every condition, cells were plated into 2 separate transwell inserts and 6 random fields from each insert were counted under the microscope, using 20x magnification.

### 3.1.9 Flow cytometry

All flow cytometry measurements were performed on a BD FACSCanto II flow cytometer, using the appropriate combination of lasers and filters and FACSDIVA software version 6.1.2. At least  $2 \times 10^4$  events per sample were acquired.

### Cell surface antigen staining

To determine the expression of cell surface receptors like CD24, CD44 and CD326, cells were seeded into 6-well dishes in triplicates. Two days later, cells were washed with PBS and harvested

by trypsinization. Trypsin was inactivated by addition of ice-cold PBS with 10% FCS and the suspension was transferred into 15 ml centrifuge tubes. After centrifugation, cell pellets were resuspended in 100  $\mu$ l FCS - PBS containing fluorophore-coupled antibodies or respective isotope controls in the concentration suggested by the supplier. Antibody staining was performed for 30 to 45 min on ice at 4°C in the dark. Afterwards, cells were washed 3 times with ice-cold FCS - PBS and immediately acquired on the flow cytometer.

### **Propidium iodide staining**

The cell cycle distribution of asynchronous growing cell pools can be measured by staining the DNA with intercalating dyes like propidium iodide (PI). Cells were plated onto 10 cm dishes. Before the monolayer reached confluence, supernatants were collected into 15 ml centrifuge tubes to harvest floating dead cells. Adherent cells were washed with PBS, which was collected as well. Cells were detached with trypsin, resuspended in DMEM with 10% FCS and pooled with their respective supernatants. After centrifugation, pellets were washed once with PBS and then resuspended in 1 ml PBS. 4 ml of ice-cold ethanol in 15 ml centrifuge tubes were placed on a vortex mixer and the cell suspension was added dropwise to fix the cells. Samples were kept at -20°C for at least 12 h.

Prior to FACS acquisition, samples were washed twice with ice-cold PBS to remove the ethanol and then incubated with 400  $\mu$ l PI - staining buffer for 30 min at 37°C. As PI also intercalates into double-strand RNA, an RNase digestion was performed at this step. The relative DNA content of the samples was immediately measured on the flow cytometer.

### **Annexin V / propidium iodide staining**

An early event during the apoptotic process is the inability of cells to switch the membrane component phosphatidylserine from the outer surface back to the inside. This exposed phospholipid can be stained with fluorophore-conjugated Annexin V to measure early apoptosis. In addition, during later stages of apoptosis, the appearance of holes in the cellular membrane allows to distinguish living from dead cells by labelling unfixed cells with dyes like PI.

To determine the percentage of early and late apoptotic cells in a population, cells were seeded into 6-well plates in triplicates. After cell attachment, monolayers were washed with PBS and fresh medium was added. Depending on the experiment, cells were subjected to different treatments. Prior to FACS acquisition, supernatants containing floating dead cells were collected in 15 ml centrifuge tubes. Cells were washed thoroughly with PBS, which was pooled with the supernatants and adherent cells were harvested by trypsinization. After centrifuging, cell pellets were stained with 8  $\mu$ l Pacific Blue - conjugated Annexin V in a volume of 100  $\mu$ l for 10 min at RT in the dark. 8  $\mu$ l PI were added to each sample immediately prior to acquisition on the flow cytometer.

## **3.2 Molecular biology methods**

### **3.2.1 Annealing of oligonucleotides**

In order to change the multiple cloning site (MCS) of a vector, generate fusion proteins or clone shRNAs, complementary oligonucleotides or short stretches of overlapping DNA fragments were

hybridised to generate double-stranded DNA.

Purchased oligos were resuspended in *aqua ad injectabilia* to achieve a stock concentration of 100  $\mu\text{M}$ . For cloning, oligos or DNA fragments were mixed in 0.2 ml PCR tubes at equimolar concentrations (10  $\mu\text{M}$ ) in a total volume of 50  $\mu\text{l}$  annealing buffer. PCR tubes were placed into a beaker with boiling water, which was allowed to slowly cool down to room temperature. Alternatively, samples were kept for 5 min in a hot block at 95  $^{\circ}\text{C}$ , which was then switched off, allowing to cool to room temperature. Once annealed, the resulting double-stranded DNA was digested (see section 3.2.3) or directly ligated into the target vector (3.2.6).

### 3.2.2 PCR for cloning of DNA fragments

To be able to clone into a specific vector backbone, it was sometimes necessary to add different restriction sites to a gene of interest. This was achieved by designing specific primers that included the desired sites and overlapped with the target gene sequence. Using these primers, the gene of interest was amplified from existing expression vectors via polymerase chain reaction (PCR), using the thermal cycling conditions (Table 3.1) and reaction mix below:

**Table 3.1: Thermocycling conditions for routine PCR**

| temperature                                     | time               |                     |
|---|--------------------|---------------------|
| 98 $^{\circ}\text{C}$                           | 30 s               |                     |
| 98 $^{\circ}\text{C}$                           | 10 s               | <i>18-25 cycles</i> |
| 55 - 66 $^{\circ}\text{C}$ (template dependent) | 30 s               |                     |
| 72 $^{\circ}\text{C}$                           | 15 s / kb template |                     |
| 72 $^{\circ}\text{C}$                           | 10 min             |                     |

1  $\mu\text{l}$  template DNA (50 ng/ $\mu\text{l}$ )  
 10  $\mu\text{l}$  Phusion HF- or GC-buffer (Thermo Fisher Scientific)  
 1  $\mu\text{l}$  dNTPs (10 mM)  
 2  $\mu\text{l}$  forward primer (10  $\mu\text{M}$ )  
 2  $\mu\text{l}$  reverse primer (10  $\mu\text{M}$ )  
 1.5  $\mu\text{l}$  DMSO  
 0.5  $\mu\text{l}$  Phusion High-Fidelity DNA Polymerase (Thermo Fisher Scientific)  
*ad* 50  $\mu\text{l}$  *aqua ad injectabilia*

### 3.2.3 Restriction digest of DNA fragments

To cleave DNA at specific sequences, annealed oligos, amplified PCR fragments or expression vectors were incubated with the desired restriction enzymes (Thermo Fisher Scientific or New England Biolabs). Appropriate buffers for each restriction digest were chosen according to the companies' recommendations for single enzymes or double digests. The following reaction mixture was incubated for 1-4 h at 37  $^{\circ}\text{C}$ :

1  $\mu\text{g}$  template DNA  
 1  $\mu\text{l}$  restriction enzyme 1  
 1  $\mu\text{l}$  restriction enzyme 2  
 2  $\mu\text{l}$  10 x reaction buffer  
*ad* 20  $\mu\text{l}$  *aqua ad injectabilia*

### 3.2.4 Separation of DNA fragments via gel electrophoresis

Agarose gel electrophoresis was used to separate digested DNA fragments and PCR products by size. Depending on the size of expected bands, gels were poured with a final concentration of 1-2% agarose powder in 1 x TAE buffer. To be able to visualise the DNA under UV light, ethidium bromide was added to the dissolved gel solution (0.5 µg/ml).

DNA loading buffer was added to every sample. Once solidified, agarose gels were placed into the electrophoresis units, samples were pipetted into the bottom of the wells and gels were run at 150 V for approximately 1 h. NEB 100 bp DNA Ladder was used as size standard. Separated DNA fragments were visualised on a benchtop UV transilluminator.

### 3.2.5 Purification of DNA from agarose gels

Following PCR or restriction digest, the desired DNA fragments were isolated from the agarose gel using a scalpel. Gel pieces were transferred to 1.5 ml centrifuge tubes and DNA was purified with GeneJET Gel Extraction Kit (Thermo Scientific).

### 3.2.6 Ligation of DNA fragments

The final step in construction of a new recombinant expression plasmid, is the covalent linkage of the digested vector backbone with a desired insert fragment containing matching DNA overhangs. All ligation reactions were performed using the T4 DNA ligase enzyme (Thermo Fisher Scientific). Approximately 100 ng of linearised vector backbone were used in a standard ligation reaction, usually maintaining a molar ratio of 3:1 (insert : vector). The following reaction mixture was incubated over night at room temperature:

|          |                             |
|----------|-----------------------------|
| 100 ng   | linearised plasmid          |
| x µl     | digested insert             |
| 1 µl     | T4 DNA Ligase               |
| 2 µl     | 10 x T4 DNA Ligase buffer   |
| ad 20 µl | <i>aqua ad injectabilia</i> |

### 3.2.7 Transformation of bacteria

Larger quantities of plasmid DNA can be generated by transforming bacteria which are able to amplify the desired vectors.

Competent bacteria were thawed on ice for approximately 10 min. Between 100 ng and 1 µg of DNA was added to the competent cells and mixed by gently flicking the tube. The mixture was incubated on ice for 10-20 min. Each transformation reaction was placed into a hot block set to 42 °C for 45 s ("heat shock"), after which the tubes were put back on ice for another 3 min. After addition of 500 µl LB medium, tubes were placed at 37 °C and left shaking for 30 min.

The transformation reactions were briefly centrifuged. Pelleted bacteria were resuspended in fresh LB medium and spread onto LB agar plates containing the appropriate antibiotic. After incubation at 37 °C over night, resulting colonies could be transferred into LB medium, again containing the appropriate selection marker, to amplify them on a smaller ("Mini prep") or larger scale ("Maxi prep").

### 3.2.8 Isolation of plasmid DNA from bacteria

#### Mini prep

Following the cloning procedure, mini prep cultures were prepared, that could subsequently be digested to determine if a fragment was successfully inserted into a target vector. For this purpose, 1.5 ml of 3 ml overnight cultures were centrifuged and bacterial pellets were dissolved in 200  $\mu$ l resuspension buffer (E1). After addition of 200  $\mu$ l lysis buffer (E2), the mixture was incubated for 5 min at RT to denature proteins. The reaction was stopped by addition of neutralisation buffer (E3) and tubes were centrifuged (13.000 x  $g$ ). DNA was precipitated by transferring the supernatant into fresh tubes containing 500  $\mu$ l isopropanol and a short incubation period at  $-20^{\circ}\text{C}$ . DNA was washed once with 70 % ethanol, air-dried and resuspended in 50  $\mu$ l *aqua ad injectabilia*.

#### Maxi prep

To isolate transfection-grade plasmid DNA from bacteria, colonies were picked into 3 ml pre-cultures during the day and transferred into 200 ml flasks with LB medium (including antibiotic) over night. PureLink® HiPure Plasmid Maxiprep Kit (life technologies) was used to extract  $\mu$ g amounts of DNA, following the procedures recommended by the manufacturer.

The concentration of DNA was determined on a NanoDrop spectrophotometer at a wavelength of 260 nm. Mostly, this technique was performed by Renate Metz.

### 3.2.9 Isolation of RNA from mammalian cells

Isolation of total RNA from cultured cells was achieved using peqGOLD TriFast system (peqlab). Briefly, after growth medium was completely removed, 1 ml of TriFast reagent was added directly to a cell culture dish and the resulting cell-lysate was scraped into 1.5 ml centrifuge tubes. After a 5 min incubation at RT, chloroform was added and the tubes were placed on a vortex mixer for several seconds. After a brief incubation period, centrifugation for 10 min at 13.000 x  $g$  was performed to separate the RNA containing aqueous phase, which was transferred to a fresh tube containing 500  $\mu$ l isopropanol and 1  $\mu$ g glycogen. RNA was precipitated at  $-80^{\circ}\text{C}$ , washed twice with 75 % ethanol and air-dried. After resuspending in 30  $\mu$ l of *aqua ad injectabilia*, RNA was quantified on a NanoDrop spectrophotometer.

#### 3.2.10 cDNA synthesis

Total RNA was reverse transcribed into complementary DNA (cDNA) using random hexamer primers. 2  $\mu$ g of RNA were adjusted to a final volume of 10  $\mu$ l with *aqua ad injectabilia* and placed in a PCR thermocycler. After incubation at  $65^{\circ}\text{C}$  for 1 min and cooling to  $4^{\circ}\text{C}$  to melt potential secondary structures within the template, the following master mix was added to every reaction:

|                 |  |
|-----------------|--|
| 10 µl           | 5X Reaction Buffer for M-MLV Reverse Transcriptase (Promega) |
| 1.25 µl         | dNTPs (10 mM)  |
| 2 µl            | Primer "random" (Roche)                                      |
| 0.2 µl          | RNase Inhibitor (RiboLock, Thermo Fisher Scientific)         |
| 1 µl            | M-MLV Reverse Transcriptase (Promega)                        |
| <i>ad</i> 40 µl | <i>aqua ad injectabilia</i>                                  |

First-strand synthesis was then performed by incubating the samples 10 min at 25 °C, 50 min at 37 °C and 15 min at 70 °C in the thermal cycler.

### 3.2.11 Quantitative PCR

The combination of reverse transcription and quantitative real time PCR (qRT-PCR) allows the detection and relative quantification of any expressed RNA in a sample.

1 µl of synthesised cDNA was used per reaction (see below). For every sample and mRNA to be analysed, reaction mixtures were set up in technical triplicates in a 96-well qPCR plate.

Measurements were carried out on an Agilent MX3000P system using the thermal cycling profile in Table 3.2. Data were quantified with the comparative CT (cycle over threshold) method using *RPS14* as reference for normalization.

|                 |  |
|-----------------|--|
| 10 µl           | ABSolute SYBR Green Mix (Thermo Fisher Scientific) |
| 0.4 µl          | primer mix (forward + reverse, 10 pmol/µl)         |
| <i>ad</i> 19 µl | <i>aqua ad injectabilia</i>                        |

**Table 3.2: Thermocycling conditions for qRT-PCR**

| temperature | time   |                  |
|-------------|--------|------------------|
| 95 °C       | 15 min |                  |
| 95 °C       | 60 s   | <i>38 cycles</i> |
| 60 °C       | 20 s   |                  |
| 72 °C       | 15 s   |                  |
| 95 °C       | 1 min  |                  |
| 60 °C       | 30 s   |                  |
| 95 °C       | 30 s   |                  |

The cycling profile above includes the generation of a dissociation or melt curve (by gradually increasing the temperature from 60 °C to 95 °C) , which can be used to asses whether the primers in a given reaction amplified a single, specific product.

The same cycling conditions were applied to measure relative enrichment of precipitated genomic DNA over input DNA after a chromatin immunoprecipitation (ChIP, see section 3.3.7). Only in this case, 5 µl of ChIP-DNA were used from every sample and water content in the reaction mix was adjusted accordingly.

### 3.2.12 Microarray

Gene expression profiling on a genome-wide level was performed using microarray technology. To this end, total RNA was extracted with QIAGEN RNeasy Kit and a DNase digest was performed "on-column" according to the manufacturer's instructions. Quality and integrity of isolated RNA was tested using Experion™ RNA StdSens Kit on an Experion™ Automated

Electrophoresis Station (BIO-RAD).

RNA was sent to the microarray unit at the Institute of Molecular Biology and Tumor Research, IMT, in Marburg. Labeling and hybridization were performed by Michael Krause following Agilent Two-Color Microarray Based Gene Expression Analysis protocols. Agilent Human Genome Microarray 4x44 K v2 slides were scanned on an Agilent DNA Microarray Scanner G2505C with Agilent Scan Control Version A.8.1.3 software. Data were processed by Lukas Rycak in Marburg, using Agilent Feature Extraction Software Version 10.5.1.1. The ratio of Cy5 to Cy3 (representing sample versus a pooled reference of all samples) was calculated and data were log<sub>2</sub> transformed. After background subtraction and LOWESS normalisation using R software and Bioconductor/Limma packages, an average log intensity value (A-value)  $\geq 5$  was used as a cutoff for subsequent analyses.

Microarray data generated in this thesis were uploaded to the Gene Expression Omnibus (GEO) database and are accessible under the accession number GSE59145 (SuperSeries record GSE59147).

### **3.3 Biochemistry methods**

#### **3.3.1 Preparation of whole cell lysates**

To isolate total protein, cells were washed with ice-cold PBS, and then directly lysed on the dish by addition of 200  $\mu$ l sonication buffer per 10 cm dish. Lysates were scraped into 1.5 ml centrifuge tubes and incubated on ice for at least 30 min. Afterwards, they were snap-frozen in liquid nitrogen and stored at  $-80^{\circ}\text{C}$  or directly thawed again on ice. Lysates were cleared by centrifugation at 13.000  $\times g$  for 10 min and supernatants were transferred to new tubes. Protein content was quantified as described below.

#### **3.3.2 Preparation of nuclear extracts**

To isolate nuclei, cells seeded on 15 cm dishes were washed with ice-cold PBS. 500  $\mu$ l swelling buffer were added per dish and lysates were scraped into 1.5 ml centrifuge tubes, followed by at least 10 min incubation on ice. Nuclei were pelleted by centrifuging 10 min at 200  $\times g$  and the cytoplasm containing supernatant was either transferred to new tubes or discarded. Nuclei were washed once with swelling buffer to remove residual cytoplasmic proteins and then lysed in approximately 70  $\mu$ l of sonication buffer, following the procedures described above.

#### **3.3.3 Quantification of protein concentration**

Protein concentrations of lysates were determined according to Bradford [1976]. A master mix containing 100  $\mu$ l 150 mM NaCl and 900  $\mu$ l Bradford reagent was prepared for all samples and pipetted into Semi-Micro cuvettes. 1.2  $\mu$ l protein lysate was added and mixed on a vortex mixer. Absorption was measured at a wavelength of 595 nm using the respective lysis buffer as a reference. Protein concentrations were calculated as the mean of triplicate measurements using a standard curve. Protein lysates were adjusted to the same concentration with H<sub>2</sub>O and equal amounts of protein were mixed with half the volume of 3  $\times$  SDS loading buffer. These samples were incubated for 10 min at 95  $^{\circ}\text{C}$  and then centrifuged briefly.



### 3.3.4 SDS polyacrylamide gel electrophoresis

Proteins were separated based on their mass weight using discontinuous sodium dodecyl sulfate polyacrylamide gel electrophoresis (SDS-PAGE, Laemmli [1970]). Using tris-glycine buffers with different pH, 4% stacking gels were poured on top of 7.5 - 15% mini resolving gels. Samples were separated at 80 - 130 V in a vertical electrophoresis chamber using SDS running buffer. Thermo Scientific PageRuler Prestained Protein Ladder was used as a size standard.

### 3.3.5 Western blot

Following electrophoresis, separated proteins were transferred onto a polyvinylidene difluoride (PVDF) membrane in a vertical "wet" transfer apparatus. A western blot transfer buffer with 15% methanol was used. Depending on protein size, transfer was performed at 250 - 300 mA for 2.5 - 4 h at 4 °C. To prevent nonspecific binding of antibodies, membranes were incubated in 5% non-fat milk powder dissolved in TBS-T buffer ("blocking buffer"). When antibodies against phospho-epitopes were used, blocking buffer contained 5% bovine serum albumin (BSA) instead of milk. Membranes were probed over night at 4 °C with specific primary antibodies, diluted appropriately in blocking buffer with 5% sodium azide. 5 - 6 washing steps were performed, after which membranes were incubated for 45 min at RT with horseradish peroxidase (HRP)-coupled secondary antibodies at a 1:10.000 dilution in TBS-T. Following further washing steps, signals were detected with an enhanced chemiluminescence (ECL) luminol-based substrate on a digital image analyser system (Fujifilm LAS4000).

### 3.3.6 Stripping PVDF membranes

To re-probe selected membranes with a different antibody, primary and secondary antibodies were removed from the membrane using an acidic glycine-based stripping buffer. Dried PVDF membranes were briefly incubated in methanol and washed several times in H<sub>2</sub>O and TBS-T, after which they were incubated for at least 1 h with stripping buffer at RT. After several washing steps, membranes were blocked again and subsequently re-probed with the desired antibodies.

### 3.3.7 Chromatin immunoprecipitation

To determine whether a specific protein, e.g. a transcription factor, is localised to the promoter of a target gene, the interaction between proteins and a genomic region of choice can be investigated by chromatin immunoprecipitation (ChIP). To this end, reversible cross-linking of proteins and DNA is followed by fragmentation of DNA and precipitation of the protein of interest with specific antibodies. Detection of selective co-precipitated DNA regions is achieved via qPCR.

#### Cross-linking

ChIP was performed from MCF10A cells grown on 15 cm dishes. At least three dishes at 70 - 80% confluence were used per antibody and condition. Cells were cross-linked with 1% formaldehyde at RT, by directly adding the 37% stock solution to the culture medium. After gentle shaking for 15 min, glycine was added to a final concentration of 125 mM for 5 min to quench the reaction. Cells were scraped off the dishes in ice-cold PBS containing 0.5 mM PMSF protease inhibitor and pelleted by centrifugation at 1.000 x *g* for 10 min at 4 °C.

### **Sonication**

Pellets were resuspended in a hypotonic swelling buffer, incubated on ice and cell membranes were disrupted using a dounce-type hand homogeniser. Nuclei were pelleted by centrifugation at  $800 \times g$ , resuspended in an SDS-based sonication buffer and sonicated for 30 min in a Branson sonifier. A protocol with 35 % amplitude, whereby each pulse of 15 s was followed by a 45 s pause, was used to generate fragments between 200 and 1.000 base pairs (bp).

### **Size-check**

To verify the size of the obtained DNA fragments, 60  $\mu$ l aliquots of chromatin were taken from every sample and incubated at 65 °C in a thermoshaker in the presence of 500 mM NaCl over night. Subsequently, chromatin was successively digested with RNase A and Proteinase K at 37 °C and 42 °C, respectively, purified via GeneJET Purification Columns (Thermo Scientific) and loaded onto a 2 % agarose gel.

### **Antibody coupling**

Per IP, 2  $\mu$ g antibody were coupled to 20  $\mu$ l Dynabeads® supermagnetic beads for 6 h at 4 °C in a final volume of 500  $\mu$ l blocking solution (5 mg/ml BSA in PBS). Following this incubation period, beads were washed once with blocking solution.

### **Immunoprecipitation**

Chromatin was centrifuged at  $14.000 \times g$  and 4 °C for at least 30 min to pellet cellular debris. Supernatant was added to antibody-coupled Dynabeads® that were resuspended in 1/10 the volume blocking solution. An aliquot of 1 % of the added chromatin was taken as input control and stored at -20 °C. Precipitation of proteins was carried out over night at 4 °C on a rotating wheel.

Beads were washed at least 5 times (2 x sonication buffer, 2 x high salt buffer, 1 x LiCl buffer) and the reaction tube was changed after the last washing step.

### **Elution and de-cross-linking**

Supernatant was completely removed after the last wash step, beads were resuspended in 230  $\mu$ l elution buffer and incubated in a thermoshaker at 65 °C while shaking at 1.000 rpm. After 15 min, 200  $\mu$ l eluate were transferred to a fresh tube and 200  $\mu$ l of fresh elution buffer were added to the beads, repeating the procedure.

Cross-linking was reversed by incubating the pooled 400  $\mu$ l of eluted chromatin in the presence of 210 mM NaCl for at least 6 h at 65 °C in a thermoshaker (1.000 rpm).

Stored input chromatin was treated the same way.

The next day, samples were digested with Proteinase K for 2 h at 42 °C.

### **DNA purification**

To purify DNA, a phenol/chloroform extraction of the de-cross-linked material was performed. To this end, an equal volume (420  $\mu$ l) of a phenol/chloroform/isoamyl alcohol solution (25:24:1) was added to every sample and vigorously mixed on a vortex mixer. After centrifugation ( $14.000 \times g$ ,

10 min) at RT, the aqueous layer was transferred into a new reaction tube. 1/10 the volume (36  $\mu\text{l}$ ) 3 M sodium acetate were added, followed by addition of 2.5 x the volume 100 % ethanol (900  $\mu\text{l}$ ) and 3  $\mu\text{g}$  glycogen. DNA was allowed to precipitate for at least 1 h at  $-80^\circ\text{C}$  and was subsequently washed once with 80 % ethanol after a 30 min centrifugation step (14.000 x  $g$ ,  $4^\circ\text{C}$ ). Pellets were air dried and resuspended in 220  $\mu\text{l}$  *aqua ad injectabilia*. 5  $\mu\text{l}$  of ChIP-DNA were used per qPCR triplicate (see 3.2.11).

### 3.3.8 ChIP-sequencing

Chromatin immunoprecipitation (ChIP) followed by high-throughput DNA sequencing (ChIP-seq) is used for mapping transcription factor occupancy across the genome.

To determine genome-wide binding sites of MYC-ER and MIZ1, the ChIP protocol described in 3.3.7 was followed, except that chromatin from approximately  $100 \times 10^6$  MCF10A cells was used per IP and condition. All other reagents (e.g. beads, antibodies) were scaled up accordingly.

The DNA pellet was resuspended in 30  $\mu\text{l}$  of *aqua ad injectabilia* and quantified using a fluorescence-based PicoGreen® assay (Life Technologies).

Sample preparation for ChIP-Seq was performed with NEBNext ChIP Prep Master Mix Set for Illumina, closely following the instructions. First, sonicated ChIP-DNA was end-repaired to create blunt ends, a step that also includes the phosphorylation of 5' ends through T4 Polynucleotide Kinase. To prevent concatamer formation during subsequent ligation steps, a 3' dAMP was added ("dA-Tailing"). In a ligation step, adaptors that are compatible with the Illumina platform were added to dA-tailed DNA. Because these adaptors are shaped like a hairpin, an additional reaction had to be performed, making use of an enzyme that generates a single nucleotide gap at the location of an uracil, thereby cleaving the hairpin (Uracil-Specific Excision Reagent, USER). Size selection of adaptor ligated DNA was performed on an agarose gel, by cutting out gel fragments at the height of approximately 200 bp with a scalpel.

Following each of the above described reactions, DNA was purified using spin columns of QIAquick PCR Purification or Gel Extraction Kits (Qiagen).

Size-selected adaptor ligated DNA was enriched by 18 cycles of PCR with Illumina primers, and DNA library integrity was analysed with Experion DNA 1K Analysis Kit (BIO-RAD). Samples were diluted according to Illumina recommendations (TruSeq Cluster Generation Kit Reagent Preparation Guide for Single-Read Runs) after quantification with PicoGreen® assay. Following cluster generation, multiplexed Single-Read sequencing runs were performed on an Illumina GAIIx sequencer, that was operated by Wolfgang Hädelt, Elmar Wolf and Carsten Ade.

After the run, sequencing reads were processed with the standard Illumina software pipeline CASAVA, to perform base calling and quality assessment steps. Resulting demultiplexed FASTQ files were analysed as described below (3.4.1).

Some ChIP-seq data generated in this thesis were published in Muthalagu et al. [2014] and are available at GEO under GSE59001. Additional data are accessible under the accession number GSE59146 (SuperSeries record GSE59147).

## 3.4 Bioinformatic and statistical analyses

All bioinformatic and statistical analyses were performed in Microsoft Excel and R [R Core Team, 2014], or with other GNU project General Public License (GPL) software described in

the following sections.

Unless stated otherwise, data were presented as mean + standard deviation (SD) or standard error of the mean (SEM) of at least three biological replicates.

Two determine if an observed difference between two groups was statistically significant, an unpaired Student's t-test was performed. p-values larger than 5 % were not considered significant (ns) and a star code was used in the figures to indicate significance levels for p-values smaller than 5 %: \*:  $p \leq 0.05$ ; \*\*:  $p \leq 0.01$ ; \*\*\*:  $p \leq 0.001$ ; \*\*\*\*:  $p \leq 0.0001$ .

To calculate the probability of an overlap between two lists, e.g. list of genes, the dhyper function in R was used, which is the density function for the hypergeometric distribution.

To measure relationships between two variables, either Pearson's coefficient or Spearman's rank order coefficient was calculated. p-values to determine the significance of either correlation were calculated with the cor.test function in R.

To test whether the slopes of two regression lines differ significantly, an analysis of covariance (ANCOVA) was performed with the aov function in R.

### 3.4.1 Bioinformatic analysis of ChIP-seq data

Sequencing read data for downstream analysis (generated by CASAVA software as described in 3.3.8) were obtained in FASTQ file format, which includes the FASTA formatted sequence and its quality data. FASTQ files from all sequenced input samples were merged to create a mixed input control as reference.

#### Alignment to the human genome and normalisation of read counts

The Bowtie algorithm (Bowtie v0.12.8, Langmead [2010]) was used to align sequences to the human genome, version hg19, with the following command:

```
bowtie -t -p 14 hg19 data_input.fastq
```

The bowtie output contained the number of processed reads and the percentage of successful alignment (between 93 and 98 %), which could be used to cut the FASTQ files of all samples to approximately equal read counts for the purpose of normalisation.

Afterwards, bowtie was run again, this time with the -S option to produce alignment files in SAM (Sequence Alignment/Map) format:

```
bowtie -t -S -p 14 hg19 data_input.fastq data_output.sam
```

#### Peak calling

SAM files were converted to their binary form (BAM) with the free software package SAMtools [Li et al., 2009] and the following command:

```
samtools view -bS -o data_output.bam data_output.sam
```

The open source software MACS (Model-based Analysis of ChIP-Seq, v1.4.2, Zhang et al. [2008]) was then used to identify "peaks", regions in the genome that are significantly enriched as determined by multiple aligned reads in the ChIP sample relative to the input control:

```
macs14 -t ChIP_sample.bam -c Input_sample.bam - -format BAM - -name output_name  
- -space 10 - -wig
```

Among the output files generated by MACS is a list of peaks in BED format, containing chromosome name as well as genomic coordinates defining start and end of the peak. In

addition, significance of enrichment is indicated by an empirical false discovery rate (FDR). For all further analyses, an FDR of 0.1 (10%) was used as a threshold for significant binding.

In addition, MACS produces a wiggle track format file (.wig), which, after further processing, can be used to visualise the distribution of tags across the genome graphically. For this purpose, files were loaded into the Integrated Genome Browser software 8.0 [Nicol et al., 2009].

### Annotation of peaks

To assign the obtained peak coordinates to the closest genomic feature, the `closestBed` command of the BEDTools utilities (v2-17.0) was used [Quinlan and Hall, 2010]:

```
closestBed -t first -a sample -b reference >output
```

Using a reference dataset containing the coordinates of all human polymerase II transcriptional start sites including strand orientation (UCSC refGene, GRCh37/hg19, generated by Elmar Wolf), all peaks were annotated to the closest TSS.

The location of the highest read density within a defined peak is called the summit. The distance from the summit to the closest TSS was calculated in Excel, taking strand orientation into account. Sublists of promoter-proximal peaks (defined as +/- 1.5 kb from TSS) and more broad binding (+/- 5 kb from TSS) were generated in R.

### Overlapping genomic features

Another part of the BEDTools suite is the tool `intersectBed` that compares coordinates in two different .bed files and delivers an output list of shared genomic features, e.g. binding sites:

```
intersectBed -wa -wb -a list a -b list b >output
```

To calculate the significance of overlapping binding sites, a hypergeometric distribution function (`dhyper`) in R was used, taking the number of base pairs covered by either each transcription factor alone or together. To this end, the `intersectBed` command was run without the `-wa -wb` options, yielding a file with only the jointly bound base pairs of both lists. A window of +/- 1.5 kb around the TSS of all human RefSeq genes, covering 120.669.000 bp was used as population size.

### Generation of ChIP-seq read profiles

Read profiles in the form of histograms or heatmaps allow the visualisation of ChIP-seq tag distribution with respect to specific genomic features, such as TSSs or binding sites of other factors.

To compare average tag densities between different datasets, the density array method of the seqMINER platform was used [Ye et al., 2011]. First, a list of specific reference coordinates in .bed format was fed into the program. Second, normalised aligned read files in .bam format were loaded. The distribution of tags in different datasets was then calculated in 50 bp steps in a window of +/- 5 kb around the reference coordinates. An output file that contained a matrix of 200 columns per sample for every reference feature (row) was exported.

Using these data, normalised tag density plots in form of histograms were created in R (R script written by Björn von Eyss).

To visualise the distribution of reads in form of a heatmap, seqMINER output files were sorted in

Excel according to the parameter of interest, e.g. MYC occupancy. Subsequently, Java Treeview software was used for graphical representation of the results [Saldanha, 2004].

### **Analysis of DNA binding motifs**

In order to search for enriched DNA binding motifs in sequences around identified ChIP-seq peaks the MEME-ChIP web tool of the MEME Suite was used [Bailey et al., 2009; Machanick and Bailey, 2011].

To this end, sequences surrounding the peak summits (+/- 50 bp) were extracted with the `fastaFromBed` command of the BEDTool suite. Afterwards, the resulting file was uploaded to the MEME-ChIP data submission form and the search was performed with default options.

### **3.4.2 Functional analysis of microarray data**

#### **Database for Annotation, Visualization and Integrated Discovery (DAVID)**

Functional activities or common biological roles of regulated target genes were identified with the online bioinformatic tool DAVID (<http://david.abcc.ncifcrf.gov>, Huang et al. [2009]). List of genes ("official gene symbol") were submitted and analysed with the Functional Annotation Tool for enriched GO Terms (biological process (BP), molecular function (MF), cellular component (CC)) or pathway components (KEGG pathway).

#### **Gene Set Enrichment Analysis (GSEA)**

Differentially expressed sets of genes between two conditions were identified by gene set enrichment analysis [Subramanian et al., 2005]. Either the Molecular Signature Database (MSigDB) collection of curated gene sets ("C2") or motif gene sets ("C3") were used. In addition, custom gene sets of bound SRF targets were created and formatted according to GSEA guidelines with a `.gmt` extension.

Similarly, M-values (log ratio of red/green intensity) obtained from the microarray analysis were saved as tab delimited file, matching the `.gct` format.

To annotate Agilent probe IDs with gene names, `.chip` annotation files were generated, allowing GSEA to collapse these probe IDs into HUGO gene symbols.

The described files were loaded into GSEA and two different phenotypes to compare were defined "on-the-fly" by inserting names of the respective samples, e.g. WT versus VD or 4-OHT versus control.

The permutation type was set to "gene\_set" and GSEA was run with n= 1.000 permutations.

## Chapter 4

# Results

### 4.1 Different levels of MYC produce diverse biological outputs

It is not well understood, how exactly cells discriminate between normal and oncogenic amounts of MYC and are able to respond with the appropriate biological response. To investigate the underlying molecular mechanisms, we constitutively overexpressed MYC in the immortalised but non-tumorigenic mammary epithelial cell line MCF10A. We generated lentiviruses with two different promoters: the cellular phosphoglycerate kinase (PGK) promoter and the retroviral enhancer-promoter of the spleen focus-forming virus (SFFV). These promoters have been reported to mediate relatively weak and supraphysiological levels of transgene expression, respectively [Zychlinski et al., 2008; González-Murillo et al., 2010].

MCF10A cells have three copies of the *MYC* gene, hence endogenous levels are elevated in comparison to other immortalised primary cells (Fig. 4.1 A, compare MCF10A to HMLE cells). Apparently, MYC protein levels in MCF10A cells are also higher than the ones observed in some breast cancer cell lines, as shown here for MDA-MB-231 and MDA-MB-468 cells.

Overexpressing MYC under the control of the PGK promoter resulted in an approximately 2-fold increase of the protein relative to endogenous levels (Fig 4.1 B). MYC driven from the stronger viral SFFV promoter accumulated to levels roughly 7-10-fold above endogenous MYC (Fig 4.1 C), which was similar to levels found in HeLa or HCT116 cancer cell lines.

Importantly, as judged based on cell morphology, only those levels of MYC reached by transduction with the SFFV promoter-driven viruses were sufficient to induce apoptosis (compare right panels in Fig 4.1 B and C). This is consistent with *in vivo* studies showing that only high levels of MYC elicit apoptotic responses in multiple tissues [Murphy et al., 2008].

Interestingly, overexpression of MYC V394D ("MYC VD"), a point mutant that is unable to bind to MIZ1, failed to induce apoptosis in MCF10A cells, although expression levels were identical (Fig 4.1 C and Herold et al. [2002]).

With the aforementioned tools, we wanted to investigate further, which aspects of MYC biology in mammary epithelial cells (MECs) are executed at different expression levels, which of them require the interaction with MIZ1 and, more specifically, whether it is the association with MIZ1 that allows cells to discriminate supraphysiological from physiological levels of MYC.

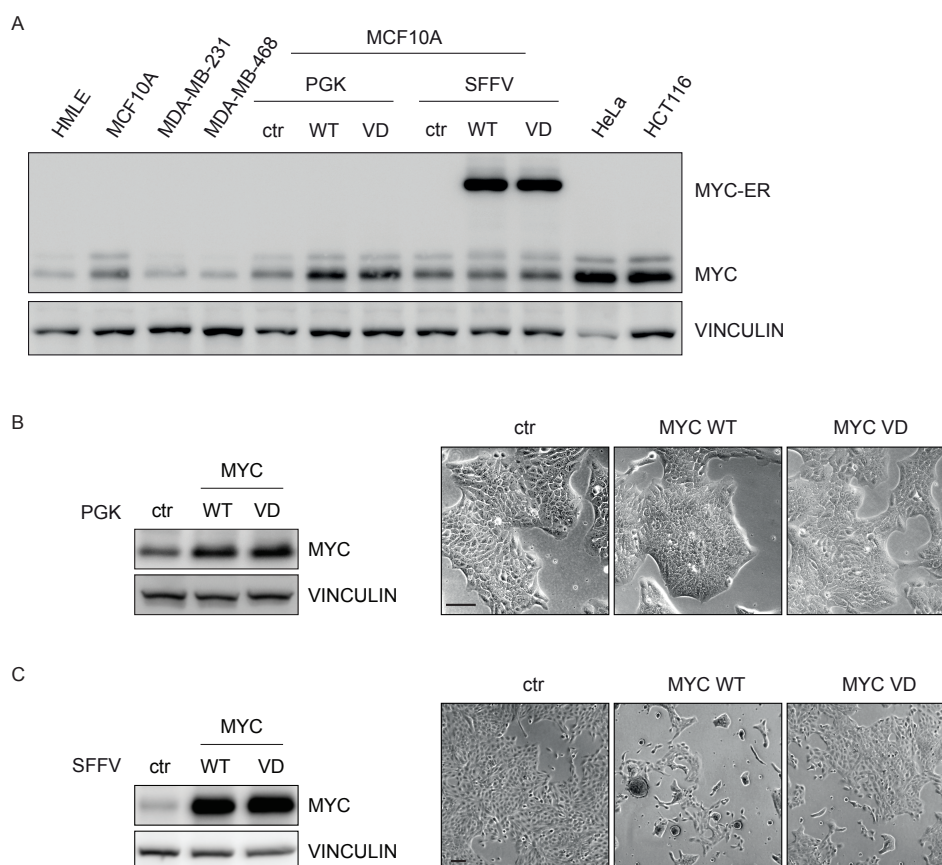


**Figure 4.1: Comparison of different Myc expression levels<sup>1</sup>**

- A Immunoblot comparing endogenous MYC levels in HMLE, MCF10A, MDA-MB-231 and -468, HeLa and HCT116 cells to overexpressed MYC in MCF10A cells driven from either the PGK or SFFV (shown for MYC-ER) promoter, respectively. An empty vector backbone is designated "ctr". Vinculin was used as loading control.
- B Left panel: Immunoblot from MCF10A cells, expressing MYC WT or MYC V394D ("VD") driven by the PGK promoter. Right panel: Morphology of these cells in culture. Bar = 100  $\mu$ m.
- C Left panel: Immunoblot from MCF10A cells, expressing MYC WT or VD driven by the SFFV promoter. Right panel: Morphology of these cells in culture. Bar = 100  $\mu$ m.

<sup>1</sup>Parts of this figure were published in similar form in Wiese et al. [2015].

#### 4.1.1 Biological functions of MYC in MECs at moderate expression levels

##### Induction of proliferation

A well documented biological effect of deregulated MYC is an enhanced G1 to S phase transition and the induction of cell proliferation [Bouchard et al., 1998]. To test whether this also happens in MCF10A mammary epithelial cells in a MIZ1-dependent manner, the proliferation rate of transduced cell pools was determined with a cumulative growth curve.

In contrast to results observed previously in a different immortalised mammary epithelial cell line, IMECs, neither MYC nor MYC VD had significant effects on the growth rate of MCF10A cells under standard culture conditions (Fig 4.2 A and Cowling et al. [2007]). Consistently, there was no apparent difference in cell cycle distribution when cells were stained with propidium iodide and analysed by flow cytometry (Fig 4.2 B, "full medium").

Furthermore, no increase in sub-G1 DNA content in MYC WT or VD overexpressing cells could be observed, validating that expression levels reached by the PGK promoter in these experiments were too low to cross the apoptotic threshold. This was also true for cultures that were deprived



of serum and other medium supplements within a 24 h timeframe (Fig 4.2 B, "starved"). About 90 % of control cells accumulated in the G1 phase of the cell cycle, as did MYC WT and VD overexpressing cells.

While elevated MYC levels did not promote proliferation in asynchronously growing cells, they could, however, accelerate progression through the cell cycle when cells were released from starvation into full medium (Fig 4.2 B, "16 h release" and "18 h release"). Notably, this was the case for MYC WT as well as VD overexpressing cell pools, indicating that stimulating cell cycle re-entry is not a MIZ1-dependent function of MYC in MCF10A cells.

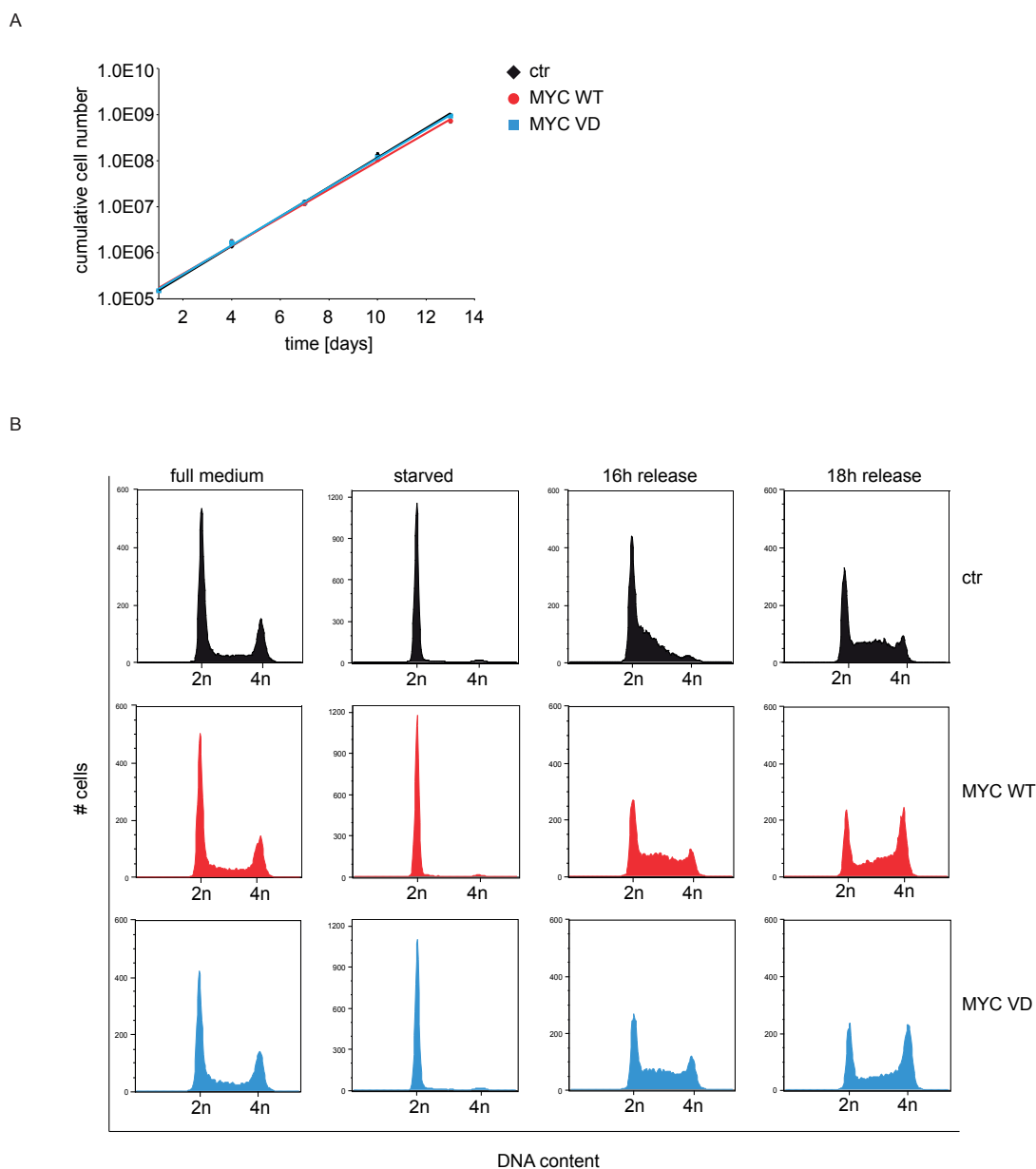


**Figure 4.2: MYC and MYC VD accelerate cell cycle re-entry after starvation<sup>1</sup>**

A Cumulative growth curve of MCF10A cells transduced with the indicated PGK-driven expression vectors. The graph represents mean  $\pm$  standard deviation (SD) from 3 independent biological experiments, each performed in triplicates.

B Propidium iodide FACS to analyse cell cycle distribution of the indicated MCF10A pools. Samples were taken from cells cultured in full medium, from cells after 24 h starvation and after release into full medium for 16 or 18 h, respectively. Representative cell cycle profiles are shown ( $n = 6$ ).

## Induction of self-renewal

With an *in vitro* technique called mammosphere assay, MECs grow under serum-free non-adherent conditions and produce spherical colonies that are enriched in early progenitor and stem cells. This system is widely used to assess the self-renewal potential of cultured primary tissues and mammary epithelial cell lines [Dontu et al., 2003]. As MYC overexpression has been reported to induce mammosphere formation efficiency in MCF10A cells, we aimed to test whether this effect requires complex formation with MIZ1 [Liu et al., 2009].

Primary spheres overexpressing MYC and MYC VD were larger than spheres which formed from control infected cells. (Fig 4.3 A). Furthermore, a 2-3-fold increase in the amount of primary mammospheres formed could be observed in both MYC WT and MYC VD cells relative to control cells (Fig 4.3 A and B, left panel). However, because self-renewal property can only be judged from serial passaging, the ability of primary mammospheres to generate secondary spheres was tested. Approximately 3 times more secondary mammospheres formed in MYC overexpressing cells than in control cells and again there was no significant difference observed between WT and VD (Fig 4.3 B, right panel). Compared with normal 2D culture conditions, the overall levels of MYC were lower in secondary mammospheres, however, there was still a 2-fold overexpression of both wildtype and the mutant protein (Fig 4.3 C). Taken together, MIZ1 does not appear to influence the induction of self-renewal capabilities by MYC.

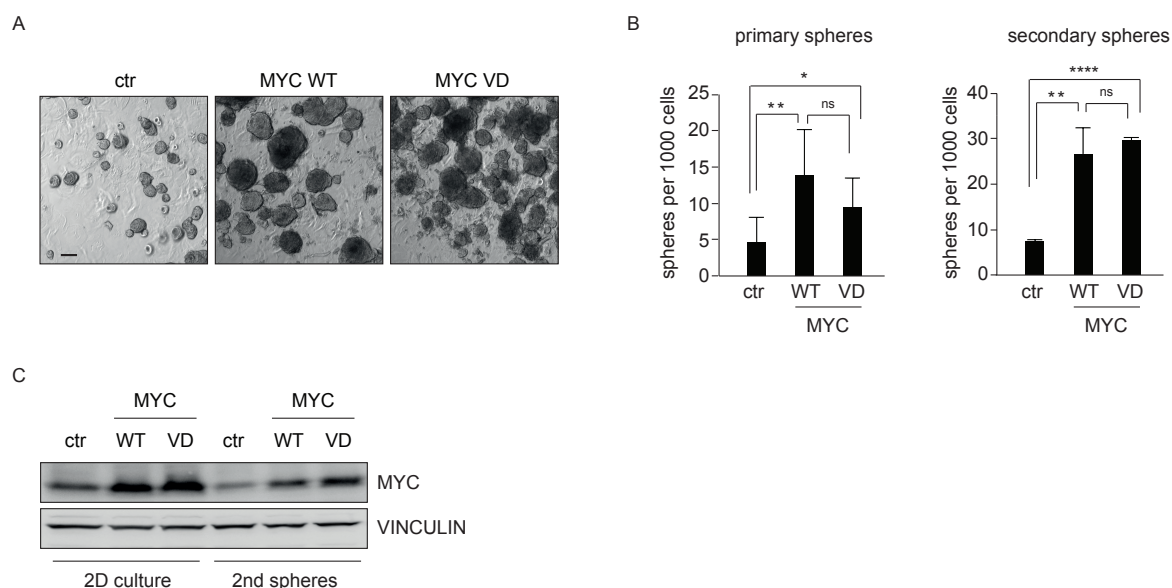


**Figure 4.3: MYC and MYC VD enhance mammosphere formation<sup>1</sup>**

- A Representative pictures of primary mammospheres generated from the indicated pools of MCF10A cells. Bar = 50  $\mu\text{m}$ .
- B Left panel: Quantification of primary mammosphere forming efficiency. Results represent mean + SD of 9 biological experiments, each performed in technical triplicates. Right panel: Quantification of secondary mammosphere formation. Results are mean + SD of 3 biological replicates each performed in technical replicates. p-values were calculated using Student's t-test (ns:  $p > 0.05$ ; \*:  $p \leq 0.05$ ; \*\*:  $p \leq 0.01$ ; \*\*\*\*:  $p \leq 0.0001$ ).
- C Immunoblot comparing MYC levels in MCF10A cells from standard 2D and secondary mammosphere culture conditions. VINCULIN was used as loading control.

## Inhibition of migration

During standard 2D monolayer culture, we had noticed that MCF10A cells overexpressing WT MYC display an altered cellular morphology as compared to vector or MYC VD infected cells (Fig. 4.1 B): They appeared more compact and grew in tighter clusters.

Such morphological alterations can be the result of changes in cytoskeletal architecture which could, in turn, have an impact on substrate adhesion and cell migration. MYC overexpression has already been shown to reduce migration of primary keratinocytes and retinal pigment epithelium cells and this effect is dependent on MIZ1 [Frye et al., 2003; Gebhardt et al., 2006; Alfano et al., 2010]. To confirm these results in mammary epithelial cells, we tested the migratory behaviour of infected MCF10A cell pools using transwell migration assays.

In line with the previous findings, less cells were able to migrate through the pores after ectopic expression of MYC WT (Fig 4.4 A and B). Although there was also a significant difference between control and MYC VD cells ( $p < 0.01$ ), MYC WT was significantly more potent in inhibiting migration of MCF10A cells than MYC VD, suggesting an involvement of MIZ1-mediated repression in this process.

Similar results were obtained when the migration potential of infected cell pools was tested with *in vitro* wound healing ("scratch") assays (data not shown).

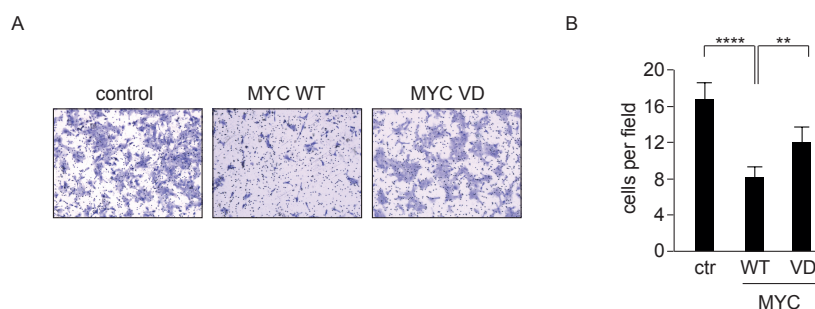


**Figure 4.4: Inhibition of migration by MYC is partially MIZ1-dependent**

- A Representative pictures of transwell assays. Cells that migrated through the pores of the transwell inserts were stained with crystal violet.
- B Quantification (mean + SD,  $n = 6$ ) of transwell migration assays performed with the indicated pools of MCF10A cells. For every condition, 6 random fields from two transwell inserts were counted, using a 20x objective. p-values were calculated using Student's t-test (\*\*:  $p <= 0.01$ ; \*\*\*\*:  $p <= 0.0001$ ).

## Sensitisation to apoptosis

The observation that deregulated MYC expression induces apoptosis was first made in IL-3 deprived myeloid cells and serum-starved fibroblasts [Askew et al., 1991; Evan et al., 1992].

To date, MYC has been shown to sensitise mammalian cells to numerous other stimuli, including DNA damage and glutamine starvation [Nesbit et al., 1998; Yuneva et al., 2007].

Since MCF10A cells did not display increased sensitivity after serum- and growth factor withdrawal (Fig 4.2 B), we tested whether MYC WT and MYC VD differed in their ability to sensitise MCF10A cells to apoptosis using glutamine deprivation and the DNA damaging agent doxorubicin. To quantify the amount of apoptosis, cells were stained with Annexin V and propidium iodide (PI) and analysed by FACS.

Already for control cells, an increase in apoptotic cells was observed after 24 h for both glutamine

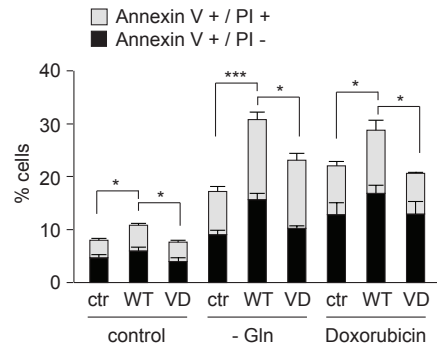


**Figure 4.5: Sensitisation to apoptosis by MYC is mostly MIZ1-dependent<sup>1</sup>**

Quantification of Annexin V / propidium iodide apoptosis stainings in MCF10A cells grown under control or glutamine-deprived conditions for 24 h ("-Gln"). Where indicated, doxorubicin was added for the same time (0.1  $\mu\text{g}/\text{ml}$ ). Annexin V + / PI - cells are an indicator of early apoptosis, double positive cells define late apoptotic cells. The results are represented as mean + SD and p-values were calculated for the sum of apoptotic cells with Student's t-test ( $n = 3$ ; \*:  $p \leq 0.05$ ; \*\*\*:  $p \leq 0.001$ ).

starvation and doxorubicin treatment (Fig. 4.5, compare first bar with 4th and 7th bar). As expected, MYC WT was able to further enhance sensitivity, leading to an increase in apoptosis in both glutamine-deprived and DNA-damaged situations.

Even though we had not observed increased apoptosis with MYC expression driven by the PGK promoter before, in this particular experiment, MYC WT was also able to promote a slight but yet significant 1.3-fold increase in the amount of apoptotic cells without any prior stimulus (Fig 4.5, "control" condition). Importantly, compared to MYC WT, MYC VD was significantly impaired in promoting apoptosis in all tested conditions, leading us to the conclusion that sensitisation to apoptosis by MYC is dependent on the association with MIZ1.

#### 4.1.2 Biological functions of MYC in MECs at oncogenic expression levels

##### Induction of stem cell markers

MYC protein overexpression has been found in more than 40 % of human breast tumours and is often correlated with poor prognosis [Chrzan et al., 2001; Xu et al., 2010].

It is widely accepted that only a small population of cells within a tumour has high tumourigenic potential. In the case of breast cancer, the surface marker combination  $\text{CD44}^{\text{high}} / \text{CD24}^{\text{low}}$  has been identified as the phenotype of both tumour initiating cancer cells and normal mammary epithelial stem cells [Al-Hajj et al., 2003; Sleeman et al., 2006]. Besides,  $\text{CD44}^{\text{high}} / \text{CD24}^{\text{low}}$  cells isolated from HMLE cells display enhanced self-renewal potential in mammosphere assays and are capable of differentiating into luminal and basal lineages [Mani et al., 2008].

As we had already seen induction of self-renewal with low levels of MYC and MYC VD using mammosphere assays (Fig. 4.3), we wanted to test the effect of higher, oncogenic levels on the induction of potential breast cancer initiating cells.

Therefore, we performed cell surface stainings against CD44 and CD24 in both HMLE and MCF10A cells and analysed the expression by FACS.

In HMLE cells, overexpression of MYC WT and MYC VD induced an approximately 3-fold increase in the percentage of  $\text{CD44}^{\text{high}} / \text{CD24}^{\text{low}}$  cells (Fig. 4.6 A and D). Whereas others had reported  $\text{CD44}^{\text{high}} / \text{CD24}^{\text{low}}$  cells to be positive for expression of a third marker, ESA (also EpCAM or CD326, Al-Hajj et al. [2003]), our experiments showed that the CD24 and

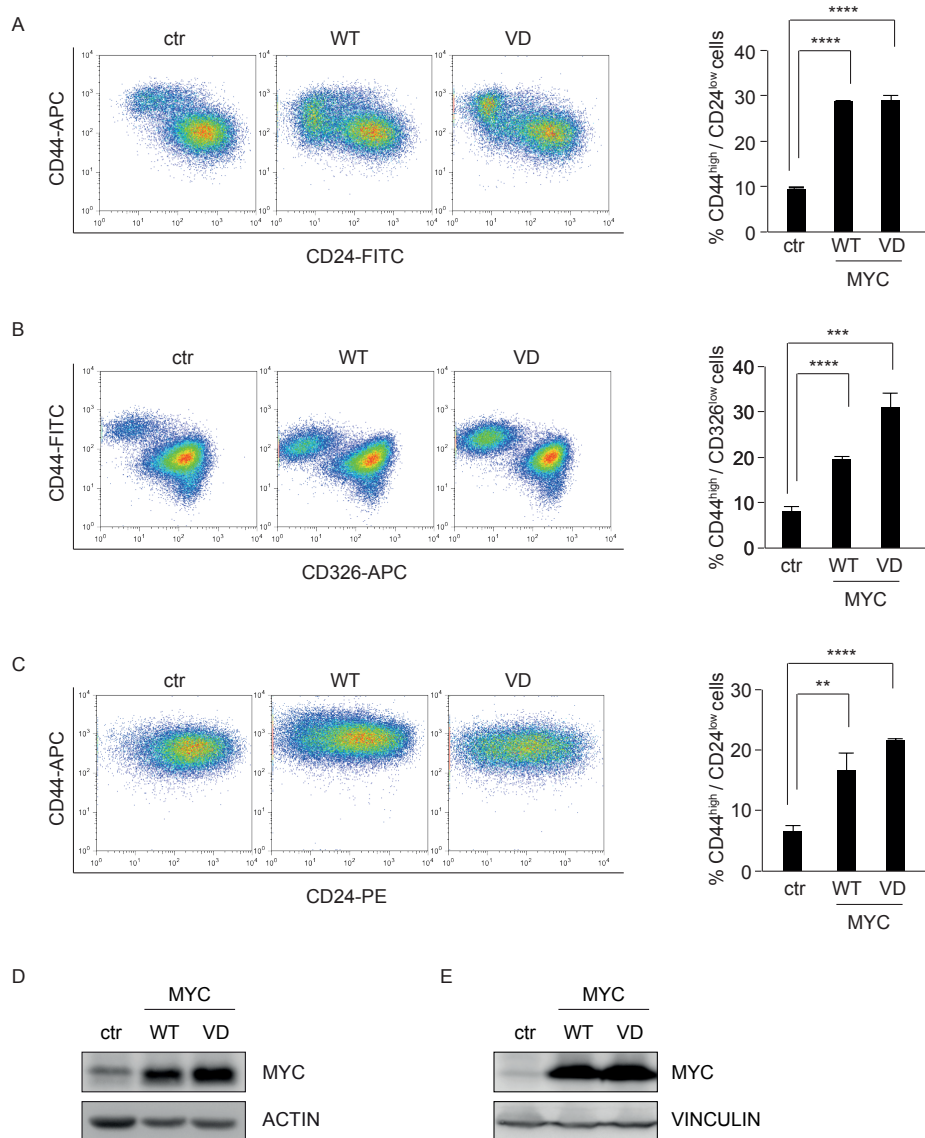


**Figure 4.6: MYC and MYC VD induce a mammary stem cell surface marker profile<sup>1</sup>**

A Cell surface FACS with antibodies directed against CD44 (APC-labeled) and CD24 (FITC-labeled) in pools of HMLE cells transduced with SFFV-driven control, MYC WT or MYC VD lentiviruses. Left panel: representative FACS plot. Right panel: Quantification of CD44<sup>high</sup> / CD24<sup>low</sup> cells (mean + SD of 3 biological replicates.  $p$ -values were calculated with Student's  $t$ -test ( \*\* :  $p \leq 0.01$ ; \*\*\* :  $p \leq 0.001$ ; \*\*\*\* :  $p \leq 0.0001$ ).

B Cell surface FACS like in A, only with antibodies directed against CD44 (FITC-labeled) and CD326 (EpCAM, APC-labeled). Left panel: representative FACS plot. Right panel: Quantification of CD44<sup>high</sup> / CD326<sup>low</sup> cells ( $n=3$ ).

C Cell surface FACS with antibodies directed against CD44 (APC-labeled) and CD24 (PE-labeled) in pools of MCF10A cells transduced with the same vectors as in A. Left panel: representative FACS plot. Right panel: Quantification of CD44<sup>high</sup> / CD24<sup>low</sup> cells ( $n = 3$ ).

D Immunoblot documenting overexpression of SFFV-driven MYC WT and MYC VD in HMLE cells. ACTIN was used as loading control.

E Immunoblot documenting overexpression of SFFV-driven MYC WT and MYC VD in MCF10A cells. VINCULIN was used as loading control.

CD326 stainings were largely interchangeable: The percentage of CD44<sup>high</sup> / CD326<sup>low</sup> cells was increased between 2- and 3-fold in MYC or MYC VD overexpressing cells, respectively (Fig. 4.6 B).

Although resolution between the different populations was not as obvious in MCF10A cells, a shift towards the same surface phenotype could be detected when MYC or MYC VD were present (Fig. 4.6 C and E).

These results are consistent with the mammosphere assays and demonstrate that induction of self-renewal capabilities by low and high levels of MYC is MIZ1-independent.

### Induction of apoptosis

As noted before, MYC levels driven by SFFV promoter containing lentiviruses induced overt apoptosis in MCF10A cells under standard culture conditions (Fig 4.1 C).

To visualise the effect on colony growth, freshly infected cells were plated at equal density and stained with crystal violet after several days in culture.

Colony formation was suppressed in pools overexpressing MYC WT but not MYC VD (Fig. 4.7 A), confirming the initial observations.

To exclude the possibility that surviving cells had simply shut down expression of MYC VD, we infected MCF10A and HMLE cells with control, MYC WT and MYC VD vectors and analysed MYC protein levels over time.

While MYC and MYC VD were equally abundant three days after transduction, MYC WT expression decreased substantially within 10 days of culture (Fig. 4.7 B). In contrast, MYC VD expression was tolerated better in both cell lines.

Taken together, these observations indicate that there is a strong selective pressure against high levels of MYC WT in mammary epithelial cells.

To have a better tool for a comprehensive analysis of the molecular mechanisms underlying MYC-induced and MIZ1-dependent apoptosis, we chose to switch to an inducible mode of MYC overexpression. This can be achieved by fusing MYC to the modified ligand binding domain of the estrogen receptor (MYC-ER), which sequesters MYC in the cytoplasm [Eilers et al., 1989; Littlewood et al., 1995]. Activation of MYC-ER and translocation to the nucleus can be triggered by addition of the synthetic anti-estrogen metabolite 4-Hydroxytamoxifen (4-OHT).

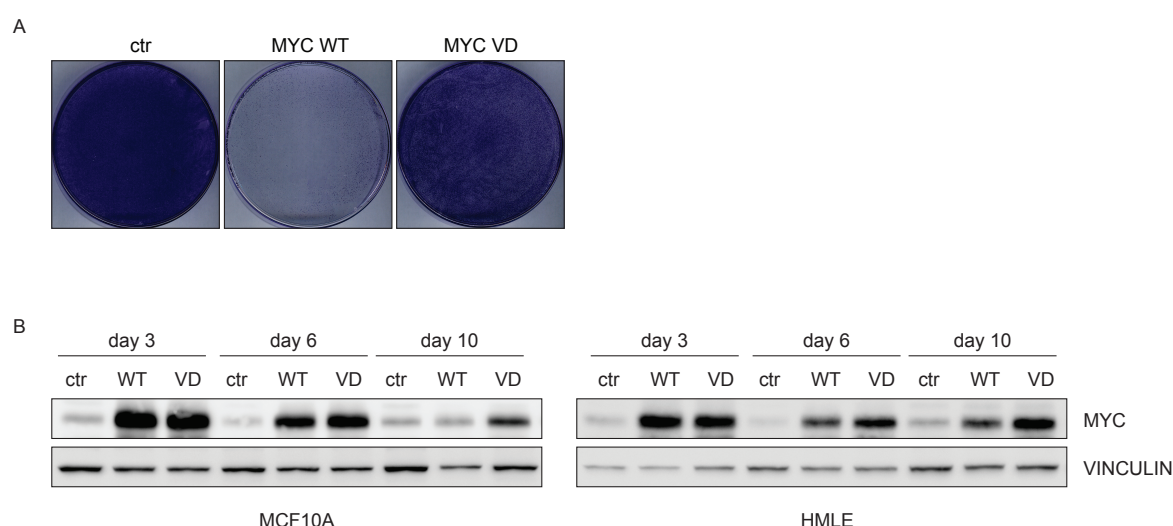


**Figure 4.7: Epithelial cells select against high levels of MYC WT but not MYC VD<sup>1</sup>**

A Colony forming assay of MCF10A cells transduced with the indicated expression vectors. Representative of 3 independent experiments.

B Immunoblots documenting expression of MYC WT and MYC VD in MCF10A (left panel) or HMLE (right panel) cells over time. Samples for protein lysates were taken at the indicated time points after transduction from cells expressing SFFV-driven MYC WT, MYC VD or empty backbone control. VINCULIN was used as loading control.

We fused MYC and MYC VD to a triple mutant form of the human estrogen receptor that is insensitive to physiological estrogenic hormones [Feil et al., 1997]. Subsequently, we generated lentiviral vectors, enabling us to express MYC-ER and MYCVD-ER fusion proteins under control of the SFFV promoter.

We performed a number of experiments to confirm the results we had obtained with constitutive high-level expression and validate the ER-fusion proteins as tool for further investigations. Steady state levels of MYC-ER and MYCVD-ER fusion proteins in MCF10A cells were comparable to levels of constitutively SFFV-driven MYC proteins before (compare Fig. 4.8 A with 4.1 C).

Using cycloheximide assays, we calculated the half-life of both fusion proteins after addition of 4-OHT (Fig. 4.8 B). With roughly 27 min, half-lives were identical for MYC-ER and MYCVD-ER and similar to values obtained for endogenous MYC proteins, which are usually reported to lie between 20 and 30 min [Salghetti et al., 1999].

Importantly, addition of 100 nM 4-OHT induced cell death in MYC-ER, but not in MYCVD-ER MCF10A cells (Fig. 4.8 C).

According to a molecular subtype classification that can be used to group normal epithelial cells and breast cancer samples, MCF10A cells cluster with the Basal-like subtype. Hence, they are "triple-negative" and lack expression of both estrogen and progesterone receptor, as well as the receptor tyrosine kinase HER2 [Subik et al., 2010]. Nevertheless, we wanted to exclude unspecific effects of the anti-estrogen 4-OHT in these cells. To this end, control cells, MYC-ER and MYCVD-ER cells were super-infected with a vector encoding the red fluorescent protein (RFP). Next, cells were mixed in a ratio of 60 to 40 % with non-fluorescent control cells and flow cytometry measurements were performed to confirm equal amounts of RFP-positive cells in all conditions. Afterwards, cells were cultured in the presence or absence of 4-OHT and the percentage of RFP-positive cells was monitored over time.

Addition of 4-OHT to control cells had no effect on the growth rate of MCF10A cells (Fig. 4.8 D, compare grey triangle (4-OHT) with grey circle (ethanol control)). Similarly, addition of ethanol ("ctr") to MYC-ER and MYCVD-ER cultures did not change the ratio of non-fluorescent to RFP-positive cells (Fig. 4.8 D, red and blue circle). However, after addition of 4-OHT, the fraction of red cells was decreased by 50 % within four days after MYC-ER activation (Fig. 4.8 D, red triangle), whereas expression of MYCVD-ER seemed to confer only a minor growth disadvantage (Fig. 4.8 D, blue triangles).

Finally, to exclude that MYC-induced apoptosis in MCF10A cells is an artefact of monolayer 2D culture, we used a protocol of three-dimensional basement membrane culture that mimics glandular epithelium morphogenesis *in vivo* [Debnath et al., 2003]. As expected, MCF10A cells formed acinar structures in 3D culture. Intriguingly, activating MYC-ER induced rapid cell death also under these more physiological conditions. Again, cells expressing MYCVD-ER were not affected by addition of 4-OHT (Fig. 4.8 E). In conclusion, also the inducible expression of MYC promotes MIZ1-dependent apoptosis in MCF10A cells.

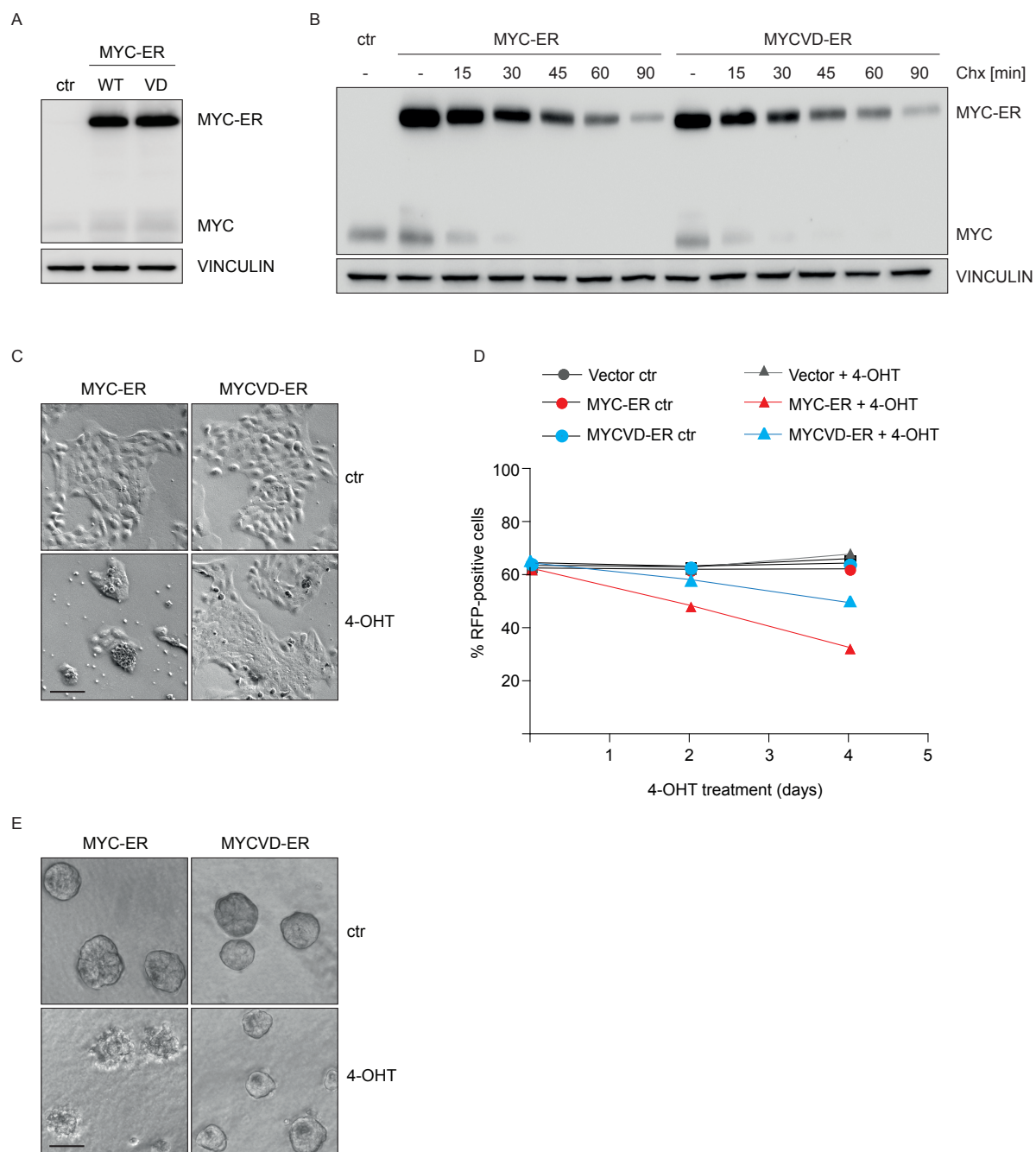


**Figure 4.8: Inducible expression of MYC but not MYC VD increases apoptosis<sup>1</sup>**

- A Immunoblot documenting expression of MYC-ER and MYCVD-ER fusion proteins relative to endogenous MYC in MCF10A cells. VINCULIN was used as loading control.
- B Cycloheximide assay to determine stability of MYC-ER and MYCVD-ER fusion proteins. Cells were treated with 100 nM 4-OHT to activate ER fusion proteins for 1 h and then 100  $\mu$ M cycloheximide (Chx) was added for the indicated time. Cells were harvested and protein expression was analysed. VINCULIN was used as loading control.
- C Morphology of MYC-ER and MYCVD-ER expressing cells treated with 4-OHT or ethanol ("ctr") for 48 h. Bar = 50  $\mu$ m.
- D Color competition assay to document loss of cells expressing active MYC-ER over time. Cells were super-infected with RFP, mixed 60:40 with non-fluorescent control cells and treated with 4-OHT or ethanol. Percentage of RFP-positive cells was measured by FACS on day 2 and 4.
- E Morphology of MYC-ER and MYCVD-ER acini treated with 4-OHT or ethanol ("ctr") for 3 days. Pictures were taken on day 4 of 3D culture. Bar = 50  $\mu$ m.



## 4.2 Characterisation of MYC/MIZ1-mediated apoptosis

MYC-mediated apoptosis has long been studied in both cell culture based and *in vivo* models. In all these systems, a positive correlation between MYC levels and apoptosis rate has been noted [Evan et al., 1992; Murphy et al., 2008]. In addition, multiple ways of how the apoptotic potential of MYC is executed on a molecular level have been proposed, involving either p53-dependent or -independent mechanisms as well as alterations of pro- and antiapoptotic BCL-2 family members [Hoffman and Liebermann, 2008].

However, the contribution of MIZ1 to these processes has not been investigated in detail.

### 4.2.1 MYC/MIZ1-mediated apoptosis is dose-dependent

Incubation of U2OS-MYC-ER cells with low amounts of 4-OHT is sufficient for enhanced S-phase entry, whereas sensitisation to apoptosis only occurs with higher 4-OHT concentrations [Liu et al., 2012b].

To determine the concentration of 4-OHT necessary to induce MYC/MIZ1-dependent apoptosis

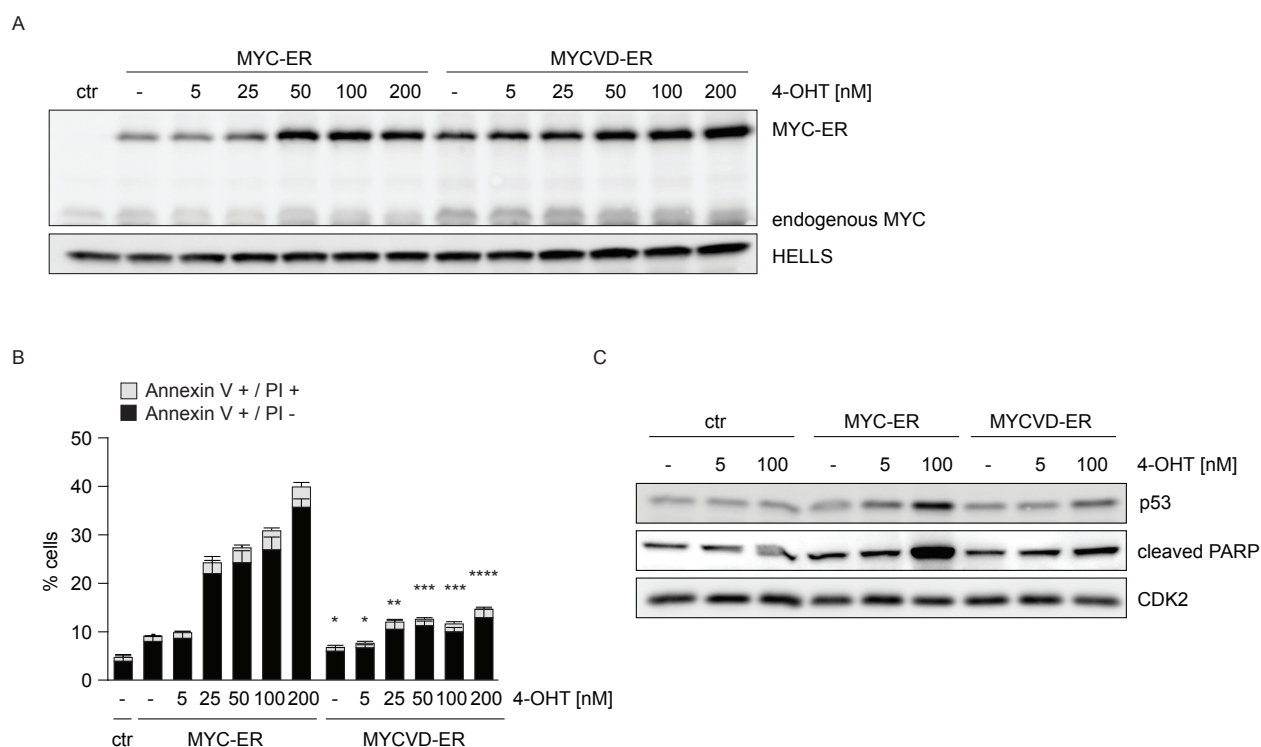


**Figure 4.9: Dose- and MIZ1-dependent induction of apoptosis<sup>1</sup>**

- A Titration of MYC-ER and MYCVD-ER in MCF10A nuclei. Immunoblot documents nuclear expression of fusion proteins and endogenous MYC after treatment with indicated concentrations of 4-OHT for 24 h. HELLS was used as loading control.
- B Annexin V / propidium iodide FACS analysis from cells that were treated as in A, except staining was performed after 48 h of 4-OHT treatment. Bars represent mean + SD of 3 replicates. p-values were calculated with Student's t-test and refer to the difference between MYC-ER and MYCVD-ER (\*:  $p \leq 0.05$ ; \*\*:  $p \leq 0.01$ ; \*\*\*:  $p \leq 0.001$ ; \*\*\*\*:  $p \leq 0.0001$ ).
- C Immunoblot documenting accumulation of p53 and cleaved PARP. Control, MYC-ER and MYCVD-ER cells were treated with ethanol ("-"), 5 or 100 nM 4-OHT for 24 h and whole cell lysates were prepared. CDK2 was used as loading control.

in MCF10A cells, we initially verified that increasing the 4-OHT dose results in an increase in nuclear MYC-ER and MYCVD-ER proteins (Fig. 4.9 A). Of note, a considerable amount of MYC- and MYCVD-ER was already localised inside the nucleus in ethanol treated cells (compare "ctr" with 2nd and 8th lane).

Cell death, as determined by Annexin V / PI FACS analysis, was correlated with nuclear levels of MYC-ER: The apoptotic response paralleled the increasing MYC levels caused by higher concentrations of 4-OHT (Fig. 4.9 B). Intriguingly, in all conditions, levels of apoptosis induced by MYCVD-ER were significantly lower, demonstrating that binding to MIZ1 is critical for apoptosis induction in mammary epithelial cells.

The tumour suppressor p53 is a major mediator of apoptosis in response to virtually all cancer-associated stress stimuli [Bálint E and Vousden, 2001]. Similarly, cleavage of PARP by activated caspase-3 is a hallmark of apoptotic cells. To further quantify apoptotic signalling at different levels of MYC, and assess the difference between WT MYC and MYC VD, we treated control, MYC-ER and MYCVD-ER cells with low (5 nM) and high (100 nM) concentrations of 4-OHT. Subsequently, we analysed accumulation of p53 and cleavage of PARP by Western Blot.

In 4-OHT-treated control cells, neither p53 nor PARP levels were altered (Fig. 4.9 C). High levels of MYC-ER were necessary to induce accumulation of p53 and cleavage of PARP in MCF10A cells. In cells expressing MYCVD-ER at 100 nM 4-OHT, levels of both markers were comparable to MYC-ER cells at 5 nM and hardly above background, again indicating, that MIZ1 might mediate cellular stress responses to increased levels of MYC.

#### 4.2.2 Molecular players involved in MYC-mediated apoptosis

To uncover the reasons for the attenuated apoptotic phenotype of MYC VD, known molecular players of MYC-mediated cell death were investigated.

Increased ARF expression and subsequent p53 stabilisation is the paradigm model of how oncogenic MYC activation results in apoptosis [Zindy et al., 1998]. However, due to a translocation, MCF10A cells have lost the *CDKN2A/B* locus and thus do not express ARF (Fig. 4.10 A and Worsham et al. [2006]). Still, they are able to accumulate high levels of p53 (Fig. 4.9 C). On the other hand, HMLE cells are immortalised by expression of *hTERT*, SV40 small t and large T antigens and should therefore have functionally inactive p53 [Elenbaas et al., 2001]. Yet, both cell lines select against oncogenic MYC levels in a MIZ1-dependent manner (see Fig. 4.7 B).

To formally show that MIZ1-mediated apoptosis is not restricted to MCF10A cells, we first constitutively overexpressed MYC in HMLE cells. As expected, elevated MYC levels in these cells resulted in accumulation of ARF and cell death (Fig. 4.10 B and data not shown). Importantly, although MYC VD levels were higher, this was not sufficient to induce ARF to the same extent. HMLE cells engineered to overexpress MYC-ER also induced apoptosis and this effect was significantly weaker in cells with activated MYCVD-ER, as determined by Annexin V / propidium iodide FACS (Fig. 4.10 C).

Thus, in contrast to the situation in ARF-deficient MCF10A cells which accumulate p53, apoptosis in HMLE cells might involve ARF but is most likely p53-independent. Yet, in response to oncogenic MYC levels both cells induce apoptosis in a MIZ1-dependent manner.

Intracellular stress signals, including oncogenic stress, are not only monitored by ARF and p53, but also by the BCL-2 family of proteins. The balance between pro- and anti-apoptotic family

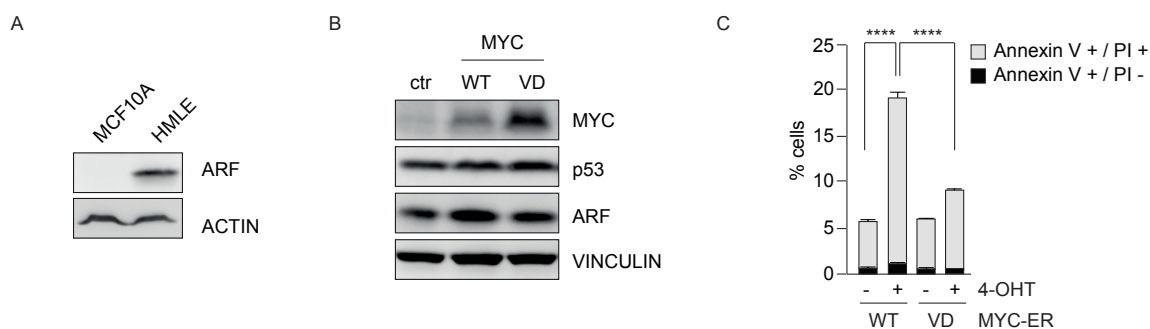


**Figure 4.10: MYC/MIZ1-mediated apoptosis in HMLE cells is p53-independent but could be mediated by ARF<sup>1</sup>**

- A Immunoblot documenting expression of p14<sup>ARF</sup> in MCF10A and HMLE mammary epithelial cells. ACTIN was used as loading control.
- B Immunoblot documenting expression of the indicated proteins in HMLE cells constitutively overexpressing SFFV-driven MYC or MYC VD. VINCULIN was used as loading control.
- C Annexin V / propidium iodide FACS in HMLE cells expressing MYC-ER or MYCVD-ER driven by SFFV. Apoptosis was analysed after 48 h of treatment with 200 nM 4-OHT (mean + SD of 3 experiments, p-values were calculated with Student's t-test).

members constitutes a major checkpoint for life and death decisions that is frequently disrupted during MYC-induced apoptosis.

BIM, a pro-apoptotic member of the family, is a direct target of the transcription factor and a critical mediator of MYC-induced apoptosis in different animal models [Egle et al., 2004; Muthalagu et al., 2014]. In addition, a MIZ1-dependent role for MYC in decreasing the anti-apoptotic buffer by repression of *BCL2* has already been demonstrated [Patel and McMahon, 2007].

To examine modulations in levels of different pro- and anti-apoptotic proteins after MYC overexpression in more detail, MYC-ER and MYCVD-ER pools were treated with 4-OHT for either 24 or 96 h.

As a first step, we analysed protein expression of BIM and p53. The largest of the three BIM isoforms, BIM-EL, was induced 2-fold after 4-OHT treatment. (Fig. 4.11 A). The other isoforms were not as abundant, however, a slight increase could also be detected. In addition, a robust accumulation of p53 was observed. The increase in total p53 levels was not accompanied by an additional increase in phosphorylation of serine 15 ("p53 P-S15"), suggesting that p53 stabilisation is not mediated via DNA damage-induced pathways.

After four days of MYC induction, cells still displayed elevated p53 protein levels and a slight increase in BIM protein levels (Fig. 4.11 B).

Compared to WT MYC, effects on BIM and p53 after 24 h were weaker when MYCVD-ER was active. This was also the case for p53 induction after four days, when the difference between MYC WT and VD was even more pronounced. However, at day 4, MYCVD-ER cells treated with 4-OHT induced BIM to a stronger extend than corresponding MYC-ER pools. Strikingly, similar to the loss of WT MYC over time (Fig. 4.7 B), also MYC-ER expression was counterselected and barely visible after 4 days of 4-OHT treatment. MYCVD-ER levels, despite the robust induction of BIM, were unaltered, which could indicate that higher BIM levels are better tolerated in the context of MYC VD.

To detect alterations in levels of several other BCL-2 family members, we extracted RNA from MYC-ER and MYCVD-ER cells after a 24 h 4-OHT treatment and determined the expression by qRT-PCR.

In contrast to the situation in fibroblasts, *BCL2* was not repressed by MYC induction in mam-

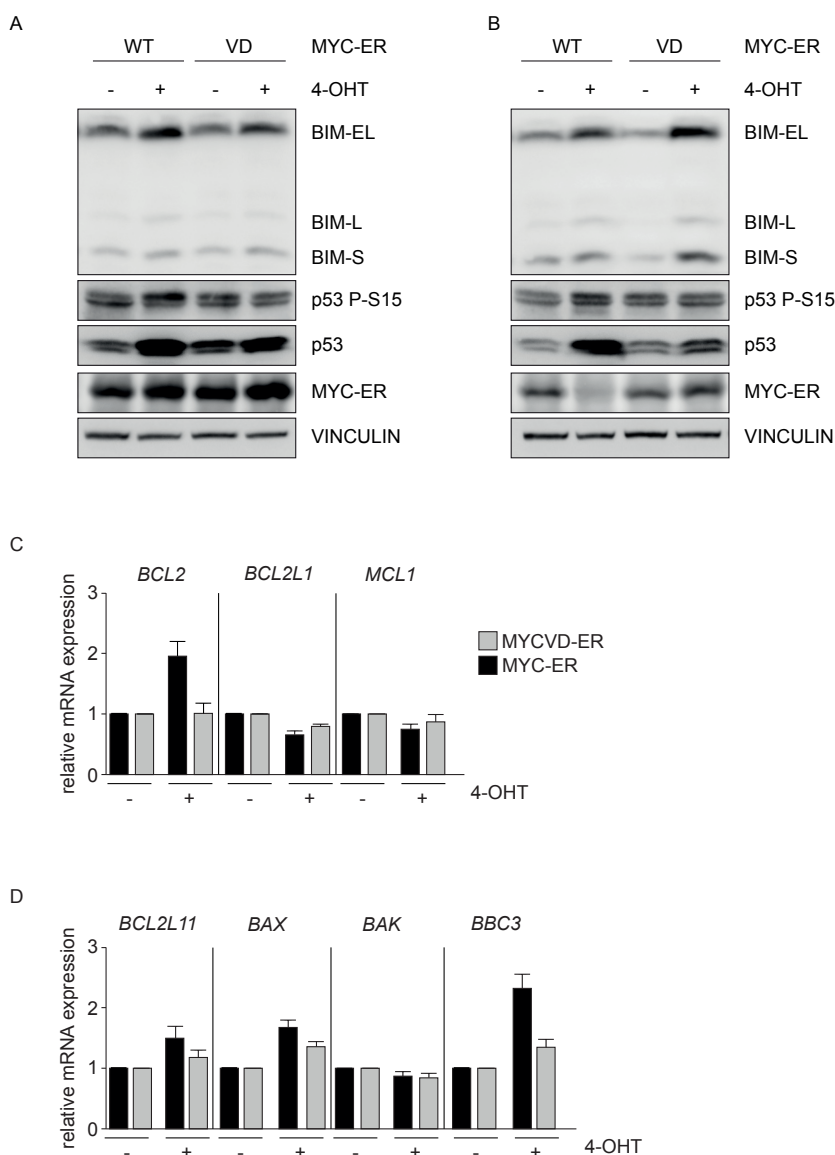


**Figure 4.11: Differential induction of p53 between MYC-ER and MYCVD-ER<sup>1</sup>**

- A Immunoblot documenting expression of the indicated proteins in MYC-ER or MYCVD-ER cells after 24 h of 4-OHT treatment. VINCULIN was used as loading control.
- B Same as in A, except that lysates were prepared after 96 h of 4-OHT treatment.
- C Expression analysis of anti-apoptotic BCL-2 family members. Same cells as in A were treated for 24 h with 200 nM 4-OHT and total RNA was isolated. cDNA was analysed via qRT-PCR with primers specific for the indicated genes. Values were normalised to *RPS14* and represented as relative expression compared to the respective control cells (mean + SEM of 4 independent biological experiments).
- D Same samples and analysis as in C, except here expression of pro-apoptotic family members is shown.

mary epithelial cells. Instead, the mRNA was consistently induced in several experiments (Fig. 4.11 C) which was not observed when MYCVD-ER was activated. Similar to results in myeloid and lymphoid progenitors, *BCL2L1* which encodes BCL-XL, was repressed by MYC about 1.5-fold, but there was no significant difference to MYC VD [Eischen et al., 2001b]. Comparable results were obtained for the *MCL1* mRNA (Fig. 4.11 C).

Analysis of mRNA expression levels of pro-apoptotic family members revealed a weak induction of *BCL2L11* by MYC-ER, consistent with the results on BIM protein levels (Fig. 4.11 D). Whereas *BAK* expression was not altered, we observed an induction of two other targets, *BBC3*, coding for PUMA, and *BAX*. This induction was impaired in the presence of MYCVD-ER. As

both of these genes are also targets of p53, the results are consistent with the differential accumulation of p53 protein in MYC WT and VD cells.

In summary, overexpression of MYC-ER seems to alter the expression of both pro- and anti-apoptotic BCL-2 family members in favour of apoptosis. Furthermore, differential stabilisation and activation of p53 is a constant feature that helps to explain the phenotypic differences between MYC WT and VD.

### Restoring the balance of pro- and anti-apoptotic BCL-2 family members

To test whether the observed changes in ratios between different BCL-2 family members are necessary to induce apoptosis in response to high levels of MYC, we manipulated the balance by either alleviating the pro-apoptotic load or restoring the anti-apoptotic buffer. In particular, we tested whether MYC-induced apoptosis in MCF10A cells can be rescued by decreasing levels of BIM or elevating levels of BCL-2, respectively.

Lentiviral shRNA-mediated depletion of BIM in MYC-ER MCF10A cells was confirmed on protein level (Fig. 4.12 A). Treatment with 4-OHT resulted in a robust induction of BIM that could be decreased to background levels with the shRNA. Annexin V / PI stainings revealed that background apoptosis was lower after knockdown of BIM. Moreover, after treatment with

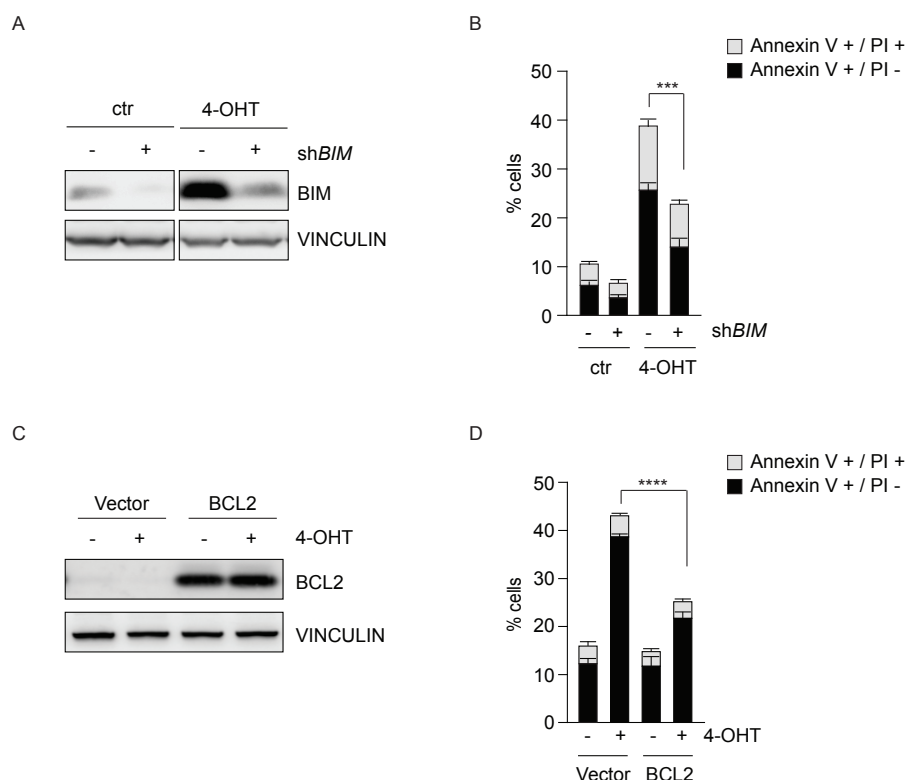


**Figure 4.12: Apoptosis is rescued by knockdown of BIM or overexpression of BCL-2<sup>1</sup>**

- A Immunoblot documenting knockdown of BIM. MYC-ER MCF10A cells were superinfected with lentiviral shRNA vectors targeting luciferase ("ctr") or *BIM*. Cells were treated with 4-OHT for 48 h. VINCULIN was used as loading control. Note that 4-OHT and control panels are from the same exposure on one membrane.
- B Annexin V / propidium iodide FACS measurements were performed after 48 h 4-OHT treatment with cells described in A (n=3; p-value obtained by Student's t-test; \*\*\*:  $p \leq 0.001$ ).
- C Immunoblot confirming BCL-2 overexpression after superinfection of MYC-ER MCF10A cells with retroviral control or BCL-2 expression vectors.
- D Annexin V / propidium iodide FACS to measure apoptosis in cells from C. Cells were treated 48 h with 4-OHT before FACS measurement (n=3; \*\*\*\*:  $p \leq 0.0001$ ).

4-OHT, the amount of MYC-induced apoptosis in the absence of BIM was significantly reduced by 20% but could not reach background levels (Fig. 4.12 B).

Overexpression of BCL-2 in MYC-ER cells was confirmed by Western blot (Fig. 4.12 C). Expectedly, treatment with 4-OHT resulted in a 3-fold increase in apoptosis. This response was significantly attenuated in cells overexpressing BCL-2 (Fig. 4.12 D).

In summary, although apoptosis could not be abolished completely, altering the stoichiometry of BCL-2 family members can significantly rescue MYC-induced apoptosis in MCF10A cells.

### Rescue by knockdown of p53

Depending on cell type and apoptotic stimulus, MYC-induced apoptosis can be either p53-dependent or -independent. Because a differential effect on p53 protein levels and target gene activation had been observed between MYC-ER and MYC-VDER (Fig. 4.11), the effect of targeted p53 depletion was investigated in MYC-ER cells.

Knockdown of p53 was achieved by lentiviral shRNA in MCF10A cells overexpressing MYC-ER. Initially, knockdown efficiency was confirmed on RNA level (Fig. 4.13 A, left panel). Reduction of p53 was functional, because a 2-fold reduction in target gene levels relative to cell expressing an shRNA against luciferase ("ctr") could be observed already under non-stressed conditions (Fig. 4.13 A, right panel). When MYC-ER cells expressing the control shRNA were treated with 4-OHT and analysed by flow cytometry, more cells stained positive for Annexin V and propidium iodide, as was detected before. Strikingly, the apoptotic response was almost completely

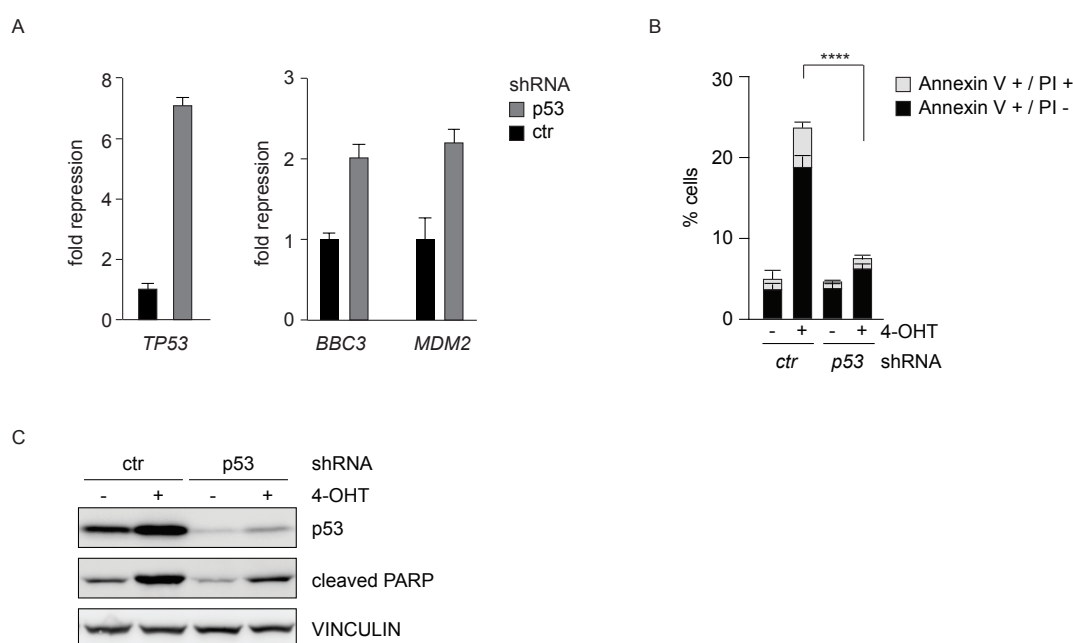


**Figure 4.13: Apoptosis is rescued by knockdown of p53<sup>1</sup>**

A Left panel: Relative *TP53* mRNA levels in MCF10A MYC-ER cells, superinfected with lentiviral shRNA vectors targeting luciferase ("ctr") or p53. Right panel: Relative mRNA levels of two p53 target genes, *BBC3* (PUMA) and *MDM2* in the same cells. Data are represented as fold repression relative to control cells and were normalised to *RPS14* (mean + SD of technical triplicates).

B Cells used in A were treated with ethanol or 4-OHT for 24 h and stained with Annexin V/ propidium iodide to measure apoptosis by FACS (mean + SD of n = 3 experiments). p-value stating significance of rescue effect was calculated with Student's t-test (\*\*\*\*;  $p < 0.0001$ ).

C Cells were treated like in B. Immunoblots document expression of the indicated proteins. VINCULIN was used as loading control.

abrogated when p53 was absent (Fig 4.13 B).

Comparable results were obtained when cells were analysed by Western blot for the presence of cleaved PARP, a marker of apoptotic cells (Fig. 4.13 C): In MYC-ER cells expressing the luciferase shRNA, 4-OHT treatment induced accumulation of p53 as well as cleavage of PARP. The shRNA against p53 reduced the amounts of p53 protein as expected. With addition of 4-OHT, there was still an increase in p53 and the cleaved form of PARP, however, levels were almost as low as in control shRNA infected cells without 4-OHT.

Taken together, MYC-induced apoptosis in MCF10A cells is dependent on p53.

### Rescue by abrogation of transcriptional activity

Apart from a few exceptions, virtually all known functions of MYC require dimerisation with MAX and target gene regulation mediated by DNA-binding [Eilers and Eisenman, 2008].

To validate that transcriptional activity of MYC is necessary for MYC/MIZ1-mediated apoptosis in MCF10A cells, we tested two transcription-deficient mutants of MYC: MYC  $\Delta$ BR, which lacks the basic region and is hence not able to bind DNA, and MYC D, a triple-phospho-mimic mutant (T358D/S373D/T400D) that is impaired in DNA- as well as MAX-binding [Chen et al., 2010a; Huang et al., 2004].

MCF10A cells were transduced with SFFV-driven constitutive vectors to overexpress WT MYC, MYC  $\Delta$ BR and MYC D. Western blot analysis confirmed that wildtype and mutants were expressed at comparable levels (Fig. 4.14 A). When lysates were probed for presence of cleaved PARP, only cells expressing WT MYC showed an induction relative to control cells. Furthermore, while there was a significant increase in apoptotic cells with MYC WT,  $\Delta$ BR MYC was completely incapable of apoptosis induction (Fig. 4.14 B). Consistent with absence of cleaved PARP, apoptosis in cells expressing the phospho-mutant MYC D was barely above background.

In a second approach, MYC-ER and MYCVD-ER pools were superinfected with an inducible shRNA against MAX. Addition of doxycycline reduced endogenous MAX protein to approximately 50 % (Fig. 4.14 C). In MYC-ER cells, addition of 4-OHT resulted in accumulation of cleaved PARP, which was reduced when MAX was depleted. Interestingly, activation of MYCVD-ER cells induced only a minor change in PARP levels, which was completely abolished in the absence of MAX. Identical results were obtained when Annexin V staining was used as a readout for apoptosis (Fig. 4.14 D).

In conclusion, apoptosis induction by oncogenic levels of MYC in MCF10A cells is most likely a response that is triggered by changes in transcriptional regulation of target genes.

## 4.3 MIZ1-dependent transcriptional changes

To gain a comprehensive overview of global gene expression changes in response to supra-physiological levels of MYC and MYC VD, we performed microarray analysis in MCF10A cells. Triplicate biological infections of MYC-ER and MYCVD-ER cells were treated with 100 nM 4-OHT or ethanol for 24 h and total RNA was sent to the Microarray Unit at the Institute of Molecular Biology and Tumor Research (IMT, Marburg, Germany), where samples were analysed on an Agilent-based DNA Microarray platform by Dr. Michael Krause.

Data processing, normalisation and generation of log<sub>2</sub>-transformed lists representing ratios of

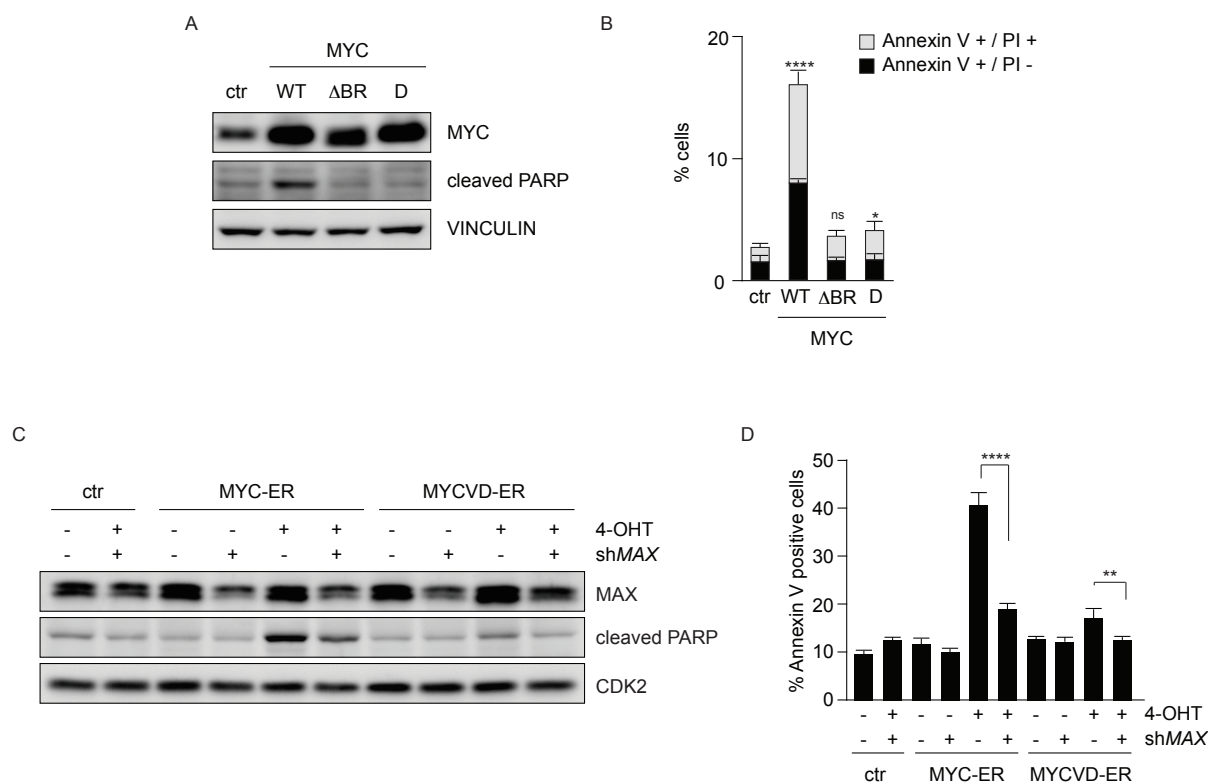


**Figure 4.14: Apoptosis is rescued by knockdown of MAX or inhibition of DNA binding<sup>1</sup>**

- A Immunoblot to document expression of different MYC mutants. MCF10A cells were transduced with constitutive SFFV-driven expression vectors, coding for MYC WT, MYC  $\Delta$ BR, which lacks the basic region, or MYC D, a triple-phospho mutant defective in both DNA-binding and binding to MAX. VINCULIN was used as loading control.
- B Annexin V / propidium iodide FACS to measure apoptosis of cells described in A ( $n = 3$ ;  $p$ -value was calculated with Student's  $t$ -test; ns:  $p > 0.05$ ; \*:  $p \leq 0.05$ ; \*\*\*\*:  $p \leq 0.0001$ ).
- C MCF10A cells expressing either control vector, MYC-ER or MYCVD-ER were superinfected with a doxycycline-inducible shRNA targeting MAX. Where indicated, cells were treated with Dox for 24h ("+" shMAX), then ER-fusion proteins were activated by addition of 4-OHT (200 nM). After 48 h, protein lysates were prepared. CDK2 was used as loading control.
- D Cells were treated as in A, except that Annexin V staining was performed to measure apoptotic cells by flow cytometry. Propidium iodide staining had to be omitted due to red fluorescence of the lentiviral shRNA vector used. Graph shows mean + SD of 3 experiments ( \*\*:  $p \leq 0.01$ ; \*\*\*\*:  $p \leq 0.0001$ ).

each sample versus a pooled reference were carried out by Lukas Rycak.

Comparison of significantly regulated Agilent probe identifiers (probe IDs) between MYC-ER and MYCVD-ER (log<sub>2</sub>FC 4-OHT versus control) revealed, that 2,278 probe IDs were regulated significantly in both sets ( $p \leq 0.05$ , Fig. 4.15 A). Surprisingly, this overlap was rather low, considering that MYC-ER regulated 5,568 probe IDs, whereas MYCVD-ER regulated 4,849 probe IDs in total. We assumed this discrepancy was more likely due to technical reasons (e.g. A-value threshold) than a true biological phenotype. Therefore, we went on to analyse the regulation of joint probe IDs: 1,243 were activated by MYC-ER relative to controls, and 1,035 were repressed (Fig. 4.15 B, left panel for activated, right panel for repressed probe IDs). All probes except 21 were also activated in response to MYCVD-ER, corresponding to 1,195 activated genes. For repressed probes, 978 of the 1,035 were also regulated by MYCVD in the same direction, which yielded a total number of 971 repressed genes.

To correlate the strength of gene regulation between WT and VD, log<sub>2</sub> fold changes (4-OHT versus control) of significantly regulated joint probe IDs were plotted (Fig. 4.15 C). As indicated



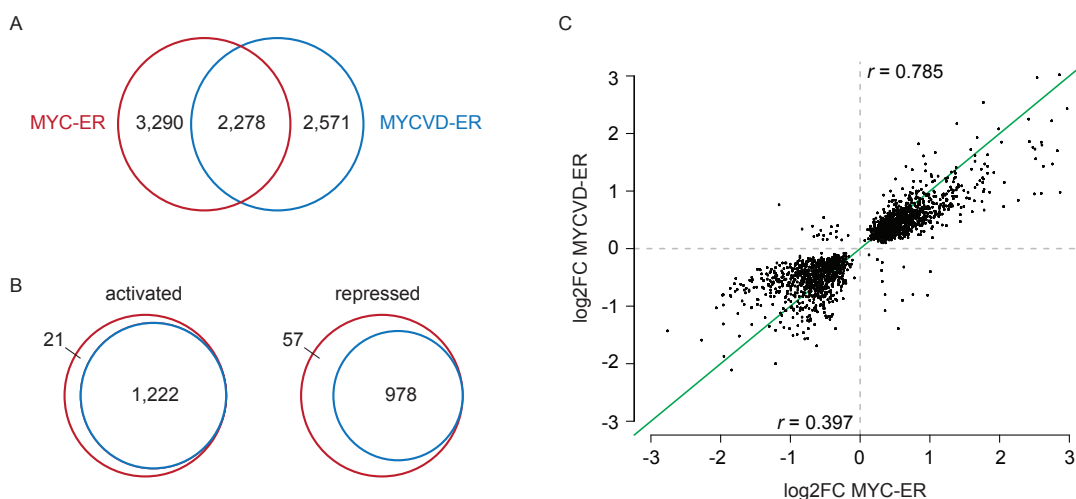


**Figure 4.15: Identification of MIZ1-dependent transcriptional changes<sup>1</sup>**

- A Venn diagram illustrating overlap of significantly regulated ( $p \leq 0.05$ ) Agilent probe IDs from microarray analysis of MCF10A MYC-ER (4-OHT and control) and MYCVD-ER (4-OHT and control) cells. Log<sub>2</sub> fold changes (4-OHT versus control) and p-values were generated with Agilent Feature Extraction software by Lukas Rycak. Three biological replicates of each condition were analysed. Red: Probe IDs with significant log<sub>2</sub> fold change (log<sub>2</sub>FC) in 4-OHT treated relative to control MYC-ER cells (5,568 in total). Blue: Probe IDs with significant log<sub>2</sub>FC in 4-OHT treated relative to control MYCVD-ER cells (4,849 in total). 2,278 probe IDs were jointly regulated (overlap).
- B Regulation of jointly regulated probe IDs. Left panel: Overlap of MYC-ER activated probe IDs (1,243 in total, red) with probe IDs activated by MYCVD-ER (blue). Right panel: Overlap of probe IDs that are repressed by MYC-ER relative to control (1,035 in total, red), with MYC VD (blue).
- C Dot plot of jointly regulated probe IDs to compare MYCVD-ER and MYC-ER induced transcriptional changes. Y-axis displays log<sub>2</sub>FC of 4-OHT versus control treated MYCVD-ER cells for every probe ID. X-axis shows the same in MYC-ER cells. Pearson's correlation coefficient  $r$  is indicated for activated and repressed genes, respectively. Green line with slope of 1 is drawn to simulate a hypothetical perfect correlation.

by a correlation coefficient of 0.785, the ability of MYC VD to activate target genes was very similar to that of wildtype MYC. Strikingly, MYC VD appeared to be selectively compromised in gene repression, which was reflected in a low Pearson correlation of 0.397. Furthermore, when the slopes of separate regression lines for activated or repressed genes were calculated, they differed significantly (0.68 versus 0.35;  $p < 2.2 \times 10^{-16}$ ), highlighting that the intensity of regulation by MYCVD-ER is lower especially for repressed genes.

### 4.3.1 MIZ1-dependent repression of target genes

Instead of examining the expression changes of individual genes, more unbiased approaches to interpret microarray data are available. For example, unfiltered expression datasets can be analysed by testing whether certain signalling pathways or groups of functionally related genes are statistically overrepresented in a certain phenotype. A collection of different curated gene sets, containing pathways, published transcription factor target genes as well as gene signatures identified by previous microarray studies, is compiled in the "Molecular Signatures Database" ([www.broadinstitute.org](http://www.broadinstitute.org)). This collection can be used with a software called Gene Set Enrichment Analysis (GSEA) to determine whether a particular gene set shows a statistically significant difference between two expression datasets [Mootha et al., 2003; Subramanian et al., 2005].

We separately performed GSEA with datasets from either MYC-ER or MYCVD-ER expressing cells (4-OHT versus control). As indicated by a positive normalised enrichment score (NES), MYC and MYC VD activated genes in MCF10A cells were similar to previously published MYC

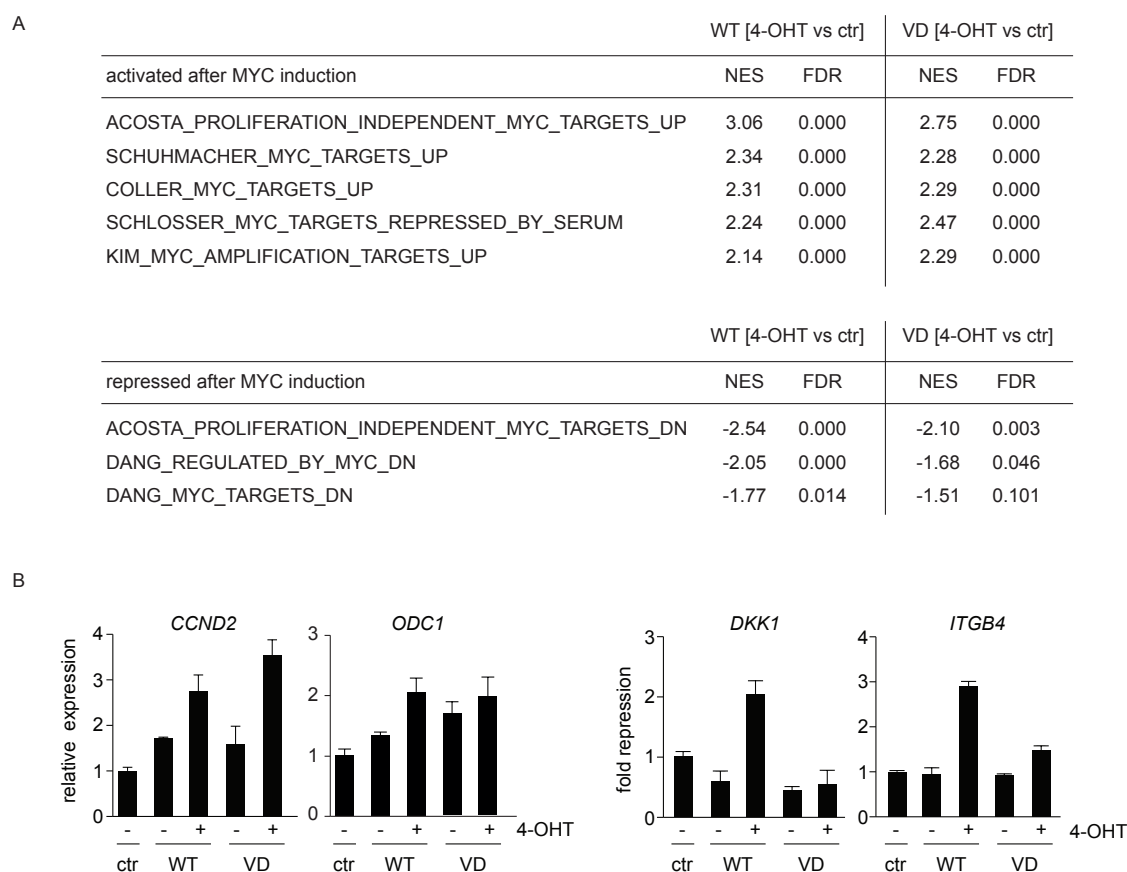


**Figure 4.16: MYC VD is selectively impaired in gene repression<sup>1</sup>**

- A Table summarising results of Gene Set Enrichment Analyses (GSEA) performed with either MYC-ER ("WT") or MYCVD-ER ("VD") expression datasets. Upper part: Selected examples of significantly enriched, previously published MYC-activated gene sets. Lower part: Selected examples of published sets containing repressed MYC target genes, that are also significantly repressed in MYC-ER cells. NES: normalised enrichment score; FDR: false discovery rate.
- B qRT-PCRs of selected MYC-activated (left 2 panels) and MYC-repressed (right 2 panels) target genes in response to 4-OHT treatment of either MYC-ER or MYCVD-ER cells. CT-values of technical triplicates were normalised to *RPS14* and are displayed relative to empty vector control cells ("ctr") as "relative expression" for activated genes and "fold repression" for repressed genes, respectively.

target genes from different studies (Fig. 4.16 A, upper part, e.g. from Acosta et al. [2008]; Schuhmacher et al. [2001]). Whereas, on average, enrichment scores were the same for activated genes, gene sets usually repressed after MYC induction had lower enrichment scores in MYCVD-ER cells (Fig. 4.16 A, lower part, e.g. Zeller et al. [2003]).

In summary, MYCVD-ER is compromised in repression of standard MYC targets.

To validate the selective impairment of MYC VD to repress genes, relative mRNA levels of *CCND2*, *ODC1*, *DKK1* and *ITGB4* were measured after 24 h of 4-OHT treatment in MYC-ER and MYCVD-ER MCF10A cells. The first two genes represent standard activated target genes, the latter two are generally repressed by MYC. In agreement with the microarray analysis, activation of target genes was similar, whereas repression by MYC VD was severely attenuated (Fig. 4.16 B).

These findings are consistent with the model, that MYC-dependent repression of target genes requires MIZ1.

### Elevated levels of MYC are required for MIZ1-dependent repression

Apoptosis in MCF10A cells occurs as a response to elevated MYC levels and MYC VD shows a significantly attenuated phenotype (see Fig. 4.9). If MIZ1-mediated repression of target genes was, at least in part, responsible for that phenotype, it should only occur at high levels of MYC WT and not with MYC VD.

To further investigate whether repression correlated with induction of apoptosis by MYC, we generated a list of genes that are differentially repressed between WT and VD. When mRNA levels of some of these genes were examined after MYC-ER activation, repression was observed predominantly with 100 nM 4-OHT (Fig. 4.17 A). Activation with 5 nM had only mild effects on the same genes. Importantly, treatment of MYCVD-ER cells with high concentrations of 4-OHT affected all target genes only weakly, in a magnitude similar to low level activation of the wildtype protein.

Gene ontology (GO) terms are used to group genes according to their molecular functions or the biological processes they belong to. To identify which processes are target of MYC/MIZ1-mediated repression, we performed an enrichment analysis of functional annotations with the list of differentially repressed genes, using DAVID bioinformatic tools [Huang et al., 2009]. Processes repressed by MYC in a MIZ1-dependent manner included angiogenesis, differentiation, migration, adhesion and the regulation of apoptosis (Fig. 4.17 B). Almost all of these functions have been described before to be repressed by MYC and for some of them the involvement of MIZ1 has already been demonstrated [Herkert and Eilers, 2010; Gebhardt et al., 2006].

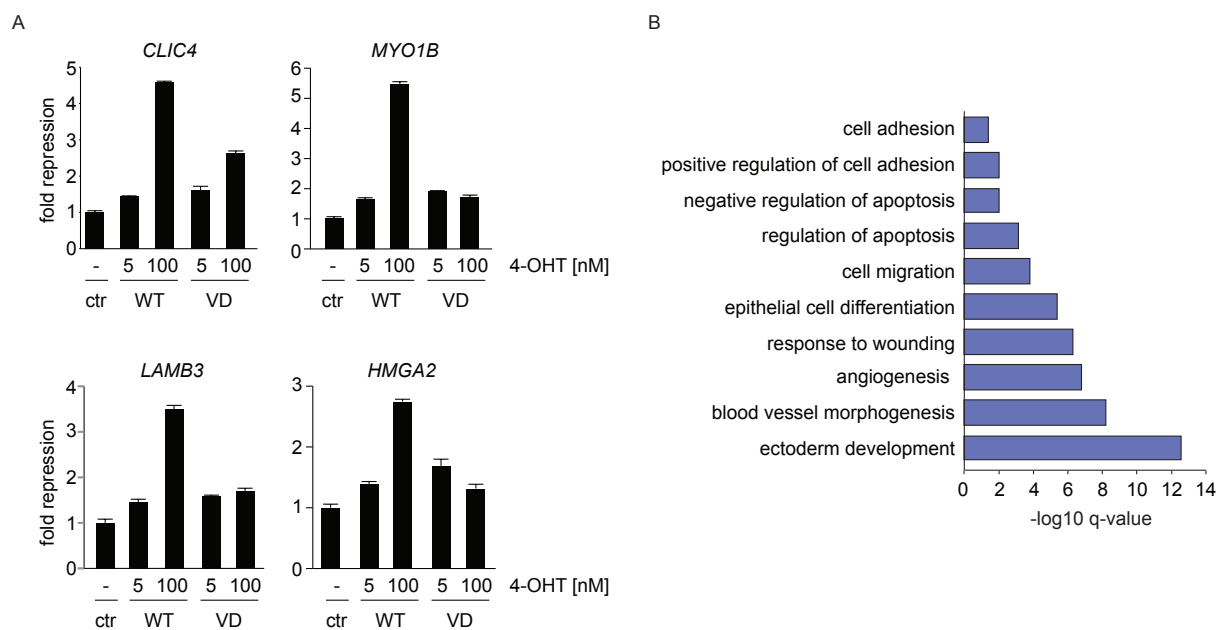


**Figure 4.17: MIZ1-mediated repression occurs at high levels of MYC<sup>1</sup>**

A qRT-PCRs of the indicated genes in MYC-ER and MYCVD-ER cells after exposure to low (5 nM) and high (100 nM) concentrations of 4-OHT. Values were normalised to *RPS14* and represent fold repression relative to empty vector control cells (mean + SD of technical triplicates, representative of 2 biological experiments).

B Functional classes of differentially repressed genes. A list of genes less repressed by MYCVD-ER than by MYC-ER ( $p \leq 0.05$  and  $\log_2\text{FC} \leq -0.5$  for WT, with a difference of  $\log_2\text{FC} \geq 0.5$  to VD) was used to perform a gene annotation enrichment analysis using DAVID. Top 10 enriched processes are shown. Significance is indicated by  $-\log_{10}$  q-values (Benjamini) from DAVID output.

### Effect of MYC VD on MYC repressed genes mimics MIZ1 depletion

Directly testing the role of endogenous MIZ1 for MYC-mediated repression in MCF10A cells was not possible because depletion of MIZ1 was unfortunately not tolerated by MCF10A cells (data not shown). Therefore, we used previously published RNA-sequencing data from U2OS cells where similar effects of MYC VD and depletion of MIZ1 on MYC-repressed target genes had been demonstrated [Walz et al., 2014].

We first analysed whether MYC repressed similar genes in a MYC VD dependent manner in mammary epithelial cells and the U2OS osteosarcoma cell line. Using the same criteria for

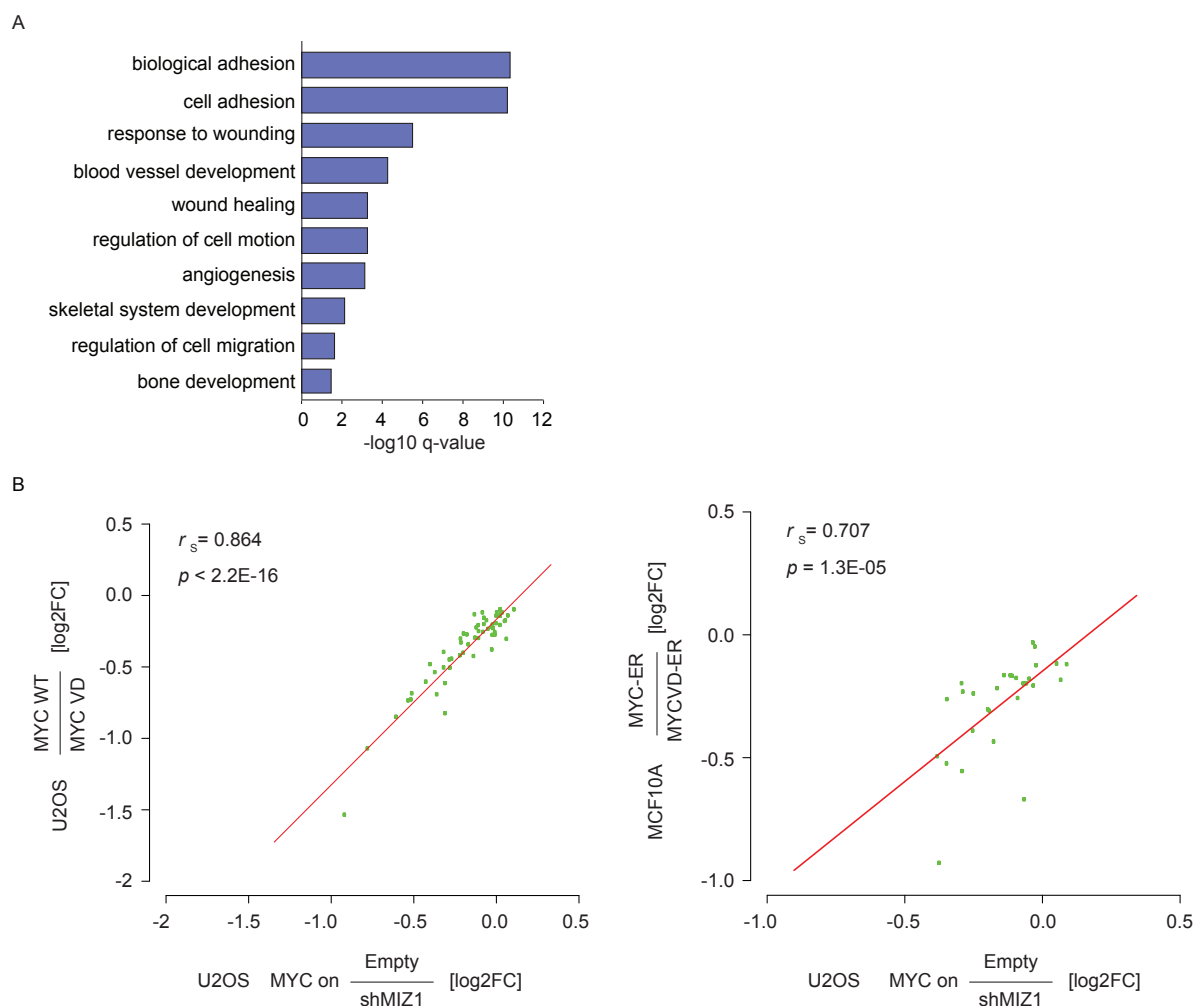


**Figure 4.18: Overexpression of MYC VD and MIZ1 depletion have similar effects on MYC target genes<sup>1</sup>**

- A Differentially repressed genes belong to similar functional classes in different cell types. The same selection criteria as in Fig. 4.17 B were applied to an RNA-seq dataset obtained from U2OS cells overexpressing MYC WT and MYC VD [Walz et al., 2014] and DAVID analysis was performed. Significance is indicated by  $-\log_{10} q\text{-values}$  (Benjamini).
- B Left panel: Effect on MYC-repressed genes in the presence of MYC VD (y-axis) or after depletion of MIZ1 (x-axis) in U2OS cells. Raw data were taken from [Walz et al., 2014]. For all genes repressed by MYC, the ratio of fold changes in WT versus VD situation was calculated and  $\log_2$  transformed. Data were merged with a second list from U2OS cells overexpressing MYC WT together with a control shRNA or an shRNA against MIZ1. Again, the ratio of fold changes was calculated, this time from control versus shMIZ situations. Data were sorted according to strength of repression, grouped into 58 bins of 70 genes each (green dots) and then plotted. Regression line is shown in red. p-value indicates significance of Spearman's rank correlation  $r_s$ . Right panel: Same analysis as before, except MYC-ER versus MYCVD-ER ratios from MCF10A cells were used (y-axis) and correlated with MYC repressed genes in the context of MIZ1-depletion from the second U2OS dataset (x-axis). Genes were grouped into 30 bins with 70 genes each.

differential repression between MYC WT and MYC VD, the overlap of genes between the two cell lines yielded only 95 genes (data not shown). However, when differentially repressed genes in U2OS cells were used in a DAVID analysis, enriched GO terms were almost identical to the results obtained in MCF10A cells (Fig. 4.18 A, compare with 4.17 B). Taken together, even though individual genes repressed by MYC are most likely cell type specific, repressed genes seem to belong to conserved molecular processes.

Next, we partially reproduced an analysis performed by Walz et al. [2014] in U2OS cells to show, that for all genes repressed by MYC, reduced repression in the context of MYC VD is correlated with reduced repression seen in MYC overexpressing cells depleted of MIZ1 (Fig. 4.18 A, left panel). Using the same method, genes repressed by MYC in MCF10A cells were analysed: The ratio of fold changes in MYC-ER and MYCVD-ER situations was calculated and log<sub>2</sub> transformed. Using the RNA-sequencing data from MYC-overexpressing U2OS cells, the ratio of control shRNA versus MIZ1 shRNA was calculated the same way. Common genes were ranked according to the strength of repression by MYC in MCF10A cells. To reduce noise and visualise potential trends, genes were combined in 30 groups of 70 genes ("bins") and plotted (Fig. 4.18 B, right panel). The magnitude of de-repression observed in U2OS cells after MIZ1 knockdown was significantly correlated with reduced repression in MCF10A cells expressing MYCVD-ER, thereby suggesting that impaired repression by the mutant is based on its disability to bind MIZ1.

#### 4.4 Chromatin binding of MYC/MIZ1 complexes

The structural view of the MYC/MAX dimer indicates that mutation of valine 394 to aspartate in MYC ("VD") should not affect binding to MAX or to DNA, as it localises to the outside of the helix-loop-helix domain (see Fig. 1.6 and Wiese et al. [2013]). However, the interaction of MYC VD with chromatin had not been analysed in detail so far.

To investigate DNA binding properties of MYC-ER, MYCVD-ER and MIZ1 in MCF10A cells, we performed chromatin immunoprecipitation (ChIP) experiments with anti-ER, anti-MIZ1 or control antibodies under different experimental conditions: Chromatin was isolated from control cells as well as from cells overexpressing MYC-ER and MYCVD-ER fusion proteins with or without 4-OHT treatment (see Fig. 4.19 A for expression levels of MYC-ER and endogenous MIZ1). Analysis of the strongly bound MYC target *GNL3* revealed, that MYC-ER and MYCVD-ER were both recruited to the transcriptional start site of this gene after addition of 4-OHT, however, a small enrichment was already observed in ethanol-treated conditions. Importantly, binding of MYCVD-ER to DNA appeared to be weaker (Fig. 4.19 B, upper left panel). Endogenous MIZ1 was not detectable at the *GNL3* promoter but was enriched under all experimental conditions at the *MRPS23* promoter (Fig. 4.19 B, upper right panel). Neither ER fusion proteins nor MIZ1 were significantly enriched at an intergenic control region, documenting specificity of the ChIP results (Fig. 4.19 B, lower panel).

To investigate more thoroughly the difference in binding affinity between MYC-ER and MYCVD-ER, we verified that expression levels of MYC-ER and MYCVD-ER upon 4-OHT addition were equal in MCF10A nuclei, when lysates were prepared with the same buffers as used for the ChIP assays (Fig. 4.20 A).

Upon overexpression of MYC, endogenous *MYC* expression is repressed via negative feedback

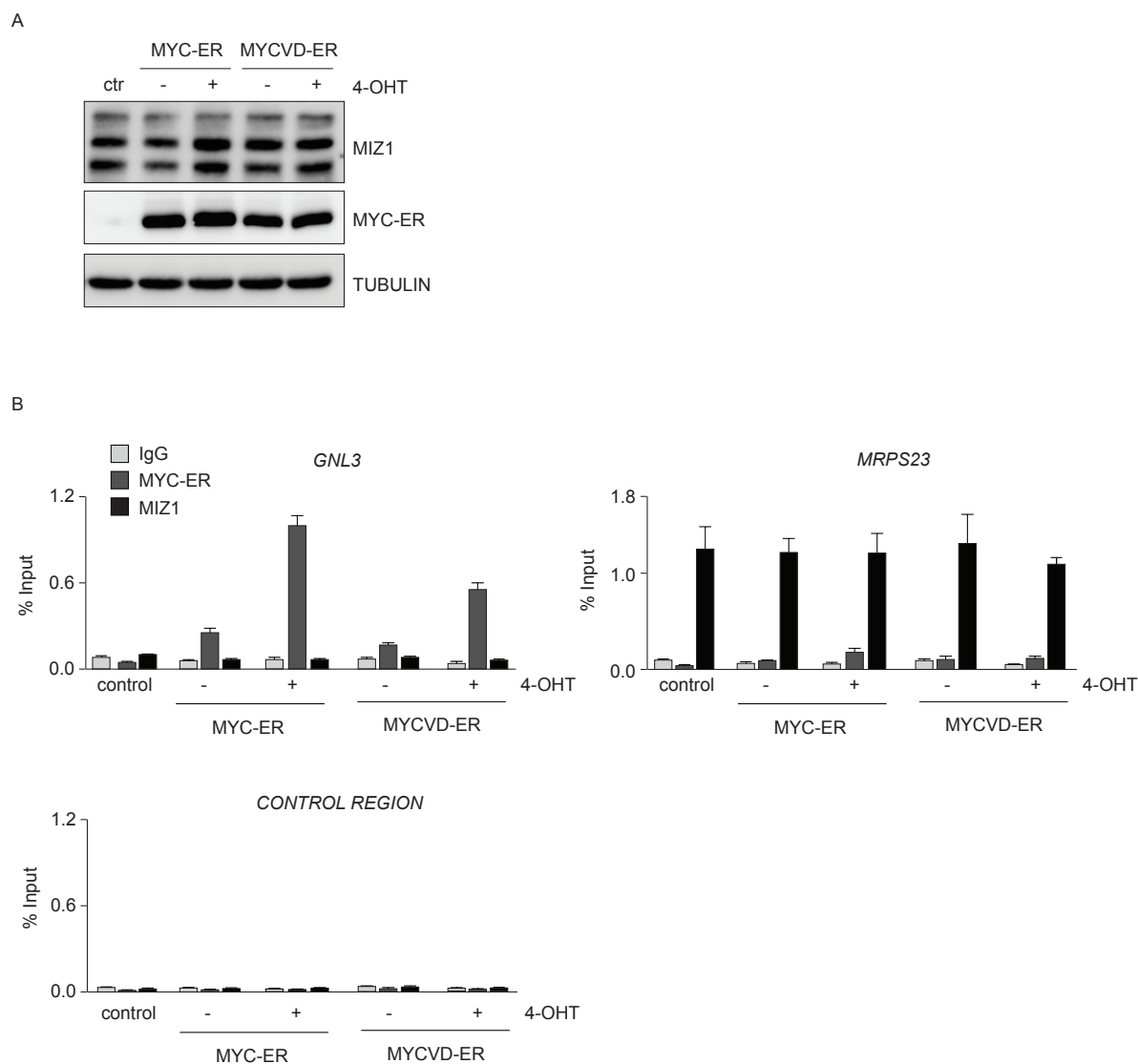


**Figure 4.19: DNA binding of MYC-ER and MIZ1<sup>1</sup>**

A Immunoblot documenting expression of MYC-ER and MYCVD-ER fusion proteins as well as endogenous MIZ1 in MCF10A cells. TUBULIN was used as loading control.

B ChIP to analyse DNA binding of ER fusion proteins and endogenous MIZ1. Chromatin was isolated from MCF10A control cells and cells overexpressing MYC-ER or MYCVD-ER. Where indicated, cells were treated for 1 h with 4-OHT. IPs were performed using control antibody ("IgG"), an antibody against MIZ1 or the ER-moiety and binding to promoters of the *GNL3* and *MRPS23* genes or an intergenic control region was analysed by qPCR. Data are presented as percentage of input DNA (mean + SD of technical triplicates).

regulation [Penn et al., 1990; Grignani et al., 1990]. In our experimental system, ER fusion proteins would have to compete with endogenous MYC at target sites. Therefore, one reason for the observed attenuated binding of MYCVD-ER to the *GNL3* promoter could be that endogenous MYC cannot be displaced as effectively as by the wildtype protein.

To prevent competition with endogenous MYC at promoters, MCF10A cells were starved for 24h. Under these conditions, endogenous MYC cannot be detected by Western Blot anymore (data not shown). ER fusion proteins were activated by addition of 4-OHT and ChIP experiments were carried out as described before. Analysis of several standard MYC targets revealed that binding of MYCVD-ER was weaker at all promoters (shown for *GNL3*, *NCL* and *FBXW8* in Fig. 4.20 B).

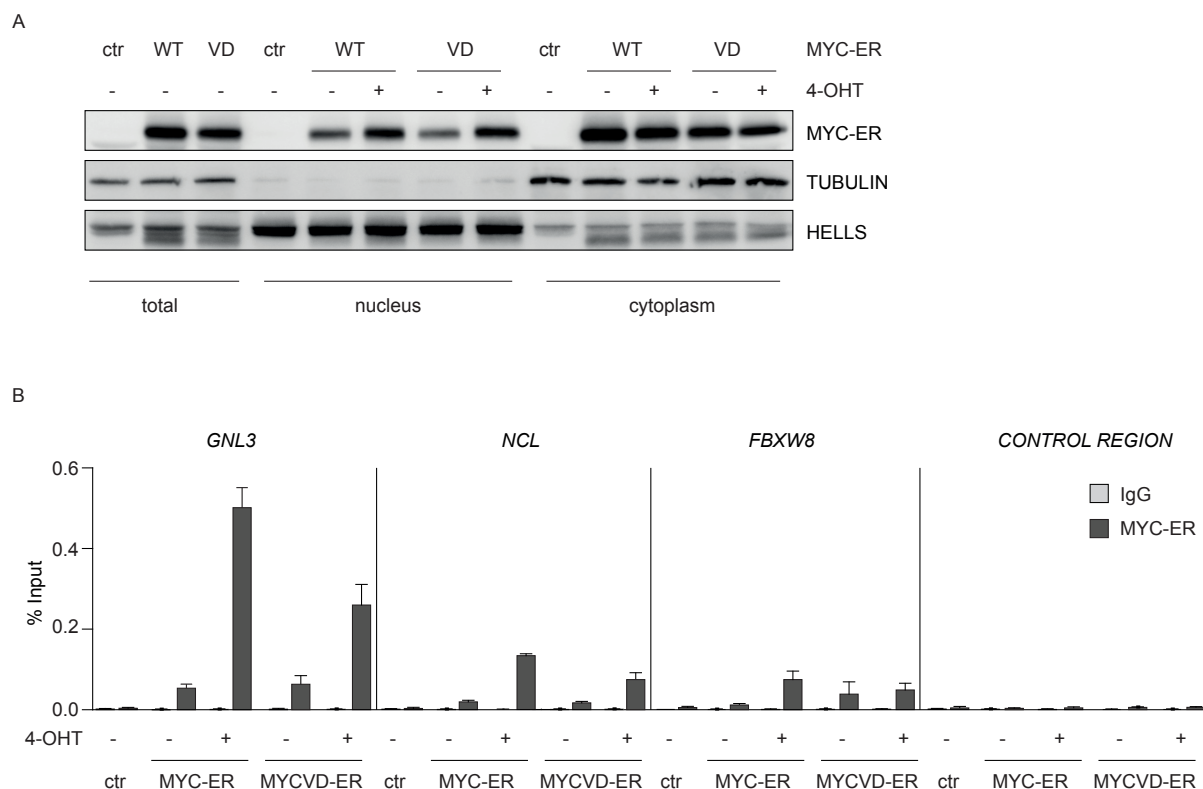


**Figure 4.20: Binding of MYCVD-ER to standard MYC targets is weaker**

- A** Fractionation assay to verify equal levels of ER fusion proteins in the nucleus. Whole cell lysates ("total"), or nuclear and cytoplasmic fractions of MCF10A cells treated for 1 h with 4-OHT were analysed by Western Blot. TUBULIN was used as loading control for the cytoplasmic, HELLS for the nuclear fraction, respectively.
- B** ChIP with control or anti-ER ("MYC-ER") antibodies to document enrichment of fusion proteins at the indicated promoters of well known MYC targets or an intergenic control region. Before treatment with 4-OHT, MCF10A cells were starved for 24 h to deplete endogenous MYC proteins. Enrichment is presented as % Input and mean + SD of technical triplicates (n = 2).

Exogenous co-immunoprecipitation experiments showed that binding of MYC VD to MAX is identical to MYC/MAX complex formation (data not shown). Therefore, reduced association of MYC VD to DNA is likely to be the result of its weakened interaction with MIZ1.

#### 4.4.1 Global analysis of MIZ1, MYC-ER and MYCVD-ER binding sites

Results of the presented transcriptomic data (Section 4.3) supported a model, in which MYC VD is impaired in apoptosis induction due to strongly attenuated transcriptional repression. In order to further elucidate which of these transcriptional effects are direct, we performed chromatin immunoprecipitation followed by high throughput sequencing (ChIP-seq) to map genome-wide binding sites of MYC-ER, MYCVD-ER and endogenous MIZ1 in MCF10A cells.

ChIP-seq DNA libraries were prepared from MYC-ER and MYCVD-ER cells treated with ethanol ("ctr") or 4-OHT as well as from empty vector cells. Fusion proteins were precipitated with anti-ER $\alpha$  antibody (HC20). An anti-MIZ1 antibody (10E2) was used to pull down endogenous MIZ1 protein under all described experimental conditions. Sequencing was performed on an Illumina Genome Analyzer IIx which was operated by Wolfgang Hädelt, Elmar Wolf and Carsten Ade.

Initial bioinformatic analyses of the sequencing data confirmed, in line with multiple published datasets, that a large number of genomic loci were bound by activated MYC-ER proteins (see

**Table 4.1: Statistics of ChIP-sequencing results**

| sample          | mapped reads | called peaks | peaks FDR < 0.1 | peaks +/- 5 kb from TSS FDR < 0.1 | peaks +/- 1.5 kb from TSS FDR < 0.1 |
|-----------------|--------------|--------------|-----------------|-----------------------------------|-------------------------------------|
| Input           | 15,040,211   | reference    | n.d.            | n.d.                              | n.d.                                |
| HC20-Vector     | 15,119,997   | 3,549        | 7               | 2                                 | 1                                   |
| HC20-WtER ctr   | 15,120,524   | 12,541       | 7,033           | 2,457                             | 1,891                               |
| HC20-WtER 4-OHT | 15,118,730   | 43,946       | 43,946          | 14,593                            | 10,887                              |
| HC20-VDER ctr   | 15,120,129   | 9,475        | 1,948           | 608                               | 455                                 |
| HC20-VDER 4-OHT | 15,114,488   | 24,180       | 24,174          | 7,979                             | 5,977                               |
| 10E2-Vector     | 13,314,598   | 7,572        | 5,992           | 1,766                             | 1,288                               |
| 10E2-WtER ctr   | 13,317,836   | 10,959       | 9,892           | 3,049                             | 2,212                               |
| 10E2-WtER 4-OHT | 13,312,133   | 16,330       | 16,330          | 5,117                             | 3,718                               |
| 10E2-VDER ctr   | 13,314,951   | 9,757        | 8,124           | 2,333                             | 1,698                               |
| 10E2-VDER 4-OHT | 13,312,529   | 11,856       | 11,855          | 3,489                             | 2,474                               |

Incorporating % alignment to the human genome (hg19), total sequencing reads for every sample were normalised to equal counts within the antibody sets ("mapped reads", HC20 = anti-ER $\alpha$ , 10E2 = anti-MIZ1). For peak calling with MACS, an equal mixture of all input samples was taken as reference control ("called peaks"). For further analysis, only peaks with an FDR < 0.1 were taken into account. Using BEDtools, every peak was annotated to the closest TSS and sublists with defined windows around the TSS were generated in R by calculating the distance from the peak summit. WtER: MYC-ER; VDER: MYCVD-ER; TSS: transcriptional start site; FDR: false discovery rate; n.d.: not determined.

Table 4.1 for statistics summary). Even though DNA binding of ER fusion proteins could already be detected in cells treated with ethanol, promoter occupancy was augmented after incubation with 4-OHT for both MYC-ER and MYCVD-ER.

Within a window of 3 kb around human RNA polymerase II (Pol II) transcriptional start sites (TSS), more than 10,000 binding sites were detected for MYC-ER in cells treated with 4-OHT (Fig. 4.21 A and Table 4.1). Similarly to weaker enrichments observed at individual promoters (Fig 4.20 B), overall DNA occupancy of MYCVD-ER was lower, resulting in a 1.8-fold reduction of detectable genomic binding sites.

ChIP experiments on selected MIZ1 target genes had not indicated changes in MIZ1 occupancy between different experimental conditions (Fig. 4.19 B). Interestingly, on a genome-wide scale, activation of MYC-ER yielded an almost 3-fold increase in the number of identified MIZ1 peaks compared to vector MCF10A cells, whereas this effect was only 2-fold with MYCVD-ER present (Table 4.1 and Fig. 4.21 A).

Inspection of tag density profiles for individual target genes confirmed that MYC and MIZ1 bind as a complex because both proteins could be detected at strongly bound standard target genes of one another, even in the absence of their own consensus binding site (Fig. 4.21 B and data not shown).



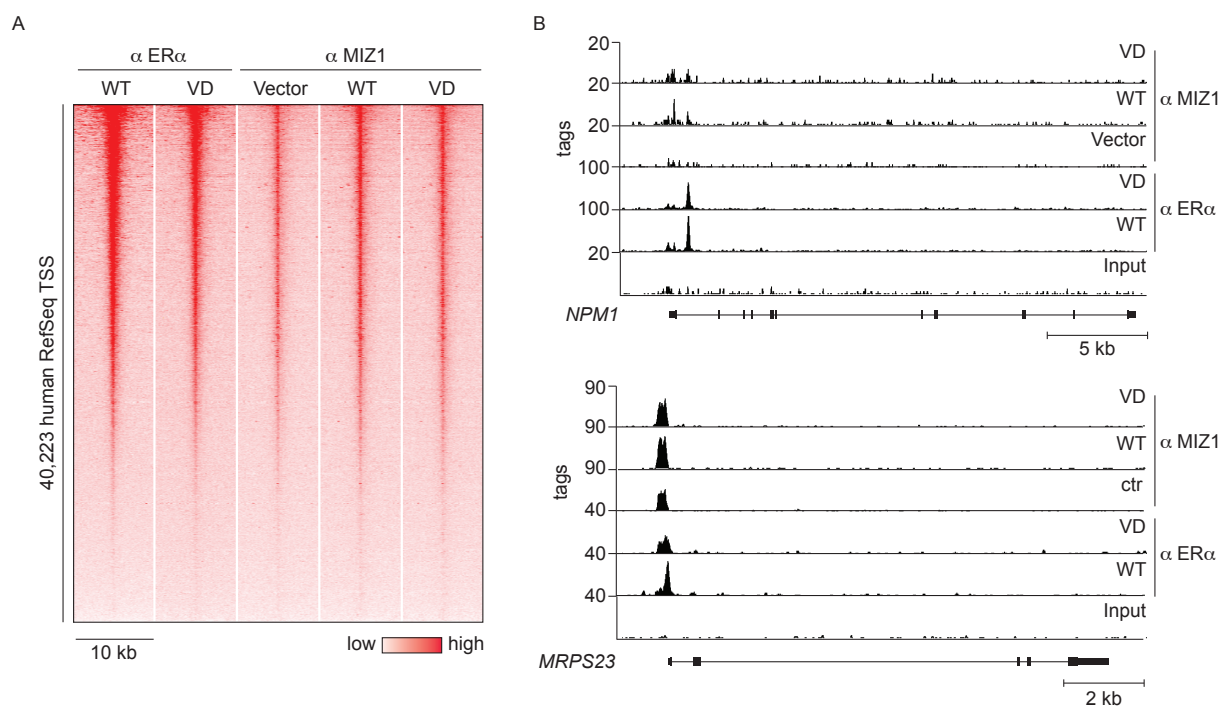


**Figure 4.21: ChIP-seencing identifies direct target genes of MYC and MIZ1 in MCF10A cells<sup>1</sup>**

- A Heatmap documenting distribution of tag densities obtained by ChIP-seencing of the indicated experimental conditions in a window  $\pm$  5 kb around all annotated human RefSeq TSS (hg19). For overexpression of MYC-ER ("WT") and MYCVD-ER ("VD") only 4-OHT conditions are shown. All conditions are ranked according to MYC-ER occupancy.
- B Example tracks of ChIP-seencing results for the indicated experimental conditions. Normalised ChIP read density files were visualised with Integrated Genome Browser software. *NPM1* is an example for a classical MYC target gene. *MRPS23* is one of the most strongly bound MIZ1 targets. Gene structure (UTRs and exons, indicated by boxes or vertical lines) are indicated below the profiles.

Collapsing the number of identified peaks into individual gene names yielded about 6,000 genes bound by MYC-ER in the 4-OHT situation. One quarter of these genes was occupied to a detectable degree under control conditions (Fig. 4.22 A, upper left panel). In the case of MYCVD-ER, an almost 10-fold increase in bound genes was observed after 4-OHT treatment. In total, once activated, roughly 4,000 different genes were bound by MYCVD-ER. (Fig. 4.22 A, upper right panel). The overlap between genes bound by activated MYC-ER and MYC-VD proteins was highly significant, suggesting that there is not a qualitative but only a quantitative difference in target genes (Fig. 4.22 A, lower panel).

In control as well as 4-OHT treated cells, overlaps between genes bound by endogenous MIZ1 and MYC-ER or MIZ1 and MYCVD-ER were significant. However, the fraction of shared genes was larger in the context of MYC WT (4.22 B).

#### 4.4.2 MYC and MIZ1 bind cooperatively to core promoters

Treatment of MYC-ER cells with 4-OHT increased the overall number of MIZ1 peaks that could be identified whereas activation of MYCVD-ER did not lead to such a strong response (see statistics in Table 4.1).

To visualise binding strength of MIZ1 and MYC on direct MIZ1 target genes, distribution of ChIP-seq tags from all samples were plotted in a window of 10 kb around coordinates of MIZ1

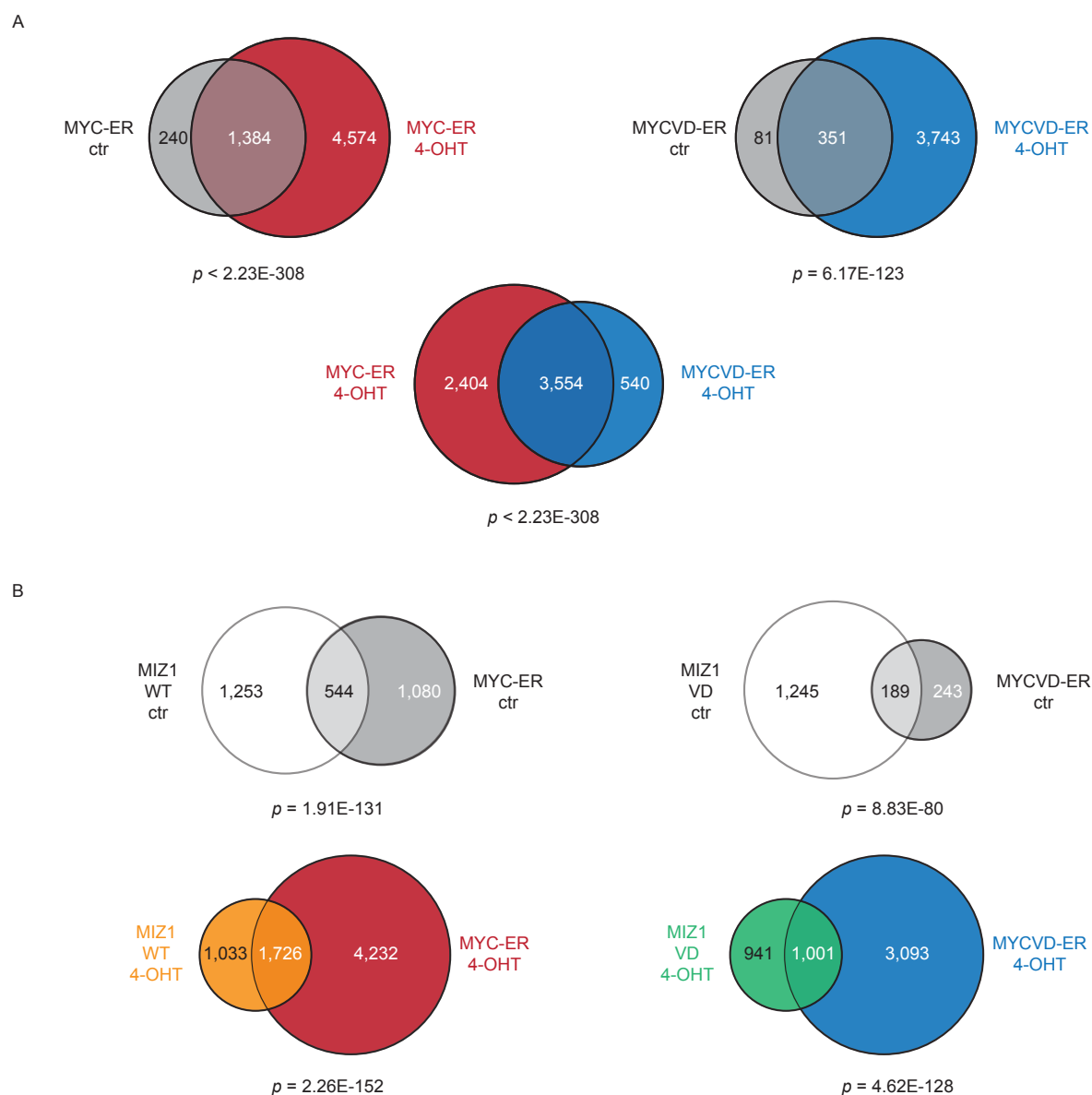


**Figure 4.22: Overlap of MYC/MIZ1 bound genes in MCF10A cells**

A Venn diagrams documenting overlap of bound genes between MYC-ER or MYCVD-ER in control versus 4-OHT conditions (upper panels) or genes bound by MYC-ER and MYCVD-ER after 4-OHT treatment (lower panel). Only genes bound within a window of  $\pm 1.5$  kb around the TSS were taken into account.  $p$ -values stating significance of overlaps are based on a hypergeometric distribution using 14,807 human RefSeq genes as population size. Diagrams are not drawn to scale.

B Venn diagrams documenting overlap of bound genes between different MIZ1 and MYC-ER or MYCVD-ER ChIPs. Upper panels: control treated samples. Lower panels: 4-OHT treated samples. Analysis was performed as in A.

peaks. Binding of MIZ1 to promoters of its target genes was increased when MYC-ER was activated (Fig. 4.23 A, upper panel). Similarly, binding of MYC-ER to MIZ1 target genes was stronger after addition of 4-OHT (Fig. 4.23 A, lower panel). MYCVD-ER occupancy at the same sites was detectable but significantly lower. Interestingly, although an increase in bound MYC VD after 4-OHT treatment was observed (Fig. 4.23 B, lower panel), this was not paralleled by a simultaneous recruitment of MIZ1 to core promoters (Fig. 4.23 B, upper panel).

The same trends were observed when tag densities around all transcriptional start sites or MYC binding sites were studied (data not shown).

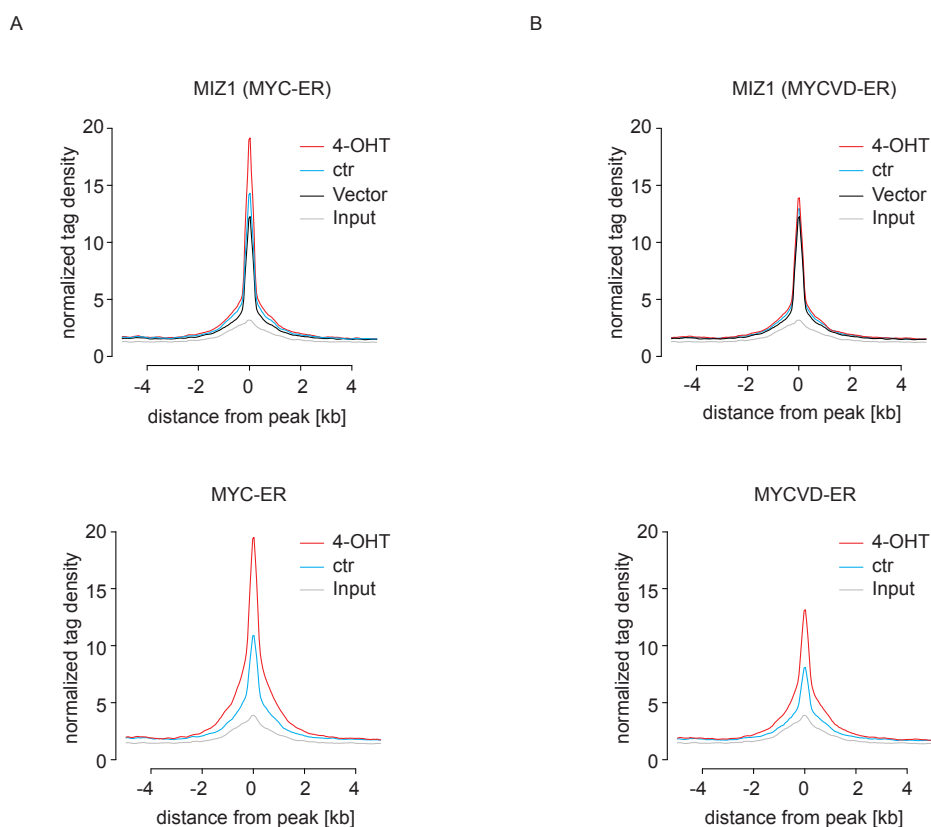


**Figure 4.23: MYC WT but not MYC VD enhances MIZ1 binding to core promoters<sup>1</sup>**

- A MIZ1 peaks identified +/- 1.5 kb around the closest TSS in MYC-ER 4-OHT treated cells were used as reference coordinates and the distribution of MIZ1 (upper panel) and MYC-ER (lower panel) ChIP-seq tags around these peaks were plotted under the indicated experimental conditions. Input tags were used as control.
- B MIZ1 (upper panel) and MYCVD-ER (lower panel) tag distribution analysed the same way as in A, except control and 4-OHT samples are from MYCVD-ER overexpressing cells.

Together, these data argue that MYC and MIZ1 bind cooperatively to their target sites and recruit each other to core promoters, which could also explain reduced DNA binding affinity of MYC VD.

#### 4.4.3 MYC/MIZ1 complexes can bind to low-affinity sites

MYC/MAX heterodimers bind to a specific DNA consensus sequence called E-box [Blackwood and Eisenman, 1991]. On the other hand, a long non-palindromic motif was identified as binding site of MIZ1 in most of its target genes [Wolf et al., 2013].

To investigate the enrichment of different DNA binding motifs in identified ChIP-seq peaks, sequences were analysed using web-based tools of the MEME Suite [Bailey et al., 2009].

We chose two different subgroups of MYC-bound target genes for the analysis (see Venn diagram in Fig.4.24): First, the overlap of peaks found under conditions of active MYC-ER and MYCVD-ER ("MYC-ER + MYCVD-ER joint"), and second, the overlap between MYC-ER and MIZ1 at those sites, where no MYCVD-ER had been detected ("MYC-ER only + MIZ1 joint").

The most strongly enriched motif in this unbiased analysis was a canonical E-box (*CACGTG*, left part of Fig 4.24) when MYC/MYC VD joint peaks were used as input sequences.

In contrast, no E-box-like motif was enriched in sequences bound by MYC WT and MIZ alone. Instead, when the top motif was analysed with the TOMTOM Motif Comparison Tool of MEME Suite, there was a significant resemblance to a consensus Sp1 motif ("GC box",  $p = 4.86E-07$ ,

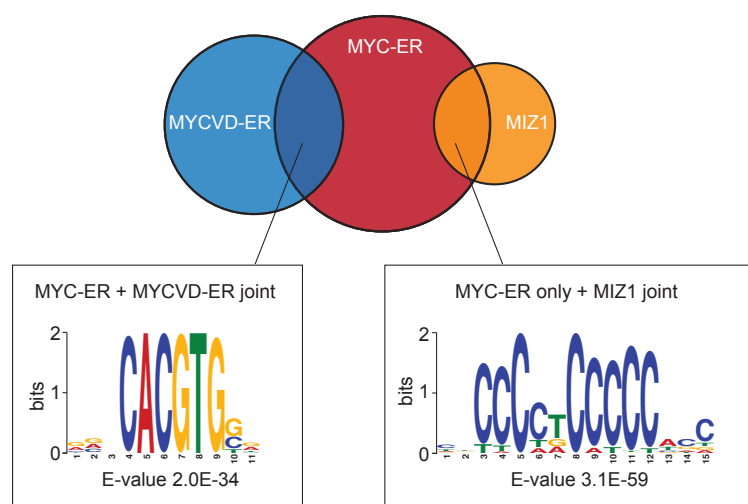


**Figure 4.24: Different DNA binding motifs are enriched in subgroups of MYC-bound genes**

A MEME analysis was performed with those groups of peaks that were either bound by MYC-ER and MYCVD-ER after 4-OHT treatment, or not bound by MYCVD-ER but only by MYC-ER together with MIZ1. The lower part represents the top motif found by MEME in the submitted sequences. E-value reported by MEME indicates statistical significance of found motifs.

right part of Fig. 4.24).

These data imply that genes with high affinity MYC binding sites can be bound in a MIZ1-dependent or -independent manner. However, some genes, that seem to be bound preferentially in a complex with MIZ1, most likely have low affinity sites for both proteins and / or are bound in collaboration with other interaction partners.

In a next step, we aimed to correlate occupancy of MYC and MIZ1 at a given promoter with the direction of the transcriptional response. To this end, genes bound by MYC-ER after 4-OHT addition were merged with results from the microarray analysis and divided into activated and repressed datasets (Fig. 4.25).

Overall binding of MYC at activated genes appeared stronger than on repressed genes (Fig. 4.25, left panel). MIZ1 occupancy at the same target sites was low, but did not differ between MYC activated and repressed genes (right panel). This observation is similar to previous results in

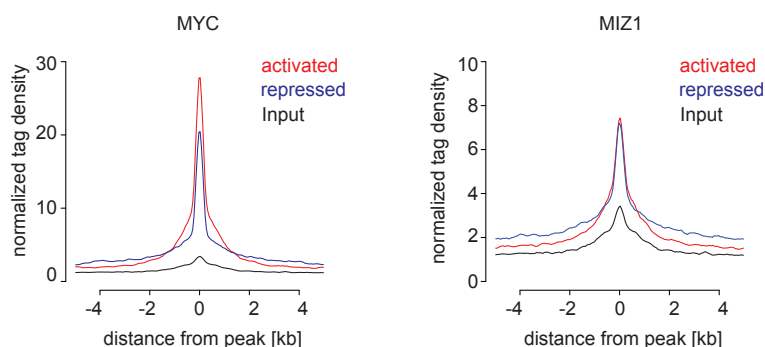


**Figure 4.25: MYC/MIZ1 ratio changes on activated and repressed genes<sup>1</sup>**

ChIP-seq data were filtered for MYC activated and repressed genes that had been identified in the microarray analysis. Peaks found in the promoters of these regulated genes were used as reference coordinates and distribution of MYC (left panel) and MIZ1 (right panel) tags was analysed.

HeLa cells, where the ratio between MYC and MIZ1 at a given promoter correlates with the direction of the transcriptional output [Walz et al., 2014].

In conclusion, the combination of microarray and ChIP-seq data supports a model in which high levels of MYC bind to MIZ1, enabling invasion of low-affinity sites and subsequent repression of target genes.

## 4.5 SRF-regulated genes are repressed by MYC/MIZ1

Mechanistically, the results obtained so far had implicated MYC/MIZ1-dependent repression as a potential cause of MYC-induced apoptosis. Repression, in turn, could be mediated via binding to low affinity sites, maybe even in a complex with other factors.

To further link these mechanistic insights to a specific group of repressed genes or a biological pathway, we re-analysed the microarray data, running GSEA software with gene sets that share predicted promoter motifs. To find transcription factor binding sites that are specifically enriched in promoters of MYC WT- but not MYC VD-repressed genes, we directly compared MYC-ER versus MYCVD-ER datasets.

Consensus binding motifs of several transcription factor families could be identified in genes repressed by MYC-ER relative to MYCVD-ER (Fig. 4.26 A). Most prominently enriched were motifs similar to the CArG box sequence of the serum response element (SRE), a motif that is bound by the MADS transcription factor SRF (serum response factor, Fig. 4.26 A and B).

Depending on the associated cofactor, two classes of SRF targets can be distinguished: One group is regulated by SRF and ternary complex factors (TCFs) which are activated downstream of Ras-MAPK signalling. The second class of genes is regulated by SRF together with myocardin-related

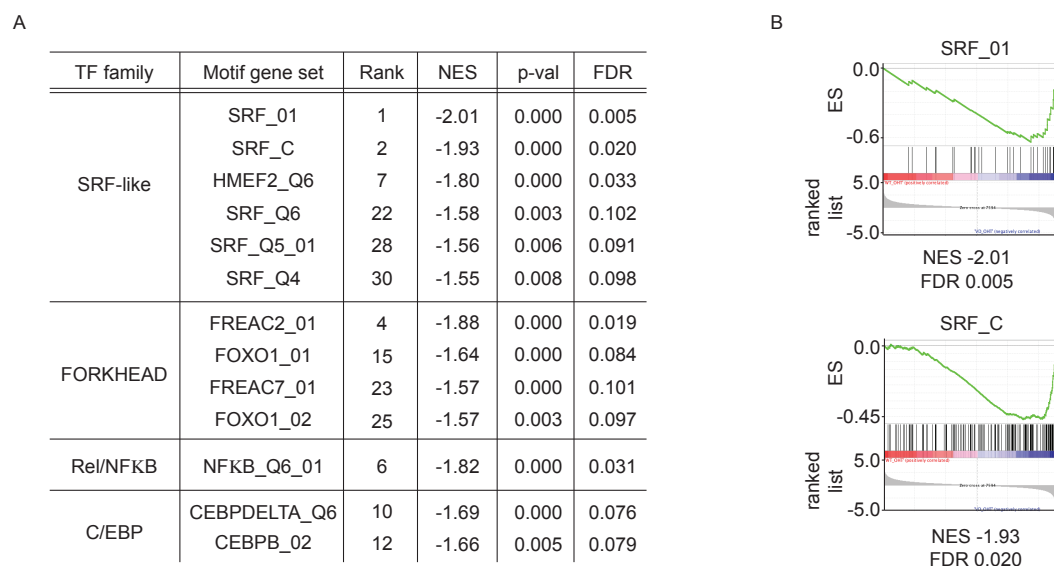


**Figure 4.26: Identification of enriched promoter motifs in MYC-repressed genes<sup>1</sup>**

A Summary of GSEA analysis (C3: conserved cis-regulatory motif gene sets) comparing MYC-ER with MYCVD-ER. Sets in this collection are comprised of genes that share a specific regulatory motif in a region of +/- 2kb around their transcriptional start site. Table shows all transcription factor (TF) families identified within the top 10 ranks of gene sets that are repressed by MYC-ER relative to MYCVD-ER. Additional matching gene sets are listed if found within the top 30 motifs. Unknown motifs were excluded.

B Example plots for the first two SRF gene sets shown in A.

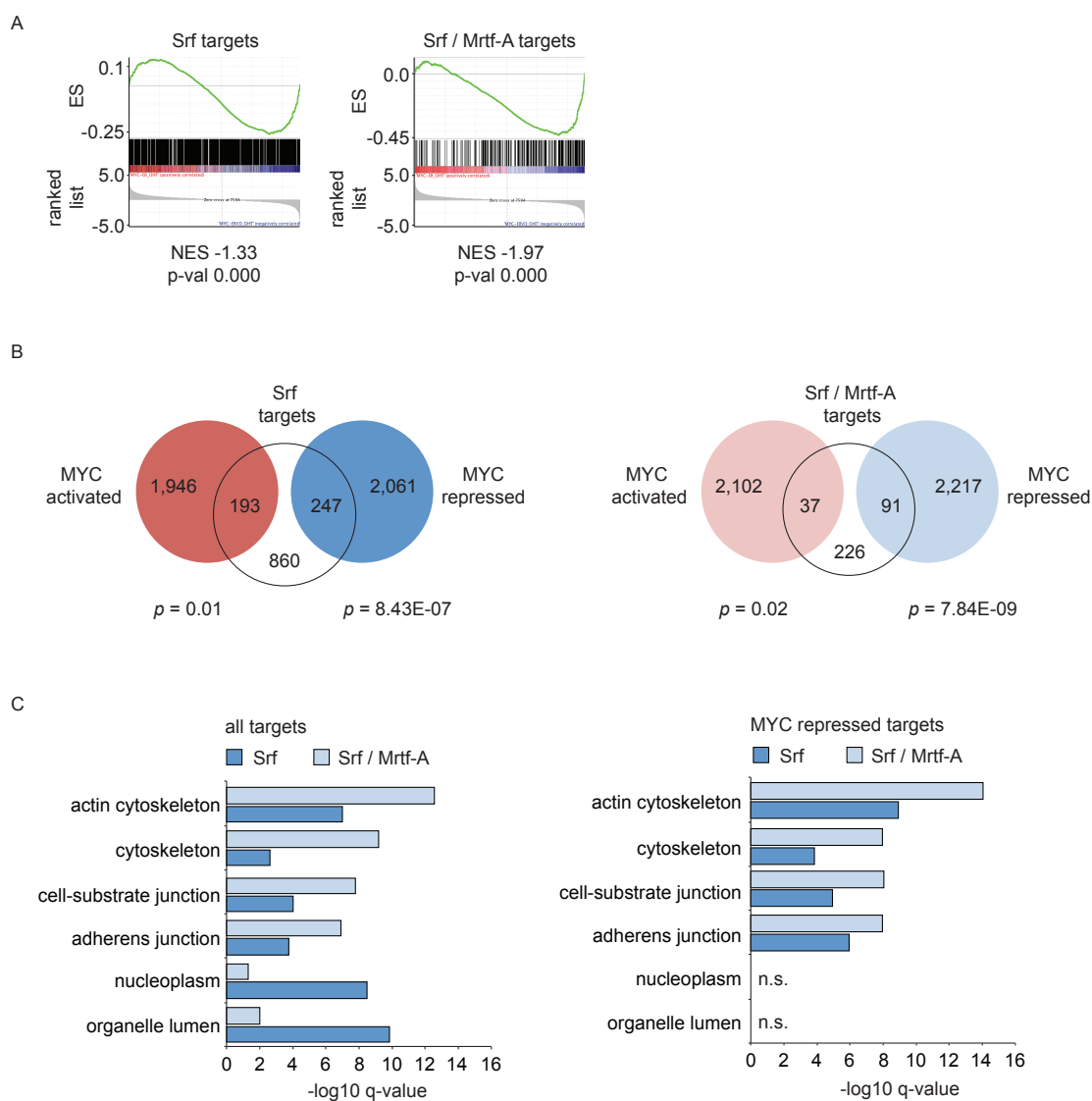


**Figure 4.27: MYC represses genes regulated by SRF and its coactivator MRTF-A<sup>1</sup>**

- A GSEA analysis testing MYC/MIZ1-dependent repression of Srf (left panel) or Srf/Mrtf-A targets (right panel) identified in murine fibroblasts [Esnault et al., 2014]. Peaks found in a window of 10 kb around a TSS, bound by either Srf alone or Srf and Mrtf-A together, were uploaded to UCSC LiftOver tool and converted to human genes. Both lists were used as gene sets in a GSEA analysis as described before.
- B Overlap of gene sets from A (left: Srf; right: Srf/Mrtf-A), with genes regulated by MYC-ER in MCF10A cells (see section 1.3).  $p$ -values indicating significance of overlaps are calculated with hypergeometric distributions.
- C Results of a DAVID analysis of functional annotations for either all Srf or Srf/Mrtf-A targets (left panel) or the overlap of those genes with genes repressed by MYC (right panel).

transcription factors (MRTFs) in response to RhoA signalling and actin dynamics [Gineitis and Treisman, 2001; Posern and Treisman, 2006].

Recently, genome-wide binding sites of the serum response factor and its cofactors have been identified in murine fibroblasts [Esnault et al., 2014].

To validate the GSEA results with an experimentally defined set of target genes, we used the ChIP-seq data from Esnault and colleagues to generate our own customised sets of SRF target genes: First, we isolated all Srf peaks found +/- 5 kb from a TSS and converted the coordinates from murine to the human genome, which yielded a list of 1,300 potential human SRF target genes. In a second step, a list of 354 SRF targets that were also bound by the cofactor MRTF-A was generated the same way.

Subsequently, we performed another gene set enrichment analysis, testing whether those experimentally validated Srf targets were also repressed by MYC in a MIZ1-dependent manner in MCF10A cells. Indeed, both gene sets were significantly repressed by MYC-ER relative to MYCVD-ER (Fig. 4.27 A). Interestingly, the enrichment score was better when joint SRF/MRTF-A genes were analysed, indicating that this specific group of SRF-regulated genes might be the primary target of MYC/MIZ1-mediated repression.

Next, we analysed the overlap between genomic targets of SRF and all genes regulated in response to MYC-ER in MCF10A cells. Although there was also a significant overlap between MYC-activated genes and SRF- or SRF/ MRTF-A-bound genes, the fraction of SRF/MRTF-A genes repressed by MYC was larger (Fig. 4.27 B).

To understand the biological roles of these target genes in more detail, we used functional annotation tools provided by DAVID. Consistent with previous analyses, SRF targets fell into two major functional classes: On the one hand, genes important for actin cytoskeleton and cell adhesion processes. On the other hand, genes involved in cell proliferation and chromatin function, as indicated by gene ontology terms like nucleoplasm (Fig. 4.27 C, left panel, dark blue bars). As expected, GO terms like "actin cytoskeleton" could be further enriched by analysing joint SRF/MRTF-A target genes. Interestingly, those SRF or SRF/MRTF target genes that overlapped with MYC-repressed genes, were exclusively enriched for functional annotations associated with cytoskeleton and adhesion functions (Fig. 4.27 C, right panel). Target genes that overlapped with MYC-activated genes, did not fall into any of these categories (data not shown). In summary, we could demonstrate that specifically SRF/MRTF-A regulated genes involved in actin cytoskeleton dynamics and adhesion are repressed by the MYC/MIZ1 complex.

In response to RhoA signalling and subsequent changes in actin polymerisation, MRTF proteins shuttle into the nucleus and are able to co-activate SRF target genes [Miralles et al., 2003].

To test whether MYC interferes with RhoA activity and might thereby indirectly regulate SRF/MRTF signalling, we superinfected MCF10A MYC-ER cells with a mutant form of RhoA, RhoA Q63L. This mutant cannot hydrolyse GTP anymore and is hence constitutively active. Analysis of three target genes of SRF revealed, that all were repressed in response to activation of MYC-ER (Fig. 4.28, "ctr" conditions). Similarly, all three genes were induced by overexpression of active RhoA, indicating that they are indeed MRTF-regulated SRF targets.

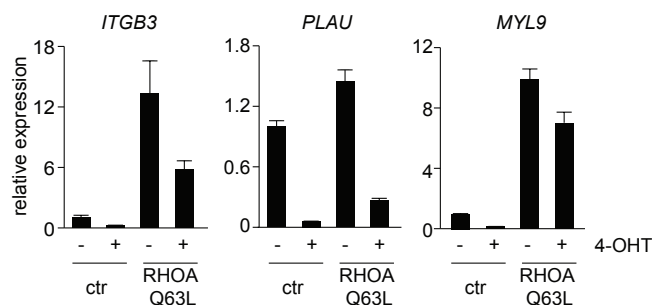


**Figure 4.28: MYC-mediated repression of SRF targets is downstream of RhoA<sup>1</sup>**

qRT-PCRs of the indicated SRF target genes that are repressed by activation of MYC-ER in the presence and absence of a constitutively active RhoA allele (Q63L). Values were normalised to *RPS14* and relative expression relative to control treated empty vector cells is shown (mean + SD of technical triplicates, n = 2).

Importantly, repression of SRF target genes by MYC also occurred in the presence of RhoA Q63L, demonstrating that it is most likely not mediated via indirect effects on RhoA signalling.

In accordance with our data documenting MYC/MIZ1-mediated repression of direct SRF targets, MYC/MIZ1 complexes were also present at the promoters of more than 20% of SRF target genes (Fig. 4.29 A). When the distribution of MYC and MIZ1 tags around SRF peaks at joint SRF/MRTF-A targets was analysed, an enrichment of both MYC and MIZ1 tags could be detected at the same sites. Identical to analyses before, binding of MYC-ER was stronger than binding of MYCVD-ER, and occupancy of MIZ1 was enhanced in the presence of active MYC-ER (Fig. 4.29 B). Interestingly, although MYC/MIZ1 and SRF binding sites seemed to be in close vicinity in most of the cases, distribution of tags was more widespread, indicating that binding sites do not necessarily overlap at all target genes.

To confirm this hypothesis, we analysed several target genes by visualising ChIP-seq density profiles with the Integrated Genome Browser [Nicol et al., 2009]. To be able to show SRF binding at the same loci, a publicly available SRF ChIP-seq from the human breast cancer cell line MCF7 was used. As expected, binding sites of MYC, MIZ1 and SRF were often close to the TSS of their target genes (Fig. 4.29 C, left panel *PLEKHG2*). However, they did not overlap in all cases

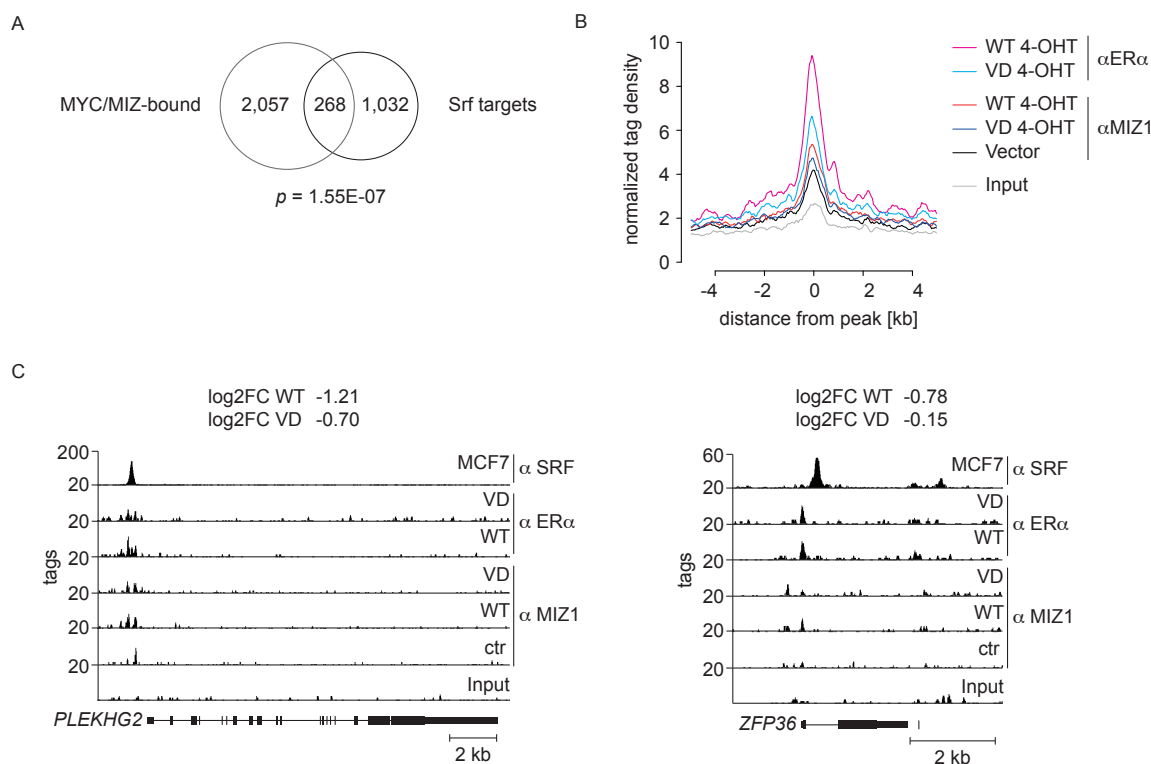


**Figure 4.29: SRF target genes are bound by MYC/MIZ1 complexes<sup>1</sup>**

- A Venn diagram documenting overlap of genes bound by MYC-ER together with MIZ1 (4-OHT condition, +/- 5 kb around TSS) and SRF targets (list from Esnault et al. [2014] after LiftOver to hg19, +/- 5 kb around TSS).  $p$ -value based on hypergeometric distribution.
- B Distribution of MYC-ER, MYCVD-ER or MIZ1 tags (experimental conditions are indicated) at SRF/MRTF-A target genes. Binding was analysed around the peaks of SRF/MRTF-A target genes found within +/- 5 kb of a TSS after LiftOver to human coordinates.
- C Example ChIP-seq density profiles at two SRF target genes, *PLEKHG2* and *ZFP36*, which were differentially repressed in the microarray (see  $\log_2FC$  above the tracks for regulation in response to MYC-ER ("WT") or MYCVD-ER ("VD"), respectively). To confirm SRF binding in human cells, a published dataset from the MCF7 breast cancer cell line was used (GSM1010839).



(e.g. Fig. 4.29 C, right panel *ZFP36*), which strongly suggests that binding of SRF/MRTF-A and MYC/MIZ1 complexes occurs independently of each other.

It should be noted, that occupancy of both MYC and MIZ1 at SRF targets was very weak in comparison to binding strength at their respective standard target genes, which is in line with our hypothesis, that high levels of MYC recruit MIZ1 to low affinity target sites.

In conclusion, MYC directly represses a subset of SRF target genes involved in cell adhesion and cytoskeleton function via MIZ1.

#### 4.5.1 Repression of SRF target genes is rescued by constitutively active MRTF-A

Functional annotation analysis had suggested that a class of RhoA- and not MAPK-dependent SRF target genes is specifically affected by MYC/MIZ-dependent repression. Furthermore, interference with SRF activity is probably downstream of RhoA, because repression of target genes still happens in the presence of a constitutively active variant. The cofactor that specifically links cellular actin dynamics with SRF-mediated transcriptional activation downstream of RhoA is MRTF-A.

To further investigate at which step MYC/MIZ1 complexes inhibit SRF transcriptional activity, we used a constitutively active mutant of the cofactor:  $\Delta$ N-MAL, an N-terminally truncated allele of MRTF-A, lacks two RPEL motifs responsible for actin binding and nuclear-cytoplasmic shuttling [Vartiainen et al., 2007; Brandt et al., 2009].

Doxycycline-inducible expression of  $\Delta$ N-MAL in MYC-ER MCF10A cells induced SRF target genes on protein and mRNA level (Fig. 4.30 A and B). Whereas SRF protein expression itself

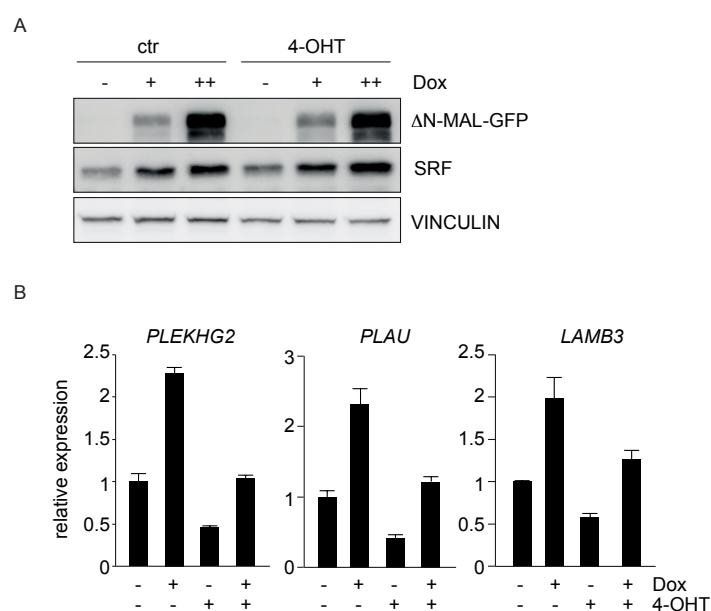


**Figure 4.30:  $\Delta$ N-MAL rescues expression of SRF target genes<sup>1</sup>**

- A** Immunoblot documenting overexpression of a doxycycline-inducible GFP-tagged constitutive active form of MRTF-A,  $\Delta$ N-MAL. MCF10A MYC-ER cells were either treated with ethanol ("ctr") or 4-OHT. Doxycycline ("Dox") was added in two different concentrations: + = 0.025  $\mu$ g/ml; ++ = 1  $\mu$ g/ml Expression of endogenous SRF was used as control for target gene induction. VINCULIN was used as loading control.
- B** Relative expression of SRF target genes after  $\Delta$ N-MAL ("Dox") and / or MYC-ER ("4-OHT") activation for 24 h. CT values were normalised to *RPS14*, vehicle treated control cells were set to 1. Bars are mean + SD of technical triplicates.

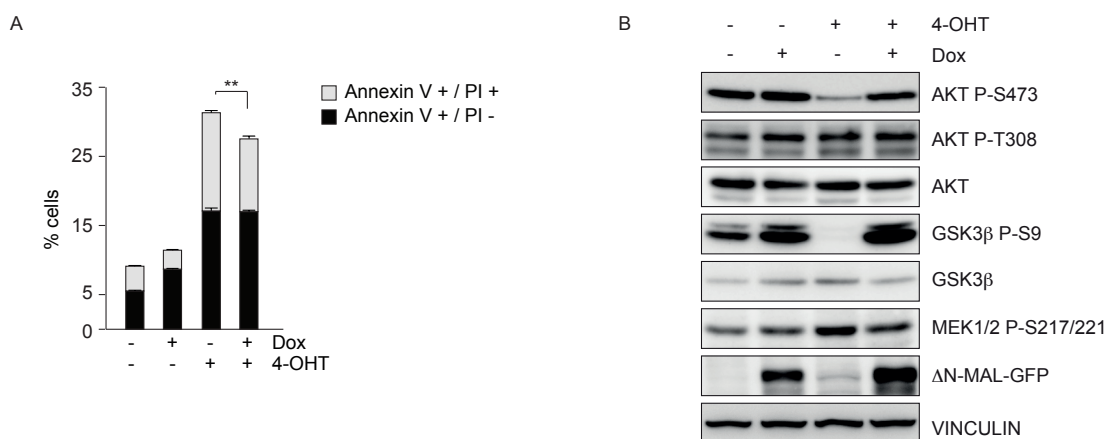


**Figure 4.31: MYC represses MRTF/SRF-induced survival signalling via AKT<sup>1</sup>**

**A** Annexin V / propidium iodide FACS to measure apoptosis in MCF10A MYC-ER cells with or without expression of  $\Delta$ N-MAL. Where indicated, cells were treated with Dox and / or 4-OHT. Apoptosis was measured after 48 h. Bars represent mean + SD (n = 3). \*\*:  $p < 0.01$  (Student's t-test).

**B** MCF10A MYC-ER cells were superinfected with Dox-inducible  $\Delta$ N-MAL. Cells were treated for 24 h with Dox and / or 4-OHT as indicated. Protein lysates were probed with the indicated antibodies. VINCULIN was used as loading control. A representative experiment is shown (n = 3).

was not inhibited by activation of MYC-ER (Fig. 4.30 A), several other targets were repressed on mRNA level, which was consistent with analyses before (shown for *PLEKHG2*, *PLAU* and *LAMB3* in Fig. 4.30 B). Importantly, activation of MYC-ER in the presence of  $\Delta$ N-MAL still repressed target gene activation. However, compared to activation of MYC-ER alone, expression of SRF targets was restored to levels found in control cells.

Taken together, MYC represses SRF target gene activation at a point downstream of MRTF-A nuclear translocation.

To test whether restoration of SRF target gene expression by  $\Delta$ N-MAL was sufficient to block MYC-induced apoptosis, Annexin V / propidium iodide stainings were performed in MYC-ER MCF10A cells. Identical to previous results, activation of MYC-ER resulted in an increased percentage of Annexin V - and Annexin V / propidium iodide double-positive cells. Concomitant activation of  $\Delta$ N-MAL was able to mildly alleviate overt induction of apoptosis by MYC (Fig. 4.31 A).

These data imply, that inhibition of SRF signalling contributes to induction of MYC/MIZ1-mediated apoptosis.

Many target genes of SRF that are repressed by MYC/MIZ1 are involved in cell adhesion processes, among them several integrins and laminins. Failure to attach to extracellular matrix (ECM) or improper adhesion signals inhibit pro-survival pathways and can induce a form of apoptosis that is commonly referred to as anoikis [Chiarugi and Giannoni, 2008].

We hypothesised that MYC-mediated repression of SRF target genes could decrease activity of survival pathways due to improperly weakened cellular adhesion. Signals critically involved in physiological protection from anoikis are, amongst others, transferred via the PI3K/AKT pathway, which can act downstream of cell-ECM as well as cell-cell contacts to promote cell survival. Therefore, we tested the phosphorylation status of AKT in cells with active MYC-ER, active SRF (mediated via  $\Delta$ N-MAL) or both (Fig. 4.32). Induction of  $\Delta$ N-MAL slightly increased phosphorylation of AKT at S473 and T308, which was followed by a phosphorylation of the

downstream target GSK3 $\beta$  at serine 9. Interestingly, activation of MYC-ER led to a strong selective reduction of serine 473 AKT phosphorylation, whereas it did not have consistent effects on the threonine 308 site. In agreement with our hypothesis, activation of  $\Delta$ N-MAL could restore AKT activity in the presence of MYC-ER.

Taken together, MYC-induced repression of SRF target genes contributes to decreased survival signalling via AKT.

# Chapter 5

## Discussion

Various environmental signals induce expression of the proto-oncogene *MYC* and, in turn, the transcription factor translates these cues into gene expression patterns that are crucial for the maintenance of most cell types and tissues [Grandori et al., 2000].

In the vast majority of human tumours, *MYC* is overexpressed due to either gene amplification or release from negative upstream regulatory signals and the protein sequence requires no alterations to transform into a potent driver of tumourigenesis [Lee et al., 2006]. Hence, once "deregulated", its normal physiological function appears to be sufficient to become oncogenic.

Yet, one question that is still debated is the causal mechanism for *MYC*'s oncogenic activities: Does it simply amplify its physiological gene expression patterns or is there a "gain of function" after all, related to newly acquired and tumour-specific target genes?

Evidence from multiple experimental systems suggests that *MYC*'s inherent ability to induce apoptosis safeguards against the inappropriate pro-proliferative and hence pro-tumourigenic signals caused by its deregulated activity [Shortt and Johnstone, 2012]. In contrast to proliferation, induction of apoptosis by *MYC* is a response that is specifically observed at high expression levels [Murphy et al., 2008]. Because multicellular organisms must balance proliferation with apoptosis to ensure tissue homeostasis and restrain aberrant growth, mammalian cells must have evolved to interpret different levels of the transcription factor as either "safe" or "dangerous".

Dissecting the mechanistic principles underlying *MYC*-induced apoptosis could therefore contribute to understanding the difference between *MYC*'s physiological and tumourigenic actions.

### 5.1 Why levels matter: MIZ1-dependent and -independent functions of *MYC* in MECs

*MYC* is one of the most commonly amplified oncogenes in human breast cancer and overexpressed on RNA as well as protein level [Bièche et al., 1999; Blancato et al., 2004]. Interestingly, *MYC* overexpression in the murine mammary gland *in vivo* increases both proliferation and apoptosis [Hundley et al., 1997; D'Cruz et al., 2001].

Therefore, mammary epithelial cells (MECs) are an ideal model system to study the molecular consequences of low- and high-level *MYC* overexpression.

A couple of well-established functions of *MYC* were analysed to test which aspects of *MYC* biology are executed at different levels of deregulation. We induced low (2- to 3-fold) and high levels (7- to 10-fold) of *MYC* by driving expression from the mammalian PGK or viral SFFV

promoter, respectively. The V394D mutant of MYC, which cannot bind MIZ1 was used to determine which of these processes require the interaction with MIZ1 [Herold et al., 2002].

### 5.1.1 Regulation of proliferation

MYC regulates a variety of transcriptional programmes that prepare cells for S-phase entry [Leone et al., 1997; Bouchard et al., 1999; Morrish et al., 2008]. Yet, in MCF10A cells, neither MYC nor MYC VD has any significant effect on proliferation under standard 2D culture conditions (Fig. 4.2 A and 4.8 D for MYC-ER). A similar effect is observed when MCF10A cells are cultured under serum-free but non-adherent conditions in a mammosphere assay (Fig. 4.3): MYC as well as MYC VD expressing cells form larger primary spheres which indicates an increased responsiveness to growth factors [Pastrana et al., 2011].

Due to a gene amplification, MYC levels in MCF10A cells are significantly higher than in other primary mammary epithelial cell lines such as HMLE and IMECs (Fig. 4.1 A and Worsham et al. [2006]; Jänicke [2014]). The failure to elicit a proliferative response in these cells might therefore be due to the fact that binding sites in promoters of proliferation-related target genes are already saturated. This has been demonstrated recently for MYC target genes involved in processes such as ribosome biogenesis and translation, for example. Those genes are already occupied by the high levels of MYC present in human cancer cells and their expression does not change in response to a further increase in MYC levels [Walz et al., 2014]. In agreement with these findings, our assays show that, when the endogenous protein is depleted due to starvation, moderately overexpressed MYC is able to accelerate S-phase entry upon growth factor stimulation (Fig. 4.2 B).

Similar to the starvation experiments, basal MYC levels in the mammosphere assay are lower than in 2D culture (Fig. 4.3 C) and promoters of target genes might not be fully engaged, hence allowing additional MYC recruitment and transcriptional activation.

One of the best documented functions of MYC/MIZ1 complexes, is the joint repression of the cell cycle inhibitors p15Ink4b and p21Cip1 which antagonises anti-mitogenic signals [Seoane et al., 2002; van Riggelen et al., 2010]. Notably, MCF10A cells do not express p15INK4b [Cowell et al., 2005] and p21Cip1 repression appears to be only relevant in response to DNA damage and differentiation signals [Seoane et al., 2002; Wu et al., 2003; Hönnemann et al., 2012]. In line with these observations, MYC VD is equally capable of promoting cell cycle re-entry after starvation in our experiments, indicating that repression of cell cycle inhibitors by the MYC/MIZ1 complex is not required in this context.

One point of discussion in the field is whether it is really the absolute amount of MYC protein inside a cell ("over-expression"), or more the failure to modulate and adapt expression in response to physiological stimuli ("deregulation"), that mediates its oncogenic activities [Murphy et al., 2008; Evan, 2014]. The latter argument is based on the observation that "deregulating" almost physiological levels of MYC *in vivo* is sufficient to drive proliferation and tumourigenesis [Murphy et al., 2008].

As moderately increasing MYC levels in MCF10A cells does not result in a proliferative phenotype unless endogenous MYC is eliminated by starvation, this indicates that the amount of MYC required to induce proliferation is indeed very low but that constitutive, deregulated expression is not a sufficient signal to drive ectopic proliferation in this context. Furthermore, it suggests

that there is also an "upper" limit of expression, after which cells are no longer responsive to react with a certain phenotype. As discussed above, this is nicely explained by the amount of MYC that can still be recruited to target gene promoters [Walz et al., 2014].

### 5.1.2 Regulation of self-renewal

*In vivo*, MYC deletion in basal mammary epithelial cells is characterised by impaired self-renewal potential and a diminished regenerative capacity [Moumen et al., 2012]. Conversely, we can show that a moderately increased abundance of MYC in MCF10A cells is sufficient for more efficient propagation of mammospheres in secondary cultures, a readout that is commonly used to assess self-renewal capacity of MECs (Fig. 4.3; Dontu et al. [2003]). Additionally, higher levels of MYC expression in MCF10A and HMLE cells induce a shift towards a surface marker phenotype that enriches for cells with increased self-renewal and tumourigenic potential (Fig. 4.6; Al-Hajj et al. [2003]; Sleeman et al. [2006]).

Isolated CD44<sup>high</sup>/CD24<sup>low</sup> cells form mammospheres and express markers indicative of epithelial mesenchymal transition (EMT; Mani et al. [2008]). Interestingly, the increase in sphere formation and self-renewal capacity by MYC in MCF10A cells has been proposed to depend on repression of p21 and a concurrent induction of EMT, which would implicate a participation of MIZ1 in this process [Liu et al., 2009]. Although the mechanism is unclear, MIZ1 has also been suggested to mediate the MYC-induced increase in self-renewal of neuronal progenitor cells, as MYC VD was not able to promote this phenotype [Kerosuo et al., 2008].

However, in our hands, MYC VD is at least as potent as the wildtype protein in all "stem cell assays" and *CDKN1A* is not repressed, suggesting that MIZ1-independent activation of target genes is the predominant underlying mechanism for this phenotype (Fig. 4.3, 4.6 and data not shown).

Furthermore, although MYC reduces expression of *CDH1* (encoding E-Cadherin) in both HMLE and MCF10A cells on RNA levels, we did not observe any change in protein expression or characteristic morphological alterations that would indicate a complete epithelial to mesenchymal transition in these cells (data not shown). On the contrary, moderately increased levels of MYC consistently cause MCF10A cells to grow in more densely packed and tight colonies which is more indicative of enhanced cell-cell interaction (Fig. 4.1 B, right panel). In addition, while EMT is usually associated with a pro-migratory phenotype, MYC overexpressing cells are strongly impaired in different migration assays, an effect that is partially dependent on MIZ1 (Fig. 4.4; see also discussion section 5.2.1).

Yet, further surface profiling of CD44<sup>high</sup>/CD24<sup>low</sup> cells in HMLE cells reveals a simultaneous decrease in CD326/EpCAM expression (Epithelial Cell Adhesion Molecule) in response to MYC and MYC VD (Fig. 4.6 B). Although this is in contrast to a previous study from Al-Hajj et al. [2003], which stated that CD44<sup>high</sup>/CD24<sup>low</sup> cells are positive for the surface glycoprotein, loss of this epithelial marker may reflect a step towards a partial EMT phenotype in response to high levels of MYC.

An additional aspect that has to be mentioned, is the observation that activation of MYC in HMLE cells, in spite of changing the CD44/CD24 surface marker expression towards a "stem cell" phenotype, represses the transcriptional regulators YAP/TAZ to restrict the self-renewal capability of mammary stem cells [von Eyss et al., 2015]. Although MYC-mediated antagonisa-

tion of YAP/TAZ also occurs in MCF10A cells (data not shown), secondary sphere formation is increased after MYC activation in this cell type (Fig. 4.3). The basis for this phenotypic difference is currently unknown but might be due to cell-type specific effects of MYC that are determined by the differentiation status of the particular cell in which it is activated.

As a matter of fact, the role for MYC in stem cell biology is quite diverse and context dependent: On the one hand, MYC is required for self-renewal and pluripotency of ES cells (ESC) and greatly enhances the efficiency of iPSC (induced pluripotent stem cell) formation [Cartwright et al., 2005; Takahashi and Yamanaka, 2006]. MYC also possesses the unique ability to induce the expression of an ESC-like gene expression programme in primary human mammary epithelial cells [Wong et al., 2008]. On the other hand, it strongly inactivates a gene module that is reminiscent of an adult stem cell programme [Wong et al., 2008]. Indeed, ectopic expression of MYC in the skin depletes epidermal stem cells and drives them into differentiation, which is most likely due to reduced adhesive interactions with the stem cell niche [Waikel et al., 2001; Frye et al., 2003; Berta et al., 2010]. A similar phenotype has been reported for MYC in the bone marrow, where depletion of the transcription factor leads to an accumulation of hematopoietic stem cells because they are retained in the local niche microenvironment [Wilson et al., 2004]. Of note, this unexpected role of MYC has been proposed as fail-safe mechanism to prevent uncontrolled proliferation in the stem cell compartment [Watt et al., 2008; Berta et al., 2010]. Interestingly, repression of adhesion genes by MYC depends on MIZ1 in several experimental systems [Gebhardt et al., 2006; Herkert et al., 2010].

Considering these observations, one could speculate that, while MYC promotes self-renewal in more differentiated cells like the basal MCF10A cells, additional protective mechanisms prevent neoplastic conversion of cells with a higher regenerative capability in response to MYC activation. Indeed, HMLE cells are characterised by a high lineage plasticity and have even been proposed to spontaneously convert into a stem-like state [Chaffer et al., 2011].

Thus, while induction of self-renewal in mammary epithelial cells does not seem to depend on MIZ1, a protective barrier against inappropriate activation of MYC in adult stem cells could require this interaction.

### 5.1.3 MYC-induced apoptosis requires association with MIZ1

While a two- to threefold increase in MYC protein is not sufficient to promote cell death, mammary epithelial cells strongly select against MYC WT during culture once levels of approximately 7- to 10-fold above endogenous MYC are reached (Fig. 4.1 C, 4.7 and 4.8). Importantly, the extend of deregulation correlates with the magnitude of the apoptotic response (Fig. 4.9), suggesting that threshold-dependent phenotypes observed *in vivo* are also operational in this cell culture model [Murphy et al., 2008]. Of note, in compliance with previous reports, low levels of deregulated MYC are sufficient to induce apoptosis in the presence of additional stress stimuli, like glutamine starvation or induction of DNA damage (Fig. 4.5 and Juin et al. [1999]; Yuneva et al. [2007]).

Association with MIZ1 has previously been suggested to affect apoptosis induction by MYC in cell culture models and *in vivo* [Patel and McMahon, 2006, 2007; van Riggelen et al., 2010].

Importantly, also in mammary epithelial cells, both sensitisation to apoptosis at low levels and frank apoptosis in response to high levels of MYC are dependent on the interaction with MIZ1, as MYC VD is strongly impaired in these experiments (e.g. Fig. 4.5 and 4.9). Notably, although

MYC VD is able to trigger a mild apoptotic response, the difference between wildtype and mutant protein becomes more pronounced with increasing MYC levels, suggesting that the impact of association with MIZ1 gains in importance (Fig. 4.9 B).

Apoptosis is one of the most complex processes in mammalian cell biology and thousands of published articles deal with the question how MYC proteins are entangled into its regulatory networks (e.g. reviewed in Nilsson and Cleveland [2003]). In general, it appears that the relative importance of different apoptotic regulators varies between cell types. For example, MYC-induced apoptosis in MCF10A cells is dependent on p53 (Fig. 4.13), although these cells are ARF-deficient. On the other hand, HMLE cells are likely to require ARF but not p53 for apoptosis (Fig. 4.10). Indeed, there is evidence that MYC-induced apoptosis *in vivo* can occur in the absence of either ARF or p53 [Hsu et al., 1995; Blyth et al., 2000; Finch et al., 2006; Muthalagu et al., 2014].

Mechanistically, this is possible because MYC tips the balance of several pro- and antiapoptotic proteins towards mitochondrial cytochrome c release (see Fig. 1.10 and Fig. 4.11). In a mouse model of human Burkitt's lymphoma, MYC proteins carrying mutations in the conserved region MYC box I can activate p19<sup>ARF</sup> and p53, however, these mutants are unable to promote apoptosis because they fail to induce Bim [Hemann et al., 2005]. Again, it seems to be dependent on the particular context, which apoptotic target genes are regulated: although both *Puma* and *Bim* deficiency accelerates MYC-induced lymphomagenesis, loss of *Bim* abrogates apoptosis in response to MYC activation in a variety of solid tissues, whereas *Puma* is dispensable [Egle et al., 2004; Garrison et al., 2008; Muthalagu et al., 2014].

Although *BCL2* is not repressed by MYC in MCF10A cells (Fig. 4.11 C), an overexpression of BCL-2 protein significantly rescues apoptosis induction by MYC (Fig. 4.12 D). Conversely, depletion of BIM attenuates MYC-induced cell death (Fig. 4.12 B). Hence, it appears to be more important to restore a correct balance between anti- and pro-apoptotic proteins, no matter which of the BCL-2 family members might be directly regulated by MYC.

However, rescues in these experiments are not complete, suggesting the existence of additional mechanisms for apoptosis induction (discussed in section 5.2). In line with this thought, MYC VD is able to induce expression of *BCL2L11* (BIM) to levels comparable with induction by MYC WT, yet there is no selective pressure to lose expression of the mutant protein (Fig. 4.11 B).

In conclusion, the described experiments are consistent with a model, in which the palette of molecular functions is expanded with increasing amounts of MYC (Fig. 5.1). While MIZ1 does not seem to play a role in processes that are already regulated by limited amounts of MYC under physiological conditions (e.g. proliferation), the consequences of deregulated MYC (e.g. apoptosis sensitisation) seem to correlate with an increased dependence on association with MIZ1. This could indicate that formation of a repressive complex may be a stress response to potentially oncogenic MYC levels, leaving cells in an alerted state, ready to execute apoptosis once circumstances deteriorate.



## 5.2 Sensing danger: MYC/MIZ1-mediated repression puts cells on the alert

One possible scenario how cells differentiate oncogenic from normal levels of MYC involves stability control of the ARF tumour suppressor: only oncogenic levels of MYC are capable of blocking ARF degradation by the ubiquitin ligase ULF, leading to p53 accumulation and apoptosis [Chen et al., 2013].

However, while this mechanism does not involve transcriptional regulation, in the majority of cases, MYC-induced apoptosis is dependent on association with MAX [Amati et al., 1993; Huang et al., 2004]. For example, the stress kinase Pak2 phosphorylates MYC at three sites (T358, S373, T400) which impairs binding to MAX and DNA. A phospho-mimetic mutant ("MYC D") does not have transcriptional activity anymore and cannot induce apoptosis [Huang et al., 2004]. Correspondingly, overexpression of MYC D, or MYC  $\Delta$ BR which lacks the DNA binding region, does not induce apoptosis in mammary epithelial cells (Fig. 4.14 A). The same result is obtained in MAX-depleted cells (Fig. 4.14 B), strongly indicating that transcriptional activity of MYC is required for apoptosis induction in ARF-deficient MCF10A cells.

As expected, the main defect of the V394D mutation in MYC manifests as selective impairment in target gene repression (Fig. 4.15 C, 4.16). Notably, more than 95 % of regulated genes are identical between wildtype and mutant protein (Fig. 4.15 B), however, fold repression induced by MYC VD is considerably weaker.

It has been suggested that both activating MYC/MAX and repressive MYC/MAX/MIZ1 complexes coexist on most MYC-bound promoters and that the ratio of both complexes determines the transcriptional response [Walz et al., 2014]. Due to its inability to bind MIZ1, selective impairment of the V394D mutant MYC to repress target genes is thus consistent with an altered balance between activating and repressive complexes on promoters (see section 5.2.2).

Because MYC VD is capable of mediating other MYC-associated molecular functions but compromised in pro-apoptotic activity, the consequent corollary of this is that induction of apoptosis

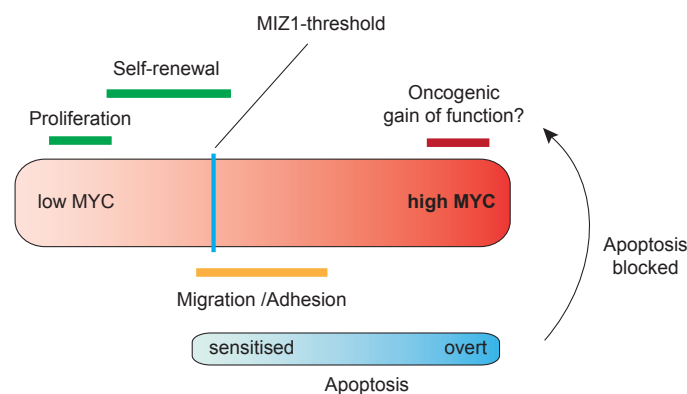


**Figure 5.1: Proposed model for the continuum of MYC functions with increasing levels**

Low levels of MYC are necessary but also sufficient for proliferation and induction of self-renewal. With increasing MYC levels, the requirement for MIZ1 seems to gain more importance, which is illustrated as "MIZ1-threshold". Sensitisation to apoptosis is already evident at moderate MYC expression levels and the response (as well as the dependence on MIZ1) become more apparent once the amount of MYC protein reaches supra-physiological levels ("high MYC") and apoptosis is induced even in the absence of additional stress stimuli ("overt"). However, once apoptotic networks are disabled, there might be an oncogenic gain of function for high levels of MYC/MIZ1 complexes, such as enforcing proliferation in response to anti-mitogenic signals (discussed in section 5.3).

must be connected to the repression of specific MYC target genes.

Interestingly, the ability of MYC to induce apoptosis has already been linked to target gene repression in several studies [Xiao et al., 1998; Conzen et al., 2000; Oster et al., 2003; Qi et al., 2004]. Most strikingly, this was shown by the ability of ARF to differentially block activation of MYC target genes, which inhibits proliferation and transformation, whereas repression by MYC is unaffected and apoptosis is enhanced [Qi et al., 2004]. Furthermore, naturally occurring N-terminal deleted versions of MYC, MYC-S (S for short) proteins, that are defective in transactivation and transforming abilities are still able to induce transcriptional repression and apoptosis [Spotts et al., 1997; Xiao et al., 1998].

MIZ1-dependent gene repression by MYC primarily affects genes with a function in cell adhesion, regulation of apoptosis and epithelial cell differentiation (Fig. 4.17 B) which is consistent with multiple previous studies [Coller et al., 2000; Gebhardt et al., 2006; Herkert et al., 2010]. While individual genes are largely non-overlapping between different cell types, functional categories of repressed genes seem to be conserved also in the osteosarcoma cell line U2OS for example (Fig. 4.18). Importantly, repression of these genes requires high levels of MYC and hence coincides with induction of apoptosis by MYC (Fig. 4.17). Of note, gene repression precedes the induction of apoptosis and is therefore more likely a cause than a consequence of cell death (data not shown).

Thus, complex formation with MIZ1 and transcriptional repression of specific sets of target genes might be a way how epithelial cells "sense" oncogenic levels of MYC.

The model that selected target genes are repressed is somewhat at odds with MYC's role as a general amplifier of pre-existing gene expression patterns inside a cell [Lin et al., 2012a; Nie et al., 2012]. However, MYC activation in MCF10A cells does neither lead to cell growth nor the increase in total RNA levels that is observed in activated B lymphocytes for example, suggesting that the transcription factor might not act as a universal amplifier in this cellular context. Hence, repressed genes are actually repressed, not just genes that are "less amplified" [Lovén et al., 2012; Wiese et al., 2015; Wolf et al., 2015].

But what is the exact functional connection between gene repression by MYC/MIZ1 and the induction of apoptosis? A novel finding of the work presented here, is the observation that repressed genes overlap with target genes of the serum response factor, SRF (Fig. 4.26).

### 5.2.1 Inhibition of SRF blocks survival signalling via AKT

The SRF transcription factor regulates the expression of target genes downstream of Ras-MAPK and Rho-Actin signalling (Fig. 5.2 and Gineitis and Treisman [2001]). Following extracellular stimuli, SRF transcriptional activity is controlled by interaction with either TCF (ternary complex factor) or MRTF (myocardin-related transcription factor) cofactors. Target genes include mitogen-responsive immediate-early genes as well as genes encoding cytoskeleton and adhesion proteins [Sun et al., 2006; Esnault et al., 2014].

The first indication that SRF activity is also regulated downstream of cytoskeletal dynamics was the observation that depletion of the cytoplasmic G-actin pool is necessary and sufficient for induction of a subset of target genes [Sotiropoulos et al., 1999; Posern et al., 2002]. Subsequently, MRTFs were identified as the crucial cofactors linking RhoA signalling to SRF target gene activation: MRTFs are retained in the cytoplasm as long as they are bound to G-actin. Activation of the RhoA GTPase decreases the concentration of free G-actin by stimulating actin

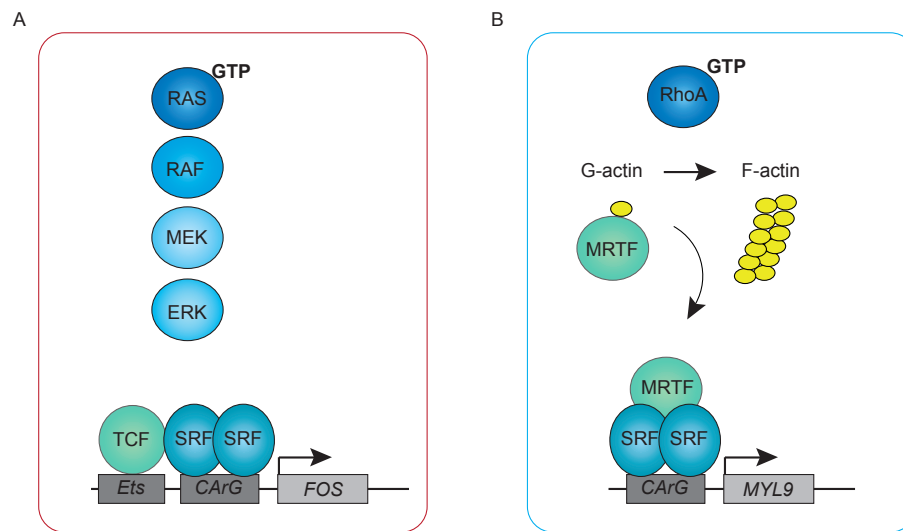


**Figure 5.2: A cofactor switch determines differential SRF activity and function**

- A The RAS-MAPK pathway converges on members of the TCF family (e.g. Elk-1) which bind to "Ets" sites next to the consensus SRF binding motif (CArG box) to control expression of immediate-early genes like *FOS*.
- B Among the SRF target genes downstream of RhoA-Actin signalling are genes involved in adhesion and cytoskeleton dynamics. The MRTF/MAL coactivator translocates to the nucleus after RhoA mediated F-actin polymerisation and is recruited to chromatin via SRF. Note that MRTFs also contact DNA but no consensus sequence has been identified. Adapted from Posern and Treisman [2006].

polymerisation, which releases MRTFs and promotes nuclear translocation [Wang et al., 2002; Miralles et al., 2003].

Conserved cis-regulatory motifs resembling the so-called CArG box or serum response element (SRE) are significantly enriched in promoters of MYC-repressed genes (Fig. 4.26). Validating the promoter analysis, genes bound by Srf in murine fibroblasts are repressed by MYC in a MIZ1-dependent manner in MCF10A cells (Fig. 4.27 and Esnault et al. [2014]). In particular, more than a quarter of joint Srf/Mrtf targets is repressed by MYC.

Of note, there is also an overlap between MYC-activated and SRF target genes (Fig. 4.27 B). This is not surprising, since similar to MYC, SRF regulates many target genes involved in cell growth and proliferation [Selvaraj and Prywes, 2004; Sun et al., 2006]. For example, the list of commonly upregulated genes includes *CCNT2*, encoding a Cyclin T isoform that is a subunit of P-TEFb [Peng et al., 1998].

In line with previous observations that SRF is a master regulator of cytoskeletal dynamics, overlapping repressed genes fall exclusively into functional categories related to actin cytoskeleton and adhesion processes (Fig. 4.27 C and Miralles et al. [2003]; Esnault et al. [2014]).

MCF10A cells seem to grow in more compact and tighter clusters when MYC, but not MYC VD, is overexpressed at moderate levels (Fig. 4.1 B). With increasing levels, these clusters get more densely packed and rounded and subsequently detach (Fig. 4.1 C). Although we did not analyse the morphological phenotype in detail, these changes in cell shape are consistent with cytoskeletal alterations and have been noted before after MYC overexpression in other cell types [Frye et al., 2003; Liu et al., 2012a]. MYC deregulation in murine skin for example, results in a severe impairment in wound healing and migration of keratinocytes and is also associated with loss of adhesion due to repression of integrins [Frye et al., 2003; Gebhardt et al., 2006]. Furthermore, MYC inhibits integrins  $\alpha v$  and  $\beta 3$  in human breast cancer cell lines, leading to a reduction in

focal adhesions and a phenotype that is characterised by reduced motility and invasiveness [Liu et al., 2012a]. Finally, in the luminal breast cancer cell line MCF7, a MYC-mediated reduction in motility has been associated with MIZ1-dependent repression of the chemokine CCL5/RANTES [Cappellen et al., 2007].

Control of migration is a complex process that is regulated by integration of various signals ranging from cytoskeletal polarity to stimuli received via cell-cell and cell-matrix adhesion. Notably, migration of epithelial cells is restricted by cell-cell contacts [Friedl and Wolf, 2010]. Consistent with the change in cell morphology and the studies described above, when expressed at sub-apoptotic levels, MYC impairs the migratory potential of MCF10A cells in transwell migration and *in vitro* wound healing assays, in a partially MIZ1-dependent manner (Fig. 4.4 and data not shown).

Migration of breast tumour cells for example, can be promoted through an interaction of the extracellular matrix protein laminin 322 with the  $\alpha 6 \beta 4$  integrin receptor [Zahir et al., 2003]. Concordantly, several integrins, such as *ITGA6*, *ITGB3* and *ITGB4* (Fig. 4.16 and 4.28 and data not shown) as well as the genes coding for  $\beta$ - and  $\gamma$ -chains of laminin 322 (*LAMB3*, *LAMC2*; Fig. 4.30 and data not shown) are among genes repressed by MYC in MCF10A cells.

Consistent with the view that activation of adhesion and cytoskeletal genes by SRF is predominantly controlled via the RhoA-MRTF-axis, overexpression of constitutively active RhoA (Q63L) or MRTF-A ( $\Delta$ N-MAL) alleles induces common MYC/SRF target genes (Fig. 4.28 and 4.30). Importantly, because one of the joint targets, *PLEKHG2*, is a guanine nucleotide exchange factor (GEF) for the Rho GTPase family (RhoGEF), we confirmed that MYC does not repress SRF indirectly via effects on RhoA (Fig. 4.28 and Sato et al. [2013]).

Although MYC-induction still suppresses SRF-dependent gene expression in presence of the constitutively nuclear  $\Delta$ N-MAL allele, expression levels of several target genes are restored to background levels (Fig. 4.30). Hence, repression of SRF occurs downstream of MRTF nuclear import (see section 5.2.2; Vartiainen et al. [2007]).

Laminin 322 and integrins are a major component of attachment structures like focal adhesions and stable anchoring contacts (SACs) [Marinkovich, 2007]. The assembly of this adhesion complexes is not only dependent on interactions with the extracellular matrix (ECM), but also on connections with the cytoskeleton. Adhesion to the ECM triggers pro-survival signals that activate kinases like FAK (focal adhesion kinase) and ILK (integrin-linked kinase), and that finally converge on PI3K/AKT and ERK signalling pathways [Paoli et al., 2013]. Disruption of these interactions induces apoptosis, which is also called "anoikis" in this case [Meredith et al., 1993; Frisch and Francis, 1994; Meredith and Schwartz, 1997].

Several studies suggest that a polarised three-dimensional architecture can protect epithelial cells from MYC-induced apoptosis [Partanen et al., 2007; Simpson et al., 2011]. However, resistance to different apoptosis-inducing stimuli in 3D cultures is critically dependent on ligation of  $\beta 4$  integrins [Weaver et al., 2002]. As *ITGB4* is one of the differentially repressed target genes, this explains, why high levels of MYC, but not MYC VD, are also able to induce apoptosis in MCF10A cells cultured in 3D and excludes that the observed effects are due to 2D-culture artefacts (Fig. 4.8 E).

Interestingly, SRF knockout (-/-) ES cells are severely compromised in adhesion and migration due to aberrant actin dynamics and show increased apoptosis under differentiating conditions, hence phenocopying MYC overexpression in MCF10A cells [Schratt et al., 2002, 2004].

If MYC-induced apoptosis was caused by repression of SRF-dependent adhesion signalling, consequently, re-activation of SRF signalling should rescue MYC-induced apoptosis. At oncogenic MYC expression levels, activation of  $\Delta$ N-MAL/MRTF-A expression has only a mild protective effect (Fig. 4.31 A). However, apoptosis is substantially inhibited by re-addition of  $\Delta$ N-MAL or constitutive active SRF-VP16 in assays of MYC-induced sensitisation to apoptotic stimuli at lower expression levels (experiments performed by Heidi M. Haikala, Wiese et al. [2015]).

One potential explanation for this phenotypic difference might be that, in addition to SRF, other pathways are additionally repressed by oncogenic MYC levels that are not yet repressed by lower levels of MYC. While a huge fraction of SRF/MRTF-target genes is repressed by MYC (approximately 25%), these genes in turn comprise only a small fraction of the total amount of MYC-repressed genes (Fig. 4.27). In agreement with this notion, we identified binding sites of other transcription factors in genes that are differentially repressed between oncogenic levels of MYC and MYC VD (see table in Fig. 4.26 A). Most notably, Rel/NF- $\kappa$ B transcription factors can have potent anti-apoptotic activity, as demonstrated in keratinocytes and breast cancer cell lines, for example [Sovak et al., 1997; Kothny-Wilkes et al., 1998; Barkett and Gilmore, 1999]. In addition, MYC-induced sensitisation to TNF-mediated apoptotic stimuli has been described to require inhibition of NF- $\kappa$ B and the transcription factor is also the critical downstream effector mediating apoptosis-resistance downstream of integrin signalling [You et al., 2002; Weaver et al., 2002].

In fibroblasts, MYC-induced apoptosis can be suppressed via PI3K/AKT signalling downstream of Ras [Kauffmann-Zeh et al., 1997]. Activity of AKT is mainly controlled via phosphorylations at threonine 308 (T308) and serine 473 (S473), which are mediated by PDK1 (phosphoinositide dependent kinase 1) and mTORC2 (mammalian target of rapamycin complex-2), respectively [Alessi et al., 1997; Sarbassov et al., 2005].

Importantly, major survival pathways downstream of integrin-mediated adhesion signalling in epithelial cells also converge on the AKT kinase [King et al., 1997; Khwaja et al., 1997; Velling et al., 2004]. Consistently, oncogenic levels of MYC lead to a diminished phosphorylation of AKT at S473 and conversely, the constitutively active viral oncogene version of AKT, *v-akt*, is able to rescue MYC-dependent apoptosis in MCF10A cells (Fig. 4.31 B and Wiese et al. [2015]). Although SRF inhibition may not be the only consequence of deregulated MYC activity in epithelial cells, it still contributes considerably to the apoptotic phenotype. This is further supported by the fact, that the MYC-dependent decrease in AKT activity can be reverted by  $\Delta$ N-MAL induction (Fig. 4.31 B). In addition, inhibition of AKT with either siRNA or the inhibitor MK-2206, abrogates the ability of  $\Delta$ N-MAL to rescue MYC-induced apoptosis, suggesting that SRF/MRTF signalling is likely to provide epithelial cells with survival signalling upstream of AKT [Wiese et al., 2015].

Although we did not completely resolve the mechanistic details, ILK as well as FAK have been proposed to promote AKT activation downstream of adhesion signalling and indeed, inhibition of both kinases abrogates phosphorylation of serine 473 in MCF10A cells, making them potential candidates [Wiese et al., 2015; Persad et al., 2000; Xia et al., 2004; Nho et al., 2005]. Of note, ILK has been proposed to promote S473 phosphorylation and AKT function without affecting T308, which is consistent with the observation that MYC-induction does not consistently alter T308 phosphorylation status in MCF10A cells (Fig. 4.31 B and Persad et al. [2000, 2001]). Yet,

activity of AKT is severely reduced as judged by the reduced phosphorylation of the downstream target GSK3 $\beta$  at serine 9 (S9, Fig. 4.31 B).

Interestingly, several studies have also connected mTORC2 to regulation of cytoskeletal dynamics and adhesion: mTORC2 as well as its upstream regulator TSC1/Hamartin seem to be involved in regulation of cytoskeleton organisation and adhesion [Lamb et al., 2000; Sarbassov et al., 2004; Jacinto et al., 2004]. Importantly, integrin-dependent cellular tension causes so-called mechanical or force activation of mTORC2 which can be downstream of FAK [Roca-Cusachs et al., 2013; Thompson et al., 2013]. Strikingly, mTORC2-mediated phosphorylation at S473 in AKT is sufficient for the downstream mechanical regulation of GSK3 $\beta$  and is independent of T308 phosphorylation and growth factor signalling [Case et al., 2011].

Activation of AKT promotes survival via phosphorylation of a variety of substrates, including BAD, BAX, MDM2, FOXO and GSK3 [Datta et al., 1997; Gardai et al., 2004; Ogawara et al., 2002; Brunet et al., 1999; Cross et al., 1995]

As noted before, MYC VD is able to induce expression of the pro-apoptotic protein BIM similar to WT MYC, which is not sufficient to induce apoptosis though. In contrast, suppression of SRF and AKT by MYC WT would additionally activate BAD and BAX, and might therefore be needed to tip the scale towards apoptosis.

Interestingly, suppression of AKT activity by oncogenic MYC would also lead to an activation of GSK3 $\beta$  (by reducing S9 phosphorylation), which in turn promotes T58 phosphorylation of MYC and subsequent ubiquitin-mediated turnover [Welcker et al., 2004; Yeh et al., 2004]. However, phosphorylation at T58 is also required for MYC-mediated upregulation of BIM and apoptosis [Hemann et al., 2005; Wang et al., 2011]. Therefore, one could speculate, that repression of SRF and AKT activity is an additional fail-safe mechanism that triggers apoptosis in cells which cannot degrade MYC anymore. Interestingly, MIZ1 is also phosphorylated by AKT which results in its sequestration by a 14-3-3 protein and inhibition of DNA binding [Wanzel et al., 2005]. Inhibition of AKT by MYC might therefore also provide a positive feedback loop to enhance MIZ1's association with chromatin.

Taken together, repression of cytoskeletal and adhesion related genes by MYC/MIZ1 disrupts critical survival circuits in epithelial cells. Most notably, these effects are mediated via SRF/MRTF and AKT (Fig. 5.3).

### 5.2.2 Joint invasion of new genomic territories

Many studies have already demonstrated that an increase in MYC protein from physiological to oncogenic levels leads to an "invasion" of promoter and enhancer sequences until almost all active chromatin regions are occupied [Guccione et al., 2006; Lin et al., 2012b; Sabò et al., 2014; Walz et al., 2014]. In addition, analysis of binding sites reveals a higher frequency of low affinity sites, including non-canonical E-box variants and other motifs, with increasing MYC levels [Fernandez et al., 2003; Walz et al., 2014]. These observations allow the assumption that oncogenic levels of MYC might regulate additional targets and that changes in their expression allow cells to discriminate physiological from supraphysiological amounts of MYC [Lin et al., 2012b; Sabò et al., 2014; Walz et al., 2014].

In line with previous studies, activation of MYC-ER in MCF10A cells results in an increased genomic occupancy and more than 4,500 "new" promoters are bound (Table 4.1, Fig. 4.21 and

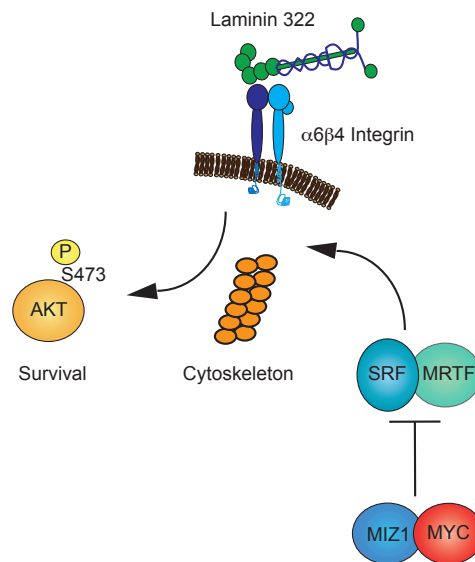


**Figure 5.3: Repression of adhesion and cytoskeleton dependent survival signalling by MYC**

In normal cells, adhesion to the extracellular matrix provides critical survival signals that result in activation of the AKT kinase (e.g. phosphorylation at serine 473). MYC/MIZ1 mediated repression of SRF/MRTF abrogates this signalling through alteration of adhesion and cytoskeletal pathways. Target genes include components of laminin ECM proteins and integrin receptors.

4.22). Furthermore, apart from the conserved MIZ1 target genes that had been identified in murine neuronal progenitor cells (NPCs) and that contain the MIZ1-binding motif, endogenous MIZ1 can be detected at promoters of more than 1,000 genes in MCF10A cells (Fig. 4.21 and Wolf et al. [2013]; Wiese et al. [2015]).

Similar to other cellular systems, there is a large overlap between MYC and MIZ1 binding sites, and MYC WT, but not MYC VD, is able to increase MIZ1 occupancy on promoters, indicating that they bind to DNA cooperatively and recruit each other to target sites (Fig. 4.23).

Altogether, there seems to be a correlation between the levels of MYC in a particular system and the number of target sites that are co-occupied by MIZ1: Whereas only a few hundred genes are bound by MIZ1 in NPCs in a MYC-independent manner, elevated levels of MYC in MCF10A cells recruit MIZ1 to thousands of target sites and even more promoters are jointly bound in human and murine cancer cell lines [Wolf et al., 2013; Walz et al., 2014].

In addition, MIZ1 is present in low but equal amounts at both MYC activated and repressed promoters in MCF10A cells (Fig. 4.25). As proposed previously, overall MYC occupancy is higher on activated than on repressed genes, confirming a correlation between the relative ratio of MYC/MIZ1 on a promoter and the direction of the transcriptional response [Walz et al., 2014]. Genomic occupancy of MYC VD appears lower, which leads to a smaller number of significant binding sites that can be detected but almost 90 % of genes bound by MYC VD are also bound by MYC WT (Fig. 4.22). Valine 394 in MYC is located in the second helix of the HLH domain and considering the crystal structure, mutation of this residue should not interfere with DNA binding or the interaction with MAX (Fig. 1.6). Indeed, exogenous co-immunoprecipitation experiments show that MYC VD can precipitate MAX as efficiently as the wildtype protein (data not shown). In addition, although both helices mediate the interaction with MAX, mutation of threonine 400 to aspartate (T400D) for example, which is very close to V394, does not interfere with binding to MAX or DNA [Davis and Halazonetis, 1993; Huang et al., 2004]. Unfortunately, depletion of

MIZ1 is not tolerated in MCF10A cells (data not shown), preventing us from corroborating that the defects of MYC VD are indeed mimicked by MIZ1 depletion in MYC overexpressing cells. However, de-repression of MYC target genes upon knockdown of MIZ1 in U2OS cells correlates significantly with the difference in gene expression between MYC WT and MYC VD in MCF10A cells (Fig. 4.18 B). Taken together, it is most likely that the reduced affinity of MYC VD for DNA as well as its impaired ability to repress target genes is connected to a weakened interaction with MIZ1.

Although binding sites that are occupied by MYC WT and MYC VD together are enriched for high affinity E-box sequences (Fig. 4.24 and Wiese et al. [2015]), more than half of the analysed peaks lack a consensus MYC binding motif. This finding is consistent with a recent study claiming that the overall MYC occupancy in the genome correlates significantly better with presence of Pol II and the general transcription machinery than with E-boxes [Guo et al., 2014]. In addition, the cooperative DNA binding with other transcriptional activators, such as GABPA and AP1, has been proposed to mediate MYC binding to low affinity sites in several studies [Neph et al., 2012; Sabò and Amati, 2014]. In fact, GABPA consensus binding motifs are present in a significant fraction of analysed MYC (or MYC VD) binding sites in MCF10A cells (data not shown).

Neither canonical E-Boxes nor non-canonical variants are enriched in promoters of genes that are bound by MYC/MIZ1 but not MYC VD (Fig. 4.24 and Wiese et al. [2015]). Instead, the top enriched motif resembles the reverse complement of a consensus binding site of the zinc finger transcription factor SP1 (5'-(G/T)GGGCGG(G/A)(G/A)(C/T)-3'; Song et al. [2001]). The formation of repressive complexes between MYC and SP1/SP3 or N-MYC/MIZ1 and SP1 has been described before and a similar DNA consensus motif is enriched in the promoters of MYC-repressed genes in HeLa cells [Gartel et al., 2001; Iraci et al., 2011; Walz et al., 2014].

Interestingly, the analysis of MYC/MIZ1 bound genes also reveals a significant enrichment of a so-called "secondary motif" for SRF (data not shown), which is not the consensus sequence of the CArG-box but an alternate recognition site that is nevertheless bound with high preference [Badis et al., 2009].

In line with this and the findings described in section 5.2.1, MYC/MIZ1 bound genes overlap significantly with target genes of the serum response factor (Fig. 4.29 A). Similar to MYC, the majority (almost 70 %) of SRF binding sites is located close to the transcriptional start site (TSS) of its target genes [Esnault et al., 2014]. However, it is highly likely that binding occurs independently of each other, since MYC and SRF ChIP-seq peaks do not overlap at most target genes and neither MYC nor MIZ1 interacts with SRF in co-immunoprecipitation experiments (Fig. 4.29 B and C; Wiese et al. [2015]; Wolf and Walz [2014]). Interestingly, similar to our analysis of MYC/MIZ1 bound genes, SRF binding sites are associated with SP1 motifs when the CArG consensus sequence is weak or absent and SRF and SP1 have been shown to interact with MyoD to regulate muscle-specific genes for example [Biesiada et al., 1999; Esnault et al., 2014].

The exact mechanism for MYC/MIZ1-mediated repression of SRF target genes is still unclear. For example, we did not investigate whether SRF/MRTF complexes might be displaced from chromatin after MYC activation. MYC/MIZ1 and SRF peaks are on average approximately 2 kb apart, excluding the possibility of steric hindrance [Wiese et al., 2015]. Interestingly, several studies link SRF function with recruitment of histone acetyltransferases. For instance,



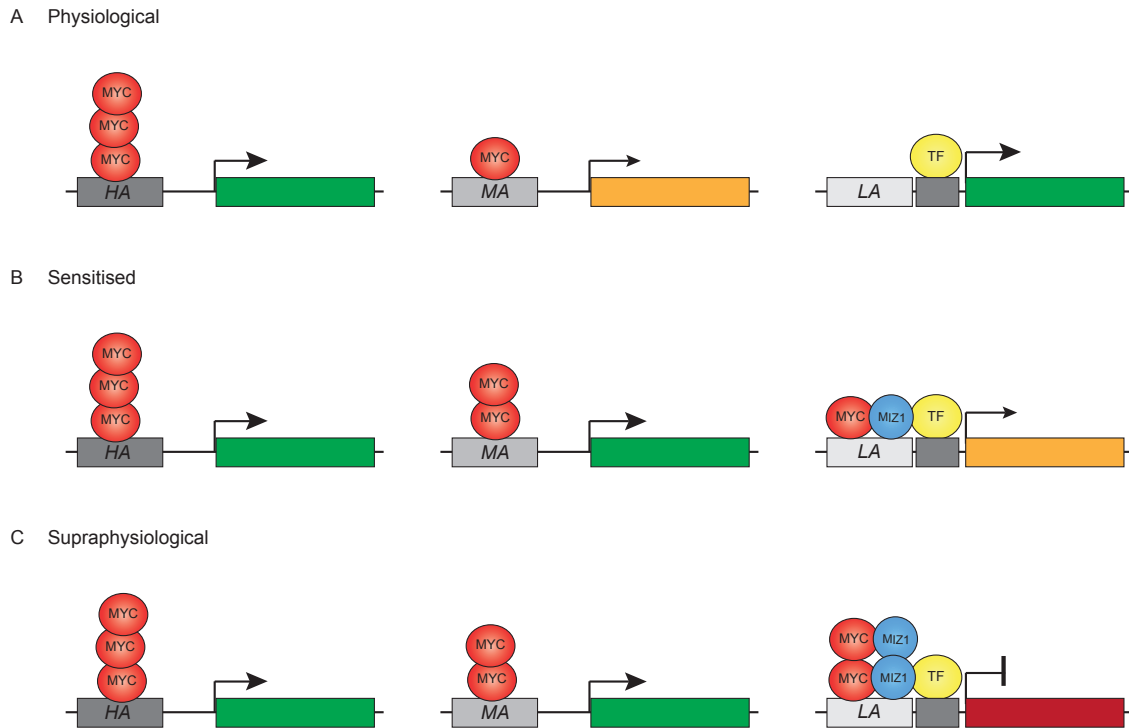


**Figure 5.4: Mechanistic model for the differential effects on target gene expression after MYC deregulation**

- A Physiological levels: MYC proteins bind to promoters containing high affinity ("HA") sites and activate gene expression (left, green). Certain genes might have intermediate affinity sites ("MA") and are only weakly activated (middle, orange). Other genes (right, green) with low affinity ("LA") sites are not bound by MYC at physiological levels but are activated by other transcription factors (TF), such as SRF.
- B Moderately deregulated levels: No change in gene expression is observed at promoters with high affinity sites. Instead, recruitment of additional MYC leads to increased expression of genes whose promoters were not fully saturated (middle). Association with MIZ1 might recruit MYC to low affinity sites and dampen the transcriptional response on these genes (right). Recruitment could be mediated by other transcription factors such as SP1 (not shown).
- C Supra-physiological levels: Enhanced complex formation with MIZ1 leads to transcriptional repression at LA sites. Note that MAX is present in all complexes and MIZ1 can also be present on HA and MA promoters without influencing the transcriptional response (not shown).

the interaction with the CBP coactivator is required for regulation of *c-fos* and conversely, histone H4 deacetylase activity blocks SRF association with chromatin [Ramirez et al., 1997; McDonald et al., 2006]. As repression by MYC/MIZ1 correlates with histone de-acetylation, access of SRF to CArG box elements could therefore be prevented [Walz et al., 2014].

Collectively, the results obtained in this thesis are thus consistent with the following model (Fig. 5.4): At physiological levels, MYC binds to high affinity binding sites and regulates genes involved in cell growth and proliferation. A gradual increase in MYC levels results in an invasion of additional promoters, which is consistent with the transient amplifier model. However, high levels of MYC associate with MIZ1, leading to further invasion of low affinity sites which can be facilitated via protein-protein interactions with other transcriptional regulators. The ratio of MYC/MIZ1 complexes is lower at these promoters, leading to repression of non-physiological target genes and thus antagonisation of nonlinear amplification. As discussed above, these targets include genes involved in cell adhesion and cytoskeletal dynamics which usually promote survival signalling in epithelial cells. Hence, repression of these genes ultimately results in apoptosis.

### 5.3 Balancing act: oncogenic and tumour suppressive consequences of the MYC/MIZ1 interaction

The view that apoptosis restricts MYC-induced tumour formation is most strikingly demonstrated in mouse models of lymphomagenesis and evidenced by the cooperation of MYC with many different apoptotic regulators, such as ARF, BCL-2 and BAX [Eischen et al., 1999; Schmitt et al., 1999; Eischen et al., 2001a; Finch et al., 2006]. In addition, so-called "double-hit" lymphomas with MYC as well as BCL-2 rearrangements in human patients are correlated with aggressive clinical course and poor prognosis [Li et al., 2013].

Similarly, although high-level MYC expression drives mammary gland tumourigenesis in transgenic mouse models, tumours arise with long latencies, suggesting that additional genetic lesions are also required in this context [Stewart et al., 1984; Schoenenberger et al., 1988; D'Cruz et al., 2001]. Consistently, cooperating alterations that suppress apoptosis accelerate MYC-induced mammary gland tumourigenesis and include signalling events downstream of activated EGF-Receptor (EGFR), PI3K and TGF $\alpha$  pathways [Nass et al., 1996; Amundadottir et al., 1996; Amundadottir and Leder, 1998].

It is tempting to speculate that the quantitative and qualitative changes in gene expression patterns that are described in this thesis, provide an alarm signal in response to oncogenic MYC levels in epithelial cells and that association of repressive MYC/MIZ1 complexes is therefore designed to serve as protection from cancer development by promoting apoptosis.

It is also very well possible, that these mechanisms are based on a physiological role of MYC in the mammary gland, namely the regulation of apoptosis during involution [Sutherland et al., 2006]. Similar to MYC, MIZ1 is expressed in the mammary epithelium at different developmental stages and interestingly, a functional role for p19<sup>ARF</sup> has also been proposed during mammary gland development, where deletion of ARF disrupts normal apoptosis during involution [Yi et al., 2004; Sanz-Moreno et al., 2014].

As mentioned above ARF promotes assembly of MYC/MIZ1 complexes and shifts MYC function towards apoptosis [Herkert et al., 2010; Boone et al., 2011]. However, as MCF10A cells do not express ARF, other mechanisms of currently unknown nature may facilitate association of MYC with MIZ1. Interestingly, ARF is dispensable for apoptosis in response to oncogenic stress in a mouse brain tumour model, suggesting the existence of more complex regulatory pathways for p53-mediated tumour suppression [Tolbert et al., 2002].

Despite all evidences for tumoursuppressive countermeasures against MYC, elevated MYC pathway activation has been documented in triple negative human breast cancer and high levels of MYC can be detected in immunohistochemical stainings of these tumours [Horiuchi et al., 2012; Wiese et al., 2015]. Interestingly, high levels of MIZ1 expression are present in both low- and high-grade tumours, whereas MYC levels seem to only rise gradually with tumour grade [Wiese et al., 2015]. The same trend is obvious when gene expression datasets from human breast cancer patients are analysed: Using a previously published set of MYC-activated genes as a measure for MYC activity, the fraction of tumours showing high MYC activity increases with increasing tumour grade and high MYC activity correlates with poor prognosis. Remarkably, MYC/MIZ1-mediated repression is not lost in human tumours, becomes equally pronounced with increasing tumour grade and is associated with a poor survival rate similar to target gene activation [Wiese et al., 2015].

However, the presence of target gene repression is significantly associated with simultaneous mutations of the tumour suppressor p53 in these patients. In line with the experiments of this thesis, this strongly suggests that MYC/MIZ1-mediated repression is tolerated once mechanisms to escape apoptosis are available.

Furthermore, it could even indicate that there is an oncogenic gain of function for repression of target genes once apoptotic pathways are disabled which would also explain the results of murine tumour models in which MYC V394D alleles display delayed tumourigenesis [Wiese et al., 2013]. For example, a delay in lymphoma formation with the V394D transgene is due to a derepression of *cdkn2b* (p15) and *cdkn1c* (p57), demonstrating that suppression of cell-cycle inhibitors, while not required under physiological conditions, is critical for an escape from senescence in response to TGF $\beta$  [van Riggelen et al., 2010]. Similarly, once apoptosis is prevented, changes in adhesive interactions and cytoskeletal dynamics might facilitate tumour progression and enable metastasis and indeed MYC regulates a poor-prognosis metastatic gene signature in human breast cancer cells [Wolfer et al., 2010].

MYC inactivation in established tumours often leads to tumour regression and it has been suggested that tumour cells depend on elevated levels of MYC and its activated target genes [Nilsson et al., 2005; Arvanitis and Felsher, 2006; Barna et al., 2008]. It will be interesting to determine whether human tumours depend as well on a MYC/MIZ1-repressed gene signature.

# Bibliography

- Acosta, J. C., Ferrándiz, N., Bretones, G., Torrano, V., Blanco, R., Richard, C., O'Connell, B., Sedivy, J., Delgado, M. D., and León, J. (2008). Myc inhibits p27-induced erythroid differentiation of leukemia cells by repressing erythroid master genes without reversing p27-mediated cell cycle arrest. *Mol Cell Biol*, 28(24):7286–7295.
- Adams, J. M. (2003). Ways of dying: multiple pathways to apoptosis. *Genes Dev*, 17(20): 2481–2495.
- Adhikary, S., Peukert, K., Karsunky, H., Beuger, V., Lutz, W., Elsässer, H.-P., Möröy, T., and Eilers, M. (2003). Miz1 is required for early embryonic development during gastrulation. *Mol Cell Biol*, 23(21):7648–7657.
- Adhikary, S., Marinoni, F., Hock, A., Hulleman, E., Popov, N., Beier, R., Bernard, S., Quarto, M., Capra, M., Goettig, S., Kogel, U., Scheffner, M., Helin, K., and Eilers, M. (2005). The ubiquitin ligase hecth9 regulates transcriptional activation by myc and is essential for tumor cell proliferation. *Cell*, 123(3):409–421.
- Al-Hajj, M., Wicha, M. S., Benito-Hernandez, A., Morrison, S. J., and Clarke, M. F. (2003). Prospective identification of tumorigenic breast cancer cells. *Proc Natl Acad Sci U S A*, 100 (7):3983–3988.
- Alessi, D. R., Deak, M., Casamayor, A., Caudwell, F. B., Morrice, N., Norman, D. G., Gaffney, P., Reese, C. B., MacDougall, C. N., Harbison, D., Ashworth, A., and Bownes, M. (1997). 3-phosphoinositide-dependent protein kinase-1 (pdk1): structural and functional homology with the drosophila dstpk61 kinase. *Curr Biol*, 7(10):776–789.
- Alfano, D., Votta, G., Schulze, A., Downward, J., Caputi, M., Stoppelli, M. P., and Iaccarino, I. (2010). Modulation of cellular migration and survival by c-myc through the downregulation of urokinase (upa) and upa receptor. *Mol Cell Biol*, 30(7):1838–1851.
- Amati, B., Littlewood, T. D., Evan, G. I., and Land, H. (1993). The c-myc protein induces cell cycle progression and apoptosis through dimerization with max. *EMBO J*, 12(13):5083–5087.
- Amundadottir, L. T. and Leder, P. (1998). Signal transduction pathways activated and required for mammary carcinogenesis in response to specific oncogenes. *Oncogene*, 16(6):737–746.
- Amundadottir, L. T., Nass, S. J., Berchem, G. J., Johnson, M. D., and Dickson, R. B. (1996). Cooperation of tgf alpha and c-myc in mouse mammary tumorigenesis: coordinated stimulation of growth and suppression of apoptosis. *Oncogene*, 13(4):757–765.

- Arabi, A., Wu, S., Ridderstråle, K., Bierhoff, H., Shiue, C., Fatyol, K., Fahlén, S., Hydbring, P., Söderberg, O., Grummt, I., Larsson, L.-G., and Wright, A. P. H. (2005). c-myc associates with ribosomal dna and activates rna polymerase i transcription. *Nat Cell Biol*, 7(3):303–310.
- Arvanitis, C. and Felsher, D. W. (2006). Conditional transgenic models define how myc initiates and maintains tumorigenesis. *Semin Cancer Biol*, 16(4):313–317.
- Ashkenazi, A. (2002). Targeting death and decoy receptors of the tumour-necrosis factor superfamily. *Nat Rev Cancer*, 2(6):420–430.
- Askew, D. S., Ashmun, R. A., Simmons, B. C., and Cleveland, J. L. (1991). Constitutive c-myc expression in an il-3-dependent myeloid cell line suppresses cell cycle arrest and accelerates apoptosis. *Oncogene*, 6(10):1915–1922.
- Badis, G., Berger, M. F., Philippakis, A. A., Talukder, S., Gehrke, A. R., Jaeger, S. A., Chan, E. T., Metzler, G., Vedenko, A., Chen, X., Kuznetsov, H., Wang, C.-F., Coburn, D., Newburger, D. E., Morris, Q., Hughes, T. R., and Bulyk, M. L. (2009). Diversity and complexity in dna recognition by transcription factors. *Science*, 324(5935):1720–1723.
- Bailey, T. L., Boden, M., Buske, F. A., Frith, M., Grant, C. E., Clementi, L., Ren, J., Li, W. W., and Noble, W. S. (2009). Meme suite: tools for motif discovery and searching. *Nucleic Acids Res*, 37(Web Server issue):W202–W208.
- Barkett, M. and Gilmore, T. D. (1999). Control of apoptosis by rel/nf-kappab transcription factors. *Oncogene*, 18(49):6910–6924.
- Barna, M., Pusic, A., Zollo, O., Costa, M., Kondrashov, N., Rego, E., Rao, P. H., and Ruggero, D. (2008). Suppression of myc oncogenic activity by ribosomal protein haploinsufficiency. *Nature*, 456(7224):971–975.
- Basu, S., Liu, Q., Qiu, Y., and Dong, F. (2009). Gfi-1 represses cdkn2b encoding p15ink4b through interaction with miz-1. *Proc Natl Acad Sci U S A*, 106(5):1433–1438.
- Benchimol, S. (2001). p53-dependent pathways of apoptosis. *Cell Death Differ*, 8(11):1049–1051.
- Bentley, D. L. and Groudine, M. (1986). A block to elongation is largely responsible for decreased transcription of c-myc in differentiated hl60 cells. *Nature*, 321(6071):702–706.
- Berta, M. A., Baker, C. M., Cottle, D. L., and Watt, F. M. (2010). Dose and context dependent effects of myc on epidermal stem cell proliferation and differentiation. *EMBO Mol Med*, 2(1):16–25.
- Beverly, L. J. and Varmus, H. E. (2009). Myc-induced myeloid leukemogenesis is accelerated by all six members of the antiapoptotic bcl family. *Oncogene*, 28(9):1274–1279.
- Biesiada, E., Hamamori, Y., Kedes, L., and Sartorelli, V. (1999). Myogenic basic helix-loop-helix proteins and sp1 interact as components of a multiprotein transcriptional complex required for activity of the human cardiac alpha-actin promoter. *Mol Cell Biol*, 19(4):2577–2584.
- Bièche, I., Laurendeau, I., Tozlu, S., Olivi, M., Vidaud, D., Lidereau, R., and Vidaud, M. (1999). Quantitation of myc gene expression in sporadic breast tumors with a real-time reverse transcription-pcr assay. *Cancer Res*, 59(12):2759–2765.

- Blackwell, T. K., Kretzner, L., Blackwood, E. M., Eisenman, R. N., and Weintraub, H. (1990). Sequence-specific dna binding by the c-myc protein. *Science*, 250(4984):1149–1151.
- Blackwell, T. K., Huang, J., Ma, A., Kretzner, L., Alt, F. W., Eisenman, R. N., and Weintraub, H. (1993). Binding of myc proteins to canonical and noncanonical dna sequences. *Mol Cell Biol*, 13(9):5216–5224.
- Blackwood, E. M. and Eisenman, R. N. (1991). Max: a helix-loop-helix zipper protein that forms a sequence-specific dna-binding complex with myc. *Science*, 251(4998):1211–1217.
- Blancato, J., Singh, B., Liu, A., Liao, D. J., and Dickson, R. B. (2004). Correlation of amplification and overexpression of the c-myc oncogene in high-grade breast cancer: Fish, in situ hybridisation and immunohistochemical analyses. *Br J Cancer*, 90(8):1612–1619.
- Blyth, K., Stewart, M., Bell, M., James, C., Evan, G., Neil, J. C., and Cameron, E. R. (2000). Sensitivity to myc-induced apoptosis is retained in spontaneous and transplanted lymphomas of cd2-mycer mice. *Oncogene*, 19(6):773–782.
- Boatright, K. M., Renshaw, M., Scott, F. L., Sperandio, S., Shin, H., Pedersen, I. M., Ricci, J. E., Edris, W. A., Sutherlin, D. P., Green, D. R., and Salvesen, G. S. (2003). A unified model for apical caspase activation. *Mol Cell*, 11(2):529–541.
- Boone, D. N., Qi, Y., Li, Z., and Hann, S. R. (2011). Egr1 mediates p53-independent c-myc-induced apoptosis via a noncanonical arf-dependent transcriptional mechanism. *Proc Natl Acad Sci U S A*, 108(2):632–637.
- Bouchard, C., Staller, P., and Eilers, M. (1998). Control of cell proliferation by myc. *Trends Cell Biol*, 8(5):202–206.
- Bouchard, C., Thieke, K., Maier, A., Saffrich, R., Hanley-Hyde, J., Ansorge, W., Reed, S., Sicinski, P., Bartek, J., and Eilers, M. (1999). Direct induction of cyclin d2 by myc contributes to cell cycle progression and sequestration of p27. *EMBO J*, 18(19):5321–5333.
- Bouchard, C., Marquardt, J., Brás, A., Medema, R. H., and Eilers, M. (2004). Myc-induced proliferation and transformation require akt-mediated phosphorylation of foxo proteins. *EMBO J*, 23(14):2830–2840.
- Bouchard, C., Lee, S., Paulus-Hock, V., Loddenkemper, C., Eilers, M., and Schmitt, C. A. (2007). Foxo transcription factors suppress myc-driven lymphomagenesis via direct activation of arf. *Genes Dev*, 21(21):2775–2787.
- Bradford, M. M. (1976). A rapid and sensitive method for the quantitation of microgram quantities of protein utilizing the principle of protein-dye binding. *Anal Biochem*, 72:248–254.
- Brandt, D. T., Baarlink, C., Kitzing, T. M., Kremmer, E., Ivaska, J., Nollau, P., and Grosse, R. (2009). Scai acts as a suppressor of cancer cell invasion through the transcriptional control of beta1-integrin. *Nat Cell Biol*, 11(5):557–568.
- Brenner, C., Deplus, R., Didelot, C., Loriot, A., Viré, E., De Smet, C., Gutierrez, A., Danovi, D., Bernard, D., Boon, T., Pelicci, P. G., Amati, B., Kouzarides, T., de Launoit, Y., Di Croce, L.,

- and Fuks, F. (2005). Myc represses transcription through recruitment of dna methyltransferase corepressor. *EMBO J*, 24(2):336–346.
- Brunet, A., Bonni, A., Zigmond, M. J., Lin, M. Z., Juo, P., Hu, L. S., Anderson, M. J., Arden, K. C., Blenis, J., and Greenberg, M. E. (1999). Akt promotes cell survival by phosphorylating and inhibiting a forkhead transcription factor. *Cell*, 96(6):857–868.
- Bálint E, E. and Vousden, K. H. (2001). Activation and activities of the p53 tumour suppressor protein. *Br J Cancer*, 85(12):1813–1823.
- Cain, K., Brown, D. G., Langlais, C., and Cohen, G. M. (1999). Caspase activation involves the formation of the aposome, a large (approximately 700 kda) caspase-activating complex. *J Biol Chem*, 274(32):22686–22692.
- Campone, M., Noël, B., Couriaud, C., Grau, M., Guillemin, Y., Gautier, F., Gouraud, W., Charbonnel, C., Campion, L., Jézéquel, P., Braun, F., Barré, B., Coqueret, O., Barillé-Nion, S., and Juin, P. (2011). c-myc dependent expression of pro-apoptotic bim renders her2-overexpressing breast cancer cells dependent on anti-apoptotic mcl-1. *Mol Cancer*, 10:110.
- Canman, C. E., Lim, D. S., Cimprich, K. A., Taya, Y., Tamai, K., Sakaguchi, K., Appella, E., Kastan, M. B., and Siliciano, J. D. (1998). Activation of the atm kinase by ionizing radiation and phosphorylation of p53. *Science*, 281(5383):1677–1679.
- Cappellen, D., Schlange, T., Bauer, M., Maurer, F., and Hynes, N. E. (2007). Novel c-myc target genes mediate differential effects on cell proliferation and migration. *EMBO Rep*, 8(1):70–76.
- Cartwright, P., McLean, C., Sheppard, A., Rivett, D., Jones, K., and Dalton, S. (2005). Lif/stat3 controls es cell self-renewal and pluripotency by a myc-dependent mechanism. *Development*, 132(5):885–896.
- Case, N., Thomas, J., Sen, B., Styner, M., Xie, Z., Galior, K., and Rubin, J. (2011). Mechanical regulation of glycogen synthase kinase  $\beta$  (gsk3 $\beta$ ) in mesenchymal stem cells is dependent on akt protein serine 473 phosphorylation via mtorc2 protein. *J Biol Chem*, 286(45):39450–39456.
- Chaffer, C. L., Brueckmann, I., Scheel, C., Kaestli, A. J., Wiggins, P. A., Rodrigues, L. O., Brooks, M., Reinhardt, F., Su, Y., Polyak, K., Arendt, L. M., Kuperwasser, C., Bierie, B., and Weinberg, R. A. (2011). Normal and neoplastic nonstem cells can spontaneously convert to a stem-like state. *Proc Natl Acad Sci U S A*, 108(19):7950–7955.
- Chang, T.-C., Yu, D., Lee, Y.-S., Wentzel, E. A., Arking, D. E., West, K. M., Dang, C. V., Thomas-Tikhonenko, A., and Mendell, J. T. (2008). Widespread microrna repression by myc contributes to tumorigenesis. *Nat Genet*, 40(1):43–50.
- Chen, D., Shan, J., Zhu, W.-G., Qin, J., and Gu, W. (2010)a. Transcription-independent arf regulation in oncogenic stress-mediated p53 responses. *Nature*, 464(7288):624–627.
- Chen, D., Kon, N., Zhong, J., Zhang, P., Yu, L., and Gu, W. (2013). Differential effects on arf stability by normal versus oncogenic levels of c-myc expression. *Mol Cell*, 51(1):46–56.

- Chen, L., Li, Z., Zwolinska, A. K., Smith, M. A., Cross, B., Koomen, J., Yuan, Z.-M., Jenuwein, T., Marine, J.-C., Wright, K. L., and Chen, J. (2010)b. Mdm2 recruitment of lysine methyltransferases regulates p53 transcriptional output. *EMBO J*, 29(15):2538–2552.
- Cheng, S. W., Davies, K. P., Yung, E., Beltran, R. J., Yu, J., and Kalpana, G. V. (1999). c-myc interacts with ini1/hsnf5 and requires the swi/snf complex for transactivation function. *Nat Genet*, 22(1):102–105.
- Chiarugi, P. and Giannoni, E. (2008). Anoikis: a necessary death program for anchorage-dependent cells. *Biochem Pharmacol*, 76(11):1352–1364.
- Christophorou, M. A., Ringshausen, I., Finch, A. J., Swigart, L. B., and Evan, G. I. (2006). The pathological response to dna damage does not contribute to p53-mediated tumour suppression. *Nature*, 443(7108):214–217.
- Chrzan, P., Skokowski, J., Karmolinski, A., and Pawelczyk, T. (2001). Amplification of c-myc gene and overexpression of c-myc protein in breast cancer and adjacent non-neoplastic tissue. *Clin Biochem*, 34(7):557–562.
- Cole, M. D. and Cowling, V. H. (2008). Transcription-independent functions of myc: regulation of translation and dna replication. *Nat Rev Mol Cell Biol*, 9(10):810–815.
- Coller, H. A., Grandori, C., Tamayo, P., Colbert, T., Lander, E. S., Eisenman, R. N., and Golub, T. R. (2000). Expression analysis with oligonucleotide microarrays reveals that myc regulates genes involved in growth, cell cycle, signaling, and adhesion. *Proc Natl Acad Sci U S A*, 97(7):3260–3265.
- Conzen, S. D., Gottlob, K., Kandel, E. S., Khanduri, P., Wagner, A. J., O’Leary, M., and Hay, N. (2000). Induction of cell cycle progression and acceleration of apoptosis are two separable functions of c-myc: transrepression correlates with acceleration of apoptosis. *Mol Cell Biol*, 20(16):6008–6018.
- Cowell, J. K., LaDuca, J., Rossi, M. R., Burkhardt, T., Nowak, N. J., and Matsui, S.-i. (2005). Molecular characterization of the t(3;9) associated with immortalization in the mcf10a cell line. *Cancer Genet Cytogenet*, 163(1):23–29.
- Cowling, V. H., D’Cruz, C. M., Chodosh, L. A., and Cole, M. D. (2007). c-myc transforms human mammary epithelial cells through repression of the wnt inhibitors dkk1 and sfrp1. *Mol Cell Biol*, 27(14):5135–5146.
- Cross, D. A., Alessi, D. R., Cohen, P., Andjelkovich, M., and Hemmings, B. A. (1995). Inhibition of glycogen synthase kinase-3 by insulin mediated by protein kinase b. *Nature*, 378(6559):785–789.
- Culjkovic, B., Topisirovic, I., Skrabanek, L., Ruiz-Gutierrez, M., and Borden, K. L. B. (2006). eif4e is a central node of an rna regulon that governs cellular proliferation. *J Cell Biol*, 175(3):415–426.
- Czabotar, P. E., Lessene, G., Strasser, A., and Adams, J. M. (2014). Control of apoptosis by the bcl-2 protein family: implications for physiology and therapy. *Nat Rev Mol Cell Biol*, 15(1):49–63.



- Dang, C. V. (2012). Myc on the path to cancer. *Cell*, 149(1):22–35.
- Dang, C. V., O'Donnell, K. A., Zeller, K. I., Nguyen, T., Osthus, R. C., and Li, F. (2006). The c-myc target gene network. *Semin Cancer Biol*, 16(4):253–264.
- Datta, S. R., Dudek, H., Tao, X., Masters, S., Fu, H., Gotoh, Y., and Greenberg, M. E. (1997). Akt phosphorylation of bad couples survival signals to the cell-intrinsic death machinery. *Cell*, 91(2):231–241.
- Davis, A. C., Wims, M., Spotts, G. D., Hann, S. R., and Bradley, A. (1993). A null c-myc mutation causes lethality before 10.5 days of gestation in homozygotes and reduced fertility in heterozygous female mice. *Genes Dev*, 7(4):671–682.
- Davis, L. J. and Halazonetis, T. D. (1993). Both the helix-loop-helix and the leucine zipper motifs of c-myc contribute to its dimerization specificity with max. *Oncogene*, 8(1):125–132.
- D'Cruz, C. M., Gunther, E. J., Boxer, R. B., Hartman, J. L., Sintasath, L., Moody, S. E., Cox, J. D., Ha, S. I., Belka, G. K., Golant, A., Cardiff, R. D., and Chodosh, L. A. (2001). c-myc induces mammary tumorigenesis by means of a preferred pathway involving spontaneous kras2 mutations. *Nat Med*, 7(2):235–239.
- Debnath, J. and Brugge, J. S. (2005). Modelling glandular epithelial cancers in three-dimensional cultures. *Nat Rev Cancer*, 5(9):675–688.
- Debnath, J., Muthuswamy, S. K., and Brugge, J. S. (2003). Morphogenesis and oncogenesis of mcf-10a mammary epithelial acini grown in three-dimensional basement membrane cultures. *Methods*, 30(3):256–268.
- Dontu, G., Abdallah, W. M., Foley, J. M., Jackson, K. W., Clarke, M. F., Kawamura, M. J., and Wicha, M. S. (2003). In vitro propagation and transcriptional profiling of human mammary stem/progenitor cells. *Genes Dev*, 17(10):1253–1270.
- Du, C., Fang, M., Li, Y., Li, L., and Wang, X. (2000). Smac, a mitochondrial protein that promotes cytochrome c-dependent caspase activation by eliminating iap inhibition. *Cell*, 102(1):33–42.
- Dubois, N. C., Adolphe, C., Ehninger, A., Wang, R. A., Robertson, E. J., and Trumpp, A. (2008). Placental rescue reveals a sole requirement for c-myc in embryonic erythroblast survival and hematopoietic stem cell function. *Development*, 135(14):2455–2465.
- Eberhardy, S. R. and Farnham, P. J. (2001). c-myc mediates activation of the cad promoter via a post-rna polymerase ii recruitment mechanism. *J Biol Chem*, 276(51):48562–48571.
- Eberhardy, S. R. and Farnham, P. J. (2002). Myc recruits p-tefb to mediate the final step in the transcriptional activation of the cad promoter. *J Biol Chem*, 277(42):40156–40162.
- Edlich, F., Banerjee, S., Suzuki, M., Cleland, M. M., Arnoult, D., Wang, C., Neutzner, A., Tjandra, N., and Youle, R. J. (2011). Bcl-x(1) retrotranslocates bax from the mitochondria into the cytosol. *Cell*, 145(1):104–116.

- Egle, A., Harris, A. W., Bouillet, P., and Cory, S. (2004). Bim is a suppressor of myc-induced mouse b cell leukemia. *Proc Natl Acad Sci U S A*, 101(16):6164–6169.
- Eilers, M., Picard, D., Yamamoto, K. R., and Bishop, J. M. (1989). Chimaeras of myc oncoprotein and steroid receptors cause hormone-dependent transformation of cells. *Nature*, 340(6228):66–68.
- Eilers, M. and Eisenman, R. N. (2008). Myc’s broad reach. *Genes Dev*, 22(20):2755–2766.
- Eischen, C. M., Weber, J. D., Roussel, M. F., Sherr, C. J., and Cleveland, J. L. (1999). Disruption of the arf-mdm2-p53 tumor suppressor pathway in myc-induced lymphomagenesis. *Genes Dev*, 13(20):2658–2669.
- Eischen, C. M., Roussel, M. F., Korsmeyer, S. J., and Cleveland, J. L. (2001)a. Bax loss impairs myc-induced apoptosis and circumvents the selection of p53 mutations during myc-mediated lymphomagenesis. *Mol Cell Biol*, 21(22):7653–7662.
- Eischen, C. M., Woo, D., Roussel, M. F., and Cleveland, J. L. (2001)b. Apoptosis triggered by myc-induced suppression of bcl-x(1) or bcl-2 is bypassed during lymphomagenesis. *Mol Cell Biol*, 21(15):5063–5070.
- Elenbaas, B., Spirio, L., Koerner, F., Fleming, M. D., Zimonjic, D. B., Donaher, J. L., Popescu, N. C., Hahn, W. C., and Weinberg, R. A. (2001). Human breast cancer cells generated by oncogenic transformation of primary mammary epithelial cells. *Genes Dev*, 15(1):50–65.
- Esnault, C., Stewart, A., Gualdrini, F., East, P., Horswell, S., Matthews, N., and Treisman, R. (2014). Rho-actin signaling to the mrtf coactivators dominates the immediate transcriptional response to serum in fibroblasts. *Genes Dev*, 28(9):943–958.
- Espinosa, J. M. and Emerson, B. M. (2001). Transcriptional regulation by p53 through intrinsic dna/chromatin binding and site-directed cofactor recruitment. *Mol Cell*, 8(1):57–69.
- Evan, G. I., Wyllie, A. H., Gilbert, C. S., Littlewood, T. D., Land, H., Brooks, M., Waters, C. M., Penn, L. Z., and Hancock, D. C. (1992). Induction of apoptosis in fibroblasts by c-myc protein. *Cell*, 69(1):119–128.
- Evan, G. Personal communication at joint lab retreat, Cambridge, UK, (2014).
- Farrell, A. S. and Sears, R. C. (2014). Myc degradation. *Cold Spring Harb Perspect Med*, 4(3).
- Feil, R., Wagner, J., Metzger, D., and Chambon, P. (1997). Regulation of cre recombinase activity by mutated estrogen receptor ligand-binding domains. *Biochem Biophys Res Commun*, 237(3):752–757.
- Feng, X.-H., Liang, Y.-Y., Liang, M., Zhai, W., and Lin, X. (2002). Direct interaction of c-myc with smad2 and smad3 to inhibit tgf-beta-mediated induction of the cdk inhibitor p15(ink4b). *Mol Cell*, 9(1):133–143.
- Fernandez, P. C., Frank, S. R., Wang, L., Schroeder, M., Liu, S., Greene, J., Cocito, A., and Amati, B. (2003). Genomic targets of the human c-myc protein. *Genes Dev*, 17(9):1115–1129.

- Finch, A., Prescott, J., Shchors, K., Hunt, A., Soucek, L., Dansen, T. B., Swigart, L. B., and Evan, G. I. (2006). Bcl-xl gain of function and p19 arf loss of function cooperate oncogenically with myc in vivo by distinct mechanisms. *Cancer Cell*, 10(2):113–120.
- Frank, S. R., Parisi, T., Taubert, S., Fernandez, P., Fuchs, M., Chan, H.-M., Livingston, D. M., and Amati, B. (2003). Myc recruits the tip60 histone acetyltransferase complex to chromatin. *EMBO Rep*, 4(6):575–580.
- Friedl, P. and Wolf, K. (2010). Plasticity of cell migration: a multiscale tuning model. *J Cell Biol*, 188(1):11–19.
- Frisch, S. M. and Francis, H. (1994). Disruption of epithelial cell-matrix interactions induces apoptosis. *J Cell Biol*, 124(4):619–626.
- Frye, M., Gardner, C., Li, E. R., Arnold, I., and Watt, F. M. (2003). Evidence that myc activation depletes the epidermal stem cell compartment by modulating adhesive interactions with the local microenvironment. *Development*, 130(12):2793–2808.
- Gabay, M., Li, Y., and Felsher, D. W. (2014). Myc activation is a hallmark of cancer initiation and maintenance. *Cold Spring Harb Perspect Med*, 4(6).
- Gallant, P. (2013). Myc function in drosophila. *Cold Spring Harb Perspect Med*, 3(10):a014324.
- Gao, P., Tchernyshyov, I., Chang, T.-C., Lee, Y.-S., Kita, K., Ochi, T., Zeller, K. I., De Marzo, A. M., Van Eyk, J. E., Mendell, J. T., and Dang, C. V. (2009). c-myc suppression of mir-23a/b enhances mitochondrial glutaminase expression and glutamine metabolism. *Nature*, 458(7239):762–765.
- Gardai, S. J., Hildeman, D. A., Frankel, S. K., Whitlock, B. B., Frasch, S. C., Borregaard, N., Marrack, P., Bratton, D. L., and Henson, P. M. (2004). Phosphorylation of bax ser184 by akt regulates its activity and apoptosis in neutrophils. *J Biol Chem*, 279(20):21085–21095.
- Garrison, S. P., Jeffers, J. R., Yang, C., Nilsson, J. A., Hall, M. A., Rehg, J. E., Yue, W., Yu, J., Zhang, L., Onciu, M., Sample, J. T., Cleveland, J. L., and Zambetti, G. P. (2008). Selection against puma gene expression in myc-driven b-cell lymphomagenesis. *Mol Cell Biol*, 28(17):5391–5402.
- Gartel, A. L., Ye, X., Goufman, E., Shianov, P., Hay, N., Najmabadi, F., and Tyner, A. L. (2001). Myc represses the p21(waf1/cip1) promoter and interacts with sp1/sp3. *Proc Natl Acad Sci U S A*, 98(8):4510–4515.
- Gebhardt, A., Frye, M., Herold, S., Benitah, S. A., Braun, K., Samans, B., Watt, F. M., Elsässer, H.-P., and Eilers, M. (2006). Myc regulates keratinocyte adhesion and differentiation via complex formation with miz1. *J Cell Biol*, 172(1):139–149.
- Gineitis, D. and Treisman, R. (2001). Differential usage of signal transduction pathways defines two types of serum response factor target gene. *J Biol Chem*, 276(27):24531–24539.
- Gomez-Roman, N., Grandori, C., Eisenman, R. N., and White, R. J. (2003). Direct activation of rna polymerase iii transcription by c-myc. *Nature*, 421(6920):290–294.

- González-Murillo, A., Lozano, M. L., Alvarez, L., Jacome, A., Almarza, E., Navarro, S., Segovia, J. C., Hanenberg, H., Guenechea, G., Bueren, J. A., and Río, P. (2010). Development of lentiviral vectors with optimized transcriptional activity for the gene therapy of patients with fanconi anemia. *Hum Gene Ther*, 21(5):623–630.
- Goodliffe, J. M., Wieschaus, E., and Cole, M. D. (2005). Polycomb mediates myc autorepression and its transcriptional control of many loci in drosophila. *Genes Dev*, 19(24):2941–2946.
- Grandori, C., Cowley, S. M., James, L. P., and Eisenman, R. N. (2000). The myc/max/mad network and the transcriptional control of cell behavior. *Annu Rev Cell Dev Biol*, 16:653–699.
- Grandori, C., Wu, K.-J., Fernandez, P., Ngouenet, C., Grim, J., Clurman, B. E., Moser, M. J., Oshima, J., Russell, D. W., Swisshelm, K., Frank, S., Amati, B., Dalla-Favera, R., and Monnat, R. J., Jr. (2003). Werner syndrome protein limits myc-induced cellular senescence. *Genes Dev*, 17(13):1569–1574.
- Griffiths, G. J., Dubrez, L., Morgan, C. P., Jones, N. A., Whitehouse, J., Corfe, B. M., Dive, C., and Hickman, J. A. (1999). Cell damage-induced conformational changes of the pro-apoptotic protein bak in vivo precede the onset of apoptosis. *J Cell Biol*, 144(5):903–914.
- Grignani, F., Lombardi, L., Inghirami, G., Sternas, L., Cechova, K., and Dalla-Favera, R. (1990). Negative autoregulation of c-myc gene expression is inactivated in transformed cells. *EMBO J*, 9(12):3913–3922.
- Guccione, E., Martinato, F., Finocchiaro, G., Luzi, L., Tizzoni, L., Dall’Olio, V., Zardo, G., Nervi, C., Bernard, L., and Amati, B. (2006). Myc-binding-site recognition in the human genome is determined by chromatin context. *Nat Cell Biol*, 8(7):764–770.
- Guo, J., Li, T., Schipper, J., Nilson, K. A., Fordjour, F. K., Cooper, J. J., Gordân, R., and Price, D. H. (2014). Sequence specificity incompletely defines the genome-wide occupancy of myc. *Genome Biol*, 15(10):482.
- Haggerty, T. J., Zeller, K. I., Osthus, R. C., Wonsey, D. R., and Dang, C. V. (2003). A strategy for identifying transcription factor binding sites reveals two classes of genomic c-myc target sites. *Proc Natl Acad Sci U S A*, 100(9):5313–5318.
- Hanahan, D. and Weinberg, R. A. (2011). Hallmarks of cancer: the next generation. *Cell*, 144(5):646–674.
- He, T. C., Sparks, A. B., Rago, C., Hermeking, H., Zawel, L., da Costa, L. T., Morin, P. J., Vogelstein, B., and Kinzler, K. W. (1998). Identification of c-myc as a target of the apc pathway. *Science*, 281(5382):1509–1512.
- Hemann, M. T., Bric, A., Teruya-Feldstein, J., Herbst, A., Nilsson, J. A., Cordon-Cardo, C., Cleveland, J. L., Tansey, W. P., and Lowe, S. W. (2005). Evasion of the p53 tumour surveillance network by tumour-derived myc mutants. *Nature*, 436(7052):807–811.
- Hengartner, M. O. (2000). The biochemistry of apoptosis. *Nature*, 407(6805):770–776.
- Herkert, B. and Eilers, M. (2010). Transcriptional repression: the dark side of myc. *Genes Cancer*, 1(6):580–586.

- Herkert, B., Dwertmann, A., Herold, S., Abed, M., Naud, J.-F., Finkernagel, F., Harms, G. S., Orian, A., Wanzel, M., and Eilers, M. (2010). The arf tumor suppressor protein inhibits miz1 to suppress cell adhesion and induce apoptosis. *J Cell Biol*, 188(6):905–918.
- Herold, S., Wanzel, M., Beuger, V., Frohme, C., Beul, D., Hillukkala, T., Syvaoja, J., Saluz, H.-P., Haenel, F., and Eilers, M. (2002). Negative regulation of the mammalian uv response by myc through association with miz-1. *Mol Cell*, 10(3):509–521.
- Hirao, A., Kong, Y. Y., Matsuoka, S., Wakeham, A., Ruland, J., Yoshida, H., Liu, D., Elledge, S. J., and Mak, T. W. (2000). Dna damage-induced activation of p53 by the checkpoint kinase chk2. *Science*, 287(5459):1824–1827.
- Hoffman, B. and Liebermann, D. A. (2008). Apoptotic signaling by c-myc. *Oncogene*, 27(50):6462–6472.
- Horiuchi, D., Kusdra, L., Huskey, N. E., Chandriani, S., Lenburg, M. E., Gonzalez-Angulo, A. M., Creasman, K. J., Bazarov, A. V., Smyth, J. W., Davis, S. E., Yaswen, P., Mills, G. B., Esserman, L. J., and Goga, A. (2012). Myc pathway activation in triple-negative breast cancer is synthetic lethal with cdk inhibition. *J Exp Med*, 209(4):679–696.
- Horn, H. F. and Vousden, K. H. (2007). Coping with stress: multiple ways to activate p53. *Oncogene*, 26(9):1306–1316.
- Hsu, B., Marin, M. C., el Naggar, A. K., Stephens, L. C., Brisbay, S., and McDonnell, T. J. (1995). Evidence that c-myc mediated apoptosis does not require wild-type p53 during lymphomagenesis. *Oncogene*, 11(1):175–179.
- Huang, D. W., Sherman, B. T., and Lempicki, R. A. (2009). Systematic and integrative analysis of large gene lists using david bioinformatics resources. *Nat Protoc*, 4(1):44–57.
- Huang, Z., Traugh, J. A., and Bishop, J. M. (2004). Negative control of the myc protein by the stress-responsive kinase pak2. *Mol Cell Biol*, 24(4):1582–1594.
- Hundley, J. E., Koester, S. K., Troyer, D. A., Hilsenbeck, S. G., Barrington, R. E., and Windle, J. J. (1997). Differential regulation of cell cycle characteristics and apoptosis in mmtv-myc and mmtv-ras mouse mammary tumors. *Cancer Res*, 57(4):600–603.
- Hynes, N. E. and Stoelzle, T. (2009). Key signalling nodes in mammary gland development and cancer: Myc. *Breast Cancer Res*, 11(5):210.
- Hönnemann, J., Sanz-Moreno, A., Wolf, E., Eilers, M., and Elsässer, H.-P. (2012). Miz1 is a critical repressor of cdkn1a during skin tumorigenesis. *PLoS One*, 7(4):e34885.
- Inoue, S., Hao, Z., Elia, A. J., Cescon, D., Zhou, L., Silvester, J., Snow, B., Harris, I. S., Sasaki, M., Li, W. Y., Itsumi, M., Yamamoto, K., Ueda, T., Dominguez-Brauer, C., Gorrini, C., Chio, I. I. C., Haight, J., You-Ten, A., McCracken, S., Wakeham, A., Ghazarian, D., Penn, L. J. Z., Melino, G., and Mak, T. W. (2013). Mule/huwe1/arf-bp1 suppresses ras-driven tumorigenesis by preventing c-myc/miz1-mediated down-regulation of p21 and p15. *Genes Dev*, 27(10):1101–1114.

- Iraci, N., Diolaiti, D., Papa, A., Porro, A., Valli, E., Gherardi, S., Herold, S., Eilers, M., Bernardoni, R., Della Valle, G., and Perini, G. (2011). A *sp1/miz1/mycn* repression complex recruits *hdac1* at the *trka* and *p75ntr* promoters and affects neuroblastoma malignancy by inhibiting the cell response to *ngf*. *Cancer Res*, 71(2):404–412.
- Ito, A., Kawaguchi, Y., Lai, C.-H., Kovacs, J. J., Higashimoto, Y., Appella, E., and Yao, T.-P. (2002). Mdm2-hdac1-mediated deacetylation of p53 is required for its degradation. *EMBO J*, 21(22):6236–6245.
- Jacinto, E., Loewith, R., Schmidt, A., Lin, S., Rüegg, M. A., Hall, A., and Hall, M. N. (2004). Mammalian tor complex 2 controls the actin cytoskeleton and is rapamycin insensitive. *Nat Cell Biol*, 6(11):1122–1128.
- Ji, H., Wu, G., Zhan, X., Nolan, A., Koh, C., De Marzo, A., Doan, H. M., Fan, J., Cheadle, C., Fallahi, M., Cleveland, J. L., Dang, C. V., and Zeller, K. I. (2011). Cell-type independent *myc* target genes reveal a primordial signature involved in biomass accumulation. *PLoS One*, 6(10):e26057.
- Jones, S. (2004). An overview of the basic helix-loop-helix proteins. *Genome Biol*, 5(6):226.
- Juin, P., Hueber, A. O., Littlewood, T., and Evan, G. (1999). *c-myc*-induced sensitization to apoptosis is mediated through cytochrome *c* release. *Genes Dev*, 13(11):1367–1381.
- Jänicke, L. Personal communication, Würzburg, Germany, (2014).
- Kauffmann-Zeh, A., Rodriguez-Viciano, P., Ulrich, E., Gilbert, C., Coffey, P., Downward, J., and Evan, G. (1997). Suppression of *c-myc*-induced apoptosis by *ras* signalling through *pi(3)k* and *pkb*. *Nature*, 385(6616):544–548.
- Kaur, M. and Cole, M. D. (2013). *Myc* acts via the *pten* tumor suppressor to elicit autoregulation and genome-wide gene repression by activation of the *ezh2* methyltransferase. *Cancer Res*, 73(2):695–705.
- Kerosuo, L., Piltti, K., Fox, H., Angers-Loustau, A., Häyry, V., Eilers, M., Sariola, H., and Wartiovaara, K. (2008). *Myc* increases self-renewal in neural progenitor cells through *miz-1*. *J Cell Sci*, 121(Pt 23):3941–3950.
- Kerr, J. F., Wyllie, A. H., and Currie, A. R. (1972). Apoptosis: a basic biological phenomenon with wide-ranging implications in tissue kinetics. *Br J Cancer*, 26(4):239–257.
- Khwaja, A., Rodriguez-Viciano, P., Wennström, S., Warne, P. H., and Downward, J. (1997). Matrix adhesion and *ras* transformation both activate a phosphoinositide 3-oh kinase and protein kinase *b/akt* cellular survival pathway. *EMBO J*, 16(10):2783–2793.
- Kim, S. Y., Herbst, A., Tworkowski, K. A., Salghetti, S. E., and Tansey, W. P. (2003). *Skp2* regulates *myc* protein stability and activity. *Mol Cell*, 11(5):1177–1188.
- Kim, Y. H., Girard, L., Giacomini, C. P., Wang, P., Hernandez-Boussard, T., Tibshirani, R., Minna, J. D., and Pollack, J. R. (2006). Combined microarray analysis of small cell lung cancer reveals altered apoptotic balance and distinct expression signatures of *myc* family gene amplification. *Oncogene*, 25(1):130–138.

- King, W. G., Mattaliano, M. D., Chan, T. O., Tsiichlis, P. N., and Brugge, J. S. (1997). Phosphatidylinositol 3-kinase is required for integrin-stimulated akt and raf-1/mitogen-activated protein kinase pathway activation. *Mol Cell Biol*, 17(8):4406–4418.
- Knoepfler, P. S., Zhang, X.-y., Cheng, P. F., Gafken, P. R., McMahon, S. B., and Eisenman, R. N. (2006). Myc influences global chromatin structure. *EMBO J*, 25(12):2723–2734.
- Konsavage, W. M., Jr, Jin, G., and Yochum, G. S. (2012). The myc 3' wnt-responsive element regulates homeostasis and regeneration in the mouse intestinal tract. *Mol Cell Biol*, 32(19):3891–3902.
- Kothny-Wilkes, G., Kulms, D., Pöppelmann, B., Luger, T. A., Kubin, M., and Schwarz, T. (1998). Interleukin-1 protects transformed keratinocytes from tumor necrosis factor-related apoptosis-inducing ligand. *J Biol Chem*, 273(44):29247–29253.
- Kruse, J.-P. and Gu, W. (2008). Snapshot: p53 posttranslational modifications. *Cell*, 133(5):930–30.e1.
- Kubbutat, M. H., Jones, S. N., and Vousden, K. H. (1997). Regulation of p53 stability by mdm2. *Nature*, 387(6630):299–303.
- Kurland, J. F. and Tansey, W. P. (2008). Myc-mediated transcriptional repression by recruitment of histone deacetylase. *Cancer Res*, 68(10):3624–3629.
- Laemmli, U. K. (1970). Cleavage of structural proteins during the assembly of the head of bacteriophage t4. *Nature*, 227(5259):680–685.
- Lamb, R. F., Roy, C., Diefenbach, T. J., Vinters, H. V., Johnson, M. W., Jay, D. G., and Hall, A. (2000). The tsc1 tumour suppressor hamartin regulates cell adhesion through erm proteins and the gtpase rho. *Nat Cell Biol*, 2(5):281–287.
- Langmead, B. (2010). Aligning short sequencing reads with bowtie. *Curr Protoc Bioinformatics*, Chapter 11:Unit 11.7.
- Lee, J. W., Soung, Y. H., Kim, S. Y., Nam, S. W., Park, W. S., Lee, J. Y., Yoo, N. J., and Lee, S. H. (2006). Mutational analysis of myc in common epithelial cancers and acute leukemias. *APMIS*, 114(6):436–439.
- Lemm, I. and Ross, J. (2002). Regulation of c-myc mrna decay by translational pausing in a coding region instability determinant. *Mol Cell Biol*, 22(12):3959–3969.
- Leone, G., DeGregori, J., Sears, R., Jakoi, L., and Nevins, J. R. (1997). Myc and ras collaborate in inducing accumulation of active cyclin e/cdk2 and e2f. *Nature*, 387(6631):422–426.
- Levens, D. L. (2003). Reconstructing myc. *Genes Dev*, 17(9):1071–1077.
- Li, H., Handsaker, B., Wysoker, A., Fennell, T., Ruan, J., Homer, N., Marth, G., Abecasis, G., Durbin, R., and , . G. P. D. P. S. (2009). The sequence alignment/map format and samtools. *Bioinformatics*, 25(16):2078–2079.
- Li, S., Lin, P., Young, K. H., Kanagal-Shamanna, R., Yin, C. C., and Medeiros, L. J. (2013). Myc/bcl2 double-hit high-grade b-cell lymphoma. *Adv Anat Pathol*, 20(5):315–326.

- Li, Z., Van Calcar, S., Qu, C., Cavenee, W. K., Zhang, M. Q., and Ren, B. (2003). A global transcriptional regulatory role for c-myc in burkitt's lymphoma cells. *Proc Natl Acad Sci U S A*, 100(14):8164–8169.
- Licchesi, J. D. F., Van Neste, L., Tiwari, V. K., Cope, L., Lin, X., Baylin, S. B., and Herman, J. G. (2010). Transcriptional regulation of wnt inhibitory factor-1 by miz-1/c-myc. *Oncogene*, 29(44):5923–5934.
- Lin, C. Y., Lovén, J., Rahl, P. B., Paranal, R. M., Burge, C. B., Bradner, J. E., Lee, T. I., and Young, R. A. (2012)a. Transcriptional amplification in tumor cells with elevated c-myc. *Cell*, 151(1):56–67.
- Lin, C.-W., Liao, M.-Y., Lin, W.-W., Wang, Y.-P., Lu, T.-Y., and Wu, H.-C. (2012)b. Epithelial cell adhesion molecule regulates tumor initiation and tumorigenesis via activating reprogramming factors and epithelial-mesenchymal transition gene expression in colon cancer. *J Biol Chem*, 287(47):39449–39459.
- Littlewood, T. D., Hancock, D. C., Danielian, P. S., Parker, M. G., and Evan, G. I. (1995). A modified oestrogen receptor ligand-binding domain as an improved switch for the regulation of heterologous proteins. *Nucleic Acids Res*, 23(10):1686–1690.
- Liu, H., Radisky, D. C., Yang, D., Xu, R., Radisky, E. S., Bissell, M. J., and Bishop, J. M. (2012)a. Myc suppresses cancer metastasis by direct transcriptional silencing of  $\alpha$ v and  $\beta$ 3 integrin subunits. *Nat Cell Biol*, 14(6):567–574.
- Liu, J. and Levens, D. (2006). Making myc. *Curr Top Microbiol Immunol*, 302:1–32.
- Liu, L., Ulbrich, J., Müller, J., Wüstefeld, T., Aeberhard, L., Kress, T. R., Muthalagu, N., Rycak, L., Rudalska, R., Moll, R., Kempa, S., Zender, L., Eilers, M., and Murphy, D. J. (2012)b. Deregulated myc expression induces dependence upon ampk-related kinase 5. *Nature*, 483(7391):608–612.
- Liu, M., Casimiro, M. C., Wang, C., Shirley, L. A., Jiao, X., Katiyar, S., Ju, X., Li, Z., Yu, Z., Zhou, J., Johnson, M., Fortina, P., Hyslop, T., Windle, J. J., and Pestell, R. G. (2009). p21cip1 attenuates ras- and c-myc-dependent breast tumor epithelial mesenchymal transition and cancer stem cell-like gene expression in vivo. *Proc Natl Acad Sci U S A*, 106(45):19035–19039.
- Liu, X., Kim, C. N., Yang, J., Jemmerson, R., and Wang, X. (1996). Induction of apoptotic program in cell-free extracts: requirement for datp and cytochrome c. *Cell*, 86(1):147–157.
- Liu, X., Tesfai, J., Evrard, Y. A., Dent, S. Y. R., and Martinez, E. (2003). c-myc transformation domain recruits the human staga complex and requires trrap and gcn5 acetylase activity for transcription activation. *J Biol Chem*, 278(22):20405–20412.
- Llambi, F., Moldoveanu, T., Tait, S. W. G., Bouchier-Hayes, L., Temirov, J., McCormick, L. L., Dillon, C. P., and Green, D. R. (2011). A unified model of mammalian bcl-2 protein family interactions at the mitochondria. *Mol Cell*, 44(4):517–531.
- Llanos, S., Clark, P. A., Rowe, J., and Peters, G. (2001). Stabilization of p53 by p14arf without relocation of mdm2 to the nucleolus. *Nat Cell Biol*, 3(5):445–452.



- Lovén, J., Orlando, D. A., Sigova, A. A., Lin, C. Y., Rahl, P. B., Burge, C. B., Levens, D. L., Lee, T. I., and Young, R. A. (2012). Revisiting global gene expression analysis. *Cell*, 151(3):476–482.
- Lowe, S. W., Cepero, E., and Evan, G. (2004). Intrinsic tumour suppression. *Nature*, 432(7015):307–315.
- Luo, X., Budihardjo, I., Zou, H., Slaughter, C., and Wang, X. (1998). Bid, a bcl2 interacting protein, mediates cytochrome c release from mitochondria in response to activation of cell surface death receptors. *Cell*, 94(4):481–490.
- Lüscher, B. and Vervoorts, J. (2012). Regulation of gene transcription by the oncoprotein myc. *Gene*, 494(2):145–160.
- Machanick, P. and Bailey, T. L. (2011). Meme-chip: motif analysis of large dna datasets. *Bioinformatics*, 27(12):1696–1697.
- Mani, S. A., Guo, W., Liao, M.-J., Eaton, E. N., Ayyanan, A., Zhou, A. Y., Brooks, M., Reinhard, F., Zhang, C. C., Shipitsin, M., Campbell, L. L., Polyak, K., Brisken, C., Yang, J., and Weinberg, R. A. (2008). The epithelial-mesenchymal transition generates cells with properties of stem cells. *Cell*, 133(4):704–715.
- Marinkovich, M. P. (2007). Tumour microenvironment: laminin 332 in squamous-cell carcinoma. *Nat Rev Cancer*, 7(5):370–380.
- Martinato, F., Cesaroni, M., Amati, B., and Guccione, E. (2008). Analysis of myc-induced histone modifications on target chromatin. *PLoS One*, 3(11):e3650.
- McDonald, O. G., Wamhoff, B. R., Hoofnagle, M. H., and Owens, G. K. (2006). Control of srf binding to carg box chromatin regulates smooth muscle gene expression in vivo. *J Clin Invest*, 116(1):36–48.
- McMahon, S. B., Wood, M. A., and Cole, M. D. (2000). The essential cofactor trrap recruits the histone acetyltransferase hgc5 to c-myc. *Mol Cell Biol*, 20(2):556–562.
- Menssen, A., Epanchintsev, A., Lodygin, D., Rezaei, N., Jung, P., Verdoodt, B., Diebold, J., and Hermeking, H. (2007). c-myc delays prometaphase by direct transactivation of mad2 and bubr1: identification of mechanisms underlying c-myc-induced dna damage and chromosomal instability. *Cell Cycle*, 6(3):339–352.
- Meredith, J., Jr and Schwartz, M. A. (1997). Integrins, adhesion and apoptosis. *Trends Cell Biol*, 7(4):146–150.
- Meredith, J., Jr, Fazeli, B., and Schwartz, M. A. (1993). The extracellular matrix as a cell survival factor. *Mol Biol Cell*, 4(9):953–961.
- Mihara, M., Erster, S., Zaika, A., Petrenko, O., Chittenden, T., Pancoska, P., and Moll, U. M. (2003). p53 has a direct apoptogenic role at the mitochondria. *Mol Cell*, 11(3):577–590.
- Miralles, F., Posern, G., Zaromytidou, A.-I., and Treisman, R. (2003). Actin dynamics control srf activity by regulation of its coactivator mal. *Cell*, 113(3):329–342.

- Mitchell, K. O., Ricci, M. S., Miyashita, T., Dicker, D. T., Jin, Z., Reed, J. C., and El-Deiry, W. S. (2000). Bax is a transcriptional target and mediator of c-myc-induced apoptosis. *Cancer Res*, 60(22):6318–6325.
- Mootha, V. K., Lindgren, C. M., Eriksson, K.-F., Subramanian, A., Sihag, S., Lehar, J., Puigserver, P., Carlsson, E., Ridderstråle, M., Laurila, E., Houstis, N., Daly, M. J., Patterson, N., Mesirov, J. P., Golub, T. R., Tamayo, P., Spiegelman, B., Lander, E. S., Hirschhorn, J. N., Altshuler, D., and Groop, L. C. (2003). Pgc-1alpha-responsive genes involved in oxidative phosphorylation are coordinately downregulated in human diabetes. *Nat Genet*, 34(3):267–273.
- Morrish, F., Neretti, N., Sedivy, J. M., and Hockenbery, D. M. (2008). The oncogene c-myc coordinates regulation of metabolic networks to enable rapid cell cycle entry. *Cell Cycle*, 7(8):1054–1066.
- Moumen, M., Chiche, A., Deugnier, M.-A., Petit, V., Gandarillas, A., Glukhova, M. A., and Faraldo, M. M. (2012). The proto-oncogene myc is essential for mammary stem cell function. *Stem Cells*, 30(6):1246–1254.
- Murphy, D. J., Junttila, M. R., Pouyet, L., Karnezis, A., Shchors, K., Bui, D. A., Brown-Swigart, L., Johnson, L., and Evan, G. I. (2008). Distinct thresholds govern myc’s biological output in vivo. *Cancer Cell*, 14(6):447–457.
- Murre, C., McCaw, P. S., and Baltimore, D. (1989). A new dna binding and dimerization motif in immunoglobulin enhancer binding, daughterless, myod, and myc proteins. *Cell*, 56(5):777–783.
- Muthalagu, N., Junttila, M. R., Wiese, K. E., Wolf, E., Morton, J., Bauer, B., Evan, G. I., Eilers, M., and Murphy, D. J. (2014). Bim is the primary mediator of myc-induced apoptosis in multiple solid tissues. *Cell Rep*, 8(5):1347–1353.
- Nair, S. K. and Burley, S. K. (2003). X-ray structures of myc-max and mad-max recognizing dna. molecular bases of regulation by proto-oncogenic transcription factors. *Cell*, 112(2):193–205.
- Nass, S. J., Li, M., Amundadottir, L. T., Furth, P. A., and Dickson, R. B. (1996). Role for bcl-xl in the regulation of apoptosis by egf and tgf beta 1 in c-myc overexpressing mammary epithelial cells. *Biochem Biophys Res Commun*, 227(1):248–256.
- Neph, S., Vierstra, J., Stergachis, A. B., Reynolds, A. P., Haugen, E., Vernot, B., Thurman, R. E., John, S., Sandstrom, R., Johnson, A. K., Maurano, M. T., Humbert, R., Rynes, E., Wang, H., Vong, S., Lee, K., Bates, D., Diegel, M., Roach, V., Dunn, D., Neri, J., Schafer, A., Hansen, R. S., Kutuyavin, T., Giste, E., Weaver, M., Canfield, T., Sabo, P., Zhang, M., Balasundaram, G., Byron, R., MacCoss, M. J., Akey, J. M., Bender, M. A., Groudine, M., Kaul, R., and Stamatoyannopoulos, J. A. (2012). An expansive human regulatory lexicon encoded in transcription factor footprints. *Nature*, 489(7414):83–90.
- Nesbit, C. E., Grove, L. E., Yin, X., and Prochownik, E. V. (1998). Differential apoptotic behaviors of c-myc, n-myc, and l-myc oncoproteins. *Cell Growth Differ*, 9(9):731–741.

- Nho, R. S., Xia, H., Kahm, J., Kleidon, J., Diebold, D., and Henke, C. A. (2005). Role of integrin-linked kinase in regulating phosphorylation of akt and fibroblast survival in type I collagen matrices through a beta1 integrin viability signaling pathway. *J Biol Chem*, 280(28): 26630–26639.
- Nicol, J. W., Helt, G. A., Blanchard, S. G., Jr, Raja, A., and Loraine, A. E. (2009). The integrated genome browser: free software for distribution and exploration of genome-scale datasets. *Bioinformatics*, 25(20):2730–2731.
- Nie, Z., Hu, G., Wei, G., Cui, K., Yamane, A., Resch, W., Wang, R., Green, D. R., Tessarollo, L., Casellas, R., Zhao, K., and Levens, D. (2012). c-myc is a universal amplifier of expressed genes in lymphocytes and embryonic stem cells. *Cell*, 151(1):68–79.
- Nieminen, A. I., Partanen, J. I., Hau, A., and Klefstrom, J. (2007). c-myc primed mitochondria determine cellular sensitivity to trail-induced apoptosis. *EMBO J*, 26(4):1055–1067.
- Nilsson, J. A. and Cleveland, J. L. (2003). Myc pathways provoking cell suicide and cancer. *Oncogene*, 22(56):9007–9021.
- Nilsson, J. A., Keller, U. B., Baudino, T. A., Yang, C., Norton, S., Old, J. A., Nilsson, L. M., Neale, G., Kramer, D. L., Porter, C. W., and Cleveland, J. L. (2005). Targeting ornithine decarboxylase in myc-induced lymphomagenesis prevents tumor formation. *Cancer Cell*, 7(5): 433–444.
- Ogawara, Y., Kishishita, S., Obata, T., Isazawa, Y., Suzuki, T., Tanaka, K., Masuyama, N., and Gotoh, Y. (2002). Akt enhances mdm2-mediated ubiquitination and degradation of p53. *J Biol Chem*, 277(24):21843–21850.
- Olivier, M., Hollstein, M., and Hainaut, P. (2010). Tp53 mutations in human cancers: origins, consequences, and clinical use. *Cold Spring Harb Perspect Biol*, 2(1):a001008.
- Oskarsson, T., Essers, M. A. G., Dubois, N., Offner, S., Dubey, C., Roger, C., Metzger, D., Chambon, P., Hummler, E., Beard, P., and Trumpp, A. (2006). Skin epidermis lacking the c-myc gene is resistant to ras-driven tumorigenesis but can reacquire sensitivity upon additional loss of the p21cip1 gene. *Genes Dev*, 20(15):2024–2029.
- Oster, S. K., Mao, D. Y. L., Kennedy, J., and Penn, L. Z. (2003). Functional analysis of the n-terminal domain of the myc oncoprotein. *Oncogene*, 22(13):1998–2010.
- Osthus, R. C., Shim, H., Kim, S., Li, Q., Reddy, R., Mukherjee, M., Xu, Y., Wonsey, D., Lee, L. A., and Dang, C. V. (2000). Deregulation of glucose transporter 1 and glycolytic gene expression by c-myc. *J Biol Chem*, 275(29):21797–21800.
- Palomero, T., Lim, W. K., Odom, D. T., Sulis, M. L., Real, P. J., Margolin, A., Barnes, K. C., O’Neil, J., Neuberg, D., Weng, A. P., Aster, J. C., Sigaux, F., Soulier, J., Look, A. T., Young, R. A., Califano, A., and Ferrando, A. A. (2006). Notch1 directly regulates c-myc and activates a feed-forward-loop transcriptional network promoting leukemic cell growth. *Proc Natl Acad Sci U S A*, 103(48):18261–18266.
- Paoli, P., Giannoni, E., and Chiarugi, P. (2013). Anoikis molecular pathways and its role in cancer progression. *Biochim Biophys Acta*, 1833(12):3481–3498.

- Partanen, J. I., Nieminen, A. I., Mäkelä, T. P., and Klefstrom, J. (2007). Suppression of oncogenic properties of c-myc by lkb1-controlled epithelial organization. *Proc Natl Acad Sci U S A*, 104(37):14694–14699.
- Pastrana, E., Silva-Vargas, V., and Doetsch, F. (2011). Eyes wide open: a critical review of sphere-formation as an assay for stem cells. *Cell Stem Cell*, 8(5):486–498.
- Patel, J. H. and McMahon, S. B. (2006). Targeting of miz-1 is essential for myc-mediated apoptosis. *J Biol Chem*, 281(6):3283–3289.
- Patel, J. H. and McMahon, S. B. (2007). Bcl2 is a downstream effector of miz-1 essential for blocking c-myc-induced apoptosis. *J Biol Chem*, 282(1):5–13.
- Peng, J., Zhu, Y., Milton, J. T., and Price, D. H. (1998). Identification of multiple cyclin subunits of human p-tefb. *Genes Dev*, 12(5):755–762.
- Penn, L. J., Brooks, M. W., Laufer, E. M., Littlewood, T. D., Morgenstern, J. P., Evan, G. I., Lee, W. M., and Land, H. (1990). Domains of human c-myc protein required for autosuppression and cooperation with ras oncogenes are overlapping. *Mol Cell Biol*, 10(9):4961–4966.
- Persad, S., Attwell, S., Gray, V., Delcommenne, M., Troussard, A., Sanghera, J., and Dedhar, S. (2000). Inhibition of integrin-linked kinase (ilK) suppresses activation of protein kinase b/akt and induces cell cycle arrest and apoptosis of pten-mutant prostate cancer cells. *Proc Natl Acad Sci U S A*, 97(7):3207–3212.
- Persad, S., Attwell, S., Gray, V., Mawji, N., Deng, J. T., Leung, D., Yan, J., Sanghera, J., Walsh, M. P., and Dedhar, S. (2001). Regulation of protein kinase b/akt-serine 473 phosphorylation by integrin-linked kinase: critical roles for kinase activity and amino acids arginine 211 and serine 343. *J Biol Chem*, 276(29):27462–27469.
- Peter, S., Bultinck, J., Myant, K., Jaenicke, L. A., Walz, S., Müller, J., Gmachl, M., Treu, M., Boehmelt, G., Ade, C. P., Schmitz, W., Wiegner, A., Otto, C., Popov, N., Sansom, O., Kraut, N., and Eilers, M. (2014). Tumor cell-specific inhibition of myc function using small molecule inhibitors of the huwe1 ubiquitin ligase. *EMBO Mol Med*, 6(12):1525–1541.
- Peukert, K., Staller, P., Schneider, A., Carmichael, G., Hänel, F., and Eilers, M. (1997). An alternative pathway for gene regulation by myc. *EMBO J*, 16(18):5672–5686.
- Pheffe, T. J., Myant, K. B., Cole, A. M., Ridgway, R. A., Pearson, H., Muncan, V., van den Brink, G. R., Vousden, K. H., Sears, R., Vassilev, L. T., Clarke, A. R., and Sansom, O. J. (2014). Endogenous c-myc is essential for p53-induced apoptosis in response to dna damage in vivo. *Cell Death Differ*, 21(6):956–966.
- Posern, G. and Treisman, R. (2006). Actin’ together: serum response factor, its cofactors and the link to signal transduction. *Trends Cell Biol*, 16(11):588–596.
- Posern, G., Sotiropoulos, A., and Treisman, R. (2002). Mutant actins demonstrate a role for unpolymerized actin in control of transcription by serum response factor. *Mol Biol Cell*, 13(12):4167–4178.

- 
- Pylyayeva-Gupta, Y., Grabocka, E., and Bar-Sagi, D. (2011). Ras oncogenes: weaving a tumorigenic web. *Nat Rev Cancer*, 11(11):761–774.
- Qi, Y., Gregory, M. A., Li, Z., Brousal, J. P., West, K., and Hann, S. R. (2004). p19arf directly and differentially controls the functions of c-myc independently of p53. *Nature*, 431(7009):712–717.
- Quinlan, A. R. and Hall, I. M. (2010). Bedtools: a flexible suite of utilities for comparing genomic features. *Bioinformatics*, 26(6):841–842.
- R Core Team. *R: A Language and Environment for Statistical Computing*. R Foundation for Statistical Computing, Vienna, Austria, (2014). URL <http://www.R-project.org/>.
- Rahl, P. B. and Young, R. A. (2014). Myc and transcription elongation. *Cold Spring Harb Perspect Med*, 4(1):a020990.
- Rahl, P. B., Lin, C. Y., Seila, A. C., Flynn, R. A., McCuine, S., Burge, C. B., Sharp, P. A., and Young, R. A. (2010). c-myc regulates transcriptional pause release. *Cell*, 141(3):432–445.
- Ramirez, S., Ait-Si-Ali, S., Robin, P., Trouche, D., Harel-Bellan, A., and Ait Si Ali, S. (1997). The creb-binding protein (cbp) cooperates with the serum response factor for transactivation of the c-fos serum response element. *J Biol Chem*, 272(49):31016–31021.
- Ray, S., Atkuri, K. R., Deb-Basu, D., Adler, A. S., Chang, H. Y., Herzenberg, L. A., and Felsher, D. W. (2006). Myc can induce dna breaks in vivo and in vitro independent of reactive oxygen species. *Cancer Res*, 66(13):6598–6605.
- Reisman, D., Elkind, N. B., Roy, B., Beamon, J., and Rotter, V. (1993). c-myc trans-activates the p53 promoter through a required downstream cacgtg motif. *Cell Growth Differ*, 4(2):57–65.
- Roca-Cusachs, P., del Rio, A., Puklin-Faucher, E., Gauthier, N. C., Biais, N., and Sheetz, M. P. (2013). Integrin-dependent force transmission to the extracellular matrix by  $\alpha$ -actinin triggers adhesion maturation. *Proc Natl Acad Sci U S A*, 110(15):E1361–E1370.
- Rodriguez, J. and Lazebnik, Y. (1999). Caspase-9 and apaf-1 form an active holoenzyme. *Genes Dev*, 13(24):3179–3184.
- Sabò, A. and Amati, B. (2014). Genome recognition by myc. *Cold Spring Harb Perspect Med*, 4(2).
- Sabò, A., Kress, T. R., Pelizzola, M., de Pretis, S., Gorski, M. M., Tesi, A., Morelli, M. J., Bora, P., Doni, M., Verrecchia, A., Tonelli, C., Fagà, G., Bianchi, V., Ronchi, A., Low, D., Müller, H., Guccione, E., Campaner, S., and Amati, B. (2014). Selective transcriptional regulation by myc in cellular growth control and lymphomagenesis. *Nature*, 511(7510):488–492.
- Saldanha, A. J. (2004). Java treeview—extensible visualization of microarray data. *Bioinformatics*, 20(17):3246–3248.
- Salghetti, S. E., Kim, S. Y., and Tansey, W. P. (1999). Destruction of myc by ubiquitin-mediated proteolysis: cancer-associated and transforming mutations stabilize myc. *EMBO J*, 18(3):717–726.
-

- Samuels, Y., Wang, Z., Bardelli, A., Silliman, N., Ptak, J., Szabo, S., Yan, H., Gazdar, A., Powell, S. M., Riggins, G. J., Willson, J. K. V., Markowitz, S., Kinzler, K. W., Vogelstein, B., and Velculescu, V. E. (2004). High frequency of mutations of the *pik3ca* gene in human cancers. *Science*, 304(5670):554.
- Sansom, O. J., Meniel, V. S., Muncan, V., Phesse, T. J., Wilkins, J. A., Reed, K. R., Vass, J. K., Athineos, D., Clevers, H., and Clarke, A. R. (2007). *Myc* deletion rescues *apc* deficiency in the small intestine. *Nature*, 446(7136):676–679.
- Sanz-Moreno, A., Fuhrmann, D., Wolf, E., von Eyss, B., Eilers, M., and Elsässer, H.-P. (2014). *Miz1* deficiency in the mammary gland causes a lactation defect by attenuated *stat5* expression and phosphorylation. *PLoS One*, 9(2):e89187.
- Sarbassov, D. D., Ali, S. M., Kim, D.-H., Guertin, D. A., Latek, R. R., Erdjument-Bromage, H., Tempst, P., and Sabatini, D. M. (2004). Rictor, a novel binding partner of mtor, defines a rapamycin-insensitive and raptor-independent pathway that regulates the cytoskeleton. *Curr Biol*, 14(14):1296–1302.
- Sarbassov, D. D., Guertin, D. A., Ali, S. M., and Sabatini, D. M. (2005). Phosphorylation and regulation of akt/pkb by the rictor-mtor complex. *Science*, 307(5712):1098–1101.
- Sato, K., Handa, H., Kimura, M., Okano, Y., Nagaoka, H., Nagase, T., Sugiyama, T., Kitade, Y., and Ueda, H. (2013). Identification of a rho family specific guanine nucleotide exchange factor, flj00018, as a novel actin-binding protein. *Cell Signal*, 25(1):41–49.
- Satoh, Y., Matsumura, I., Tanaka, H., Ezoe, S., Sugahara, H., Mizuki, M., Shibayama, H., Ishiko, E., Ishiko, J., Nakajima, K., and Kanakura, Y. (2004). Roles for *c-myc* in self-renewal of hematopoietic stem cells. *J Biol Chem*, 279(24):24986–24993.
- Satou, A., Taira, T., Iguchi-Arigo, S. M., and Ariga, H. (2001). A novel transrepression pathway of *c-myc*. recruitment of a transcriptional corepressor complex to *c-myc* by mm-1, a *c-myc*-binding protein. *J Biol Chem*, 276(49):46562–46567.
- Schlee, M., Hölzel, M., Bernard, S., Mailhammer, R., Schuhmacher, M., Reschke, J., Eick, D., Marinkovic, D., Wirth, T., Rosenwald, A., Staudt, L. M., Eilers, M., Baran-Marszak, F., Fagard, R., Feuillard, J., Laux, G., and Bornkamm, G. W. (2007). *C-myc* activation impairs the *nf-kappab* and the interferon response: implications for the pathogenesis of burkitt’s lymphoma. *Int J Cancer*, 120(7):1387–1395.
- Schlereth, K., Beinoraviciute-Kellner, R., Zeitlinger, M. K., Bretz, A. C., Sauer, M., Charles, J. P., Vogiatzi, F., Leich, E., Samans, B., Eilers, M., Kisker, C., Rosenwald, A., and Stiewe, T. (2010). Dna binding cooperativity of p53 modulates the decision between cell-cycle arrest and apoptosis. *Mol Cell*, 38(3):356–368.
- Schlosser, I., Hölzel, M., Hoffmann, R., Burtscher, H., Kohlhuber, F., Schuhmacher, M., Chapman, R., Weidle, U. H., and Eick, D. (2005). Dissection of transcriptional programmes in response to serum and *c-myc* in a human b-cell line. *Oncogene*, 24(3):520–524.

- Schmitt, C. A., McCurrach, M. E., de Stanchina, E., Wallace-Brodeur, R. R., and Lowe, S. W. (1999). Ink4a/arf mutations accelerate lymphomagenesis and promote chemoresistance by disabling p53. *Genes Dev*, 13(20):2670–2677.
- Schoenenberger, C. A., Andres, A. C., Groner, B., van der Valk, M., LeMeur, M., and Gerlinger, P. (1988). Targeted c-myc gene expression in mammary glands of transgenic mice induces mammary tumours with constitutive milk protein gene transcription. *EMBO J*, 7(1):169–175.
- Schratt, G., Philippar, U., Berger, J., Schwarz, H., Heidenreich, O., and Nordheim, A. (2002). Serum response factor is crucial for actin cytoskeletal organization and focal adhesion assembly in embryonic stem cells. *J Cell Biol*, 156(4):737–750.
- Schratt, G., Philippar, U., Hockemeyer, D., Schwarz, H., Alberti, S., and Nordheim, A. (2004). Srf regulates bcl-2 expression and promotes cell survival during murine embryonic development. *EMBO J*, 23(8):1834–1844.
- Schuhmacher, M., Kohlhuber, F., Hölzel, M., Kaiser, C., Burtscher, H., Jarsch, M., Bornkamm, G. W., Laux, G., Polack, A., Weidle, U. H., and Eick, D. (2001). The transcriptional program of a human b cell line in response to myc. *Nucleic Acids Res*, 29(2):397–406.
- Sears, R., Ohtani, K., and Nevins, J. R. (1997). Identification of positively and negatively acting elements regulating expression of the e2f2 gene in response to cell growth signals. *Mol Cell Biol*, 17(9):5227–5235.
- Sears, R., Leone, G., DeGregori, J., and Nevins, J. R. (1999). Ras enhances myc protein stability. *Mol Cell*, 3(2):169–179.
- Selvaraj, A. and Prywes, R. (2004). Expression profiling of serum inducible genes identifies a subset of srf target genes that are mkl dependent. *BMC Mol Biol*, 5:13.
- Seoane, J., Le, H.-V., and Massagué, J. (2002). Myc suppression of the p21(cip1) cdk inhibitor influences the outcome of the p53 response to dna damage. *Nature*, 419(6908):729–734.
- Shchors, K., Shchors, E., Rostker, F., Lawlor, E. R., Brown-Swigart, L., and Evan, G. I. (2006). The myc-dependent angiogenic switch in tumors is mediated by interleukin 1beta. *Genes Dev*, 20(18):2527–2538.
- Shortt, J. and Johnstone, R. W. (2012). Oncogenes in cell survival and cell death. *Cold Spring Harb Perspect Biol*, 4(12).
- Si, J., Yu, X., Zhang, Y., and DeWille, J. W. (2010). Myc interacts with max and miz1 to repress c/ebpdelta promoter activity and gene expression. *Mol Cancer*, 9:92.
- Simpson, D. R., Yu, M., Zheng, S., Zhao, Z., Muthuswamy, S. K., and Tansey, W. P. (2011). Epithelial cell organization suppresses myc function by attenuating myc expression. *Cancer Res*, 71(11):3822–3830.
- Sleman, K. E., Kendrick, H., Ashworth, A., Isacke, C. M., and Smalley, M. J. (2006). Cd24 staining of mouse mammary gland cells defines luminal epithelial, myoepithelial/basal and non-epithelial cells. *Breast Cancer Res*, 8(1):R7.

- Smith, K. N., Singh, A. M., and Dalton, S. (2010). Myc represses primitive endoderm differentiation in pluripotent stem cells. *Cell Stem Cell*, 7(3):343–354.
- Smith, K. N., Lim, J.-M., Wells, L., and Dalton, S. (2011). Myc orchestrates a regulatory network required for the establishment and maintenance of pluripotency. *Cell Cycle*, 10(4):592–597.
- Song, J., Ugai, H., Ogawa, K., Wang, Y., Sarai, A., Obata, Y., Kanazawa, I., Sun, K., Itakura, K., and Yokoyama, K. K. (2001). Two consecutive zinc fingers in sp1 and in maz are essential for interactions with cis-elements. *J Biol Chem*, 276(32):30429–30434.
- Sotiropoulos, A., Gineitis, D., Copeland, J., and Treisman, R. (1999). Signal-regulated activation of serum response factor is mediated by changes in actin dynamics. *Cell*, 98(2):159–169.
- Soucek, L., Lawlor, E. R., Soto, D., Shchors, K., Swigart, L. B., and Evan, G. I. (2007). Mast cells are required for angiogenesis and macroscopic expansion of myc-induced pancreatic islet tumors. *Nat Med*, 13(10):1211–1218.
- Soule, H. D., Maloney, T. M., Wolman, S. R., Peterson, W., Jr, Brenz, R., McGrath, C. M., Russo, J., Pauley, R. J., Jones, R. F., and Brooks, S. C. (1990). Isolation and characterization of a spontaneously immortalized human breast epithelial cell line, mcf-10. *Cancer Res*, 50(18):6075–6086.
- Sovak, M. A., Bellas, R. E., Kim, D. W., Zanieski, G. J., Rogers, A. E., Traish, A. M., and Sonenshein, G. E. (1997). Aberrant nuclear factor-kappaB/rel expression and the pathogenesis of breast cancer. *J Clin Invest*, 100(12):2952–2960.
- Spotts, G. D., Patel, S. V., Xiao, Q., and Hann, S. R. (1997). Identification of downstream-initiated c-myc proteins which are dominant-negative inhibitors of transactivation by full-length c-myc proteins. *Mol Cell Biol*, 17(3):1459–1468.
- Staller, P., Peukert, K., Kiermaier, A., Seoane, J., Lukas, J., Karsunky, H., Möröy, T., Bartek, J., Massagué, J., Hänel, F., and Eilers, M. (2001). Repression of p15<sup>ink4b</sup> expression by myc through association with miz-1. *Nat Cell Biol*, 3(4):392–399.
- Steiger, D., Furrer, M., Schwinkendorf, D., and Gallant, P. (2008). Max-independent functions of myc in drosophila melanogaster. *Nat Genet*, 40(9):1084–1091.
- Stewart, T. A., Pattengale, P. K., and Leder, P. (1984). Spontaneous mammary adenocarcinomas in transgenic mice that carry and express mtv/myc fusion genes. *Cell*, 38(3):627–637.
- Subik, K., Lee, J.-F., Baxter, L., Strzepak, T., Costello, D., Crowley, P., Xing, L., Hung, M.-C., Bonfiglio, T., Hicks, D. G., and Tang, P. (2010). The expression patterns of er, pr, her2, ck5/6, egfr, ki-67 and ar by immunohistochemical analysis in breast cancer cell lines. *Breast Cancer (Auckl)*, 4:35–41.
- Subramanian, A., Tamayo, P., Mootha, V. K., Mukherjee, S., Ebert, B. L., Gillette, M. A., Paulovich, A., Pomeroy, S. L., Golub, T. R., Lander, E. S., and Mesirov, J. P. (2005). Gene set enrichment analysis: a knowledge-based approach for interpreting genome-wide expression profiles. *Proc Natl Acad Sci U S A*, 102(43):15545–15550.



- Sun, Q., Chen, G., Streb, J. W., Long, X., Yang, Y., Stoeckert, C. J., Jr, and Miano, J. M. (2006). Defining the mammalian cargome. *Genome Res*, 16(2):197–207.
- Sutherland, K. D., Vaillant, F., Alexander, W. S., Wintermantel, T. M., Forrest, N. C., Holroyd, S. L., McManus, E. J., Schutz, G., Watson, C. J., Chodosh, L. A., Lindeman, G. J., and Visvader, J. E. (2006). c-myc as a mediator of accelerated apoptosis and involution in mammary glands lacking socs3. *EMBO J*, 25(24):5805–5815.
- Takahashi, K. and Yamanaka, S. (2006). Induction of pluripotent stem cells from mouse embryonic and adult fibroblast cultures by defined factors. *Cell*, 126(4):663–676.
- Thompson, W. R., Guilluy, C., Xie, Z., Sen, B., Brobst, K. E., Yen, S. S., Uzer, G., Styner, M., Case, N., BurrIDGE, K., and Rubin, J. (2013). Mechanically activated fyn utilizes mtorc2 to regulate rhoa and adipogenesis in mesenchymal stem cells. *Stem Cells*, 31(11):2528–2537.
- Tolbert, D., Lu, X., Yin, C., Tantama, M., and Van Dyke, T. (2002). p19(arf) is dispensable for oncogenic stress-induced p53-mediated apoptosis and tumor suppression in vivo. *Mol Cell Biol*, 22(1):370–377.
- Vafa, O., Wade, M., Kern, S., Beeche, M., Pandita, T. K., Hampton, G. M., and Wahl, G. M. (2002). c-myc can induce dna damage, increase reactive oxygen species, and mitigate p53 function: a mechanism for oncogene-induced genetic instability. *Mol Cell*, 9(5):1031–1044.
- van Riggelen, J., Müller, J., Otto, T., Beuger, V., Yetil, A., Choi, P. S., Kosan, C., Möröy, T., Felsher, D. W., and Eilers, M. (2010). The interaction between myc and miz1 is required to antagonize tgfbeta-dependent autocrine signaling during lymphoma formation and maintenance. *Genes Dev*, 24(12):1281–1294.
- Varlakhanova, N., Cotterman, R., Bradnam, K., Korf, I., and Knoepfler, P. S. (2011). Myc and miz-1 have coordinate genomic functions including targeting hox genes in human embryonic stem cells. *Epigenetics Chromatin*, 4:20.
- Vartiainen, M. K., Guettler, S., Larijani, B., and Treisman, R. (2007). Nuclear actin regulates dynamic subcellular localization and activity of the srf cofactor mal. *Science*, 316(5832):1749–1752.
- Velling, T., Nilsson, S., Stefansson, A., and Johansson, S. (2004). beta1-integrins induce phosphorylation of akt on serine 473 independently of focal adhesion kinase and src family kinases. *EMBO Rep*, 5(9):901–905.
- Verhagen, A. M., Ekert, P. G., Pakusch, M., Silke, J., Connolly, L. M., Reid, G. E., Moritz, R. L., Simpson, R. J., and Vaux, D. L. (2000). Identification of diablo, a mammalian protein that promotes apoptosis by binding to and antagonizing iap proteins. *Cell*, 102(1):43–53.
- Vervoorts, J., Lüscher-Firzlaff, J. M., Rottmann, S., Lilischkis, R., Walsemann, G., Dohmann, K., Austen, M., and Lüscher, B. (2003). Stimulation of c-myc transcriptional activity and acetylation by recruitment of the cofactor cbp. *EMBO Rep*, 4(5):484–490.
- Vita, M. and Henriksson, M. (2006). The myc oncoprotein as a therapeutic target for human cancer. *Semin Cancer Biol*, 16(4):318–330.

- von Eyss, B., Jaenicke, L. A., Kortlever, R. M., Royla, N., Wiese, K. E., Letschert, S., Sauer, M., Rosenwald, A., Evan, G. I., Kempa, S., and Eilers, M. (2015). A myc-driven change in mitochondrial dynamics limits self-renewal of mammary stem cells. *Cancer Cell, in revision*.
- Waikel, R. L., Kawachi, Y., Waikel, P. A., Wang, X. J., and Roop, D. R. (2001). Deregulated expression of *c-myc* depletes epidermal stem cells. *Nat Genet*, 28(2):165–168.
- Wall, M., Poortinga, G., Hannan, K. M., Pearson, R. B., Hannan, R. D., and McArthur, G. A. (2008). Translational control of *c-myc* by rapamycin promotes terminal myeloid differentiation. *Blood*, 112(6):2305–2317.
- Walz, S., Lorenzin, F., Morton, J., Wiese, K. E., von Eyss, B., Herold, S., Rycak, L., Dumay-Odelot, H., Karim, S., Bartkuhn, M., Roels, F., Wüstefeld, T., Fischer, M., Teichmann, M., Zender, L., Wei, C.-L., Sansom, O., Wolf, E., and Eilers, M. (2014). Activation and repression by oncogenic myc shape tumour-specific gene expression profiles. *Nature*, 511(7510):483–487.
- Wang, D.-Z., Li, S., Hockemeyer, D., Sutherland, L., Wang, Z., Schratt, G., Richardson, J. A., Nordheim, A., and Olson, E. N. (2002). Potentiation of serum response factor activity by a family of myocardin-related transcription factors. *Proc Natl Acad Sci U S A*, 99(23):14855–14860.
- Wang, X., Cunningham, M., Zhang, X., Tokarz, S., Laraway, B., Troxell, M., and Sears, R. C. (2011). Phosphorylation regulates *c-myc*'s oncogenic activity in the mammary gland. *Cancer Res*, 71(3):925–936.
- Wang, Y., Engels, I. H., Knee, D. A., Nasoff, M., Deveraux, Q. L., and Quon, K. C. (2004). Synthetic lethal targeting of *myc* by activation of the *dr5* death receptor pathway. *Cancer Cell*, 5(5):501–512.
- Wanzel, M., Kleine-Kohlbrecher, D., Herold, S., Hock, A., Berns, K., Park, J., Hemmings, B., and Eilers, M. (2005). Akt and 14-3-3 $\beta$  regulate *miz1* to control cell-cycle arrest after dna damage. *Nat Cell Biol*, 7(1):30–41.
- Wanzel, M., Russ, A. C., Kleine-Kohlbrecher, D., Colombo, E., Pelicci, P.-G., and Eilers, M. (2008). A ribosomal protein l23-nucleophosmin circuit coordinates *miz1* function with cell growth. *Nat Cell Biol*, 10(9):1051–1061.
- Watt, F. M., Frye, M., and Benitah, S. A. (2008). Myc in mammalian epidermis: how can an oncogene stimulate differentiation? *Nat Rev Cancer*, 8(3):234–242.
- Weake, V. M. and Workman, J. L. (2010). Inducible gene expression: diverse regulatory mechanisms. *Nat Rev Genet*, 11(6):426–437.
- Weaver, V. M., Lelièvre, S., Lakins, J. N., Chrenek, M. A., Jones, J. C. R., Giancotti, F., Werb, Z., and Bissell, M. J. (2002).  $\beta$ 4 integrin-dependent formation of polarized three-dimensional architecture confers resistance to apoptosis in normal and malignant mammary epithelium. *Cancer Cell*, 2(3):205–216.
- Weber, J. D., Taylor, L. J., Roussel, M. F., Sherr, C. J., and Bar-Sagi, D. (1999). Nucleolar arf sequesters *mdm2* and activates p53. *Nat Cell Biol*, 1(1):20–26.

- Welcker, M., Orian, A., Jin, J., Grim, J. E., Grim, J. A., Harper, J. W., Eisenman, R. N., and Churman, B. E. (2004). The *fbw7* tumor suppressor regulates glycogen synthase kinase 3 phosphorylation-dependent c-myc protein degradation. *Proc Natl Acad Sci U S A*, 101(24): 9085–9090.
- Weng, A. P., Millholland, J. M., Yashiro-Ohtani, Y., Arcangeli, M. L., Lau, A., Wai, C., Del Bianco, C., Rodriguez, C. G., Sai, H., Tobias, J., Li, Y., Wolfe, M. S., Shachaf, C., Felsher, D., Blacklow, S. C., Pear, W. S., and Aster, J. C. (2006). c-myc is an important direct target of notch1 in t-cell acute lymphoblastic leukemia/lymphoma. *Genes Dev*, 20(15):2096–2109.
- Westphal, D., Kluck, R. M., and Dewson, G. (2014). Building blocks of the apoptotic pore: how bax and bak are activated and oligomerize during apoptosis. *Cell Death Differ*, 21(2):196–205.
- Whibley, C., Pharoah, P. D. P., and Hollstein, M. (2009). p53 polymorphisms: cancer implications. *Nat Rev Cancer*, 9(2):95–107.
- WHO, W. H. O. World health organization - noncommunicable diseases (ncd) country profiles, (2014). URL <http://www.who.int/>.
- Wiese, K. E., Walz, S., von Eyss, B., Wolf, E., Athineos, D., Sansom, O., and Eilers, M. (2013). The role of miz-1 in myc-dependent tumorigenesis. *Cold Spring Harb Perspect Med*, 3(12): a014290.
- Wiese, K. E., Haikala, H. M., von Eyss, B., Wolf, E., Esnault, C., Rosenwald, A., Treisman, R., Klefström, J., and Eilers, M. (2015). Repression of *srf* target genes is critical for myc-dependent apoptosis of epithelial cells. *EMBO J*, 34(11):1554–1571.
- Wilson, A., Murphy, M. J., Oskarsson, T., Kaloulis, K., Bettess, M. D., Oser, G. M., Pasche, A.-C., Knabenhans, C., Macdonald, H. R., and Trumpp, A. (2004). c-myc controls the balance between hematopoietic stem cell self-renewal and differentiation. *Genes Dev*, 18(22): 2747–2763.
- Wolf, E. and Walz, S. Personal communication, Würzburg, (2014).
- Wolf, E., Gebhardt, A., Kawauchi, D., Walz, S., von Eyss, B., Wagner, N., Renninger, C., Krohne, G., Asan, E., Roussel, M. F., and Eilers, M. (2013). Miz1 is required to maintain autophagic flux. *Nat Commun*, 4:2535.
- Wolf, E., Lin, C. Y., Eilers, M., and Levens, D. L. (2015). Taming of the beast: shaping myc-dependent amplification. *Trends Cell Biol*, 25(4):241–248.
- Wolfer, A., Wittner, B. S., Irimia, D., Flavin, R. J., Lupien, M., Gunawardane, R. N., Meyer, C. A., Lightcap, E. S., Tamayo, P., Mesirov, J. P., Liu, X. S., Shioda, T., Toner, M., Loda, M., Brown, M., Brugge, J. S., and Ramaswamy, S. (2010). Myc regulation of a "poor-prognosis" metastatic cancer cell state. *Proc Natl Acad Sci U S A*, 107(8):3698–3703.
- Wong, D. J., Liu, H., Ridky, T. W., Cassarino, D., Segal, E., and Chang, H. Y. (2008). Module map of stem cell genes guides creation of epithelial cancer stem cells. *Cell Stem Cell*, 2(4): 333–344.

- Wong, R. S. Y. (2011). Apoptosis in cancer: from pathogenesis to treatment. *J Exp Clin Cancer Res*, 30:87.
- Worsham, M. J., Pals, G., Schouten, J. P., Miller, F., Tiwari, N., van Spaendonk, R., and Wolman, S. R. (2006). High-resolution mapping of molecular events associated with immortalization, transformation, and progression to breast cancer in the mcf10 model. *Breast Cancer Res Treat*, 96(2):177–186.
- Wu, K. J., Grandori, C., Amacker, M., Simon-Vermot, N., Polack, A., Lingner, J., and Dalla-Favera, R. (1999). Direct activation of tert transcription by c-myc. *Nat Genet*, 21(2):220–224.
- Wu, S., Cetinkaya, C., Munoz-Alonso, M. J., von der Lehr, N., Bahram, F., Beuger, V., Eilers, M., Leon, J., and Larsson, L.-G. (2003). Myc represses differentiation-induced p21cip1 expression via miz-1-dependent interaction with the p21 core promoter. *Oncogene*, 22(3):351–360.
- Xia, H., Nho, R. S., Kahm, J., Kleidon, J., and Henke, C. A. (2004). Focal adhesion kinase is upstream of phosphatidylinositol 3-kinase/akt in regulating fibroblast survival in response to contraction of type i collagen matrices via a beta 1 integrin viability signaling pathway. *J Biol Chem*, 279(31):33024–33034.
- Xiao, Q., Claassen, G., Shi, J., Adachi, S., Sedivy, J., and Hann, S. R. (1998). Transactivation-defective c-mycs retains the ability to regulate proliferation and apoptosis. *Genes Dev*, 12(24):3803–3808.
- Xu, J., Chen, Y., and Olopade, O. I. (2010). Myc and breast cancer. *Genes Cancer*, 1(6):629–640.
- Yada, M., Hatakeyama, S., Kamura, T., Nishiyama, M., Tsunematsu, R., Imaki, H., Ishida, N., Okumura, F., Nakayama, K., and Nakayama, K. I. (2004). Phosphorylation-dependent degradation of c-myc is mediated by the f-box protein fbw7. *EMBO J*, 23(10):2116–2125.
- Ye, T., Krebs, A. R., Choukrallah, M.-A., Keime, C., Plewniak, F., Davidson, I., and Tora, L. (2011). seqminer: an integrated chip-seq data interpretation platform. *Nucleic Acids Res*, 39(6):e35.
- Yeh, E., Cunningham, M., Arnold, H., Chasse, D., Monteith, T., Ivaldi, G., Hahn, W. C., Stukenberg, P. T., Shenolikar, S., Uchida, T., Counter, C. M., Nevins, J. R., Means, A. R., and Sears, R. (2004). A signalling pathway controlling c-myc degradation that impacts oncogenic transformation of human cells. *Nat Cell Biol*, 6(4):308–318.
- Yi, Y., Shepard, A., Kittrell, F., Mulac-Jericevic, B., Medina, D., and Said, T. K. (2004). p19arf determines the balance between normal cell proliferation rate and apoptosis during mammary gland development. *Mol Biol Cell*, 15(5):2302–2311.
- You, Z., Madrid, L. V., Saims, D., Sedivy, J., and Wang, C.-Y. (2002). c-myc sensitizes cells to tumor necrosis factor-mediated apoptosis by inhibiting nuclear factor kappa b transactivation. *J Biol Chem*, 277(39):36671–36677.
- Yuneva, M., Zamboni, N., Oefner, P., Sachidanandam, R., and Lazebnik, Y. (2007). Deficiency in glutamine but not glucose induces myc-dependent apoptosis in human cells. *J Cell Biol*, 178(1):93–105.

- Zahir, N., Lakins, J. N., Russell, A., Ming, W., Chatterjee, C., Rozenberg, G. I., Marinkovich, M. P., and Weaver, V. M. (2003). Autocrine laminin-5 ligates alpha6beta4 integrin and activates rac and nfkappab to mediate anchorage-independent survival of mammary tumors. *J Cell Biol*, 163(6):1397–1407.
- Zanet, J., Pibre, S., Jacquet, C., Ramirez, A., de Alborán, I. M., and Gandarillas, A. (2005). Endogenous myc controls mammalian epidermal cell size, hyperproliferation, endoreplication and stem cell amplification. *J Cell Sci*, 118(Pt 8):1693–1704.
- Zeller, K. I., Jegga, A. G., Aronow, B. J., O'Donnell, K. A., and Dang, C. V. (2003). An integrated database of genes responsive to the myc oncogenic transcription factor: identification of direct genomic targets. *Genome Biol*, 4(10):R69.
- Zeller, K. I., Zhao, X., Lee, C. W. H., Chiu, K. P., Yao, F., Yustein, J. T., Ooi, H. S., Orlov, Y. L., Shahab, A., Yong, H. C., Fu, Y., Weng, Z., Kuznetsov, V. A., Sung, W.-K., Ruan, Y., Dang, C. V., and Wei, C.-L. (2006). Global mapping of c-myc binding sites and target gene networks in human b cells. *Proc Natl Acad Sci U S A*, 103(47):17834–17839.
- Zhang, Q., Spears, E., Boone, D. N., Li, Z., Gregory, M. A., and Hann, S. R. (2013). Domain-specific c-myc ubiquitylation controls c-myc transcriptional and apoptotic activity. *Proc Natl Acad Sci U S A*, 110(3):978–983.
- Zhang, Y., Liu, T., Meyer, C. A., Eeckhoutte, J., Johnson, D. S., Bernstein, B. E., Nusbaum, C., Myers, R. M., Brown, M., Li, W., and Liu, X. S. (2008). Model-based analysis of chip-seq (macs). *Genome Biol*, 9(9):R137.
- Zhu, J., Blenis, J., and Yuan, J. (2008). Activation of pi3k/akt and mapk pathways regulates myc-mediated transcription by phosphorylating and promoting the degradation of mad1. *Proc Natl Acad Sci U S A*, 105(18):6584–6589.
- Zindy, F., Eischen, C. M., Randle, D. H., Kamijo, T., Cleveland, J. L., Sherr, C. J., and Roussel, M. F. (1998). Myc signaling via the arf tumor suppressor regulates p53-dependent apoptosis and immortalization. *Genes Dev*, 12(15):2424–2433.
- Zychlinski, D., Schambach, A., Modlich, U., Maetzig, T., Meyer, J., Grassman, E., Mishra, A., and Baum, C. (2008). Physiological promoters reduce the genotoxic risk of integrating gene vectors. *Mol Ther*, 16(4):718–725.

# Abbreviations

## SI prefixes

|       |       |   |       |
|-------|-------|---|-------|
| f     | femto | m | milli |
| p     | pico  | c | centi |
| n     | nano  | d | deci  |
| $\mu$ | micro | k | kilo  |

## SI units, SI derived units and other units

|                    |                                 |
|--------------------|---------------------------------|
| A                  | ampere                          |
| kg                 | kilogram                        |
| m                  | metre                           |
| mol                | mole                            |
| s                  | second                          |
| $^{\circ}\text{C}$ | degree Celsius                  |
| V                  | volt                            |
| W                  | watt                            |
| d                  | day                             |
| h                  | hour                            |
| l                  | litre                           |
| min                | minute (time)                   |
| Da                 | dalton                          |
| M                  | mol/l                           |
| U                  | unit                            |
| v/v                | volume per volume               |
| w/v                | weight per volume               |
| g                  | rcf, relative centrifugal force |

## Greek letters

|          |                         |
|----------|-------------------------|
| $\alpha$ | alpha                   |
| $\beta$  | beta                    |
| $\delta$ | delta                   |
| $\Delta$ | Delta, for deletion     |
| $\mu$    | mu, for SI prefix micro |

**Other abbreviations and acronyms**

|          |   |
|----------|---|
| A        | Adenine   |
| AKT      | AKR mouse thymoma kinase, protein kinase B                        |
| ALL      | Acute lymphocytic leukemia  |
| AMP      | Adenosine monophosphate   |
| APS      | Ammoniumpersulfate  |
| ATCC     | American Type Culture Collection                                  |
| ATM      | Ataxia telangiectasia mutated                                     |
| ATP      | Adenosine triphosphate  |
| APAF-1   | Apoptotic protease-activating factor 1                            |
| APC      | Adenomatous polyposis coli  |
| ARF      | Alternate reading frame   |
| BAD      | Bcl-2-associated death promoter                                   |
| BAK      | Bcl-2 homologous antagonist killer                                |
| BAX      | B-cell lymphoma-associated x                                      |
| BCL-2    | B-cell lymphoma gene 2  |
| BCL-XL   | B-cell lymphoma-extra large                                       |
| BH       | BCL-2 homology  |
| bHLH     | Basic helix-loop-helix  |
| BID      | BH3 -interacting domain   |
| BIM      | Bcl-2-interacting mediator  |
| bp       | base pairs  |
| BR       | Basic region  |
| BRD4     | Vromodomain-containing protein 4                                  |
| BTB/POZ  | Bric-a-brac, Tramtrack, Broad- complex/ Pox virus and Zinc finger |
| C        | Cytosine  |
| CAD      | Caspase activated DNase   |
| CDK      | Cyclin-dependent kinase   |
| Chx      | Cycloheximide   |
| cDNA     | Complementary DNA   |
| CEBP     | CAAT Enhancer Binding Protein                                     |
| ChIP     | Chromatin immunoprecipitation                                     |
| ChIP-seq | Chromatin immunoprecipitation coupled to deep sequencing          |
| Chk2     | Checkpoint protein 2  |
| CMV      | Cytomegalovirus   |
| CRD      | Coding region instability determinant                             |
| ctr      | control   |
| D        | Aspartate   |
| dd       | Double-distilled  |
| DIABLO   | Direct IAP-binding protein with Low PI                            |
| DISC     | Death induced silencing complex                                   |
| DMEM     | Dulbecco's Modified Eagle-Medium                                  |
| DMSO     | Dimethylsulfoxide   |
| DNA      | Deoxyribonucleic acid   |
| DNMT     | DNA-methyltransferase   |
| dNTP     | Deoxynucleotide triphosphate                                      |
| DR       | Death receptor  |
| DTT      | Dithiothreitol  |
| E3       | Ubiquitin ligase  |
| E-box    | Enhancer-box  |
| ECL      | Enhanced chemoluminescence  |
| EDTA     | Ethylenediaminetetraacetic acid                                   |

---

|         |   |
|---------|---|
| e.g.    | exempli gratia, for example                         |
| EGF     | Epidermal Growth Factor                             |
| EIF4E   | Eukaryotic Translation Initiation Factor 4E         |
| EMT     | Epithelial mesenchymal transition                   |
| EpCAM   | Epithelial cell adhesion molecule                   |
| ES      | Enrichment score                                    |
| ES cell | Embryonic stem cell                                 |
| EZH2    | Enhancer of zeste homolog 2                         |
| FADD    | Fas-associated death domain protein                 |
| FBW7    | F-box and WD repeat domain containing 7             |
| FC      | Fold change   |
| FCS     | Fetal calf serum                                    |
| FDR     | False discovery rate                                |
| Fig.    | Figure  |
| G       | Guanine   |
| GFP     | Green fluorescent protein                           |
| GTP     | Guanosine triphosphate                              |
| H3/H4   | Histone 3/4   |
| HDAC    | Histone deacetylase                                 |
| HEPES   | N-2-Hydroxyethylpiperazine-N'-2-Ethanesulfonic Acid |
| HRP     | Horseradish peroxidase                              |
| HUWE1   | HECT, UBA and WWE domain containing 1               |
| IAP     | Inhibitor of apoptosis                              |
| IgG     | Immunoglobulin                                      |
| IP      | Immunoprecipitation                                 |
| iPSC    | Induced pluripotent stem cell                       |
| IRES    | Internal ribosome entry site                        |
| INK4    | Inhibitor of CDK4                                   |
| K       | Lysine  |
| kb      | kilo base pairs                                     |
| LB      | Lysogeny Broth                                      |
| log     | Logarithm   |
| LTR     | Long terminal repeat                                |
| LZ      | Leucine zipper                                      |
| MAL     | Megakaryocytic acute leukemia                       |
| MAPK    | Mitogen-activated protein kinase                    |
| MAX     | MYC Associated factor X                             |
| MCL1    | Myeloid cell leukemia 1                             |
| MDM2    | Mouse double minute 2                               |
| mRNA    | messenger RNA                                       |
| miRNA   | microRNA  |
| MRTF    | Myocardin-related transcription factor              |
| MIZ1    | Myc-interacting zinc finger protein 1               |
| MOMP    | Mitochondrial outer membrane permeabilisation       |
| mTORC   | Mammalian Target Of Rapamycin Complex               |
| MYC     | Myelocytomatosis                                    |
| NES     | Normalised enrichment score                         |
| NOXA    | NADPH oxidase activator                             |
| NPM1    | Nucleophosmin                                       |
| PCR     | Polymerase chain reaction                           |
| PDGF    | Platelet-derived growth factor                      |
| PGK     | Phosphoglycerate kinase                             |
| PI      | Propidium iodide                                    |
| PI3K    | Phosphatidylinositol-3-Kinase                       |

---



---

|             |   |
|-------------|---|
| PMSF        | Phenylmethanesulfonyl fluoride  |
| Pol         | Polymerase  |
| pTEFb       | Positive transcription elongation factor complex b                    |
| PUMA        | p53 upregulated modulator of apoptosis                                |
| qPCR        | Quantitative PCR  |
| RNA         | Ribonucleic acid  |
| rpm         | Rounds per minute   |
| RFP         | Red fluorescent protein   |
| RT          | Reverse transcriptase   |
| RT          | Room temperature  |
| S           | Serine  |
| SCF         | Skp, Cullin, F-box containing complex                                 |
| SD          | Standard deviation  |
| SDS         | Sodium dodecyl sulfate  |
| SEM         | Standard error of the mean  |
| SFFV        | Spleen focus forming virus  |
| shRNA       | Small hairpin RNA   |
| SKP2        | S-Phase Kinase-Associated Protein 2                                   |
| Smac        | Second mitochondria-derived activator of caspases                     |
| SMAD        | SMA and MAD related protein   |
| SP1/SP3     | Specificity protein 1/3   |
| SRF         | Serum response factor   |
| SWI/SNF     | Switching/sucrose nonfermenting                                       |
| T           | Thymine   |
| T           | Threonine   |
| TCF/LEF     | T cell factor/lymphoid enhancing factor                               |
| TEMED       | Tetramethylethylenediamine  |
| TF          | Transcription factor  |
| TGF         | Transforming growth factor  |
| TIP48/49/60 | Tat-interactive protein 48/49/60                                      |
| TSS         | Transcriptional start site  |
| TNF         | Tumour necrosis factor  |
| TRADD       | Tumor necrosis factor receptor type 1-associated death domain protein |
| TRAIL       | TNF-related apoptosis-inducing ligand                                 |
| TRRAP       | Transformation- transactivation domain-associated protein             |
| UTR         | Untranslated region   |
| V           | Valine  |
| VD          | Valine to aspartate mutation  |
| WHO         | World health organisation   |
| WNT         | Wingless-related integration site                                     |
| WT          | Wildtype  |

# Acknowledgements

"Silent gratitude isn't much use to anyone" - G.B. Stern

First of all, thank you, **Prof. Dr. Martin Eilers**, for taking me with you to Würzburg, for supervising me during all that time (in the end, it was almost 8 years...) and for the intellectual support, the discussions and new models that helped shaping this thesis. Thank you also for your patience in anticipation of the final version of this thesis. And last but not least, thank you for "volunteering me" as student speaker of the Transregio 17 - it was an invaluable experience and I learned a lot!

I would also like to thank **Prof. Dr. Andreas Trumpp** and **Prof. Dr. Dr. Manfred Scharl** for agreeing to be in my thesis committee as well as **Prof. Dr. Manfred Gessler** for chairing the defense.

Publication of this thesis would not have been possible without the help of **Heidi Haikala** and **Juha Klefström, Björn von Eyss**, as well as **Andreas Rosenwald** - Thank you for the fruitful collaboration!

**Andrea Schott-Heinzmann** and **Anne Catherine Bretz**: Thank you for the amazing time we had together during our services for the Transregio 17 and for the continuous moral support afterwards!

A huge thank you to all the former and present members of the **Eilers "universe"**. Working with you was the best possible combination of professionalism and fun!

I am particularly grateful to have come across some special people:

Thanks **Rosi** - for your help, dedication and all organisational stuff! **Renate**, your help was invaluable and I cannot thank you enough for all the gels you made and for dealing with my little confusions so well! **Christina**, thank you for introducing me to some of the best quotes & books and for reading huge parts of this thesis; and together with **Steffi**, thank you for all the laughs and little office chats. **Fra D, Fra L, Jiajia, Eva** and **Nathiya**: Girls, thanks for all the fun - I especially enjoyed our many "international food lunches"! **Nikita**: Thanks for sharing your amazingly complex brains and all the scientific and personal fun. **Ksenia** and **Milana**, thanks for the friendship and the many nice pictures. **Elmar, Anneli, Giacomo, Carsten, Laura, Björn**: Thank you guys for all the scientific as well as politically-correct and nonsense discussions! For sharing the possibly loudest laughs and being friends! I enjoyed to have coffee, cluster-cake and cocktails with you and it was an honour to lose all the bets (and beers)!

**Laura** - You saved me from falling so many times (figuratively & literally). You were there for me in the lab as well as outside and you always found the right word (muaahhh). Laughing with you from the very first day made everything so much better!

Thanks also to my new lab members in Amsterdam and especially to Renée van Amerongen for accepting me as a fake postdoc and for your patience and support in the final period of writing this thesis.

It is also the time to thank - and mostly apologise to - my friends: Meike, Rebecca (thanks for proofreading), Lena, Maïke, Johannes, Manja, Anna, Sabine und Anne - "sorry for the times I deserted you" and for still sticking around.

Markus, thanks for your support and believe in me in the last years. For listening to complaints and stories and for making me move to the most amazing city! Was du mir alles bietest!

Ich möchte mich am herzlichsten bei meinen Eltern, meiner Oma und dem ganzen großen Rest meiner Familie bedanken - für eure Geduld und Liebe. Auch wenn sich die Antwort auf "Wann bist du (endlich) fertig?" in den letzten vier Jahren nicht groß verändert hat ("So in ein bis zwei Jahren."), habt ihr mich konstant unterstützt und unendlich viel Verständnis gezeigt.

# Publications

Haikala HM, Klefström J, Eilers M, **Wiese KE**. "MYC-induced apoptosis in mammary epithelial cells is associated with repression of lineage-specific gene signatures.", *Cell Cycle*, in press

von Eyss B, Jaenicke LA, Kortlever RM, Royla N, **Wiese KE**, Letschert S, Sauer M, Rosenwald A, Evan GI, Kempa S, Eilers M. "A MYC-driven change in mitochondrial dynamics limits YAP/TAZ function in mammary epithelial cells and breast cancer.", *Cancer Cell*, in press

**Wiese KE**, Haikala HM, von Eyss B, Wolf E, Esnault C, Rosenwald A, Treisman R, Klefström J, Eilers M, "Repression of SRF target genes is critical for Myc-dependent apoptosis of epithelial cells.", *EMBO J*. 2015 Jun 3;34(11):1554-71

Muthalagu N, Junttila MR, **Wiese KE**, Wolf E, Morton J, Bauer B, Evan GI, Eilers M, Murphy DJ, "BIM is the primary mediator of MYC-induced apoptosis in multiple solid tissues.", *Cell Rep*. 2014 Sep 11;8(5):1347-53

Walz S, Lorenzin F, Morton J, **Wiese KE**, von Eyss B, Herold S, Rycak L, Dumay-Odelot H, Karim S, Bartkuhn M, Roels F, Wüstefeld T, Fischer M, Teichmann M, Zender L, Wei CL, Sansom O, Wolf E, Eilers M. "Activation and repression by oncogenic MYC shape tumour-specific gene expression profiles.", *Nature*. 2014 Jul 24;511(7510):483-7

**Wiese KE**, Walz S, von Eyss B, Wolf E, Athineos D, Sansom O, Eilers M. "The role of MIZ-1 in MYC-dependent tumorigenesis.", *Cold Spring Harb Perspect Med*. 2013 Dec1;3(12):a014290

**Wiese KE**, Eilers M. "Pluripotency without Max.", *Cell Stem Cell*. 2011 Jul 8;9(1):5-6

# Curriculum vitae

## Personal data

**Katrin Evelyn Wiese**

Sassenheimstraat 68-2

1059BL Amsterdam

The Netherlands

Born April 12, 1984 in Hannover, Germany

## Education and Work Experience

since 01/2015

**Researcher**

Universiteit van Amsterdam,  
Amsterdam, The Netherlands

04/2009 – 09/2014

**PhD thesis research**

Theodor Boveri Institute,  
Julius-Maximilians-Universität Würzburg, Germany  
Title: "Sensing supraphysiological levels of MYC"  
Supervisor: Prof. Dr. Martin Eilers

12/2007 – 09/2008

**Diploma thesis research**

Institute for Molecular Biology and Tumor Research,  
Philipps-Universität Marburg, Germany  
Supervisor: Prof. Dr. Martin Eilers

10/2003 – 11/2008

**Studies of Human Biology**

Medical Faculty of the Philipps-Universität Marburg, Germany  
Diploma in Human Biology (Humanbiologie)  
Major subjects: Molecular Biology and Human Genetics  
Minor subjects: Immunology

06/2003

**Abitur**

St. Ursula Schule Hannover, Germany

Würzburg, November 16, 2015

# Affidavit

I hereby confirm that my thesis entitled “Sensing supraphysiological levels of MYC - Mechanisms of MIZ1-dependent MYC-induced Apoptosis in Mammary Epithelial Cells” is the result of my own work. I did not receive any help or support from commercial consultants. All sources and/or materials applied are listed and specified in the thesis.

Furthermore, I confirm that this thesis has not yet been submitted as part of another examination process neither in identical nor in similar form.

Würzburg, November 2015